GENETICS OF ENDOCRINE AND EXOCRINE DISEASES OF THE PANCREAS

Ph.D. Thesis

Balázs Németh, M.D.

Supervisors:

Prof. Yvette Mándi, M.D., Ph.D., D.Sc.[1]

Prof. Miklós Sahin-Tóth, M.D., Ph.D.[2]

[1]Department of Medical Microbiology and Immunbiology

Faculty of Medicine

University of Szeged

[2]Department of Molecular and Cell Biology

Boston University

Henry M. Goldman School of Dental Medicine

Szeged

2014.

Publications related to the subject of the thesis:

I. Németh BC, Várkonyi T, Somogyvári F, Lengyel C, Fehértemplomi K, Nyiraty S, Kempler P, Mándi Y. (2014) Relevance of α-defensins (HNP1-3) and defensin β–1 in diabetes. *World Journal of Gastroenterology* **[Accepted for publication]**
IF: 2.547 (2012)

II. Németh BC, Sahin-Tóth M. (2014) Human cationic trypsinogen (PRSS1) variants and chronic pancreatitis. *American Journal of Physiology Gastrointestinal and Liver Physiology.* **306**, G466-73.
IF: 3.649 (2012)

III. Németh BC, Horváth Á, Szekeres M, Mándi Y, Somogyvári F. (2013) Quantitation with allele specific amplification and realtime PCR. *Acta Biologica Szegediensis* **57**, 47-50.

IV. Németh BC, Wartmann T, Halangk W, Sahin-Tóth M. (2013) Autoactivation of mouse trypsinogens is regulated by chymotrypsin C via cleavage of the autolysis loop. *Journal of Biological Chemistry* **288**, 24049-24062.

IF: 4.651 (2012)

V. Tiszlavicz Z, Németh B, Fülöp F, Vécsei L, Tápai K, Ocsovszky I, Mándi Y. (2011) Different inhibitory effects of kynurenic acid and a novel kynurenic acid analogue on tumour necrosis factor-alpha (TNF-alpha) production by mononuclear cells, HMGB1 production by monocytes and HNP1-3 secretion by neutrophils. *Naunyn-Schmiedebergs Archives of Pharmacology* **383**, 447-455.
IF: 2.647 (2011)

Publications not related to the subject of the thesis:

I. Tiszlavicz Z, Somogyvári F, Szolnoki Z, Sztriha LK, Németh B, Vécsei L, Mándi Y. (2012) Genetic polymorphisms of human beta-defensins in patients with ischemic stroke. *Acta Neurologica Scandinavica* **126**, 109-115.

IF: 2.474 (2012)

II. Tiszlavicz Z, Endrész V, Németh B, Megyeri K, Orosz L, Seprényi G, Mándi Y. (2011) Inducible expression of human β-defensin 2 by Chlamydophila pneumoniae in brain capillary endothelial cells. *Innate Immunity* **17**, 463-469.

IF: 4.000 (2011)

ABBREVIATIONS

cDNA	complementary DNA
CEL	carboxyl esther lipase
CLPS	*procolipase gene*
CN	copy number (of a gene)
CP	chronic pancreatitis
C_t	threshold cycle
CTLA4	cytotoxic T-lymphocyte-associated protein 4 gene
CTRB2	human chymotrypsinogen B2 protein
CTRC	human chymotrypsinogen C protein
Ctrb	mouse chymotrypsinogen B protein
Ctrc	mouse chymotrypsinogen C protein
CXCL1	chemokine (C-X-C motif) ligand 1
DEFA1	human α1-defensin gene
DEFA3	human α3-defensin gene
DEFB1	human β1-defensin gene
DM	diabetes mellitus
DM1	type 1 diabetes mellitus, insulin-dependent diabetes mellitus
DM2	type 2 diabetes mellitus, non-insulin dependent diabetes mellitus
DNA	deoxyribonucleic acid
DTT	dithiothreitol
EDTA	ethylenediaminetetraacetic acid
ELISA	enzyme-linked immunosorbent assay
FAM	6-carboxyfluorescein
GAPDH	glyceraldehyde-3-phosphate dehydrogenase gene
GFR	glomerular filtration rate
HBD1	human β1-defensin protein
HBD2	human β2-defensin protein
HCl	hydrogen chloride
HLA	human leukocyte antigen
HNP	human neutrophil peptide
Hu1	human cationic trypsinogen protein
Hu2	human anionic trypsinogen protein
Hu3	human mesotrypsinogen protein
IFIH1	interferon-induced helicase C domain-containing protein 1
IFNγ	interferon gamma
IL1R1	interleukin receptor type 1
IL1RN	interleukin-1 receptor antagonist

IL-1β	interleukin-1β
IL2RA	interleukin 2 receptor alpha
IL-6	interleukin-6
INS	insulin gene
LDL	low density lipoprotein
LXR	liver X receptor
MMP	matrix metalloproteinase
MODY	maturity onset diabetes of the young, monogenic diabetes
MPO	myeloperoxidase gene
mRNA	messenger ribonucleic acid
MWCO	molecular weight cut off
NaCl	sodium chloride
NCBI	National Center for Biotechnology Information, USA
NF-κB	nuclear factor-κB
OR	odds ratio
PAGE	polyacrylamide gel electrophoresis
PCR	polymerase chain reaction
PMN	polymorphonuclear immune cells
PPARμ2	peroxisome proliferator-activated receptor μ2
PRSS1	human cationic trypsinogen gene
PRSS2	human anionic trypsinogen gene
PRSS3	human mesotrypsinogen gene
PTPN22	protein tyrosine phosphatase, non-receptor type 22
PVDF	polyvinylidene fluoride
qPCR	quantitative (real time) polymerase chain reaction
RNA	ribonucleic acid
RT PCR	reverse transcription polymerase chain reaction
SBDS	Shwachman-Bodian-Diamond Syndorme gene
SDF1	stromal cell-derived factor 1 (or chemokine (C-X-C motif) ligand 12)
SDS	sodium dodecyl sulfate
SNP	single nucleotide polymorphism
SUMO4	small ubiquitin-like modifier 4 gene
TAP	trypsinogen activation peptide
TIMP	tissue inhibitors of metalloproteinases
TLR4	Toll-like receptor 4
TNF-α	tumor necrosis factor alpha
UBR1	Ubiquitin-protein ligase E3 component N-recognin 1 gene
UV	ultraviolet light

TABLE OF CONTENTS

1. INTRODUCTION

Disorders of the pancreas, both endocrine (e.g. diabetes mellitus) and exocrine (e.g. chronic pancreatitis or cystic fibrosis), can be triggered by different genetic factors. There exist specific mutations which can directly lead to the development of certain pancreatic diseases. A little more than a half century ago, mankind knew a significant amount about these disorders clinically, however at that time not much was known about their genetic background.

In 1889, Minkowski and von Mering reported, that dogs developed diabetes after pancreatectomy [112]. This was the first evidence proving the role of the pancreas in pathogenesis of diabetes mellitus. In 1921, the first effective therapy in dogs using pancreatic extracts containing insulin against diabetes mellitus was carried out by Banting and Best [11]. Today we know that genetic factors (including the insulin gene) have significant roles in the development of diabetes mellitus in combination with environmental factors. However, diabetes can also develop due to a mutation in a single gene (monogenic diabetes).

One of the most common genetic diseases among the Caucasian (white) population is cystic fibrosis (OMIM: 219700) with an incidence of 1 in 2500 live births [88]. In 1938, it was first distinguished from coeliac disease by Dorothy H. Andersen [5]. Mutations in the cystic fibrosis transmembrane conductance regulator gene (*CFTR*, OMIM: 602421) -identified in 1989 [52]- are responsible for the development of this disorder. The *CFTR* gene codes for a chloride channel whose malfunction hinders the physiological role of the pancreas and other organs of the digestive, respiratory and reproductive systems. Mutations causing cystic fibrosis can be found under the homepage http://www.cftr2.org/.

In 1896, Hans Chiari has described for the first time the *post mortem* autodigestion of the pancreas and he proposed that this might be mediated by pancreatic enzymes [23]. In 1952, Comfort and Steinberg were the first to describe a familial accumulation of chronic pancreatitis [24], and in 1996, the *PRSS1* gene encoding human cationic trypsinogen was identified as the first gene associated with chronic pancreatitis by Whitcomb et al. [116]. Since then other genes (*CTRC, SPINK1, CPA1* and the above mentioned *CFTR*) have also been shown to have roles in the development of chronic pancreatitis. Under the http://www.pancreasgenetics.org/ homepage a summary of published mutations of genes (except for *CFTR*) associated with chronic pancreatitis can be found.

In the past 2-3 decades, investigators began studying genetic factors which can lead to pancreatic diseases. Despite the fact that large steps have been made in the understanding of

the genetics and pathophisiology of pancreatic diseases, clearly, these investigations have not reached their endpoint yet. In this thesis the results of recent genetic investigations regarding hereditary chronic pancreatitis and diabetes mellitus have been reviewed together with a description of the author's experimental data in order to gain a deeper comprehension of the pathophisiology of pancreatic diseases and their complications.

1.1. GENETIC RISK FACTORS OF DIABETES

Based on the definitions provided by the American Diabetes Association, diabetes is a group of metabolic diseases characterized by hyperglycemia resulting from defects in insulin secretion, insulin action, or both. Type 1 diabetes (~5-10% of all cases of diabetes) is caused by β-cell destruction in the Langerhans islets of the pancreas, usually leading to absolute insulin deficiency. Characteristics of type 2 diabetes (~90-95% of all cases of diabetes) range from predominant insulin resistance with relative insulin deficiency to predominant insulin secretory defect with insulin resistance [3]. The long term complications affect several organs including the eyes, kidneys, nerves and blood vessels, making diabetes a lifelong disease which predisposes to secondary malfunction of almost all organs in the whole body, primarily due to the metabolic changes characteristic of diabetes.

1.1.1. Genetic risk factors of type 1 diabetes mellitus (DM1)

Type 1 diabetes mellitus (DM1, OMIM: 222100) is a genetically heterogeneous autoimmune disease of glucose homeostasis that is characterized by susceptibility to ketoacidosis in the absence of insulin therapy [111]. β-cells of the pancreas suffer autoimmune destruction in which several autoantibodies can have a pathogenic role against islet cells, including insulin, glutamic acid decarboxylase 65, and tyrosine phosphatases IA-2. In this type of diabetes patients are rarely obese [3].

Based on functional, structural and genetic evidence, haplotypes DR3 and DR4 of the human leukocyte antigene (HLA) class II loci are considered strong triggering factors, while DR2 haplotype protects from DM1 [13]. Other genes which are involved in disease pathogenesis are: *INS* (insulin gene on 11q15), *PTPN22* (protein tyrosine phosphatase, non-receptor type 22 on 1p13), *CTLA4* (cytotoxic T-lymphocyte-associated protein 4 on 2q33), *CD25* / *IL2RA* (on 10p15), interferon-induced helicase C domain-containing protein 1 (*IFIH1* gene on 2q24), small ubiquitin-like modifier 4 (*SUMO4* gene on 6q25). However, certain alleles of these genes confer relatively low risk for development of DM1 compared to HLA class II haplotypes of which genetic association studies have shown clear correlation to DM1 [13].

Since DM1 is known to be principally an autoimmune disease, genetic factors which influence the physiology of the immune system, might have a significant role in the pathophysiology. Certain alleles of the TNF-α locus, as a part of an extended haplotype of the HLA DR4 haplotype on chromosome 6, have been found to play a direct role in the pathogenesis of DM1 [82].

Lanng et al. did not find an association between certain IL-1β alleles and the development of diabetes in cystic fibrosis patients [57], however, the IL-1β*2 allele, which correlates with a high secretor phenotype was associated significant susceptibility to nephropathy in DM1 patients [62], as well as to an interleukin-1 receptor antagonist allele (IL1RN*2) [16]. Investigation of the interleukin receptor type 1 gene (IL1R1) led also to the conclusion that certain IL1R1 alleles are associated with DM1 development [14, 71].

Awata et al. suggested that a CA-repeat polymorphism within the first intron of the IFNγ gene may contribute to the pathogenesis of DM1 in patients of Japanese origin and may be a genetic marker for DM1 [9]. Pociot et al. did not find an association between the presence of the same IFNγ allele and DM1 in Danish population, however in the Finnish population they found a modestly significant disease association of the studied IFNγ allelic pattern [83].

1.1.2. Genetic risk factors of type 2 diabetes mellitus (DM2)

Type 2 diabetes mellitus (DM2, OMIM: 125853) accounts for 90–95% of those with diabetes. This type encompasses individuals who have insulin resistance and usually have relative insulin deficiency. Most patients with this form of diabetes are obese. Obesity itself is known to cause some degree of insulin resistance. Although, many different etiological factors can be responsible for the development of DM2, the specific causes are not known. In this type of diabetes, autoimmune destruction of β-cells does not occur. Ketoacidosis is not characteristic of DM2, but occurs rarely. Hyperglycaemia develops gradually and at its earlier stage it is often not severe enough for the patient to notice any of the classic symptoms of diabetes. Insulin deficiency due to β-cell dysfunction impacts skeletal muscle, liver and adipose tissues. Nevertheless, such patients are at increased risk for the development of macrovascular and microvascular complications [3, 8]. DM2 is known to be a multifactorial disease with clear association with different environmental and genetic factors.

Although there are several genes found to be associated with DM2, only genes that have a role in the function of the innate immune system, and are also associated with DM2, are reviewed in this thesis. The innate immune system is the first line of defense against

microbial, fungal and viral infections. Tumor necrosis factor alpha (TNF-α), interleukin-1β (IL-1β) and interleukin-6 (IL-6) are released when toll-like receptor 4 (TLR4) binds certain danger- or pathogen-associated molecules [70]. These molecules can directly increase insulin resistance in fat, muscle and liver cells [15, 46], which can lead to impaired glucose tolerance, the major characteristic of DM2. Different alleles of these cytokine genes may influence the innate immunity pathway resulting in altered response to dietary factors which can also bind to TLR4 [10].

Arora et al. investigated DM2 patients in a cross-sectional study, and found genetic association between several SNPs in IL-6 and triglyceride levels, furthermore between SNPs of IL-6, TNF-α and fasting insulin levels. Other associations were found also between SNPs of TNF-α, and levels of CRP and HDL cholesterol. The strongest association was observed between CRP SNPs and CRP levels; SNPs rs1205 was inversely and rs1417938 was directly associated with CRP levels [8].

Saxena et al. investigated IL-6, TNF-α and IL-10 polymorphisms in DM2 patients and controls of Indian origin. Genotypes IL-6 -597AA and TNF-α -308GG together, or -597AA, TNF-α -308GG and IL-10 -592CA together markedly increased the risk of DM2 if they were present in the same individual. However, the individual presence of the above mentioned genotypes did not lead to an increase in risk [96].

The “Pro” allele of p.P12A (rs1801282) polymorphism of peroxisome proliferator-activated receptor μ2 (PPARμ2) gene is associated with higher glucose and insulin levels in obese patients [48]. However, if the Ala allele of polymorphism p.T92A (rs225014) of type 2 deiodinase is present in the same patient together with the Ala allele of PPARμ2 p.P12A polymorphism, the chance of developing significant insulin resistance is highly elevated [31].

1.1.3. Defensins in diabetes

Defensins are small antimicrobial peptides of the innate immune system, which have 3 major type in vertebrates: α -, β- and θ-defensins. In humans only α- and β-defensins are expressed, while the genes encoding human θ-defensins are pseudogenes [20, 38, 108].

1.1.3.1. α-defensins

The human chromosome locus 8p23.1 harbors 6 different α-defensin genes (*DEFA1, DEFA3*, *DEFA1B, DEFA4, DEFA5, DEFA6*) and 5 α-defensin pseudogenes. There are 6 different types of α-defensins / human neutrophil peptides (HNP) expressed in humans. The protein product of *DEFA1*, *DEFA3*, *DEFA4* genes are HNP-1,-2,-3 and -4 derived from polymorphonuclear immune cells, while intestinal human defensins (HD-5 and HD-6) are

derived from Paneth cells and are the protein products of *DEFA5* and *DEFA6* genes [19, 22, 118].

The cluster of human α-defensin genes include *DEFA1 (OMIM:* 125220) and *DEFA3 (OMIM:* 604522) lying on chromosome 8 with high variability of copy numbers. These genes encode human neutrophil peptide 1, 2 and 3 (HNP1-3) which are almost identical in their mature peptide sequence. The only difference between these mature peptides is the N-terminal amino acid, which is Ala in the case of HNP-1, while at the same position HNP-3 has an Asp residue. Mature HNP-2 peptide lacks this amino acid residue, and this peptide might be a result of a proteolytic cleavage of the other two peptides, because no separate gene has been identified to encode HNP-2 [100]. Differencies in copy number are the major source of genetic polymorphisms in the *DEFA1* and *DEFA3* genes. These are present in a cluster that is close to but independent of the β-defensin cluster on 8p23.1. Total *DEFA1/DEFA3* copy number was found to range between four and 11 copies per diploid genome with five to nine copies being the most common [1].

Today, these peptides are characterized as danger signals (alarmins) playing important roles in inflammation and immunity [77]. In addition to antimicrobial effects, α-defensins have an important role in chemotaxis and they induce proinflammatory cytokines [19, 22, 118]. HNPs increase LDL (low density lipoprotein cholesterol) binding to the endothelial surface suggesting that α-defensins may modulate the development of atherosclerosis [86]. Neutrophil granulocytes are considered to be the primary cellular origin of HNP 1-3; which comprise 30-50 % of the granule proteins. HNPs can be released into the extracellular milieu following granulocyte activation as a consequence of degranulation, leakage, cell death, and lysis during inflammation [37]. In the formation of neutrophil extracellular traps (NETs) α-defensins are also involved [80].

1.1.3.2. β-defensins

Human β-defensins are also antimicrobial peptides, which are thought to control the microbial flora on epithelial surfaces. [38, 81]. According to currently accessible data from the HUGO Gene Nomenclature Committee (http://www.genenames.org/), 38 different genes were identified encoding potentially expressed β-defensins in humans (17 genes on 8p23.1, 1 gene on 11q13.4, 5 genes on 6p12.3, 4 genes on 20q11.1, 4 genes on 20q11.21, 6 genes on 20p13, 1 gene on 4p16.1), while 9 genes are referred to as β-defensin pseudogenes.

There is a wide body of knowledge regarding human β1-defensin, which is constitutively expressed from the *HBD1* gene (OMIM: 602056) on chromosome 8, in close

proximity to *DEFA1/DEFA3* sites. The main sources of human β1-defensin are the epithelial cells throughout in body: skin, small intestine, respiratory and urogenital tissues, pancreas, kidneys, male and female internal genital organs and thymus [121]. Human β1-defensin kills *E.coli* at micromolar concentrations, and other Gram-negative bacteria at concentrations ranging from 60 to 500 μg/μL [98]. The antibacterial and antifungal characteristics of HBD1 is well characterized [114, 119] and their function is thought to be important in protection also against viral infections [41]. In addition to their antimicrobial effects, the chemoattractive function of these defensins have been shown to play a role in immunological reactions that protect the host from various pathogens [30]. While the expression of HBD1 is generally constitutive, the levels of human β2-defensin (HBD2) is inducible by proinflammatory cytokines and bacteria [17, 26, 81].

Several SNPs have been characterized in the *HBD1* gene. Three frequent SNPs at positions c.-20G>A (rs11362), c.-44C>G (rs 1800972) and c.-52G>A (rs1799946) in the 5'-untranslated region (5' UTR) of *DEFB1* were described earlier [28]. The untranslated variants influence HBD-1 expression or function [103].

1.1.3.3. Role of defensins in diabetes mellitus

Although it has been shown that some polymorphisms in certain cytokine genes are associated either with DM1 or DM2, little is known about the genetics and the functions of α- and β-defensins in diabetes. Infections are frequent in diabetic patients, because the antimicrobial function of their immune response is impaired. It has been reported that mRNA levels of rat β1-defensin are decreased in the kidneys, which may explain the high incidence of urinary tract infections in diabetes mellitus [35]. Recently, the effect of glucose and insulin on β-defensin expression have been described [12]. However, no connection was found between genetic polymorphisms of the *HBD1* gene and diabetes in a Brasilian study investigating diabetic children [42].

Increased levels of human neutrophil peptide 1, 2 and 3 in type 1 diabetic patients with nephropathy and with cardiovascular complications has recently been reported [50, 95]. It is tempting to speculate that copy number polymorphisms and alterations of *DEFA1/DEFA3* mRNA levels in granulocytes may influence the levels of HNP1-3 in patients with diabetes type 1 and type 2.

1.1.4. Connections between endocrine and exocrine pancreatic diseases at the genomic level

Diabetes is a multifactorial disease, with both environmental and genetic factors playing a role in its development. Mutations in only a single gene, can also lead to the development of diabetes. Monogenic diabetes, also termed maturity onset diabetes of the young (MODY), develops before the age of 25, and presents as a nonketotic form of diabetes. Its inheritance follows an autosomal dominant pattern, and mutations associated with MODY cause a primary defect in the function of the beta cells of the endocrine pancreas [33]. Exocrine pancreas function is not affected in the majority of the 11 different types of MODY [34]. However, in MODY8 (CEL MODY), in which there is a defect in the carboxyl ester lipase (*CEL*, OMIM: 114840) gene, insufficiency of both endocrine and exocrine pancreatic function is observed [87].

Another example when a single malfunctioning gene may lead to both endocrine and exocrine insufficiency of the pancreas is the procolipase gene (*CLPS*, OMIM: 120105). The products of *CLPS* gene are the precursors of colipase and enterostatin. They are secreted mainly by the exocrine pancreas, but are also expressed in stomach, liver and regions of the central nervous system. The mature form of colipase is the essential cofactor of lipase, which has a significant role in the digestion of triglycerides emulsified by bile salts. Enterostatin acts as a pentapeptide hormone, which selectively down-regulates fat intake, and hampers insulin secretion in animal models. Certain SNPs of the *CLPS* gene (rs3748050 and rs378051) are associated in altered insulin secretion in non-diabetic Caucasians [115]. Furthermore, *CLPS* gene mutant p.R109C (also called p.R92C according to procolipase numbering) was found to be associated with DM2 [60]. In a functional study, the same mutant was found to be defective in its ability to anchor triglycerides to pancreatic lipase [29].

The simultaneous appearance of diabetes mellitus and exocrine pancreas insufficiency is surprisingly common. In most cases they do not develop together due to a single genetic disorder as described above in the case of *CEL* MODY, but as a result of disorders which can diffusely damage the pancreatic tissue (pancreatitis, trauma, pancreatectomy, neoplasia, cystic fibrosis, hemochromatosis, fibrocalculous pancreatopathy or surgical pancreas resection), which is classified as type 3c diabetes mellitus [3]. According to the publication by Ewald et al. [32], diabetes type 3c is often misclassified as type 2. Upon reclassification, the authors found that out of 1868 patients, 172 had type 3c diabetes mellitus (9.2%), of which 78.5% had chronic pancreatitis. In a publication by Hardt et al. [43] a high prevalence

of patients with type 1 and type 2 diabetes were found to have pathological exocrine function of the pancreas, which was correlated with an early onset of endocrine failure, long-lasting diabetes mellitus and low body mass index levels.

Though endocrine and exocrine malfunction of the pancreas usually have different genetic risk factors, they might have a common genetic origin due to certain mutations in *CLPS* and *CEL* genes mentioned above. Living with chronic pancreatitis leads to the development of endocrine pancreas disfunction over time. Therefore, investigation of the mechanisms leading to chronic pancreatitis may not only result in a deeper understanding of the function of the exocrine pancreas and related diseases, but may also elucidate the mechanism of disease pathogenesis in certain types of diabetes.

1.2. CHRONIC PANCREATITIS

Chronic pancreatitis (CP) is defined as a relapsing or continuing inflammatory disease of the pancreas and is characterized by irreversible morphological changes, upper abdominal pain and, in some patients, permanent impairment of exocrine or endocrine function or both. The incidence of CP is 3.5-23 cases / 100.000 persons [4, 69, 88]. Excessive alcohol consumption is the most frequently identified etiological factor of chronic pancreatitis. In addition, smoking can accelerate the progression of the disease [65], and increase the risk of developing pancreatic adenocarcinoma. The incidence of pancreatic cancer among chronic pancreatic patients ranges between 3% and 13% [63, 69, 74], however, the incidence is close to 70% in patients with hereditary CP [69].

1.2.1. Hereditary chronic pancreatitis

The first description of familial accumulation of chronic pancreatitis cases was provided in 1952 by Comfort and Steinberg [24]. However, it took 44 years before the first gene associated with hereditary pancreatitis was identified by Whitcomb et al. in 1996 [116]. The first reports about Hungarian cases of hereditary pancreatitis were published by Ruszinkó et al. and Oláh et al. in 2001 [76, 90], and these cases were also mentioned in a 2004 study by Howes et al. [47]. The first case report describing a Hungarian family affected by hereditary pancreatitis was published in 2012 by Major et al. [66].

The definitions of familial and hereditary pancreatitis need to be distinguished. Clinically, both are recurrent acute or chronic pancreatitis. If two first-degree relatives or three or more third-degree relatives in two or more generations are affected and have no other precipitating factors, the diagnosis of hereditary pancreatitis is established. The diagnosis of

familial pancreatitis is made if more than one affected family member was diagnosed with CP in the same generation [47].

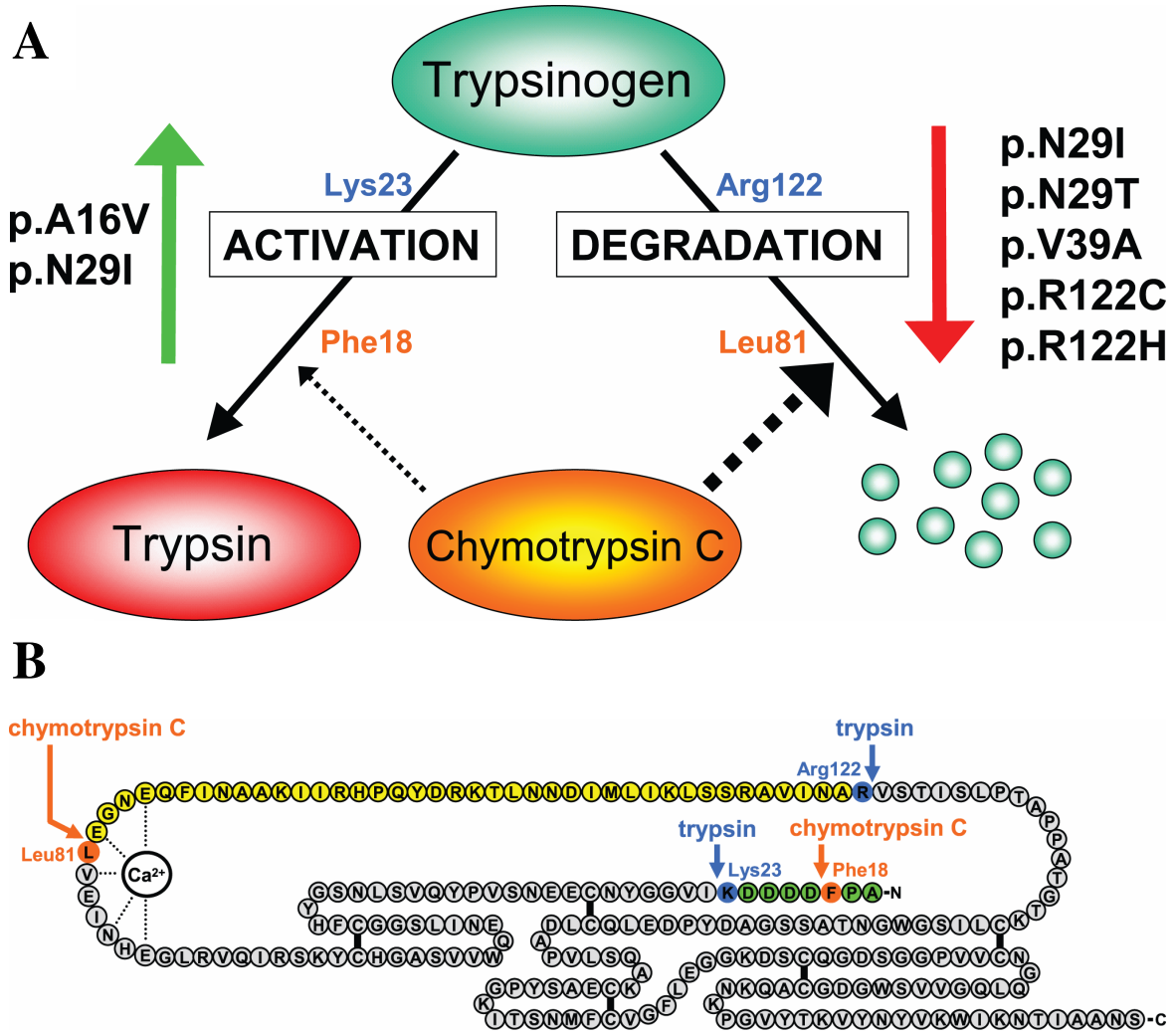

Figure 1. Effect of pancreatitis-associated *PRSS1* mutations on the chymotrypsin C (CTRC) dependent activation and degradation of human cationic trypsinogen. CTRC cleaves the Leu81-Glu82 peptide bond and trypsin cleaves the Arg122-Val123 peptide bond; these two cleavages result in the eventual degradation of trypsinogen. CTRC also stimulates autoactivation of cationic trypsinogen by cleaving the Phe18-Asp19 peptide bond in the activation peptide. The shortened activation peptide is more susceptible to trypsin-mediated activation at the Lys23-Ile24 peptide bond. The dominant effect of CTRC is degradation. **(A)** ***PRSS1* mutations** can increase conversion of trypsinogen to trypsin by inhibition of CTRC-dependent trypsinogen degradation (red arrow) or by increasing CTRC-dependent stimulation of autoactivation (green arrow). **(B) Proteolytic cleavage of human cationic trypsinogen by CTRC and trypsin.** Primary structure of trypsinogen with disulfide bonds is shown. CTRC cleavage sites are highlighted in orange and trypsin cleavage sites are shown in blue. The activation peptide is in green. Note the yellow peptide segment not stabilized by disulfide bonds between the Leu81 and Arg122 cleavage sites. Figure 1B is modified from Szmola and Sahin-Tóth (2007) [107].

Hereditary chronic pancreatitis is a human genetic disorder caused by heterozygous mutations in the serine protease 1 gene (*PRSS1,* OMIM: 276000) on chromosome 7q35 encoding human cationic trypsinogen [116], the precursor for the most abundant digestive enzyme secreted by the human pancreas [97]. Besides *PRSS1*, the locus also contains five

trypsinogen pseudogenes, a relic gene, and *PRSS2*, which encodes anionic trypsinogen, the other major human trypsinogen isoform. The *PRSS3* gene coding for mesotrypsinogen, the relatively minor third human isoform, is found on chromosome 9p13.

Mutations in the *PRSS1* gene associated with hereditary chronic pancreatitis result in early activation of trypsinogen inside the pancreas due to altered regulation by chymotrypsin C (CTRC) [106]. High penetrance trypsinogen mutations such as p.N29I and p.R122H are associated with an autosomal dominant inheritance pattern, whereas mutations with lower penetrance (e.g. mutation p.A16V), may be found not only in hereditary but also in sporadic cases without family history [109].

Figure 1 shows the functional effects of the most frequent human cationic trypsinogen mutations. Shortening of the activation peptide by CTRC-mediated cleavage of Phe18-Asp19 peptide bond results in increased autoactivation [72]. This cleavage is stimulated by pancreatitis-associated mutations p.N29I and p.A16V [106, 72]. Cleavage of the Leu81-Glu82 peptide bond in the calcium binding loop, together with the trypsin-mediated autolytic cleavage of the Arg122-Val123 peptide bond, results in rapid degradation and inactivation of cationic trypsinogen [107]. Mutations p.N29I and p.R122H inhibit CTRC-mediated degradation and thereby increase trypsinogen autoactivation [106].

1.2.2. Syndromes associated with chronic pancreatitis

Goobie et al. mapped the susceptibility gene of Shwachman-Diamond syndrome (OMIM: 260400) to chromosome 7 [40]. This disease follows an autosomal recessive inheritance pattern and is characterized mainly by exocrine pancreatic insufficiency (lipomatosis of pancreas), hematologic (neutropenia, anemia, thrombocytopenia) and skeletal abnormalities (delayed maturation, metaphyseal chondordysplasia of the long bones and thoracic-cage abnormalities with costochondrial thickening). The susceptibility gene is the Shwachman-Bodian-Diamond Syndrome gene (*SBDS*, OMIM: 607444) mapped to 7q11.21 [18].

In 1971, Johanson and Blizzard described a congenital syndrome characterized by aplasia of the alae nasi, deafness, hypothyroidism, dwarfism, absent permanent teeth and malabsorption [49]. The most consistently affected organ in this syndrome is the pancreas, and the intrauterin onset of pancreatitis is characterized by gradual destruction of previously formed acinar cells with unaffected primary zymogen synthesis and no sign of apoptosis at the cellular level. The susceptibility gene of Johanson-Blizzard syndrome (OMIM: 243800)

with multiple pathogenic alleles is the ubiquitin-protein ligase E3 component N-recognin 1 gene (*UBR1*, OMIM: 605981) at position 15q15.2, containing 47 exons [120].

1.3. MOUSE TRYPSINOGENS

Considering the widespread use of mice in experimental studies of the pancreas, it is surprising how little is known about mouse trypsinogens. In 1982, Watanabe reported the purification of three trypsinogen isoforms from the mouse pancreas [113]. In 1986, Stevenson et al. cloned a trypsinogen cDNA, corresponding to isoform T20, from the pancreas and demonstrated that the mouse genome contained multiple different trypsinogen genes [102]. This was later confirmed by Leroy Hood's laboratory in 1997 when they sequenced the mouse T cell receptor beta locus on chromosome 6 and identified 20 trypsinogen genes organized into two groups, one comprising genes T1-T7 and the other containing genes T8-T20 [39].

Using the currently accessible NCBI (National Center for Biotechnology Information, USA) online genomic database (http://www.pubmed.org/) we found that eleven of the 20 genes are potentially functional (T4, T5, T7, T8, T9, T10, T11, T12, T15, T16, T20; as shown in Suppl. Figure 1), while the other nine genes are either pesudogenes (T1, T2, T3, T14) or relic genes (T6, T13, T17, T18, T19). In 1999, Ohmura et al. cloned the cDNA for isoform T9 from sperm acrosome [75]. It remained unknown, however, which isoforms of the 11 potentially functional trypsinogen genes are expressed at the protein level in the mouse pancreas. More recently, genetic deletion of T7 indicated that this isoform may contribute to as much as 60% of pancreatic trypsinogens [25, 91]. The authors also found that despite the presence of other trypsinogen isoforms, mice deficient in T7 did not respond to secretagogue hyperstimulation with the characteristic intra-acinar cell trypsinogen activation, which is an early event in acute pancreatitis.

These findings suggest that the different mouse trypsinogen isoforms vary in their activation kinetics and highlight the need for their comparative biochemical characterization. Therefore, identification of major trypsinogen isoforms in the mouse pancreas, and a study of their autoactivation and regulation by mouse chymotrypsins is needed.

3. AIMS

Like other members of the innate immune system, defensins can also have a role in the development of type 1 and type 2 diabetes mellitus and their macro- and microvascular complications. In order to gain deeper comprehension about the role of defensins in diabetes, the aims of this study were:

- to measure plasma levels of human neutrophil peptides 1-3 (HNP 1-3) and to examine their possible association with diabetes and / or its complications,
- to determine gene copy number polymorphism and mRNA expression levels of *DEFA1/DEFA3* genes in diabetes mellitus,
- to investigate the association of single nucleotide polymorphisms c.-20G>A, c.-44C>G and c.-52G>A in the promoter region of the β1-defensin (*DEFB1)* gene with type 1 and type 2 diabetes mellitus.

Research into the pathomechanism of hereditary chronic pancreatitis has been hindered by the lack of good animal models which mimic the human disease and develop spontaneous pancreatitis. In order to create a mouse model, biochemical characterisation of mouse trypsinogens was necessary. The aims of the study of mouse trypsinogens were:

- to identify the major trypsinogen isoforms expressed in the mouse pancreas,
- to characterize the autoactivation of mouse trypsinogens and study their interaction with mouse chymotrypsins,
- to investigate the biochemical characteristics of the most frequent pathogenic human cationic trypsinogen mutation p.R122H introduced into mouse trypsinogen isoforms T7 and T8.

2. PATIENTS AND METHODS

2.1. NOMENCLATURE

Nucleotide residues are numbered starting with nucleotide A of the ATG-translation initiation codon. Amino acid residues are numbered starting with the initiator methionine of the primary translation product. Note that because of an extra Asp residue (Asp23) in the activation peptide of T7 mouse trypsinogen isoform, amino-acid numbering in this isoform is shifted by one relative to human and other mouse trypsinogens. Autolysis loop refers to the flexible region between residues 146 and 154 in trypsinogen (Suppl. Figure 1).

2.2. PATIENTS AND CONTROLS IN GENETIC ASSOCIATION STUDY

All cases and controls were of Hungarian ethnic origin and were residents of Hungary. Informed consent was obtained from all subjects, and the local Ethics Committee of University of Szeged gave prior approval to the study. All subjects consented to the study and were treated according to the Patient Right Protection Act of our institutions and international guidelines.

2.2.1. Control group

The 221 age- and gender matched members of the control group were selected from healthy blood donors from the regional Centre of Hungarian National Blood Transfusion Service, Szeged, Hungary. Blood donors with diabetes mellitus, nephropathy, hypertension or ischemic heart disease were excluded from this study.

2.2.2. Patients with diabetes mellitus

257 diabetic patients (122 men, 135 women) were enrolled in the study; which included 117 patients with type 1 and 140 patients with type 2 diabetes. Diagnosis of diabetes of all patients was based on the ADA criteria [2].

71 of the cohort had diabetic nephropathy (32 with type 1 diabetes and 39 with type 2 diabetes), defined as an albumin-to-creatinine ratio in a random spot collection higher than 3.4 mg/mM or protein content over 300 mg/day in collected urine. Abnormal kidney function was detected if glomerular filtration rate (GFR) was lower than 60 mL/min/1.73 m^2.

115 patients suffered from retinopathy (47 with type 1 diabetes and 68 with type 2 diabetes). This complication was evidenced as the presence of background or proliferative retinopathy, macular edema or diabetes-related blindness or the use of retinal photocoagulation therapy. The retinopathy status was checked by color stereo-ophtalmography and fluorescence angiography. Neuropathy was diagnosed in 95 patients (35

with type 1 and 60 with type 2 diabetes). Neuropathy was proven if abnormal peripheral sensory functions or altered lower limb tendon reflexes as well as impaired cardiovascular reflex tests were detected. 54 diabetic patients (14 with type 1 diabetes, 40 with type 2 diabetes) had previously been diagnosed with macrovascular disease including major coronary events, stroke or transient ischemic attack, peripheral artery disease or amputation. High number of patients (182) had treated hypertension. (50 with type 1 diabetes and 132 with type 2 diabetes).

2.3. METHODS USED IN GENETIC ASSOCIATION STUDY

2.3.1. DNA isolation

Genomic DNA purification was carried out from 300 µl buffy coat of the anticoagulated (EDTA), centrifuged (1200 rpm/min for 15 min), peripheral blood using the High Pure PCR Template Preparation Kit (Roche Diagnostic GmbH, Mannheim, Germany). DNA concentrations were measured with a Qubit™ fluorometer (Invitrogen, Carlsbad, CA, USA) according to the manufacturer's instructions. Genomic DNA was stored at –20ºC.

2.3.2. Determination of *DEFA1/DEFA3* gene copy number by quantitative real-time PCR

Genomic DNA was purified from peripheral blood. Gene copy number determination was carried out as previously described by Linzmeier et al. [61] with minor modifications. For quantitation BIO-RAD CFX 96 instrument (Bio-Rad, Hercules, CA, USA) was used. The reaction volume was 15 µL, containing 3 µL of DNA, 1 µM of each primers, 7,5 µL of reaction buffer (Fermentas Probe/ROX qPCR MasterMix, Fermentas, Lithuania) and 0,6 µL EVAGreen (20x EVAGreen™ Biotium Inc., Hayward, CA, USA). In order to amplify the *DEFA1/DEFA3* target genes we used the forward primer "DEFA1 1 F" (5’ TAC CCA CTG CTA ACT CCA TAC 3’), and the reverse primer "DEFA1 1 R" (5’ GAA TGC CCA GAG TCT TCC C 3’). To amplify the reference gene *MPO* (myeloperoxidase) we used the forward primer "MPO 1 F" (5’ CCA GCC CAG AAT ATC CTT GG 3’), and the reverse primer "MPO 1 R" (5’ GGT GAT GCC TGT GTT GTC G 3’). The real time PCR conditions were as follows: initial denaturation at 95 ^{o}C for 10 min followed by 40 cycles of denaturation (95 ^{o}C for 15 s) and extension (54 ^{o}C for 1 min).

Quantification was performed by monitoring the emitted fluorescence after each cycle of PCR reaction of genomic DNA samples in order to identify the exact time point at which

the logarithmic linear phase could be distinguished from the background (crossing point). Each DNA sample was analyzed in triplicate, in two independent experiments.

Using the formula "A" we calculated the ΔC_t value which was characteristic for each DNA sample. The copy number of the reference gene *MPO* was known to be 2 per diploid genome [61]. The total copy number (CN) of target genes *DEFA1* and *DEFA3* per diploid genome was calculated using the formula "B".

A: $\Delta C_t = C_{t\ reference} - C_{t\ target}$

B: $CN_{target} = 2^{\Delta Ct} \times (CN_{reference})$

2.3.3. RNA extraction and reverse transcription

For RNA extraction 300 µL buffy coat was prepared from the same peripheral blood samples which were used for genomic DNA extraction. Total RNA was extracted with High Pure RNA isolation kit (Roche) according the manufacturer's instruction. RNA concentration was determined by the A_{260} value of the sample. Complementary DNA (cDNA) was generated from 1 µg total RNA using the High-Capacity cDNA Reverse Transcription Kit (Applied Biosystems) in a final volume of 20 µL.

2.3.4. *DEFA1/DEFA3* mRNA expression measurement using quantitative RT PCR

Using the reverse transcription polymerase chain reaction (RT PCR), we examined the relative expression levels of *DEFA1/DEFA3* mRNA in 20 patients with diabetes (10 cases of type 1, and 10 cases of type 2 diabetes). RNA samples were prepared from buffy coat and quantification were performed according to our previously used method [110]. After reverse transcription, quantitative PCR amplification was carried out using Light Cycler Fast Start DNA Master^{PLUS} SYBR Green I mix (Roche). Samples were loaded into capillary tubes and placed in the fluorescence thermocycler (LightCycler). Initial denaturation at 95 °C for 10 min was followed by 45 cycles of 95 °C for 10 s, annealing at 58 °C for 8 s, and elongation at 72 °C for 12 s. To amplify specific products from cDNA of *DEFA1/DEFA3*, the following primers were used: sense 5'-TCC CAG AAG TGG TTG TTT CC-3'; and antisense, 5'-GCA GAA TGC CCA GAG TCT TC-3'. To measure expression of *GAPDH,* the housekeeping gene, sense primer 5′-AAG GTC GGA GTC AAC GGA TTT-3′; and antisense primer 5′-TGG AAG ATG GTG ATG GGA TTT-3′ were used. At the end of each run, melting-curve profiles were achieved by cooling the sample to 40 °C for 15 s and then heating the sample slowly at 0.20 °C/s up to 95 °C with continuous measurement of the fluorescence to confirm the amplification of specific transcripts. Cycle-to-cycle fluorescence emission readings were monitored and analyzed by the LightCycler software (Roche Diagnostics GmbH). Expression

data were normalized to the housekeeping *GAPDH* gene. Relative gene expression was determined using the $\Delta\Delta C_t$ method.

2.3.5. Genotyping of SNPs of human β1-defensin (*DEFB1*)

Genotyping was performed using Custom TaqMan® SNP Genotyping Assays (Applied Biosystems, CA). Fluorogenic minor groove binder probes with the dyes 6-carboxyfluorescein FAM™ (excitation, 494 nm) and VIC® (excitation, 538 nm) were used in each cases in order to determine the genotypes of different SNPs: β1-defensin (*DEFB1*) polymorphisms c.-20G>A (rs11362, Applied Biosystems code c_11636793_20), c.-44C>G (rs1800972, c_11636794_10) and c.-52G>A (rs1799946, c_11636795_20). Thermal cycling was performed on ABI Prism 7000 sequence-detection PCR systems. The amplification mix contained the following ingredients: 7.5 μL of TaqMan® universal PCR master mix (Applied Biosystems, CA), 0.375 μL of primer-probe mix, 6.375 μL of RNase- and DNase-free water (Sigma), and 0.8 μL of sample DNA, in a total volume of 15 μL per single tube reaction. Assay conditions were 2 min at 50 °C, 10 min at 95 °C, and 40 cycles of 95 °C for 15 s and 60 °C for 1 min. Each 96-well plate contained 90 samples of an unknown genotype and six reactions with reagents but no DNA. DNase-free water used as nontemplate control. Initial and post-assay analysis was performed using the Sequence Detection System version 2.1 software (Applied Biosystems, CA) as outlined in the TaqMan Allelic Discrimination Guide. Genotypes were determined visually based on the dye-component fluorescent emission data depicted in the X-Y scatter plot of the Sequence Detection System software. Genotypes were also determined automatically by the signal processing algorithms in the software. Results of each scoring method were saved in two separate output files for later comparison.

2.3.6. Assay of HNP 1-3 concentration

The same peripheral blood samples we used for genomic DNA and RNA extraction from patients and controls were also used for isolation of plasma, which was stored at -80^{o}C until further analysis. Plasma HNP1-3 concentrations were determined by ELISA (Hycult-Biotech HK324, Uden, The Netherlands) according to the instructions of the manufacturer.

2.3.7. Statistical analysis

Comparisons of plasma concentrations were carried out by Mann-Whitney test and with two-tailed paired Student's test. The level of significance of the genotype frequency of different *DEFB1* SNPs was analysed by using the χ^2 test and Fischer test. Levels $p<0.05$ indicated statistical significance. All statistical calculations were performed with the Graph Pad Prism 5.0 statistical program (GraphPad Software,San Diego, CA USA). The genotype

frequencies for each polymorphism of *DEFB1* were tested for deviation from the Hardy-Weinberg equilibrium by the χ^2 test, with 1 degree of freedom.

2.4. EXPERIMENTAL PROCEDURES USED IN MOUSE TRYPSINOGEN EXPERIMENTS

2.4.1. Plasmid construction and mutagenesis

Construction of the pTrapT7-intein-Hu1 and pcDNA3.1(-)-CTRB2 expression plasmids harboring the coding sequence for human cationic trypsinogen (Hu1) and human chymotrypsinogen B2 (CTRB2) was reported previously [54, 107]. Mutation p.S150F was introduced into human cationic trypsinogen using overlap-extension PCR mutagenesis. Expression plasmids for mouse trypsinogens were created in the pTrapT7 plasmid previously designed for bacterial expression of human trypsinogens [93, 94]. The coding DNA was PCR amplified from commercial I.M.A.G.E. clones and cloned into pTrapT7 using NcoI and SalI restriction sites. In all constructs the N-terminal secretory signal peptide was replaced with a Met-Ala sequence. In T20, the stop codon was changed from amber (TAG) to ochre (TAA). T7 was amplified from I.M.A.G.E. clone #30306963 (GenBank accession BC061093.1) using T7 NcoI sense (5'- AAA TTT CCA TGG CTC TCC CCC TGG ATG ATG ATG ATG -3', where the NcoI site is underlined) and T7 SalI antisense (5'- AAA TTT GTC GAC TTA GTT GGC AGC GAT GGT CTG CTG -3', where the SalI site is underlined) primers. T8 was amplified from I.M.A.G.E. clone #30306436 (GenBank accession BC061135.1) using T8 NcoI sense (5'- AAA TTT CCA TGG CTT TCC CTG TGG ATG ATG ATG ACA -3', where the NcoI site is underlined) and T8 SalI antisense (5'- AAA TTT GTC GAC TTA GTT TGC AGC AAT GGT GTT TTG -3,' where the SalI site is underlined) primers. T9 was amplified from I.M.A.G.E. clone #6433372 (GenBank accession CF581321.1) using T8 NcoI sense and T9 SalI antisense (5'- AAA TTT GTC GAC TTA GTT TGC GGC AAT GGT GTC CTG -3', where the SalI site is underlined) primers. T20 was amplified from I.M.A.G.E. clone #6433384 (GenBank accession CF581305.1) using T20 NcoI sense (5'- AAA TTT CCA TGG CTT TCC CTG TGG ATG ATG ATG ACA -3', where the NcoI site is underlined) and T20 SalI antisense (5'- AAA TTT GTC GAC TTA GTT GTC AGC AAT TGT GTT CTG -3', where the SalI site is underlined) primers. Mutations p.L82A, p.R123H, and p.L149A in T7 and p.R122H and p.F150S in T8 were created by overlap extension PCR and cloned into the pTrapT7 plasmid.

Expression plasmids for mouse chymotrypsinogens carrying a 10His affinity tag were created in the pcDNA3.1(-) plasmid. The coding DNA for mouse chymotrypsinogen C (Ctrc)

was PCR amplified from a cDNA preparation from CD-1 mouse pancreas, using mCTRC XhoI sense (5'-AAA TTT CTC GAG ACC TGA ACC ATG TTG GGA ATT ACA GTC-3', where the XhoI site is underlined) and mCTRC EcoRI antisense (5'-AAA TTT GAA TTC GGC GTC GAG ACT TCT GGA ACC GTC TCT-3', where the EcoRI site is underlined) primers and cloned into pcDNA3.1(-) using XhoI and EcoRI. A 10His affinity tag was added to the C terminus using gene synthesis (GenScript, Piscataway, NJ) and the XcmI and EcoRI sites. In this synthetic construct Leu268 was deleted to prevent autolytic cleavage of the His-tag. The coding DNA for mouse chymotrypsinogen B (Ctrb, GenBank accession NM_025583.2) with a C-terminal 10His tag was custom synthesized (GenScript) and cloned into pcDNA3.1(-) using XhoI and BamHI.

2.4.2. Purification and identification of trypsinogens from CD-1 mouse pancreas

Pancreata (2-3) were homogenized in 10 mL of 20 mM Na-HEPES (pH 7.4) buffer, briefly sonicated, centrifuged at 13,500 rpm for 10 min and ~4 mL supernatant was loaded onto a 2 mL ecotin column. Ecotin is a pan-serine protease inhibitor from *E. coli* which can bind the inactive zymogen forms of pancreatic serine proteases [58, 79].

The ecotin column was washed with 20 mM Tris-HCl (pH 8.0), 0.2 M NaCl and trypsinogens were eluted with 50 mM HCl. The flow-through contained no trypsinogen, as judged by the lack of trypsin activity after incubation with enteropeptidase. The ecotin-eluate contained all trypsinogen isoforms and low levels of chymotrypsinogen and proelastase. Four

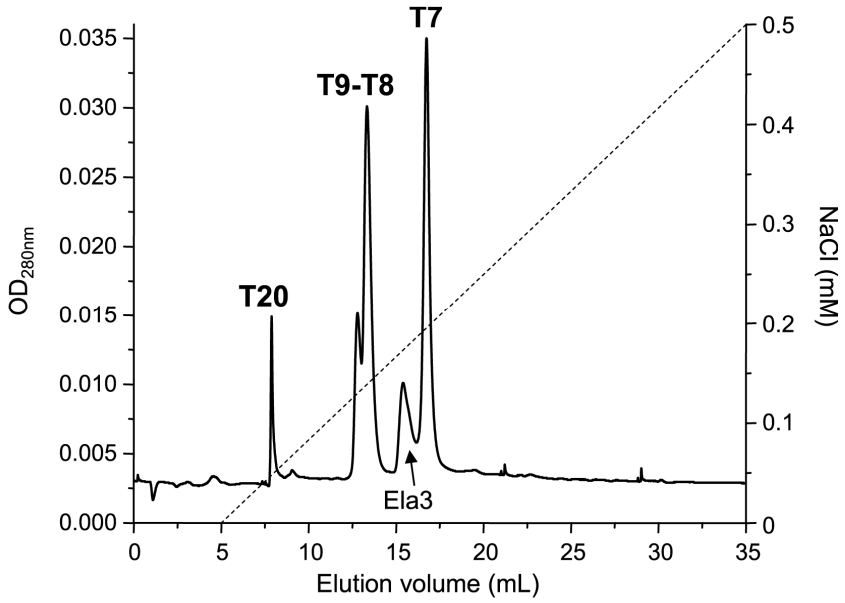

Figure 2. Identification of major trypsinogen isoforms expressed by the mouse pancreas. Chromatographic separation of trypsinogen isoforms. Trypsinogens were purified from pancreas tissue extracts of CD-1 mice using ecotin affinity chromatography and the ecotin eluate was loaded onto a MonoS column equilibrated with 20 mM Na-acetate (pH 5.0). The column was developed with a linear gradient of 0-0.5 M NaCl. Peaks were analyzed by SDS-PAGE, N-terminal sequencing and mass spectrometry.

mL eluate was loaded onto a 2 mL MonoS column equilibrated with 20 mM Na-acetate (pH 5.0) and trypsinogens were eluted with a 0-0.5 M NaCl gradient at 1 mL/min flow rate (Figure 2). The eluted proteins were separated by SDS-PAGE, transferred to PVDF membrane and individual bands were subjected to N-terminal protein sequencing by Edman degradation (Midwest Analytical, St. Louis, MO). Peaks corresponding to T8, T9 and T20 were also subjected to in-gel digestion followed by LC-MS/MS mass spectrometry (ProtTech, Phoenixville, PA). Relative abundance of trypsinogen isoforms were calculated from the peak areas corrected for the ultraviolet extinction coefficient differences. The T9-T8 peaks were also corrected for Ctrb contamination, which was determined from the relative trypsin and chymotrypsin activities after activation with enteropeptidase. Because of the poor separation of T8 and T9, these two isoforms were calculated as one.

2.4.3. Expression and purification of trypsinogens

Human cationic trypsinogen was expressed in the aminopeptidase P deficient LG-3 *E. coli* strain as fusions with a self-splicing mini-intein, as decribed in [53, 54]. Mouse trypsinogens were expressed in *E. coli* BL21(DE3), as described for human trypsinogens previously [93, 94]. Isolation of cytoplasmic inclusion bodies, *in vitro* refolding and purification with ecotin affinity chromatography were performed according to published protocols [53, 54, 58, 93, 94]. The preparations were more than 90% pure, as judged by SDS-PAGE and Coomassie Blue staining. Concentrations of trypsinogen solutions were calculated from their UV absorbance at 280 nm using the following extinction coefficients: 37,525 $M^{-1}cm^{-1}$ (human cationic trypsinogen), 39,140 $M^{-1}cm^{-1}$ (mouse T7), 34,670 $M^{-1}cm^{-1}$ (mouse T8 and T9) and 43,150 $M^{-1}cm^{-1}$ (mouse T20).

2.4.4. Expression and purification of chymotrypsinogens

Human CTRB2, mouse Ctrb and Ctrc carrying 10His affinity tags were expressed in transiently transfected HEK 293T cells using Lipofectamine® 2000 (Life Technologies) and purified from 450 mL conditioned medium using nickel-affinity chromatography as reported previously [105, 106]. Aliquots (75 µL) of the eluted 5 mL fractions were analyzed by 15% SDS-PAGE and Coomassie Blue staining and peak fractions with >90% purity were pooled and dialyzed for 72 hours against three changes of 1 liter of 0.1 M Tris-HCl (pH 8.0) buffer containing 150 mM NaCl. The dialyzed chymotrypsinogen solutions were concentrated using a Vivaspin 20 concentrator (10 kDa MWCO). Chymotrypsinogens were activated with trypsin and active chymotrypsin concentrations were determined by active site titration with ecotin, as described [104].

2.4.5. Trypsinogen autoactivation

Trypsinogen at 2 µM concentration was incubated in the absence or presence of 25 nM chymotrypsin, as indicated. Autoactivation was induced by 10 nM trypsin in 0.1 M Tris-HCl (pH 8.0), 1 or 10 mM $CaCl_2$ and 0.05% Tween 20 (final concentrations) at 37 ºC. At given times, 1.5 µL aliquots were withdrawn and mixed with 48.5 µL assay buffer containing 0.1 M Tris-HCl (pH 8.0), 1 mM $CaCl_2$, and 0.05% Tween 20. Trypsin activity was measured by adding 150 µL 200 µM N-CBZ-Gly-Pro-Arg-p-nitroanilide substrate dissolved in assay buffer and following the release of the yellow p-nitroaniline at 405 nm in a SpectraMax plus384 microplate reader (Molecular Devices, Sunnyvale, CA) for 1 min. Reaction rates were calculated from fits to the initial linear portions of the curves.

2.4.6. Trypsinogen activation with enteropeptidase

Complete activation of 2 µM trypsinogen (100 mM Tris-HCl (pH 8.0), 10 mM $CaCl_2$ and 0.05% Tween 20 as final concentrations) was carried out using 140 ng/mL final concentration of human enteropeptidase (R&D Systems, Minneapolis MN) on 37 ºC for 1 hour. Maximal trypsin activity was measured as described above. This activity was designated as 100% and trypsin activity measured in autoactivation experiments was expressed relative to this value. The 100% values corresponded to 500 (T7), 400 (T8), 400 (T9) and 300 (T20) mOD / min readings.

2.4.7. SDS polyacrylamide gel electrophoresis

Seventy-five µL of 2 µM trypsinogen samples were precipitated with 10 % trichloroacetic acid (final concentration). After centrifugation at 13.000 rpm for 10 minutes, the supernatant was discarded and the precipitate was dissolved in 15 µL Laemmli sample buffer (20% glycerol, 120 mM Tris, pH=6.8, 2% SDS, 0.003% bromphenol blue) containing 100 mM DTT (final concentration). The precipitate was heat-denatured at 95 °C for 5 min. 15% SDS-PAGE mini gels (running gel: 15% acrilamide, 375 mM Tris, 0.1% SDS, pH=8.8 and stacking gel: 5% acrilamide, 125 mM Tris, 0.1% SDS, pH=6.8) were used for electrophoretic separation in standard Tris-glycine buffer (24.76 mM Tris, 19.18 mM glycine and 0.1 % SDS). Gels were stained with Coomassie blue (containing 3 grams of Brilliant Blue R-250 dissolved in 50% methanol and 10% acetic acid). The Coomassie stained gels were destained in a solution containing 60% methanol and 10% acetic acid as described earlier [56]. Quantitation of bands was carried out with the GelDoc XR+ gel documentation system and Image Lab 3.0 software (Bio-Rad, Hercules, CA).

3. RESULTS

3.1. α-DEFENSINS IN DIABETES

3.1.1. Plasma levels of HNP1-3 in patients with type 1 and type 2 diabetes

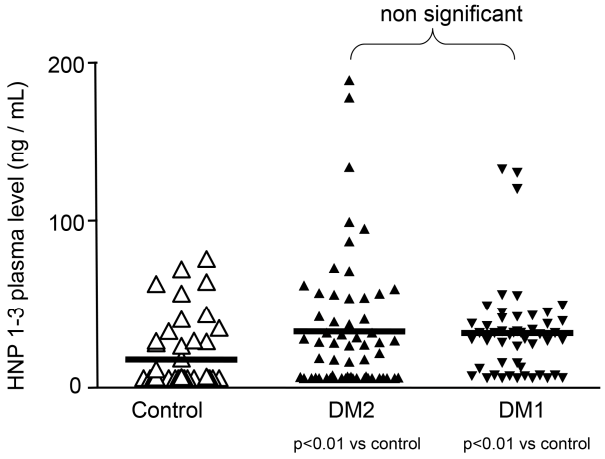

Figure 3. Plasma levels of human neutrophil peptides (HNP1-3) in patients with type 1 and type 2 diabetes (DM1 and DM2) and healthy controls. The lines represent the mean plasma levels of HNP1-3. Significant differences determined by Mann-Whitney test are indicated.

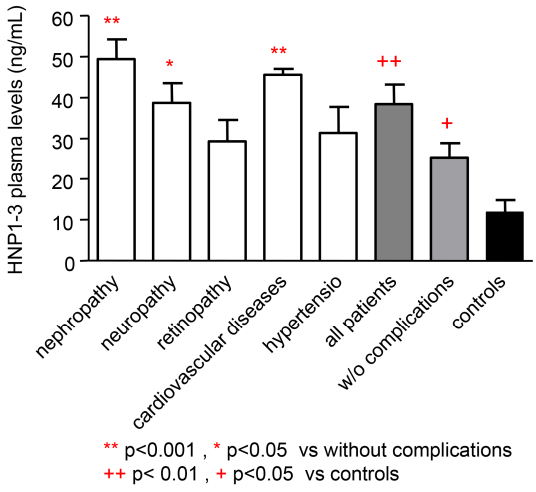

Figure 4. Plasma levels of human neutrophil peptides (HNP1-3) in diabetic patients with different complications relative to those without complications, and to healthy controls. Mean and S.E.M. are indicated; significant differences between groups were determined by unpaired *t test.*

Plasma levels of α-defensin -human neutrophil peptide- (HNP1-3) in 50 patients with type 1 and in 60 patients with type 2 diabetes were determined and compared to 50 healthy blood donors. There was high individual variation in plasma levels of α-defensin, but a significant difference between healthy subjects and both groups of diabetic patients was observed. The mean value ± S.E.M. was 28.78 ± 4.2 ng/mL in type 1 diabetes, and 29.82 ± 5.36 ng/mL in type 2 diabetes, versus 11.94 ± 2.96 ng/mL in controls; $p<0.01$ respectively. No significant difference was found concerning the high plasma concentrations of HNP 1-3 between the patients with type 1 and type 2 diabetes (Figure 3).

3.1.2. Plasma levels of HNP1-3 in diabetic patients with complications

Subsequent investigations were focused on the generally high levels of HNP1-3 found in the peripheral blood of both group (type 1 and type 2) of diabetic patients, which were further divided in subgroups with different diabetes-related complications. Nephropathy was diagnosed in 71 patients (32 with type 1 and 39 with type 2 diabetes), and neuropathy in 95 cases (35 with type 1 and 60 with type 2 diabetes). 115

patients suffered from retinopathy (47 with type 1, and 68 with type 2 diabetes), 54 patients (14 with type 1 diabetes, 40 with type 2 diabetes) had cardiovascular diseases and 182 (50 with type 1 and 132 with type 2 diabetes) had hypertension. Data of these subgroups concerning HNP1-3 levels were compared with 67 patients who did not suffer from these complications, and with the data of 100 healthy subjects (Figure 4). The highest concentrations of α-defensin levels were found in diabetic patients with nephropathy (49.4 ± 4.8 ng/mL), and with neuropathy (38.7 ± 4.8 ng/mL) or with cardiovascular complications (45.6.± 1.45 ng/mL) which were significantly higher in comparison with HNP1-3 plasma levels of diabetic patients without complications (25.4 ± 3.5 ng/mL). These data are in accordance with previous observations [50, 95] reporting high level of HNP 1-3 in type 1 diabetic patients with cardiovascular mortality, or in type 1 diabetic patients with nephropathy. These results suggest that in diabetic complications, such as nephropathy, neuropathy and cardiovascular diseases, HNP 1-3 is elevated in the circulation independently of the type of diabetes. In summary, all of the diabetic patients, with or without complications exerted significantly higher levels of HNP1-3 in their plasma, than controls.(Figure 4)

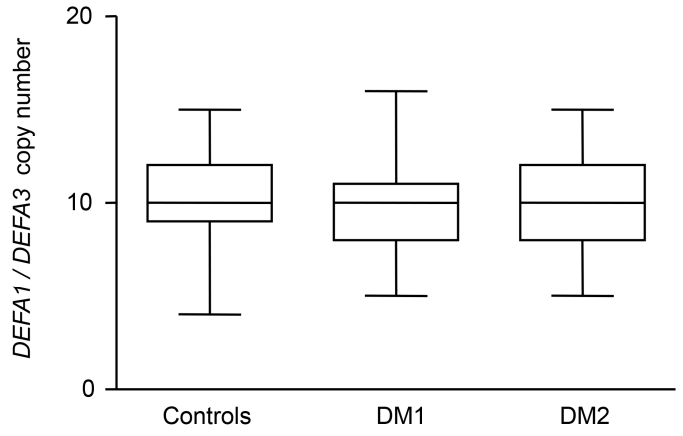

Figure 5. Genomic copy number of *DEFA1/DEFA3* in patients with diabetes and in healthy blood donors. Quantitative box-plot analysis (median, minimum, maximum value, 25% and 75% percentiles) of *DEFA1/A3* copy numbers determined in DNA samples from 133 controls, 100 patients with type 1 diabetes (DM1) and 100 patients with type 2 diabetes (DM2).

3.1.3. Copy number polymorphism of *DEFA1/DEFA3*

The cumulative copy numbers of *DEFA1/DEFA3* were detected using quantitative PCR analysis. From the control population 133 DNA samples were used for copy number determination, and 100-100 DNA samples of diabetic patients with type 1 or type 2 diabetes were investigated. There was no significant difference in *DEFA1/DEFA3* copy number between controls and patients or between patients in the two types of diabetes groups (Figure 5). In the control group *DEFA1/DEFA3* copy numbers ranged from 4 to 15 per genome, with a median number of 10 copies. The median copy number of *DEFA1/DEFA3* in the patients with type 1 diabetes was 10 copies per genome (from 5 to 16 copies) and the median copy number of *DEFA1/DEFA3* in patients with type 2

diabetes was also 10 (ranging from 5 to 15). No significant correlation was observed between α-defensin plasma levels and genomic *DEFA1/DEFA3* copy numbers ($r^2 = 0.01$; Figure 6).

3.1.4. *DEFA1/DEFA3* gene expression

Furthermore, determination of relative mRNA expression levels of *DEFA1/DEFA3* in peripheral leukocytes from diabetic patients was carried out. *DEFA1/DEFA3* mRNA were obtained from blood samples of patients (10 with type 1 and another 10 with type 2 diabetes). Relative expression levels of *DEFA1/DEFA3* were compared to the *DEFA1/DEFA3* copy number of the same patients. Our data support that peripheral leukocytes have the ability to transcribe *DEFA1/DEFA3* genes and to produce HNP1-3 peptides. However, no positive correlation was observed between the copy numbers and the expression levels of the human neutrophil peptide 1-3 (Figure 7).

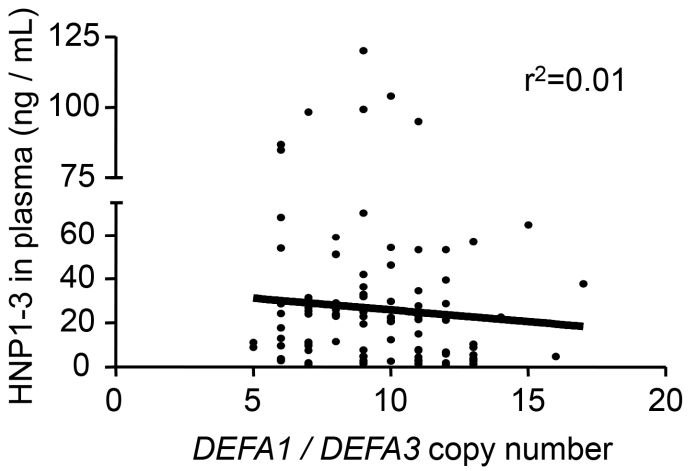

Figure 6. Plasma levels of human neutrophil peptides (HNP1-3) in diabetic patients versus copy number of *DEFA1/DEFA3*. The *DEFA1/A3* copy number were determined by quantitative PCR analysis and compared to the HNP1-3 plasma level of the same patient (50 with type 1 and 50 with type 2 diabetes).

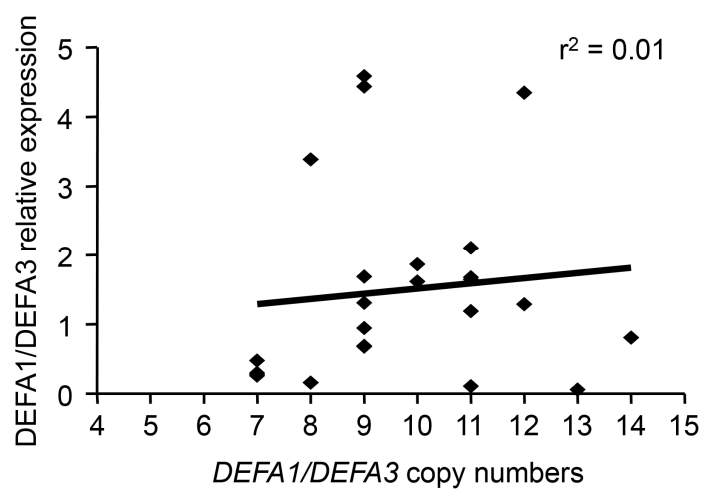

Figure 7. Relative mRNA expression levels of *DEFA1/DEFA3* in diabetic patients versus copy numbers of *DEFA1/DEFA3*. The *DEFA1/A3* copy numbers were determined by quantitative PCR analysis and compared to the *DEFA1/DEFA3* mRNA measured by RT-PCR of the same patient (10 with type 1 and 10 with type 2 diabetes).

3.2. *DEFB1* C.-20G>A, C.-52G>A AND C.-44C>G POLYMORPHISMS IN DIABETES

The distribution of the *DEFB1* c.-20G>A genotypes (Table 1) was in accordance with the Hardy-Weinberg equilibrium both in the control population and in the patients.(p = 0.449 and p = 0.989, respectively). There was no significant difference in genotype distribution between the patients overall and the healthy controls. Similarly, no significant differences in genotypes were observed when the patients were grouped as type 1 and type 2 diabetes mellitus.

Table 1. *DEFB1* c.-20G>A genotypes in patients with diabetes

	GG	GA	AA	χ^2 test*
Patients with diabetes n = 257	82 (32 %)	131 (51 %)	44 (17 %)	0.568
Type 1 diabetes n = 117	36 (31 %)	60 (51 %)	21 (18 %)	0.775
Type 2 diabetes n = 140	46 (33 %)	71 (51 %)	23 (16 %)	0.573
Controls n = 200	62 (31 %)	96 (48 %)	42 (21 %)	

* chi square test versus control

As to the *DEFB1* c.-52G>A SNP (Table 2), distribution of the genotypes was in accordance with the Hardy-Weinberg equilibrium both in the control population and in the patients (p=0.610 and p=0.065 respectively). We did not detect significant differences in genotypes between the patients and the controls, neither in type 1 diabetes, nor in type 2 diabetes.

Table 2. *DEFB1* c.-52G>A genotypes in patients with diabetes

	GG	GA	AA	χ2 test*
Patients with diabetes n = 257	114 (44 %)	104 (40 %)	39 (15 %)	0.572
Type 1 diabetes n = 117	52 (44 %)	47 (40 %)	18 (17 %)	0.702
Type 2 diabetes n = 140	62 (44 %)	57 (41 %)	21 (15 %)	0.658
Controls n = 200	80 (40 %)	84 (42 %)	36 (18 %)	

* chi square test versus control

Table 3. DEFB1 c.-44G>C genotypes in patients with diabetes

	CC	CG	GG	χ2 test*
Patients with diabetes n = 257	156 (61 %)+	95 (37 %)	6 (2 %) **	0.002
Type 1 diabetes n = 117	70 (60 %)	44 (37 %)	3 (2.5 %)	0.01
Type 2 diabetes n = 140	86 (61 %)	51 (36 %)	3 (2 %)	0.003
Controls n = 200	90 (45 %)	92 (46 %)	18 (9 %)	

* chi square test versus control
** Fisher test versus control p = 0.001, OR = 9.136, 95 % CI: 3.512 – 23.82
\+ Fisher test versus control p = 0.0009, OR = 2.005, 95 % CI: 1.218- 2.746

The genotypic distribution of *DEFB1* c.-44C>G polymorphism is shown in Table 3, where the distribution of genotypes was also in accordance with the Hardy-Weinberg equilibrium among the patients with diabetes (p =0.610, χ^2 = 0.260) and also in the control population (p=0.597, χ^2=0.279). There was a significant difference in genotype distribution between patients and healthy controls (χ^2 test, p = 0.002). The frequency of GG genotype was significantly lower in both types of diabetes (2.5% and 2%, respectively) than in healthy controls (9%), (Fisher test versus control p=0.002, OR=4.121, 95% CI: 1.604 – 10.59). Conversely, the prevalence of the CC genotype was 61% in the group of diabetic patients vs. 45 % of controls (Fisher test: p = 0.02, OR = 2.055, 95% CI: 1.27 – 3.745). When the patients were sorted according to their diabetic complications, lower frequency of GG genotype among the patients with nephropathy and among the patients with neuropathy was found (1.4% and 1% respectively).

3.3. RESULTS OF MOUSE TRYPSINOGEN EXPERIMENTS

3.3.1. Identification of major trypsinogen isoforms in the mouse pancreas

Ecotin affinity chromatography was used to purify trypsinogen isoforms from the mouse pancreas. Outbred CD-1 mice expressed 4 trypsinogen isofroms to high levels (T7, T8, T9 and T20), which were identified from homogenized whole mouse pancreata using N-terminal sequenceing and mass spectrometry. Trypsinogens were eluted under acidic conditions from the ecotin column and immediately loaded onto a MonoS cation exchange column equilibrated with 20 mM Na-acetate (pH 5.0). The MonoS column was developed with a NaCl gradient, resulting in five peaks (Figure 2).

Edman-degradation identified the small fourth peak as elastase 3 (N terminus is CGQPS) and the large fifth peak as the cationic T7 trypsinogen isoform, which has a unique N-terminal sequence, LPLDD (Suppl. Figure 1 and Suppl. Figure 2A). The same N-termini (FPVDD) was observed in case of the other three peaks, which proved to be trypsinogens. These were subjected to in-gel tryptic digestion followed by mass spectrometric nanosequencing, which revealed the identity of the first peak as isoform T20. The second and third peaks were indistinguishable from each other, however it was proven that they are T9 and T8 isoforms (Figure 2), which are almost identical in their amino-acid sequence (99% identity, Suppl. Figure 1 and Suppl. Figure 2B). They had a slight difference in their ionic character, which helped to assign T9 as the second peak and T8 as the third peak.

Identification strategy of trypsinogen isoforms based on N-terminal sequenceing is shown in Figure 8. N-terminal sequencing of the combined second/third peaks after activation of trypsinogen to trypsin indicated a mixture of Val/Ile amino-acids at position 35 (IVGGYTCRENS(**V/I**)P), with a preponderance of Val, confirming that the smaller second

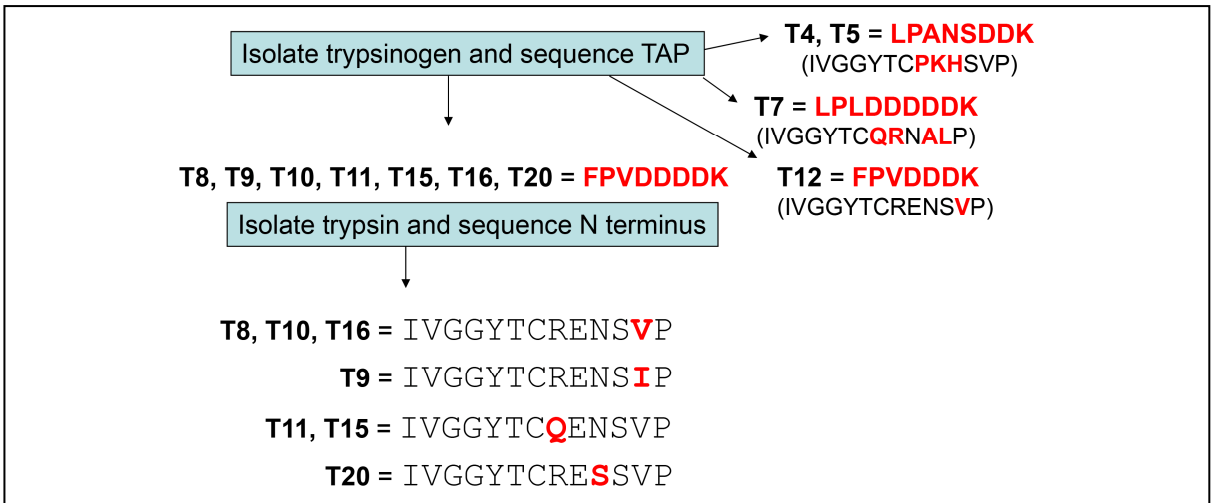

Figure 8. Strategy for the the identification of mouse trypsinogen isoforms by N-terminal sequencing. T4, T5, T7 and T12 trypsinogens have unique N-termini which allowed us to distinguish them from other isoforms, which were identical in their N-terminal sequences. Therefore, these isoforms were activated to trypsin, which allowed us to distinguish them from each other by N-terminal sequencing. Unique amino acid residues in the N-terminal sequence of given isoforms are in red letters.

peak is T9 (containing Ile35) and the larger third peak is T8 (containing Val35) (Figure 2). Both N-terminal sequencing (CGVPA) and mass spectrometry indicated that the T9/T8 peaks were contaminated with some Ctrb. Quantitative evaluation of trypsinogen peaks were performed as described under *Patients and Methods* and the following relative expression levels were obtained (mean±SD, n=4): 41 ± 1 % for T7; 47 ± 3 % for T8 and T9 combined and 12 ± 2 % for T20.

3.3.2. Autoactivation of mouse trypsinogens.

Large-scale purification of different trypsinogen isoforms from the mouse pancreas is impractical and preparations may be contaminated with low levels of other pancreatic proteases. In contrast, recombinant expression should provide highly purified, homogeneous enzyme preparations. Reliable methodology for the expression and purification of human trypsinogens [93, 94] is well known and the same approach has been used to obtain functionally competent mouse trypsinogen preparations. Trypsinogens were expressed in *E. coli* as inclusion bodies, renatured *in vitro* and purified by ecotin-affinity chromatography. When mouse trypsinogens were incubated in 1 mM $CaCl_2$ at pH 8.0, isoforms T7, T8 and T9 autoactivated and reached about 40-60% of potentially attainable trypsin levels, indicating that some autocatalytic (trypsin-mediated) degradation occurred (Figure 9A) during autoactivation. In contrast, T20 did not autoactivate under these conditions. As expected, high concentrations of calcium (10 mM) increased the rate of autoactivation and stabilized trypsinogens against degradation, yielding 80-100% of attainable trypsin levels. The stimulatory effect of calcium on the autoactivation of T20 was particularly striking (Figure 9B).

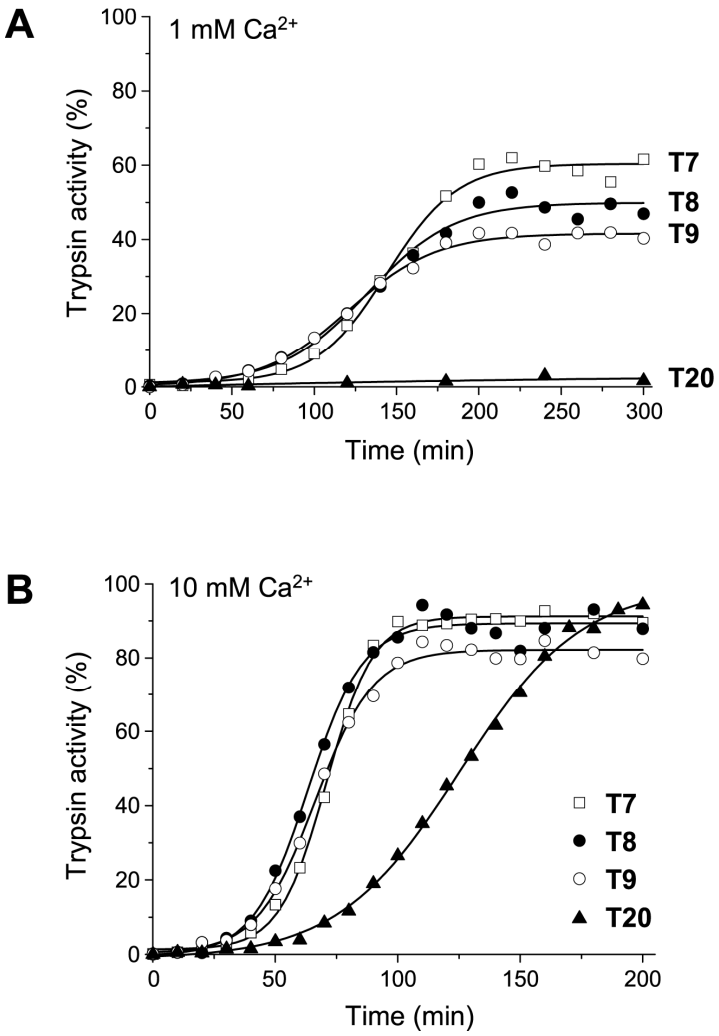

Figure 9. Autoactivation of mouse trypsinogens. Trypsinogens were incubated at 2 µM concentration with 10 nM initial trypsin in 0.1 M Tris-HCl (pH 8.0), 1 mM $CaCl_2$, (**A**) or 10 mM $CaCl_2$ (**B**) and 0.05% Tween 20, at 37 °C. Aliquots (1.5 µL) were withdrawn at the indicated times and trypsin activity was determined as described in *Patients and Methods*. Trypsin activity was expressed as percentage of the maximal activity determined by full activation with enteropeptidase. Representative experiments from four replicates are shown.

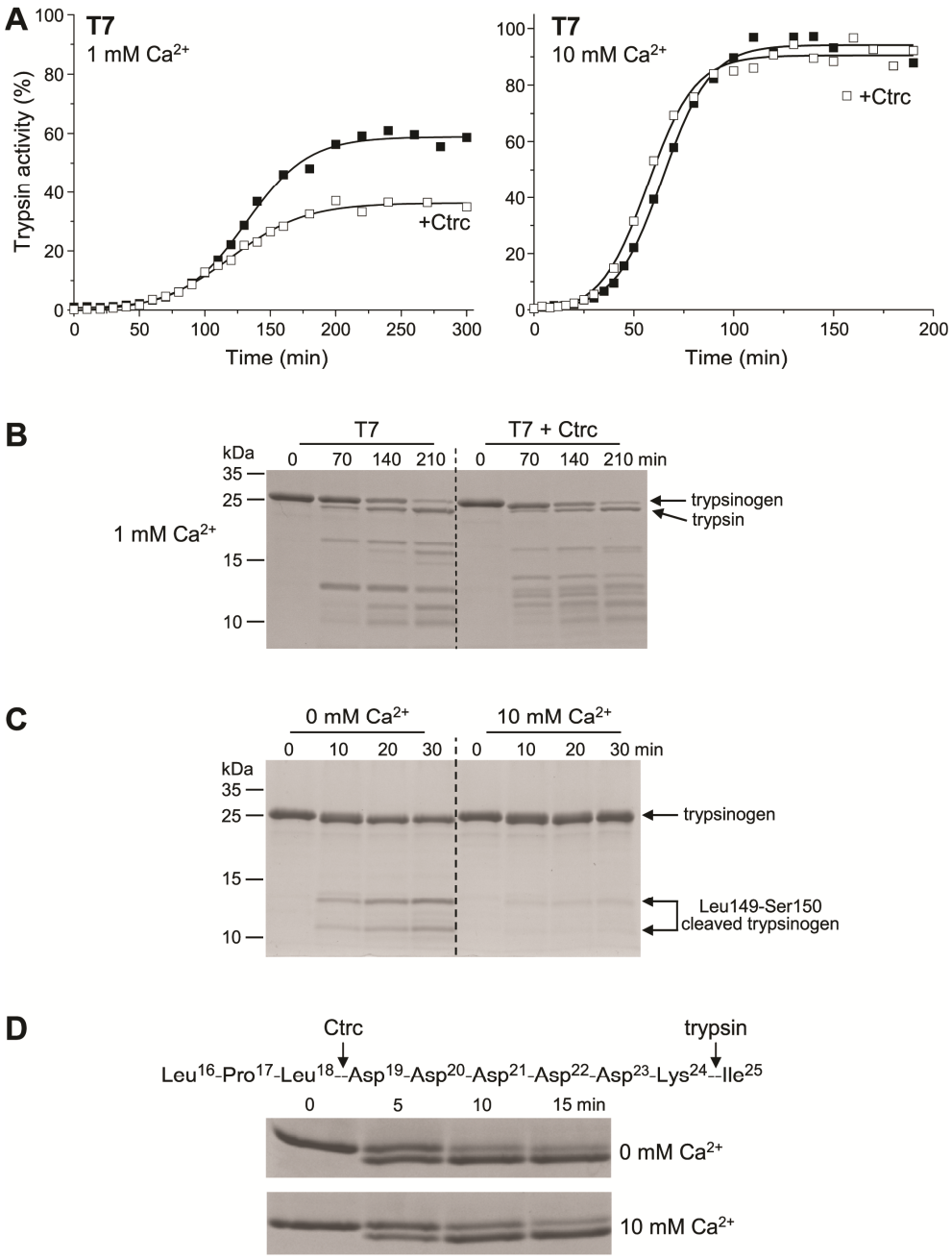

Figure 10. Effect of mouse chymotrypsin C (Ctrc) on mouse trypsinogen T7. (**A**) Autoactivation was measured in 1 mM and 10 mM $CaCl_2$, in the absence (solid symbols) or presence (open symbols) of 25 nM mouse Ctrc, as described in *Patients and Methods*. (**B**) **SDS-PAGE analysis of autoactivation in 1 mM $CaCl_2$.** Samples were withdrawn at the indicated time points, precipitated with trichloroacetic acid, electrophoresed and stained as described in *Patients and Methods*. (**C**) **Cleavage of T7 trypsinogen by 25 nM mouse Ctrc**. Incubations were performed with 2 µM trypsinogen in 0.1 M Tris-HCl (pH 8.0) in the absence or presence of 10 mM $CaCl_2$. Samples were precipitated with trichloroacetic acid and analyzed by SDS-PAGE and Coomassie blue staining. Representative experiments from three replicates are shown. (**D**) **Cleavage of the activation peptide of trypsinogen T7 by mouse Ctrc**. Primary structure of the native T7 activation peptide with proteolytic cleavage sites for Ctrc and trypsin are also indicated. Note that the N-terminal amino acid of mature trypsinogen is Leu16, as the 15 amino-acid long secretory signal peptide is removed in the endoplasmic reticulum. Trypsinogen was incubated at 2 µM concentration with 25 nM Ctrc in 0.1 M Tris-HCl (pH 8.0) and 0 or 10 mM $CaCl_2$ (final concentrations), at 37 °C. To prevent autoactivation, 25 nM human SPINK1 trypsin inhibitor was included. At the indicated times reactions were terminated by precipitation with 10% trichloroacetic acid (final concentration) and samples were analyzed by 15% non-reducing SDS-PAGE and Coomassie Blue staining. Relevant segments of representative gels (from two replicates) demonstrate the small mobility shift of the trypsinogen band caused by Ctrc-mediated cleavage of the Leu18-Asp19 peptide bond. Note that the rapid rate of cleavage is partly due to the added Met-Ala sequence at the N terminus of recombinant T7.

3.3.3. Effect of mouse Ctrc on T7 trypsinogen

Mouse chymotrypsin C (Ctrc) in 25 nM final concentration reduced the final mouse T7 trypsin levels by ~35% during autoactivation in 1 mM $CaCl_2$, while in 10 mM $CaCl_2$ it slightly stimulated the rate of autoactivation (Figure 10A).

In the absence of Ctrc, SDS-PAGE analysis of the autoactivation reaction in 1 mM calcium confirmed conversion of the T7 trypsinogen band to trypsin and also indicated degradation fragments generated by cleavages of trypsin-sensitive peptide bonds Arg123-Val124 and Lys194-Asp195 (Figure 10B, left panel, see also Suppl. Figure 1 and Suppl. Figure 2A). These were identified by N-terminal sequencing, similarity to the published degradation fragments of rat anionic trypsinogen-2 [92] and comparison of the banding pattern with that of the T7 p.R123H mutant (Figure 12). Note that because of an extra amino acid in the activation peptide of T7, amino-acid numbering is shifted by one relative to human and other mouse trypsinogens (Suppelementary Figure 1). Cleavage after Arg123 should result in a fully active, two-chain trypsin [55, 67], whereas cleavage after Lys194 causes inactivation [92, 101]. Ctrc caused a small shift of the T7 trypsinogen band, suggesting cleavage of the activation peptide (Figure 10B, right panel). In addition, the banding pattern of degradation fragments became more complex, which is consistent with the lower trypsin activity attained during autoactivation in 1 mM calcium in the presence of Ctrc.

To identify Ctrc-mediated cleavages of trypsinogen, digestion experiments with short incubation times was performed; when no trypsinogen activation took place yet and no trypsin activity was present. Under these conditions, slow cleavage of the Leu149-Ser150 peptide bond in the autolysis loop was observed in the absence of calcium (Figure 10C, left panel) and this was completely inhibited by 10 mM calcium (Figure 10C, right panel, see also Suppl. Figure 2A). The Leu82-Glu83 peptide bond (corresponding to Leu81-Glu82 in human trypsinogens and other studied mouse isoforms) in the calcium binding loop was not cleaved to a detectable extent. This finding suggested that in T7 the moderate degradation observed during autoactivation in 1 mM calcium in the presence of Ctrc is mediated by cleavage of the Leu149-Ser150 peptide bond. To confirm this assumption, we compared autoactivation of the T7 p.L82A and p.L149A mutants in 1 mM calcium and found that only mutation p.L149A protected against degradation in the presence of Ctrc (Figure 11). Interestingly, mutant p.L82A suffered Ctrc-dependent degradation during autoactivation to an even larger extent than wild type T7.

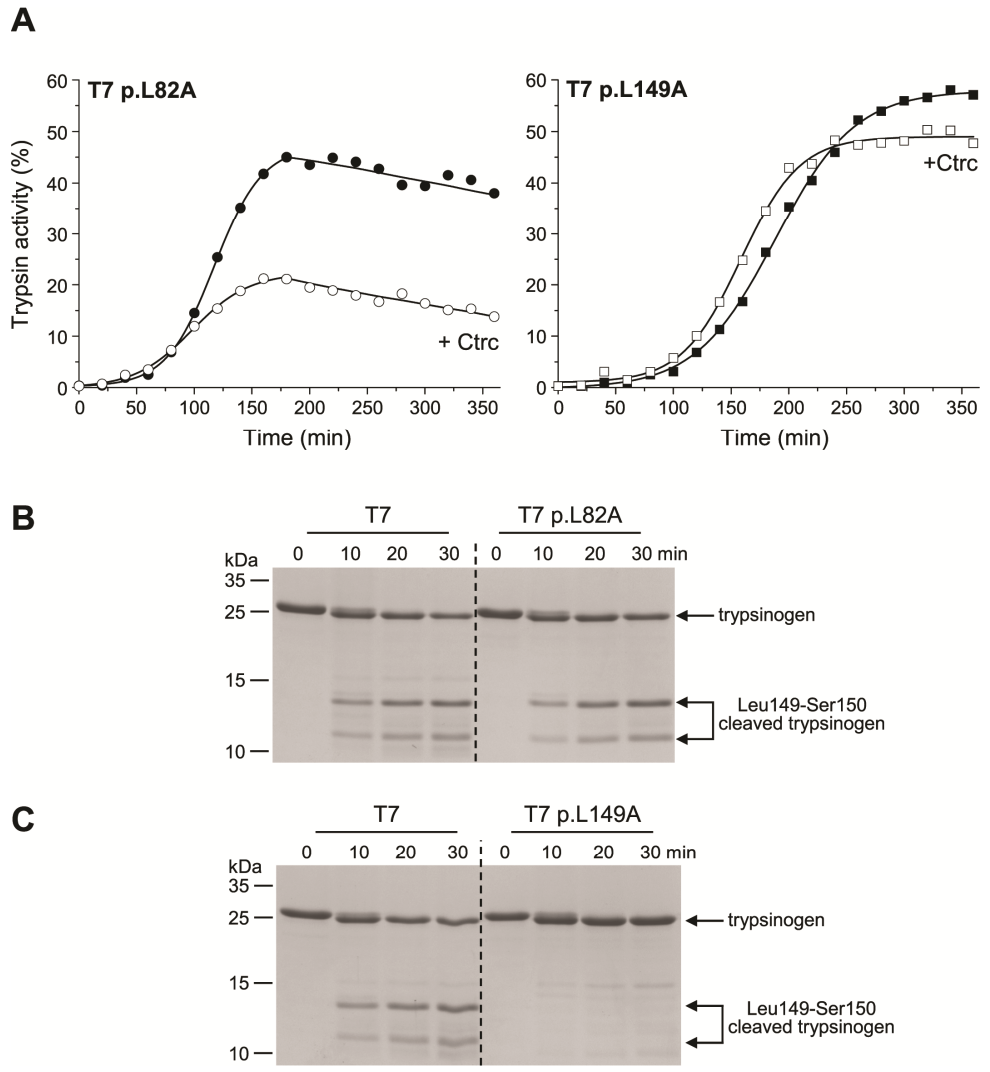

Figure 11. Effect of mutations p.L82A and p.L149A on mouse trypsinogen T7. (**A**) Autoactivation was measured in 1 mM $CaCl_2$ as described in *Patients and methods*. Trypsin activity was expressed as percentage of the maximal activity determined by full activation with enteropeptidase. (**B**) **Cleavage of wild type and p.L82A T7 trypsinogen by 25 nM mouse Ctrc.** (**C**) **Cleavage of wild type and p.L149A T7 trypsinogen by 25 nM mouse Ctrc.** Incubations were performed with 2 µM trypsinogen in 0.1 M Tris-HCl (pH 8.0) in the absence of calcium. Trypsinogen samples were precipitated with 10% trichloroacetic acid (final concentration) and analyzed by SDS-PAGE and Coomassie blue staining. Representative experiments from two replicates are shown.

3.3.4. N-terminal processing of T7 trypsinogen by mouse Ctrc

Among the activation peptide sequences of mouse trypsinogens only T7 contains a potentially Ctrc-sensitive peptide bond, Leu18-Asp19 (Suppl. Figure 1 and Suppl. Figure 2A). Inspection of Figure 10B revealed that the T7 trypsinogen band became slightly shifted as a result of treatment with Ctrc, suggesting that the activation peptide might be cleaved at Leu18-Asp19. When the samples were run under non-reducing conditions, the mobility shift caused by N-terminal processing of the T7 activation peptide became more apparent (Figure 10D) and N-terminal sequencing confirmed the predicted cleavage site. However, in contrast

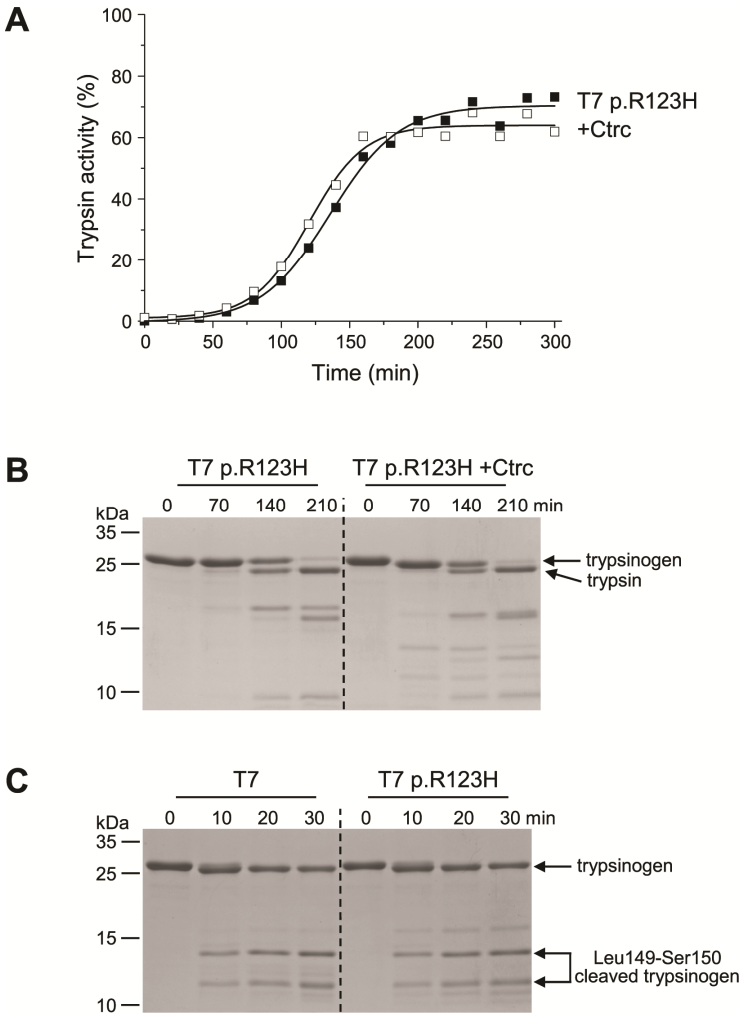

Figure 12. Effect of mutation p.R123H on mouse trypsinogen T7. (**A**) Autoactivation was measured in 1 mM $CaCl_2$ as described in *Pateints and methods*. Trypsin activity was expressed as percentage of the maximal activity determined by full activation with enteropeptidase. (**B**) **SDS-PAGE analysis of the autoactivation reaction.** Samples were withdrawn at indicated times, precipitated with trichloroacetic acid, electrophoresed and stained as described in *Pateints and methods*. (**C**) **Cleavage of wild-type and p.R123H T7 trypsinogen by 25 nM mouse Ctrc.** Incubations were performed with 2 µM trypsinogen in 0.1 M Tris-HCl (pH 8.0) in the absence of calcium. Samples were precipitated with trichloroacetic acid and analyzed by SDS-PAGE and Coomassie blue staining. Cleavage products were identified with N-terminal sequencing. Representative experiments from two replicates are shown.

to human cationic trypsinogen, the rate of autoactivation of N-terminally processed T7 was only negligibly stimulated (see Figure 10A, 10 mM calcium panel), indicating that Ctrc does not regulate activation of mouse trypsinogens through cleavage of the activation peptide.

3.3.5. Effect of the p.R123H mutation on T7 trypsinogen.

Mutation p.R123H protected T7 trypsinogen against degradation during autoactivation in 1 mM calcium in the presence of Ctrc (Figure 12); however, it had no effect on the cleavage of the Leu149-Ser150 peptide bond *per se*. This observation indicates that

moderate degradation of T7 during autoactivation is due to the combined effects of Ctrc-mediated and tryptic cleavages after Leu149 and Arg123, respectively (Suppl. Figure 2A).

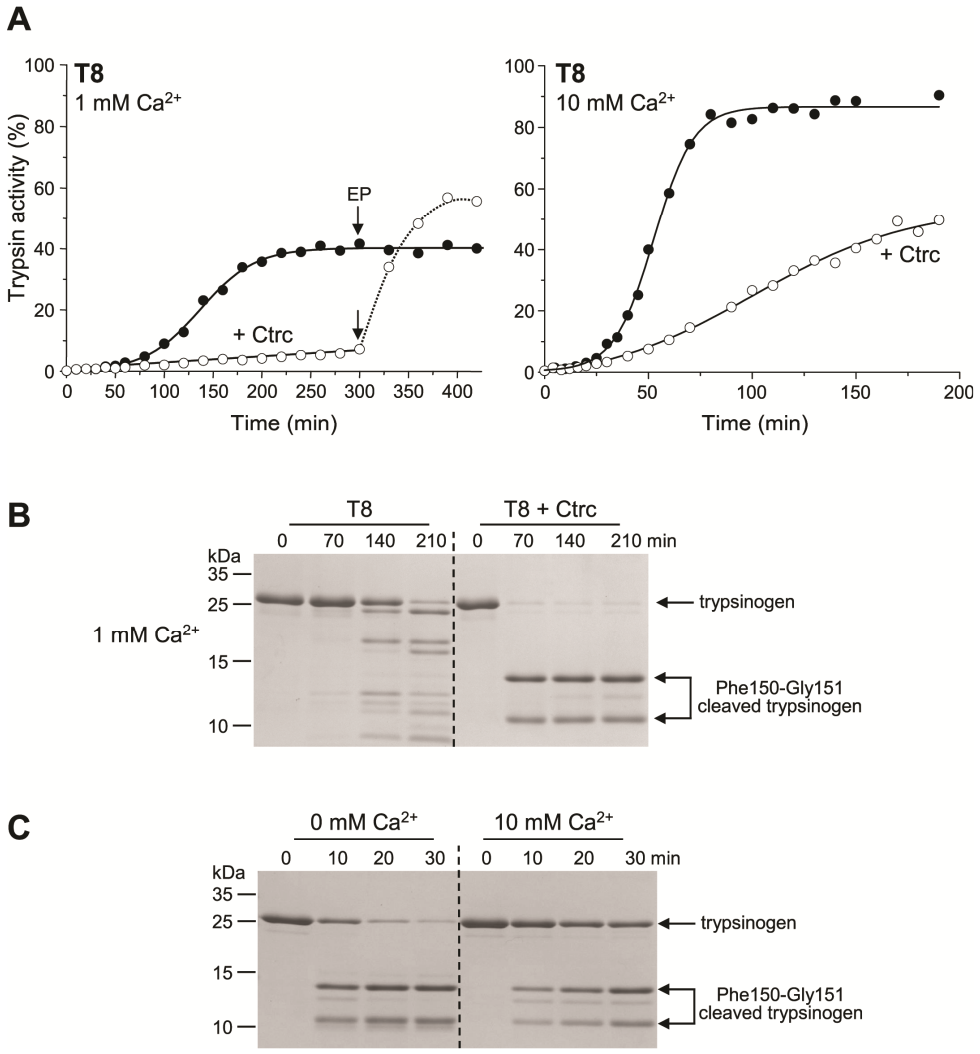

Figure 13. Effect of mouse chymotrypsin C (Ctrc) on mouse trypsinogen T8. (**A**) Autoactivation was measured in 1 mM and 10 mM $CaCl_2$, in the absence (solid symbols) or presence (open symbols) of 25 nM mouse Ctrc, as described in *Patients and Methods*. Where indicated, 2 µL of 1.4 µg/mL human enteropeptidase (EP) was added. (**B) SDS-PAGE analysis of the autoactivation reaction** in 1 mM $CaCl_2$. Samples were withdrawn at indicated times, precipitated with trichloroacetic acid, electrophoresed and stained as described in *Patients and Methods*. (**C**) **Cleavage of trypsinogen by 25 nM mouse Ctrc.** Incubations were performed with 2 µM trypsinogen in 0.1 M Tris-HCl (pH 8.0) in the absence or presence of 10 mM $CaCl_2$. Samples were precipitated with trichloroacetic acid and analyzed by SDS-PAGE and Coomassie blue staining. Cleavage products were identified with N-terminal sequencing. In the absence of calcium (left panel), the faint bands above and below the major cleavage products correspond to fragments of trypsinogen cleaved at the Leu81-Glu82 peptide bond. The faint band visible in the presence of 10 mM calcium (right panel) could not be identified. Representative experiments from three replicates are shown.

3.3.6. Effect of mouse Ctrc on T8 and T9 trypsinogen

Mouse Ctrc almost completely inhibited autoactivation of T8 and T9 trypsinogen in 1 mM calcium and markedly reduced it in 10 mM calcium (Figures 13, 14). This inhibitory effect was not due to degradation, as addition of enteropeptidase to the Ctrc-treated samples

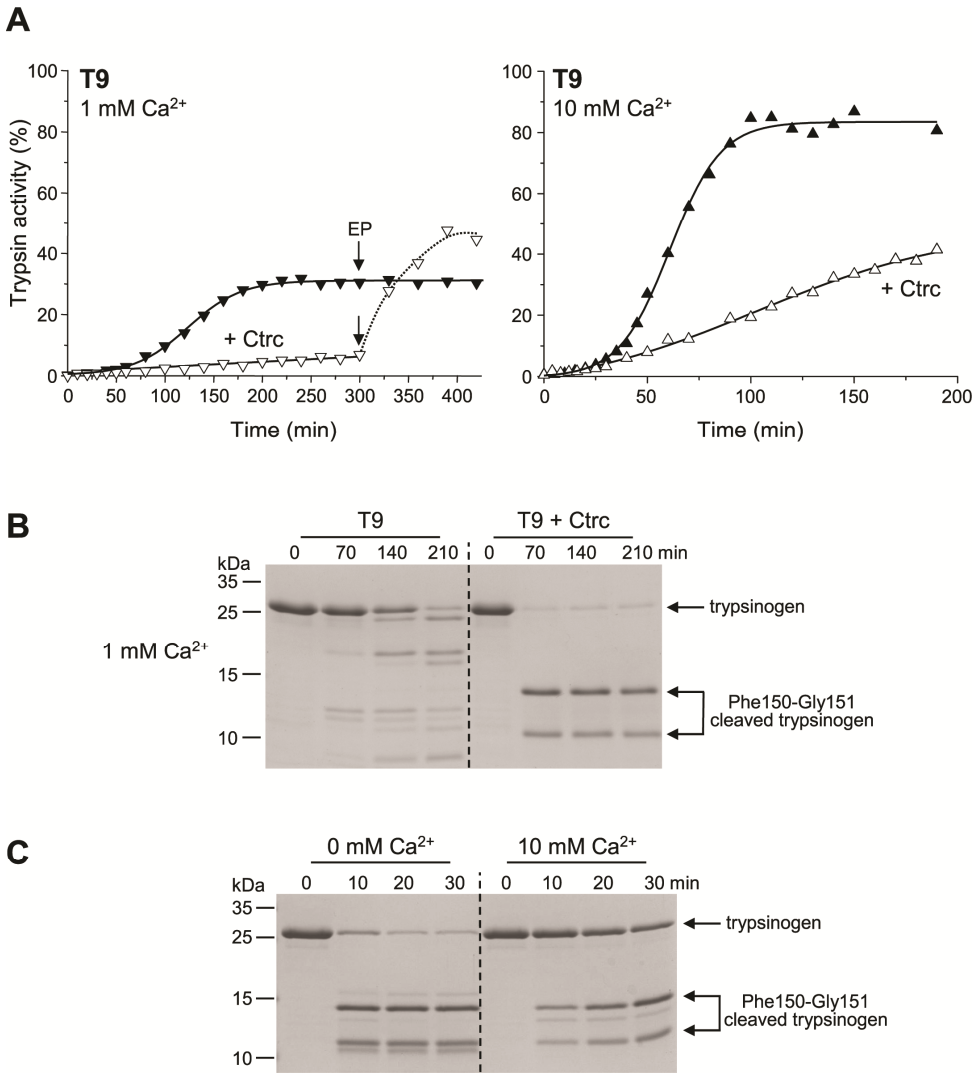

Figure 14. Effect of mouse chymotrypsin C (Ctrc) on mouse trypsinogen T9. See Figure 13 for experimental details.

resulted in the appearance of highly significant trypsin activity. SDS-PAGE analysis of autoactivation in 1 mM calcium, in the absence of Ctrc, demonstrated conversion of trypsinogen to trypsin with the characteristic degradation fragments generated by tryptic cleavage of the Arg122-Val123 and Lys193-Asp194 peptide bonds (Figures 13B, 14B, left panel, see also Suppl. Figure 2B). In dramatic contrast, when autoactivation was followed in the presence of Ctrc, no trypsin band or any of the tryptic degradation bands were observed. Instead, Ctrc rapidly and completely cleaved T8 and T9 trypsinogen at a single site, which N-terminal sequencing revealed as the Phe150-Gly151 peptide bond (Figures 13B, 14B, right panel, see also Suppl. Figure 2B). This peptide bond lies within the so-called autolysis loop, a flexible segment between residues 146 and 154 (Suppl. Figure 1). When cleavage of T8 and T9 trypsinogen by Ctrc was studied with short incubation times (i.e. before autoactivation occurred), both isoforms were primarily cleaved at the Phe150-Gly151 peptide bond, with

minimal cleavage observed at the Leu81-Glu82 peptide bond in the absence of calcium (Figures 13C, 14C). Cleavage of the Phe150-Gly151 peptide bond was slower but still readily detectable in 10 mM calcium.

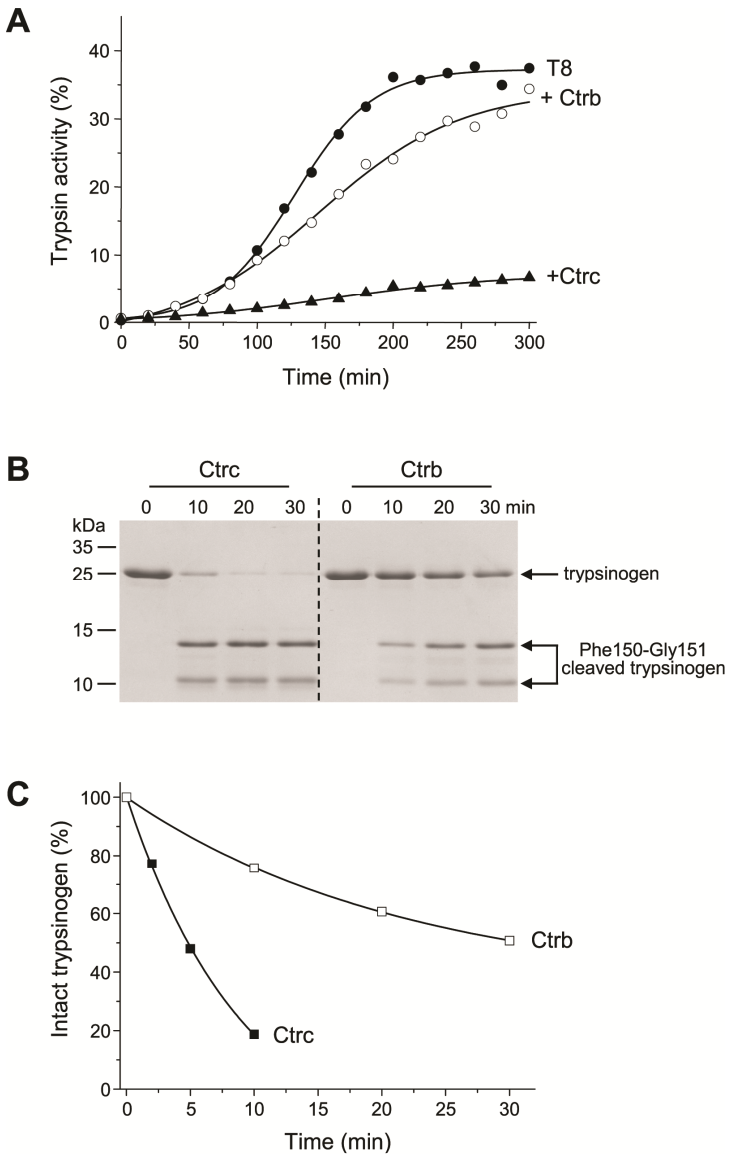

Figure 15. Effect of mouse chymotrypsin B (Ctrb) on mouse trypsinogen T8. (**A**) Autoactivation was measured in 1 mM $CaCl_2$ as described in *Patients and Methods*, in the absence or presence of 25 nM mouse Ctrb or Ctrc, as indicated. (**B**) **Cleavage of trypsinogen by 25 nM Ctrb and Ctrc** was compared in the absence of calcium, as described in Figure 13C. Representative experiments from two replicates are shown. (**C**) The disappearance of the intact trypsinogen band was quantitated by densitometry and data from two experiments were plotted. For clarity, error bars were omitted, the error was within 10% of the mean.

3.3.7. Cleavage of the Phe150-Gly151 peptide bond by mouse chymotrypsin B (Ctrb)

Regulation of autoactivation of human cationic trypsinogen by human CTRC is highly specific and other chymotrypsins and elastases do not cleave the CTRC cleavage sites. To test whether the same Ctrc specificity exists in the mouse, we compared the effect of

mouse Ctrb and Ctrc on T8 trypsinogen. As shown in Figure 15A, autoactivation of T8 was much less effectively inhibited by 25 nM Ctrb than by an equimolar concentration of Ctrc. In degradation experiments, Ctrb cleaved the Phe150-Gly151 peptide bond at a more than 7-fold slower rate than Ctrc (Figures 15B and 15C).

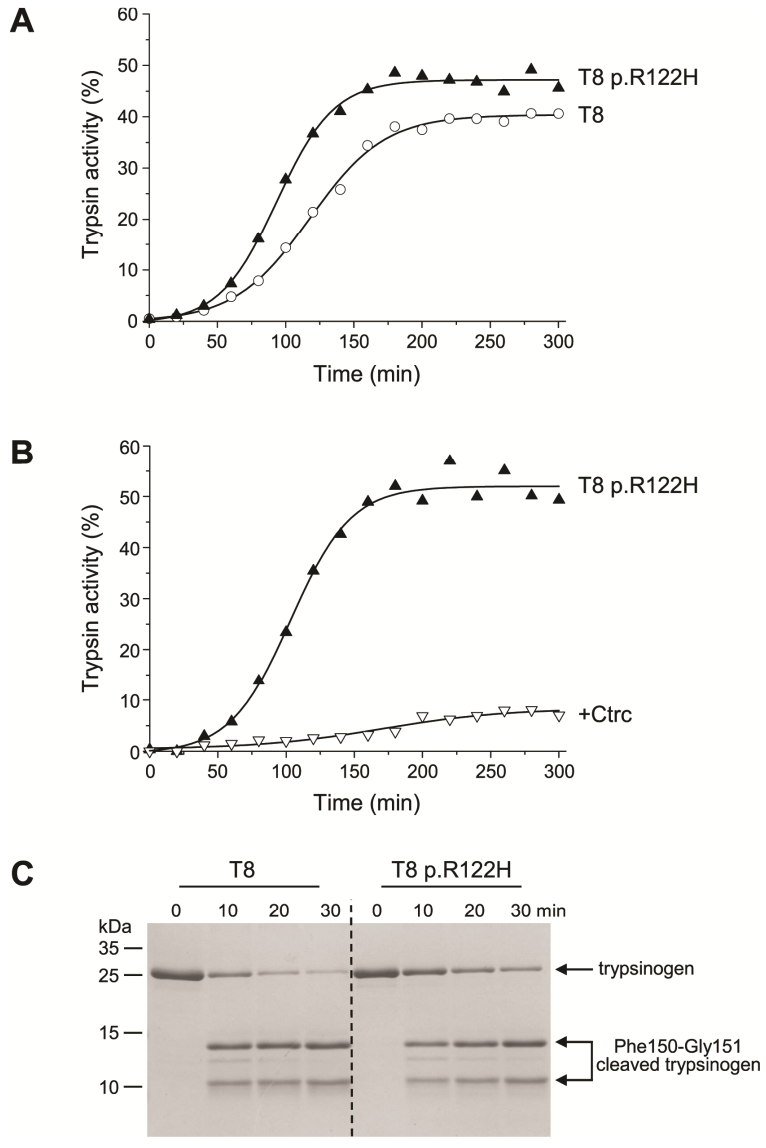

Figure 16. Effect of mutation p.R122H on mouse trypsinogen T8. (**A**) Autoactivation of wild-type and p.R122H mutant T8 trypsinogen was measured in 1 mM $CaCl_2$ as described in *Patients and Methods*. (**B**) The effect of 25 nM mouse Ctrc on the autoactivation of the p.R122H mutant T8. Conditions were the same as in panel A. (**C**) Cleavage of wild-type and p.R122H mutant T8 trypsinogen by 25 nM mouse Ctrc in the absence of calcium. Samples were incubated and analyzed as described in Figure 13C. Representative experiments from two replicates are shown.

3.3.8. Effect of the p.R122H mutation on T8 trypsinogen

Mutation p.R122H slightly stimulated autoactivation of T8 trypsinogen in 1 mM calcium, in the absence of Ctrc (Figure 16A). In the presence of Ctrc, however, autoactivation was strongly inhibited by Ctrc, approximately to the same extent as seen with wild type T8

(Figure 16B, cf. Figure 13A). Consistent with the robust inhibitory effect, the Phe150-Gly151 peptide bond was cleaved by Ctrc almost as well in T8 p.R122H trypsinogen as in wild type T8 (Figure 16C), indicating that mutation p.R122H does not influence this regulatory mechanism.

3.3.9. Cleavage of the autolysis loop in the p.S150F human cationic trypsinogen mutant inhibits autoactivation

The majority of mammalian trypsinogens do not contain Phe150 in their autolysis loop. To test whether introduction of Phe150 would reconstitute the chymotrypsin-dependent

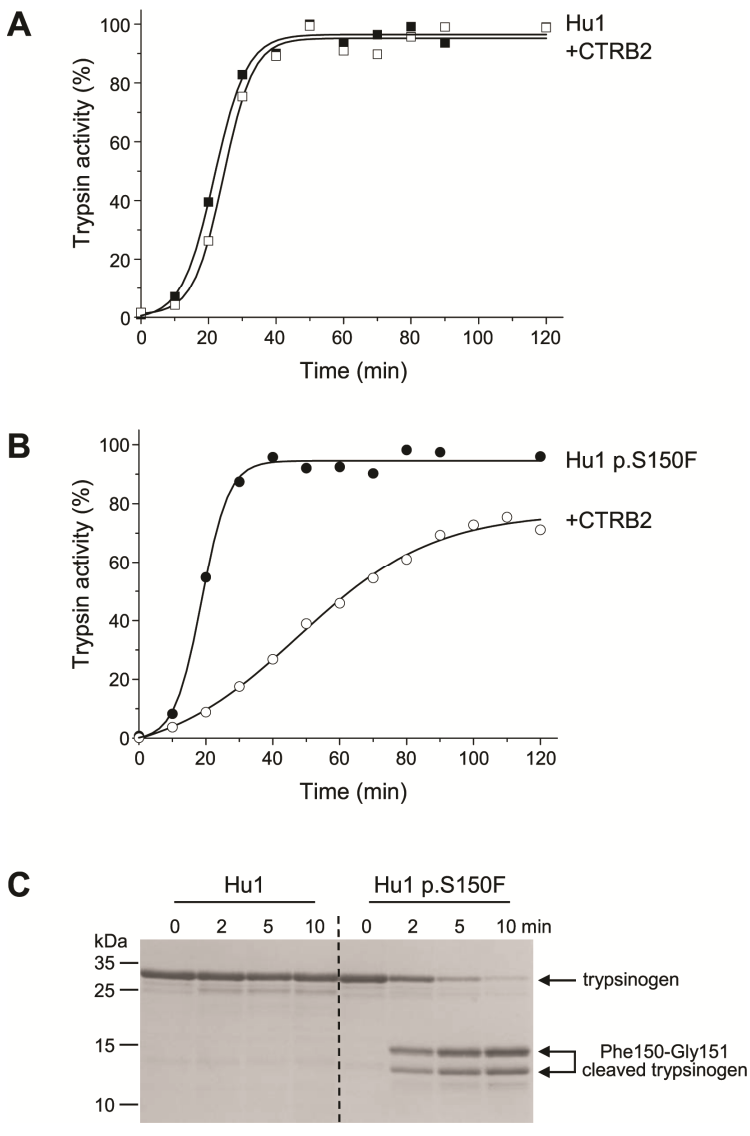

Figure 17. Effect of human chymotrypsin B2 (CTRB2) on the autoactivation of wild-type and p.S150F mutant human cationic trypsinogen (Hu1). (**A, B**) Autoactivation was measured in 1 mM $CaCl_2$, in the absence or presence of 25 nM CTRB2, as described in *Patients and Methods*. (**C**) Cleavage of wild-type and p.S150F mutant human cationic trypsinogen by 25 nM CTRB2 in the absence of calcium. Incubations were performed and samples were analyzed as given in Figure 13C. To prevent autoactivation, 25 nM human SPINK1 trypsin inhibitor was included. Representative experiments from two replicates are shown.

autoactivation inhibition in another mammalian trypsinogen, we mutated Ser150 in human cationic trypsinogen to Phe. Because human CTRC cleaves the Leu81-Glu82 peptide bond and causes trypsinogen degradation, we used human CTRB2 to selectively cleave the newly created Phe150-Gly151 peptide bond. CTRB2 at 25 nM concentration had no effect on the autoactivation of wild type cationic trypsinogen (Figure 17A), whereas it inhibited activation of the p.S150F mutant (Figure 17B), via cleavage at the Phe150-Gly151 peptide bond (Figure 17C).

3.3.10. Effect of mouse Ctrc on T20 trypsinogen

Mouse Ctrc had essentially no effect on trypsinogen T20, except for a slight stimulation of the activation rate in 10 mM calcium (Suppl. Figure 3A). On SDS-PAGE, no trypsinogen to trypsin conversion was evident in 1 mM calcium, in the absence or presence of Ctrc (Suppl. Figure 3B). Note that T20 trypsinogen ran as a doublet on gels, which seem to represent differently denatured conformers, as N-terminal sequencing and mass spectrometry indicated molecular homogeneity (not shown). Finally, cleavage of T20 with Ctrc resulted in very faint degradation bands even in the absence of calcium, indicating that this isoform is resistant to Ctrc (Suppl. Figure 3C).

4. DISCUSSION

4.1. RELEVANCE OF α-AND β-DEFENSINS IN DIABETES MELLITUS

4.1.1. The role of α-defensins

In this work, HNP1-3 levels from the plasma of venous blood were measured. From the buffy coat, copy number variation and mRNA expression levels of *DEFA1/DEFA3* genes of the same individual were investigated. Intriguingly, our results showed significantly higher HNP 1-3 plasma levels in patients with both type 1 and type 2 diabetes mellitus compared to healthy controls. Moreover, the plasma of diabetic patients with nephropathic and neuropathic complications showed the highest concentrations of HNPs. It seems possible that the elevation of HNP1-3 in the plasma of patients with nephropathy is the consequence of the decreased renal degradation of the peptides together with advanced nephropathy [95]. The cause of high levels of HNP1-3 in patients with neuropathy in type 1 and type 2 diabetes remains unknown.

Further investigations were performed in order to clarify whether increased gene expression was responsible for the elevated plasma levels of α-defensins. In our study no correlation was observed between HNP1-3 plasma levels and copy numbers of *DEFA1/DEFA3* genes. The effect of copy number variations in *DEFA1/DEFA3* on the disease or even on the plasma concentrations of the peptides remain unclear.

There are contradictory data about the correlation between *DEFA1/DEFA3* copy numbers and α-defensin peptide concentrations. Linzmeier and Ganz [61] showed that the HNP1-3 peptide levels in human neutrophils were proportional to the copy number of the *DEFA1* and *DEFA3* genes. Copy numbers of *DEFA1/DEFA3* may be proportional to the intracellular levels of HNP1-3 in neutrophil granulocytes, but possibly not to the circulating HNP1-3 levels. Additionally, a recent study in septic patients [21] showed the discrepancy between gene copy number and protein levels. There are several possibilities to explain why *DEFA1/DEFA3* copy numbers and HNP 1-3 plasma levels are not correlated. The human α-defensins are stored primarily in the granules of neutrophils and released into the circulation during the activation of neutrophils. Also, yet unrevealed transcriptional mechanisms or an increased distance between the regulators of the genes might modulate the expression of these genes [21, 45].

In our study no significant correlation was observed between the genomic copy number variation of *DEFA1/DEFA3* and the mRNA expression levels (Figure 7), suggesting

that degranulation rather than increased gene expression may be responsible for increased HNP plasma levels in diabetes. In a study by Aldred et al. [1] the combined expression levels of *DEFA1/DEFA3* and the genomic copy number were also not correlated, suggesting the superimposed influence of trans-acting factors. It is noteworthy that there are several examples for the abscence of correlation between copy number polymorphisms and relative transcription levels [45].

These results are in a good correlation with our recent observations, suggesting that modulation of the HNP1-3 secretion by neutrophils following kynurenic acid treatment might be independent from the mRNA expression levels of *DEFA1 / DEFA3* [110].

In a recent study, eosinophils with active α-defensin production have been detected in capillary blood of diabetic patients [73]. In this investigation eosinophils but not neutrophils displayed augmentation of transcriptional activation of α-defensin expression. In our study the majority of the cells in peripheral venous blood were neutrophils, therefore our purified DNA and RNA samples were derived also mostly from neutrophils.

4.1.2. Polymorphisms of β1-defensin gene

The present study has demonstrated that the distribution of *DEFB1* c.-44C>G genotypes were different between patients with diabetes and healthy controls. Our results showed that the frequency of the GG genotype was significantly higher in the control population. The presence of G allele might lead to strengthened HBD1 antimicrobial activity, which is less frequent among patients with diabetes. The G allele of the c.-44C>G SNP generates a putative binding site for nuclear factor-κB (NF-κB), and induces overexpression of HBD1 gene. The proposed effect of this SNP could partially explain why the GG genotype was considered to be a protective genotype in atopic dermatitis [84] and also in case of *Candida* colonization in diabetic patients [51]. Conversely, in these studies subjects carrying the CC genotype were at a greater risk of aquiring infection. Recently, it has been suggested that the C allele of c.-44C>G SNP probably abrogates NF-κB-dependent *DEFB1* upregulation [85].

These earlier observations are consistent with our present finding that the GG genotype could also be protective in diabetes, and the presence of CC genotype might be connected with lower expression of human β1-defensin. Among 257 patients with diabetes, only 6 (2%) were GG homozygotes, and 61% of the patients were CC homozygotes, comparing with 45% of CC homozygotes in control group. Furthermore, the number of GG homozygotes was even less (1%) in nephropathy and neuropathy. These observations draw

attention to the importance of *DEFB1* polymorphisms in diabetes, especially in case of nephropathy and neuropathy. High blood glucose itself can result in low levels of β-defensin [35] and as it was earlier mentioned, its expression might be downregulated in humans carrying the C allele of c.-44C>G polymorphism. It is noteworthy that insulin is also an important factor mediating HBD-1 expression [12].

Taken together, in our study elevated levels of α-defensin (HNP1-3) was observed in type 1 and type 2 diabetes, and this increase was more pronounced in diabetic complications. However, correlation of circulating HNP1-3 levels with *DEFA1/DEFA3* copy number was absent. Similarly, no correlation between mRNA expression and copy number variations was found. Further studies are needed to explore whether the elevated α-defensin levels of the plasma in diabetes are causally linked to this disease and its complications, or are simply the consequences of the degranulation of neutrophils in pathologic conditions. According to our results, elevated HNP1-3 levels might not be genetically determined, or at least they are independent from the copy number variation of the *DEFA1/DEFA3* genes. In contrast, the CC genotype, and the C allele of c.-44C>G SNP in the promoter region of *DEFB1* gene was more frequent among diabetic patients than in healthy controls, which drew attention to the genetic background of a potentially impaired function of hBD1 in diabetes. These data support the hypothesis that both α- and β-defensins might have important roles in the pathogenesis of diabetes and diabetic complications.

4.2. CTRC REGULATES AUTOACTIVATION OF MOUSE TRYPSINOGENS VIA CLEAVAGE OF THE AUTOLYSIS LOOP

4.2.1. Genetic mouse models of chronic pancreatitis

Available mouse models of acute and chonic pancreatitis has been reviewed in a recent publication by Lerch and Gorelick [59]. In the past decade there were several attempts to create mouse models, which develop chronic pancreatitis due to different genetic manipulations. Dimagno et al. described a *CFTR* knock out mouse model in the C57BL/6 background, which had mild pancreatic insufficiency, and developed more severe pancreatitis in response to cerulein injenction compared to wild type mice [27].

Rat elastase promoter controlled human interleukin-1β (IL-1β) expression in mice resulted in chronic pancreatitis with early onset and severe fibrosis. In this model T-cell dominated inflammatory response was seen together with increased expression of other cytokines (TNF-α), chemokines (CXCL1, SDF1), growth factors (TGF-β1), metalloproteases (MMP2, 7, 9, and TIMP1) and cyclooxigenase 2. These observations generally suggest that

IL-1β might have a major role in the persistent activation of the immune system leading to chronic pancreatitis. It is important to mention that there was no evidence whether these mice developed diabetes. Interlukin-1β is a well-described activator of pancreatic stellate cells, and also an inflammatory cytokine of the innate immune system. Cytokine polymorphisms can affect the immune response, and were shown to play an important role in the pathogenesis of pancreatitis [68].

Liver X receptors (LXRs) α and β are nuclear oxysterol receptors with a key role in cholesterol, triglyceride, and glucose metabolism and also control the expression of water transporter aquaporin-1. LXRβ−/− male and female mice developed pancreatic exocrine insufficiency at 11 month of age [36].

None of the models above tried to make an attempt to manipulate genes of digestive enzymes. Human cationic trypsinogen (*PRSS1*), chymotrypsinogen C (*CTRC*) and carboxypeptidase A1 (*CPA1*) are known to have a role in the development of pancreatitis according to described plethora of biochemical and clinical studies [72, 89, 107, 116, 117]. Transgenic mice carrying the coding DNA for human cationic trypsinogen with the p.R122H mutation (see Figure 1B and Suppl. Figure 1) did not develop spontaneous pancreatitis, although small differences in the pathological responses were noted when pancreatitis was artificially induced [99]. In contrast, when mice were made transgenic with the p.R122H mutation introduced into mouse trypsinogen isoform T8 (Suppl. Figure 2B), the resulting animals developed acute and eventually chronic pancreatitis [7], however any replication study with this last model has not been published since 2006. It is unclear whether the observed phenotype was related to the expression of the mutant trypsinogen. Nonetheless, this thesis raises the question whether the biochemical effects of the p.R122H mutation are similar in the context of mouse and human trypsinogens and whether we can utilize mouse trypsinogens to model the human condition. Although considerable progress has been made in clarifying the mechanism of *PRSS1* mutations at the biochemical level, until this time, only the two publications above [7, 99] documented attempts to generate such models. Animal models that recapitulate the characteristics of human hereditary pancreatitis are still lacking.

Genetic deletion of mouse T7 was recently shown to abolish intra-acinar trypsinogen activation in response to hyperstimulation with cerulein; while severity of acute pancreatitis was somewhat decreased but not diminished [25]. Furthermore, development of cerulein-induced chronic pancreatitis was unaffected by the absence of T7 [91]. These observations seem to call into question the direct role of trypsinogen in the development of pancreatitis. However, a more likely explanation for the apparent contradiction is that the

hyperstimulation model employed in these studies does not mimic the pathological pathway associated with human hereditary pancreatitis.

We wanted to clarify whether introduction of trypsinogen mutations associated with human hereditary pancreatitis into mouse trypsinogens would offer a viable approach to model hereditary pancreatitis in mice. Therefore, identification of the major trypsinogen isoforms expressed by the mouse pancreas and characterization of their regulation of autoactivation by mouse Ctrc was necessary.

4.2.2. Trypsinogens expressed by the mouse pancreas

Investigating the commonly used outbred mouse strain CD-1, we found that only four trypsinogen isoforms, T7, T8, T9 and T20, are expressed to high levels (Figure 2) in the mouse pancreas, even though the mouse genome contains 20 trypsinogen genes, of which 11 are potentially functional (Suppl. Figure 1). The cationic isoform T7 was deleted in the C57BL/6 strain and judging from the residual trypsinogen content the authors suggested that T7 contributes 60% of total mouse trypsinogens [25, 91]. In our investigations we found smaller values (41%), however, these difference seem to fall within experimental error and may represent strain-specificity. In our experiments we used unstimulated mouse pancreas and it is possible, even likely, that upon hormonal stimulation, the trypsinogen expression pattern may change, as shown previously for rat p23, the ortholog of mouse T4 and T5, which becomes drastically upregulated upon cerulein stimulation [64]. Marked upregulation of T5 was observed in a knock-out mouse strain deficient in interferon regulatory factor 2 [44].

4.2.3. Biochemical characteristics of mouse trypsinogens

Autoactivation of mouse trypsinogens T7, T8 and T9 was comparable, whereas T20 autoactivated more slowly, particularly in 1 mM calcium (Figure 9). Surprisingly, regulation of autoactivation by mouse Ctrc was isoform specific and mechanistically different from the actions of human CTRC on human cationic trypsinogen. Thus, Ctrc-mediated cleavage of the activation peptide was observed only with the T7 isoform, however, this N-terminal processing had no effect on autoactivation. Cleavage of the Leu81-Glu82 peptide bond in the calcium binding loop was detectable in T7 but was inefficient and resulted in minimal degradation, when compared to the effect of human CTRC on human cationic trypsinogen. Slow cleavage of the Leu81-Glu82 peptide bond was also seen in T8 and T9, whereas isoform T20 was not cleaved by Ctrc.

In contrast, isoforms T8 and T9 were rapidly cleaved at the Phe150-Gly151 peptide bond in the autolysis loop and this cleavage resulted in marked inhibition of autoactivation without degradation. The Phe150-Gly151 peptide bond was also cleaved by Ctrb at a 7-fold slower rate. However, considering that Ctrb is the most abundant chymotrypsin in the mouse pancreas, physiological regulation of activation of T8 and T9 may be also dependent on Ctrb.

The vast majority of mammalian trypsinogens do not contain Phe in position 150 in their primary amino acid sequence. Trypsinogens of some rodents has been investigated either in a functional study (guinea pig -*Cavia porcellus*- [78]), or only at the genomic level (rabbit -*Oryctolagus cuniculus*- [6]), but the Phe150 residue has not been found in the investigated rodent trypsinogen isoforms. According to the online genomic database of NCBI (http://www.pubmed.org) some rodent species (rat -*Rattus norvegicus*-, chinese hamster -*Cricetulus griseus*- and naked mole rat -*Heterocephalus glaber*-) have at least one possible trypsinogen isoform which carries a Phe residue at the 150th amino acid position. Surprisingly, in one marsupial, the tasmanian devil -*Sarcophilus harrisii*- and also, in some primates (Rhesus macaque -*Macaca mulatta*- , gorilla -*Gorilla gorilla gorilla*- and the olive baboon -*Papio anubis*-) Phe150 can be found in the primary structure of one of their potentially functional trypsinogen isoforms. More interestingly, human mesotrypsinogen also contains Phe150 (Suppl. Figure 1) and cleavage at this site by human CTRC was demonstrated previously [107], suggesting that activation of mesotrypsinogen may be under a similar regulation. Human anionic and cationic trypsinogens contain Ser at position 150, but mutation S150F of human cationic trypsinogen confers sensitivity to CTRB2-mediated cleavage of the autolysis loop, which inhibits autoactivation in a manner that is similar to the Ctrc-dependent inhibition of T8 and T9 in the mouse.

The Ctrc-dependent inhibition of autoactivation of T8 and T9 trypsinogens may have evolved as a protective mechanism to curtail unwanted trypsinogen activation in the pancreas. In this regard, this is highly analogous to the regulation of human trypsinogens by human CTRC even though mechanistic details are dissimilar. Interestingly, we found that cleavage of the Phe150-Gly151 peptide bond in T8 and T9 trypsinogens also inhibits activation by enteropeptidase, the physiological trypsinogen activator in the duodenum. Although inhibition of digestive enzyme activation in the gut may seem counterintuitive, this chymotrypsin-dependent feed-back mechanism likely ensures that intestinal trypsinogen activation proceeds with a slower, more prolonged kinetics which may be more favorable for food digestion.

Intra-acinar cell activation of trypsinogen in cytoplasmic vesicles of autophagic origin is an early event in experimental models of acute pancreatitis. Genetic deletion of T7 was recently shown to abolish intra-acinar trypsinogen activation in response to hyperstimulation with cerulein; a somewhat perplexing observation as other trypsinogen isoforms could have potentially be activated [25, 91]. The results presented in this thesis offer a plausible explanation for this puzzle. When trypsinogen activation occurs, isoforms T8 and T9 may be inhibited in a Ctrc- or Ctrb-dependent manner, whereas T7 is relatively insensitive to chymotryptic regulation. Due to its lower concentration and poor activation, isoform T20 is unlikely to contribute to intra-acinar trypsinogen activation to a detectable extent. Taken together, the biochemical properties of mouse trypsinogens suggest that T7 is the isoform responsible for intra-acinar trypsinogen activation, which is the exact conclusion that Dawra et al offered in their study [25].

Finally, our data argue that the previously published mouse model in which a T8 transgene carrying the p.R122H mutation was introduced could not have developed the described phenotypic changes as a result of a mutation-dependent increase in trypsinogen activation [7]. We found that mutation p.R122H did not affect inhibition of autoactivation by Ctrc in T8 trypsinogen, which stands in contrast to the robust negative effect of this mutation on CTRC-dependent degradation of human cationic trypsinogen [106]. Thus, it seems more likely that in the published mouse model increased gene dosage or nonspecific effects of the transgene may have been the cause of the described pancreas pathology.

5. SUMMARY AND NEW RESULTS

I.

1. We confirmed earlier findings of elevated HNP 1-3 plasma levels in patients with diabetes mellitus compared to healthy controls. Furthermore, we found that diabetic patients with nephropathy, neuropathy, or cardiovascular complications all had significantly higher HNP1-3 levels compared to diabetic patients without complications and also to healthy controls.
2. Our results demonstrated that the median gene copy number of human *DEFA1/DEFA3* gene is 10 per diploid genome in the Hungarian population; not only among controls but also in diabetic patients. *DEFA1/DEFA3* gene copy numbers did not correlate with mRNA expression levels in peripheral leukocytes, nor with the α-defensin (HNP 1-3) levels measured in the plasma of peripheral blood. Therefore the elevated HNP 1-3 levels might not be genetically determined, or at least independent of the copy number variation of the *DEFA1/DEFA3* genes.
3. The C allele of the c.-44C>G SNP located in the promoter region of the *DEFB1* gene was found to be more frequent among diabetic patients than in healthy controls, indicating that impaired human β-defensin function might have a role in the development of diabetes mellitus.

II.

1. There are 4 trypsinogen isoforms (T7, T8, T9 and T20) expressed at high levels in the mouse pancreas under physiological conditions. In 1 mM CaCl2, at pH=8.0, only T7, T8 and T9 autoactivated, while T20 did not autoactivate.
2. Ctrc and Ctrb almost completely inhibited autoactivation of T8 and T9 isoforms by enzymatic cleavage of their autolysis loop, but had no significant effect on the autoactivation of T7 isoform.
3. Introduction of the p.R123H mutation in T7, or the analogous p.R122H mutation in T8, did not significantly change the autoactivation characteristics of mouse trypsinogens. Therefore, the biochemical characteristics of these mutants did not mimic the pathogenic phenotype of the p.R122H mutation in human cationic trypsinogen.

6. REFERENCES

1. Aldred PM, Hollox EJ, Armour JA. (2005) Copy number polymorphism and expression level variation of the human alpha-defensin genes DEFA1 and DEFA3. *Hum. Mol. Genet.* **14**, 2045–2052.

2. American Diabetes Association. (2010) Diagnosis and classification of diabetes mellitus. *Diabetes Care* **33** (Suppl. 1), S62–S69.

3. American Diabetes Association. (2013) Diagnosis and classification of diabetes mellitus. *Diabetes Care* **36** (Suppl. 1) S64-S74

4. Andersen BN, Pedersen NT, Scheel J, Worning H. (1982) Incidence of alcoholic chronic pancreatitis in Copenhagen. *Scand J Gastroenterol* **17**, 247-52.

5. Andersen DH. (1938) Cystic fibrosis of the pancreas and its relation to celiac disease. *Am. J. Dis. Child.* **56**, 344.

6. Antonacci R, Giannico F, Ciccarese S, Massari S. (2014) Genomic characteristics of the T cell receptor (TRB) locus in the rabbit (Oryctolagus cuniculus) revealed by comparative and phylogenetic analyses. *Immunogenetics* **66**, 255-66.

7. Archer H, Jura N, Keller J, Jacobson M, Bar-Sagi D. (2006) A mouse model of hereditary pancreatitis generated by transgenic expression of R122H trypsinogen. *Gastroenterology* **131**, 1844-1855

8. Arora P, Garcia-Bailo B, Dastani Z, Brenner D, Villegas A, Malik S, Spector TD, Richards B, El-Sohemy A, Karmali M, Badawi A. (2011) Genetic polymorphisms of innate immunity-related inflammatory pathways and their association with factors related to type 2 diabetes. *BMC Med. Genet.* **12**, 95.

9. Awata T, Matsumoto C, Urakami T, Hagura R, Amemiya S, Kanazawa Y. (1994) Association of polymorphism in the interferon gamma gene with IDDM. *Diabetologia*, **37**, 1159-62.

10. Badawi A, Klip A, Haddad P, Cole DE, Bailo BG, El-Sohemy A, Karmali M. (2010) Type 2 diabetes mellitus and inflammation: Prospects for biomarkers of risk and nutritional intervention. *Diabetes Metab. Syndr. Obes.* **3**, 173-86.

11. Banting FG and Best CH. (1922) Internal secretion of Pancreas**.** *Jour. Lab. & Clin. Med.* **7**, 251-266.

12. Barnea M, Madar Z, Froy O. (2008) Glucose and insulin are needed for optimal defensin expression in human cell lines. *Biochem. Biophys. Res. Commun.* **367**, 452-456.

13. Baschal EE, Eisenbarth GS. (2008) Extreme genetic risk for type 1A diabetes in the post-genome era. *Journal of Autoimmunity* **31**, 1–6

14. Bergholdt R, Karlsen AE, Johannesen J, Hansen PM, Dinarello CA, Nerup J, Pociot F. (1995) Characterization of polymorphisms of an interleukin 1 receptor type 1 gene (IL1RI) promotor region (P2) and their relation to insulin-dependent diabetes mellitus (IDDM). The Danish Study Group of Diabetes in Childhood. *Cytokine* **7**, 727-33.

15. Bilan PJ, Samokhvalov V, Koshkina A, Schertzer JD, Samaan MC, Klip A. (2009) Direct and macrophage-mediated actions of fatty acids causing insulin resistance in muscle cells. *Arch. Physiol. Biochem.* **115**, 176-90

16. Blakemore AI, Cox A, Gonzalez AM, Maskil JK, Hughes ME, Wilson RM, Ward JD, Duff GW. (1996) Interleukin-1 receptor antagonist allele (IL1RN*2) associated with nephropathy in diabetes mellitus. *Hum. Genet.* **97**, 369-74.

17. Boman HG (2003) Antibacterial peptides: basic facts and emerging concepts. *J. Intern. Med.* **254**, 197-215

18. Boocock GR, Morrison JA, Popovic M, Richards N, Ellis L, Durie PR, Rommens JM. (2003) Mutations in SBDS are associated with Shwachman-Diamond syndrome. *Nat. Genet.* **33**, 97-101.

19. Bowdish DME, Davidson DJ, Hancock REW. (2005) A re-evaluation of the role of host defence peptides in mammalian immunity. *Curr. Protein Pept. Sci.* **6**, 35-51.

20. Chen H, Xu Z, Peng L, Fang X, Yin X, Xu N, Cen P. (2006) Recent advances in the research and development of human defensins. *Peptides* **27**, 931-940.

21. Chen QX., Hakimi M, Wu S, Jin Y, Cheng B, Wang HH, Xie G, Ganz T, Linzmeier RM, Fang XM. (2010) Increased Genomic Copy Number of DEFA1 / DEFA3 Is Associated with Susceptibility to Severe Sepsis in Chinese Han Population. *Anesthesiology* 2010; **112**, 1428-1834.

22. Chertov O, Yang D, Howard OMZ, Oppenheim JJ. (2000) Leukocyte granulate proteins mobilize innate host defenses and adaptive immune responses. *Immunol. Rev.* **177**, 68-78.

23. Chiari H (1896) Über Selbstverdauung des menschlichen Pankreas. *Z. Heilkd.* **17**, 69-96. [German]

24. Comfort MW, Steinberg AG. (1952) Pedigree of a family with hereditary chronic relapsing pancreatitis. *Gastroenterology* **21**, 54-63.

25. Dawra R, Sah RP, Dudeja V, Rishi L, Talukdar R, Garg P, Saluja AK. (2011) Intra-acinar trypsinogen activation mediates early stages of pancreatic injury but not inflammation in mice with acute pancreatitis. *Gastroenterology* **141**, 2210-2217

26. De Smet K and Contreras R. (2005) Human antimicrobial peptides: defensins, cathelicidins and histatins. *Biotechnol. Lett.* **27**, 1337-1347.

27. Dimagno MJ, Lee SH, Hao Y, Zhou SY, McKenna BJ, Owyang C. (2005) A proinflammatory, antiapoptotic phenotype underlies the susceptibility to acute pancreatitis in cystic fibrosis transmembrane regulator (-/-) mice. *Gastroenterology* **129**, 665-81.

28. Dork T, Stuhrmann M (1998) Polymorphisms of the human beta-defensin-1 gene. *Mol. Cell. Probes* **12**, 171-173.

29. D'Silva S, Xiao X, Lowe ME. (2007) A polymorphism in the gene encoding procolipase produces a colipase, Arg92Cys, with decreased function against long-chain triglycerides. *J. Lipid. Res.* **48**, 2478-84.

30. Durr M, Peschel A. (2002) Chemokines meet defensins: the merging concepts of chemoattractans and antimicrobial peptides in host defense. *Infect. Immun.* **70**, 6515-6517

31. Estivalet AA, Leiria LB, Dora JM, Rheinheimer J, Bouças AP, Maia AL, Crispim D. (2011) D2 Thr92Ala and PPARγ2 Pro12Ala polymorphisms interact in the modulation of insulin resistance in type 2 diabetic patients. *Obesity (Silver Spring)*. **19**, 825-32.

32. Ewald N, Kaufmann C, Raspe A, Kloer HU, Bretzel RG, Hardt PD. (2012) Prevalence of diabetes mellitus secondary to pancreatic diseases (type 3c). *Diabetes Metab. Res. Rev.* **28**, 338-42.

33. Fajans SS, Bell GI, Polonsky KS. (2001) Molecular mechanisms and clinical pathophysiology of maturity-onset diabetes of the young. *N. Engl. J. Med*. **345**, 971-80.

34. Fajans SS, Bell GI. (2011) MODY: history, genetics, pathophysiology, and clinical decision making. *Diabetes Care*. **34**, 1878-84.

35. Froy O., Hananel A., Chapnik N, Madar Z. (2007) Differential effect of insulin treatment on decreased levels of beta-defensins and Toll-like receptors in diabetic rats. *Molecular Immunology* **44**, 796-802

36. Gabbi C, Kim HJ, Hultenby K, Bouton D, Toresson G, Warner M, Gustafsson JA. (2008) Pancreatic exocrine insufficiency in LXRbeta-/- mice is associated with a reduction in aquaporin-1 expression. *Proc. Natl. Acad. Sci. U S A*. **105**, 15052-7.

37. Ganz T. (1987) Extracellular release of antimicrobial defensins by human polymorphonuclear leukocytes *Infect. Immun.* **55**, 568-571.

38. Ganz T. (2003) Defensins: antimicrobial peptides of innate immunity. *Nature Reviews Immunology* **3**, 710-720.

39. Glusman G, Rowen L, Lee I, Boysen C, Roach JC, Smit AF, Wang K, Koop BF, Hood L. (2001) Comparative genomics of the human and mouse T cell receptor loci. *Immunity* **15**, 337-349

40. Goobie S, Popovic M, Morrison J, Ellis L, Ginzberg H, Boocock GR, Ehtesham N, Bétard C, Brewer CG, Roslin NM, Hudson TJ, Morgan K, Fujiwara TM, Durie PR, Rommens JM. (2001) Shwachman-Diamond syndrome with exocrine pancreatic dysfunction and bone marrow failure maps to the centromeric region of chromosome 7. *Am. J. Hum. Genet.* **68**, 1048-54.

41. Gropp R, Frye M, Wagner TO, Bargon J (1999). Epithelial defensins impair adenoviral infection: implication for adenovirus-mediated gene therapy. *Hum. Gene Ther.* **10**, 957–964.

42. Guimarães RL, Segat L, Rocha CR, Brandão LA, Zanin V, Araujo J, Naslavsky MS, de Lima Filho JL, Crovella S. (2009) Functional polymorphisms of DEFB1 gene in type 1 diabetes Brazilian children. *Autoimmunity* **42**, 406-13.

43. Hardt PD, Hauenschild A, Nalop J, Marzeion AM, Jaeger C, Teichmann J, Bretzel RG, Hollenhorst M, Kloer HU; S2453112/S2453113 Study Group. (2003) High prevalence of exocrine pancreatic insufficiency in diabetes mellitus. A multicenter study screening fecal elastase 1 concentrations in 1,021 diabetic patients. *Pancreatology* **3**, 395-402.

44. Hayashi H, Kohno T, Yasui K, Murota H, Kimura T, Duncan GS, Nakashima T, Yamamoto K, Katayama I, Ma Y, Chua KJ, Suematsu T, Shimokawa I, Akira S, Kubo Y, Mak TW, Matsuyama T. (2011) Characterization of dsRNA-induced pancreatitis model reveals the regulatory role of IFN regulatory factor 2 (Irf2) in trypsinogen5 gene transcription. *Proc. Natl. Acad. Sci. USA* **108**, 18766-18771

45. Henrichsen CN, Chaignat E, Reymond A. (2009) Copy number variants, diseases and gene expression. *Human Molecular Genetics* **18**, R1-R8.

46. Hotamisligil GS. (2006) Inflammation and metabolic disorders. *Nature* **444**, 860-7.

47. Howes N, Lerch MM, Greenhalf W, Stocken DD, Ellis I, Simon P, Truninger K, Ammann R, Cavallini G, Charnley RM, Uomo G, Delhaye M, Spicak J, Drumm B, Jansen J, Mountford R, Whitcomb DC, Neoptolemos JP; European Registry of Hereditary Pancreatitis and Pancreatic Cancer (EUROPAC). (2004) Clinical and genetic characteristics of hereditary pancreatitis in Europe. *Clin. Gastroenterol. Hepatol.* **2**, 252-61.

48. Jermendy A, Körner A, Kovács M, Madácsy L, Cseh K. (2011) PPAR-gamma2 pro12Ala polymorphism is associated with post-challenge abnormalities of glucose homeostasis in children and adolescents with obesity. *J. Pediatr. Endocrinol. Metab.* **24**, 55-9.

49. Johanson A, Blizzard R. (1971) A syndrome of congenital aplasia of the alae nasi, deafness, hypothyroidism, dwarfism, absent permanent teeth, and malabsorption. *J. Pediatr.* **79**, 982-7.

50. Joseph G, Tarnow L, Astrup AS, Hansen TK, Parving HH, Flyvbjerg A, Frystyk J. (2008) Plasma alpha-defensin is associated with cardiovascular morbidity and mortality in type 1 diabetic patients. *J. Clin. Endocrinol. Metab.* **93**, 1470-1475.

51. Jurevic RJ, Bai M, Chadwick RB, White TC, Dale BA. (2003) Single-nucleotide polymorphisms (SNPs) in human β-defensin 1: High-throughput SNP assays and association with Candida carriage in type I diabetics and nondiabetic controls. *J. Clin. Microbiol.* **41**, 90-6.

52. Kerem B, Rommens JM, Buchanan JA, Markiewicz D, Cox TK, Chakravarti A, Buchwald M, Tsui LC. (1889) Identification of the cystic fibrosis gene: genetic analysis. *Science* **245**,1073-80.

53. Király O, Guan L, Sahin-Tóth M. (2011) Expression of recombinant proteins with uniform N-termini. *Methods Mol. Biol*. **705**, 175-194

54. Király O, Guan L, Szepessy E, Tóth M, Kukor Z, and Sahin-Tóth M. (2006) Expression of human cationic trypsinogen with an authentic N terminus using intein-mediated splicing in aminopeptidase P deficient Escherichia coli. *Protein Expr. Purif.* **48**, 104-111

55. Kukor Z, Tóth M, Pál G, Sahin-Tóth M. (2002) Human cationic trypsinogen. Arg117 is the reactive site of an inhibitory surface loop that controls spontaneous zymogen activation. *J. Biol. Chem*. **277**, 6111-6117

56. Kukor Z, Tóth M, Sahin-Tóth M. (2003) Human anionic trypsinogen: properties of autocatalytic activation and degradation and implications in pancreatic diseases. *Eur. J. Biochem*. **270**, 2047-2058

57. Lanng S, Thorsteinsson B, Pociot F, Marshall MO, Madsen HO, Schwartz M, Nerup J, Koch C. (1993) Diabetes mellitus in cystic fibrosis: genetic and immunological markers. *Acta Paediatr.* **82**, 150-4.

58. Lengyel Z, Pál G, Sahin-Tóth M. (1998) Affinity purification of recombinant trypsinogen using immobilized ecotin. *Protein Expr. Purif.* **12**, 291–294

59. Lerch MM, Gorelick FS. (2013) Models of acute and chronic pancreatitis. *Gastroenterology* **144**, 1180-93.

60. Lindner I, Helwig U, Rubin D, Li Y, Fisher E, Boeing H, Möhlig M, Spranger J, Pfeiffer A, Hampe J, Schreiber S, Döring F, Schrezenmeir J. (2005) Putative association between a new polymorphism in exon 3 (Arg109Cys) of the pancreatic colipase gene and type 2 diabetes mellitus in two independent Caucasian study populations. *Mol. Nutr. Food Res.* **49**, 972-6.

61. Linzmeier RM, Ganz T. (2005) Human defensin gene copy number polymorphisms: comprehensive analysis of independent variation in α- and β-defensin regions at 8p22-p23. *Genomics* **86**, 423-430.

62. Loughrey BV, Maxwell AP, Fogarty DG, Middleton D, Harron JC, Patterson CC, Darke C, Savage DA. (1998) An interluekin 1B allele, which correlates with a high secretor phenotype, is associated with diabetic nephropathy. *Cytokine* **10**, 984-8.

63. Lowenfels AB, Maisonneuve P, Cavallini G, Ammann RW, Lankisch PG, Andersen JR, Dimagno EP, Andrén-Sandberg A, Domellöf L. (1993) Pancreatitis and the risk of pancreatic cancer. International Pancreatitis Study *Group. N. Engl. J. Med.* **328**, 1433-7.

64. Lütcke H, Rausch U, Vasiloudes P, Scheele GA, Kern HF. (1989) A fourth trypsinogen (P23) in the rat pancreas induced by CCK. *Nucleic Acids Res.* **17**, 6736

65. Maisonneuve P, Lowenfels AB, Müllhaupt B, Cavallini G, Lankisch PG, Andersen JR, Dimagno EP, Andrén-Sandberg A, Domellöf L, Frulloni L, Ammann RW. (2005) Cigarette smoking accelerates progression of alcoholic chronic pancreatitis. *Gut* **54**, 510–4.

66. Major J, Czelecz J, Daoud S, Molnár E, Gyömörei B, Czakó L, Szabó I (2012) Recidíváló akut pancreatitis családon belüli halmozódása - Az első kationos tripszinogén gén mutációt hordozó magyar család - Esetismertetés *Gyermekgyógyászat* **63**, 21-24 [Hungarian]

67. Maroux S, Desnuelle P. (1969) On some autolyzed derivatives of bovine trypsin. *Biochim. Biophys. Acta* **181**, 59–72

68. Marrache F, Tu SP, Bhagat G, Pendyala S, Osterreicher CH, Gordon S, Ramanathan V, Penz-Osterreicher M, Betz KS, Song Z, Wang TC. (2008) Overexpression of interleukin-1beta in the murine pancreas results in chronic pancreatitis. *Gastroenterology* 135, 1277-87.

69. Mayerle J, Hoffmeister A, Werner J, Witt H, Lerh MM, Mössner J. (2013) Chronic pancreatitis-definition, etiology, investigation and treatment. *Dtsch. Arztebl. Int.* **110**, 387-93.

70. Medzhitov R, Janeway C Jr. (2000) Innate immunity. *N. Engl. J. Med*. **343**, 338-44.

71. Metcalfe KA, Hitman GA, Pociot F, Bergholdt R, Tuomilehto-Wolf E, Tuomilehto J, Viswanathan M, Ramachandran A, Nerup J. (1996) An association between type 1 diabetes and the interleukin-1 receptor type 1 gene. The DiMe Study Group. Childhood Diabetes in Finland. *Hum. Immunol.* **51**, 41-8.

72. Nemoda Z, Sahin-Tóth M. (2006) Chymotrypsin C (caldecrin) stimulates autoactivation of human cationic trypsinogen. *J. Biol. Chem*. **281**, 11879-86.

73. Neuwirth A, Dobeš J, Oujezdská J, Ballek O, Benesova M, Sumink Z, Vcelakova J, Kolouskova S, Obermannova B, Kolátr M, Stechova K, Filipp D. (2012) Eosinophils from patients with type 1 diabetes mellitus express high level of myeloid alpha-defensins and myeloperoxidase. *Cellular Immunol.* **273**, 158-163

74. Nøjgaard C. Prognosis of acute and chronic pancreatitis - a 30-year follow-up of a Danish cohort. (2010) *Dan. Med. Bull.* **57**, B4228.

75. Ohmura K, Kohno N, Kobayashi Y, Yamagata K, Sato S, Kashiwabara S, Baba T. (1999) A homologue of pancreatic trypsin is localized in the acrosome of mammalian sperm and is released during acrosome reaction. *J. Biol. Chem.* **274**, 29426-29432

76. Oláh A, Ruszinkó V, Garab E, Horváth V, Vasi I. (2001) Cholestasist okozó krónikus gyermekkori pancreatitisek műtéti megoldása és genetikai vizsgálata. *Magyar Sebészet* **54**, 23–26. [Hungarian]

77. Oppenheim JJ, Yang D. (2005) Alarmins: chemotactic activators of immune responses. *Curr. Opin. Immunol.* **17**, 359-365.

78. Ózsvári B, Hegyi P, Sahin-Tóth M. (2008) The guinea pig pancreas secretes a single trypsinogen isoform, which is defective in autoactivation. *Pancreas* **37**, 182-8

79. Pál G, Sprengel G, Patthy A, Gráf L. (1994) Alteration of the specificity of ecotin, an E. coli serine proteinase inhibitor, by site directed mutagenesis. *FEBS Lett*. **342**, 57-60

80. Papayannopoulos V, Zychlinsky A. (2009) NETs: a new strategy for using old weapons. *Trends Immunol.* **30**, 513-21.

81. Pazgier M, Hoover DM, Yang D, Lu W, Lubkowski J. (2006) Human beta-defensins. *Cell. Mol. Life Sci.* **63**, 1294-1313.

82. Pociot F, Briant L, Jongeneel CV, Mölvig J, Worsaae H, Abbal M, Thomsen M, Nerup J, Cambon-Thomsen A. (1993) Association of tumor necrosis factor (TNF) and class II major histocompatibility complex alleles with the secretion of TNF-alpha and TNF-beta by human mononuclear cells: a possible link to insulin-dependent diabetes mellitus. *Eur. J. Immunol.* **23**, 224-31.

83. Pociot F, Veijola R, Johannesen J, Hansen PM, Lorenzen T, Karlsen AE, Reijonen H, Knip M, Nerup J. (1997) Analysis of an interferon-gamma gene (IFNG) polymorphism in Danish and Finnish insulin-dependent diabetes mellitus (IDDM) patients and control subjects. Danish Study Group of Diabetes in Childhood. *J. Interferon Cytokine Res.* **17**, 87-93.

84. Prado-Montes de Oca E, García-Vargas A, Lozano-Inocencio R, Gallegos-Arreola MP, Sandoval-Ramírez L, Dávalos-Rodríguez NO, Figuera LE (2007) Association of beta-defensin 1 single nucleotide polymorphisms with atopic dermatitis. *Int. Arch. Allergy Immunol.* **142**, 211-218.

85. Prado-Montes de Oca E, Velarde-Félix JS, Ríos-Tostado JJ, Picos-Cárdenas JP, Figuera LE. (2009) SNP 668C(-44) alters of NKκB1 putative binding site in non-coding strand of human β-defensin 1 (DEFB1) and is associated with lempromatous leprosy. *Infection, Genetics, and Evolution* **9**, 612-625.

86. Quinn K, Henriques M, Parker T, Slutsky AS, Zhang H. (2008) Human neutrophil peptides: a novel potential mediator of inflammatory cardiovascular diseases. *Am. J. Physiol. Heart Circ. Physiol.* **295**, H1817-H1824.

87. Raeder H, Johansson S, Holm PI, Haldorsen IS, Mas E, Sbarra V, Nermoen I, Eide SA, Grevle L, Bjørkhaug L, Sagen JV, Aksnes L, Søvik O, Lombardo D, Molven A, Njølstad PR. (2006) Mutations in the CEL VNTR cause a syndrome of diabetes and pancreatic exocrine dysfunction. *Nat. Genet.* **38**, 54-62.

88. Rosendahl J, Bödeker H, Mössner J, Teich N. (2007) Hereditary chronic pancreatitis. *Orphanet J. Rare. Dis* **2**, 1.

89. Rosendahl J, Witt H, Szmola R, Bhatia E, Ozsvári B, Landt O, Schulz HU, Gress TM, Pfützer R, Löhr M, Kovacs P, Blüher M, Stumvoll M, Choudhuri G, Hegyi P,te Morsche RH, Drenth JP, Truninger K, Macek M Jr, Puhl G, Witt U, Schmidt H, Büning C, Ockenga J, Kage A, Groneberg DA, Nickel R, Berg T, Wiedenmann B, Bödeker H, Keim V, Mössner J, Teich N, Sahin-Tóth M. (2008) Chymotrypsin C (CTRC) variants that diminish activity or secretion are associated with chronic pancreatitis. *Nat. Genet*. **40**, 78-82.

90. Ruszinkó V, Ellis I. (2001) Krónikus Pancreatitis Gyermekkorban. *Gyermekgyógyászat* **52**, 290–293. [Hungarian]

91. Sah RP, Dudeja V, Dawra RK, Saluja AK. (2013) Caerulein-induced chronic pancreatitis does not require intra-acinar activation of trypsinogen in mice. *Gastroenterology*, **144**, 1076-1085.

92. Sahin-Tóth M. (1999) Hereditary pancreatitis-associated mutation Asn21→Ile stabilizes rat trypsinogen in vitro. *J. Biol. Chem*. **274**, 29699-29704

93. Sahin-Tóth M. (2000) Human cationic trypsinogen. Role of Asn-21 in zymogen activation and implications in hereditary pancreatitis. *J. Biol. Chem*. **275**, 22750-22755

94. Sahin-Tóth M, Tóth M. (2000) Gain-of-function mutations associated with hereditary pancreatitis enhance autoactivation of human cationic trypsinogen. *Biochem. Biophys. Res. Commun*. **278**, 286-289

95. Saraheimo M, Forsblom C, Pettersson-Fernholm K, Flyvbjerg A, Groop PH, Frystyk J; FinnDiane Study Group (2008) Increased levels of alpha-defensin (-1, -2 and -3) in type 1 diabetic patients with nephropathy. *Nephrol. Dial. Transplant.* **23**, 914-918.

96. Saxena M, Srivastava N, Banerjee M. (2013) Association of IL-6, TNF-α and IL-10 gene polymorphisms with type 2 diabetes mellitus. *Mol. Biol. Rep*. **40**, 6271-9.

97. Scheele G, Bartelt D, Bieger W. (1981) Characterization of human exocrine pancreatic proteins by two-dimensional isoelectric focusing/sodium dodecyl sulfate gel electrophoresis. *Gastroenterology* **80**, 461-473

98. Scröder J-M (1999) Epithelial antimicrobial peptides: innate local host response elements. *Cell. Mol. Life Sci.* **56**, 32-46

99. Selig L, Sack U, Gaiser S, Klöppel G, Savkovic V, Mössner J, Keim V, Bödeker H. (2006) Characterisation of a transgenic mouse expressing R122H human cationic trypsinogen. *BMC Gastroenterol*. **6**, 30.

100. Selsted ME, Ouellette AJ. (2006) Mammalian defensins in the antimicrobial immune response, *Nat. Immunol.* **6**, 551–557.

101. Smith RL, Shaw E. (1969) Pseudotrypsin. A modified bovine trypsin produced by limited autodigestion. *J. Biol. Chem*. **244**, 4704–4712

102. Stevenson BJ, Hagenbüchle O, Wellauer PK. (1986) Sequence organisation and transcriptional regulation of the mouse elastase II and trypsin genes. *Nucleic Acids Res*. **14**, 8307-8330

103. Sun CQ, Arnold R, Fernandez-Golarz C, Parrish AB, Almekinder T, He J, Ho SM, Svoboda P, Pohl J, Marshall FF, Petros JA. (2006) Human beta-defensin-1, a potential chromosome 8p tumor suppressor: control of transcription and induction of apoptosis in renal cell carcinoma. *Cancer Res.* **66**, 8542-8549.

104. Szabó A, Héja D, Szakács D, Zboray K, Kékesi KA, Radisky ES, Sahin-Tóth M, Pál G. (2011) High affinity small protein inhibitors of human chymotrypsin C (CTRC) selected by phage display reveal unusual preference for P4' acidic residues. *J. Biol. Chem*. **286**, 22535-22545

105. Szabó A, Sahin-Tóth M. (2012) Determinants of chymotrypsin C cleavage specificity in the calcium-binding loop of human cationic trypsinogen. *FEBS J*. **279**, 4283-4292

106. Szabó A, Sahin-Tóth M. (2012) Increased activation of hereditary pancreatitis-associated human cationic trypsinogen mutants in presence of chymotrypsin C. *J. Biol. Chem.* **287**, 20701-20710

107. Szmola R, Sahin-Tóth M. (2007) Chymotrypsin C (caldecrin) promotes degradation of human cationic trypsin: identity with Rinderknecht's enzyme Y. *Proc. Natl. Acad. Sci. U S A.* **104**, 11227-32.

108. Tang YQ and Selsted ME. (1993) Characterization of the disulfide motif in BNBD-12, an antimicrobial beta-defensin peptide from bovine neutrophils. *J. Biol. Chem.* **268**, 6649–6653

109. Teich N, Rosendahl J, Tóth M, Mössner J, Sahin-Tóth M. (2006) Mutations of human cationic trypsinogen (PRSS1) and chronic pancreatitis. *Hum. Mutat.* **27**, 721-730

110. Tiszlavicz Z, Németh B, Fülöp F, Vécsei L, Tápai K, Ocsovszky I, Mándi Y. (2011) Different inhibitory effects of kynurenic acid and a novel kynurenic acid analogue on tumour necrosis factor-alpha (TNF-alpha) production by mononuclear cells, HMGB1 production by monocytes and HNP1-3 secretion by neutrophils. *Naunyn-Schmiedebergs Archives of Pharmacology* **383,** 447-455.

111. Todd JA, Bell JI, McDevitt HO. (1987) HLA-DQ beta gene contributes to susceptibility and resistance to insulin-dependent diabetes mellitus. *Nature* **329**, 599-604.

112. Von Mering and Minkowski. (1889) *Arch. f. exp. Path. u. Pharmakol* **XXVI 371**

113. Watanabe T, Ogasawara N. (1982) Purification and properties of multiple forms of mouse trypsinogen. *Biochim. Biophys. Acta* **717**, 439-444

114. Weinberg A, Krisanaprakornkit S, Dale BA (1998). Epithelial antimicrobial peptides: review and significance for oral applications. *Crit. Rev. Oral. Biol. Med.* **9**, 399–414.

115. Weyrich P, Albet S, Lammers R, Machicao F, Fritsche A, Stefan N, Häring HU. (2009) Genetic variability of procolipase associates with altered insulin secretion in non-diabetic Caucasians. *Exp. Clin. Endocrinol. Diabetes* **117**, 83-7.

116. Whitcomb DC, Gorry MC, Preston RA, Furey W, Sossenheimer MJ, Ulrich CD, Martin SP, Gates LK Jr, Amann ST, Toskes PP, Liddle R, McGrath K, Uomo G, Post JC, Ehrlich GD. (1996) Hereditary pancreatitis is caused by a mutation in the cationic trypsinogen gene. *Nat. Genet.* **14**, 141-5.

117. Witt H, Beer S, Rosendahl J, Chen JM, Chandak GR, Masamune A, Bence M, Szmola R, Oracz G, Macek M Jr, Bhatia E, Steigenberger S, Lasher D, Bühler F,Delaporte C, Tebbing J, Ludwig M, Pilsak C, Saum K, Bugert P, Masson E, Paliwal S, Bhaskar S, Sobczynska-Tomaszewska A, Bak D, Balascak I, Choudhuri G, Nageshwar Reddy D, Rao GV, Thomas V,

Kume K, Nakano E, Kakuta Y, Shimosegawa T, Durko L, Szabó A, Schnúr A, Hegyi P, Rakonczay Z Jr, Pfützer R,Schneider A, Groneberg DA, Braun M, Schmidt H, Witt U, Friess H, Algül H, Landt O, Schuelke M, Krüger R, Wiedenmann B, Schmidt F, Zimmer KP, Kovacs P,Stumvoll M, Blüher M, Müller T, Janecke A, Teich N, Grützmann R, Schulz HU, Mössner J, Keim V, Löhr M, Férec C, Sahin-Tóth M. (2013) Variants in CPA1 are strongly associated with early onset chronic pancreatitis. *Nat. Genet.* **45**, 1216-20.

118. Yang D, Biragyn A, Kwak LW, Oppenheim JJ. (2002) Mammalian defensins in immunity: more than just microbibidal. *Trends Imunol.* **23**, 291-296.

119. Zasloff M (2002). Antimicrobial peptides of multicellular organisms. *Nature* **415**, 389–395.

120. Zenker M, Mayerle J, Lerch MM, Tagariello A, Zerres K, Durie PR, Beier M, Hülskamp G, Guzman C, Rehder H, Beemer FA, Hamel B, Vanlieferinghen P, Gershoni-Baruch R, Vieira MW, Dumic M, Auslender R, Gil-da-Silva-Lopes VL, Steinlicht S, Rauh M, Shalev SA, Thiel C, Ekici AB, Winterpacht A, Kwon YT, Varshavsky A, Reis A. (2005) Deficiency of UBR1, a ubiquitin ligase of the N-end rule pathway, causes pancreatic dysfunction, malformations and mental retardation (Johanson-Blizzard syndrome). *Nat. Genet.* **37**, 1345-50.

121. Zhao C, Wang I, Lehrer RI. (1996) Widespread of beta-defensin hBD-1 in human secretory glands and epithelial cells. *FEBS Letters* **396**, 319-322.

7. SUPPLEMENTARY

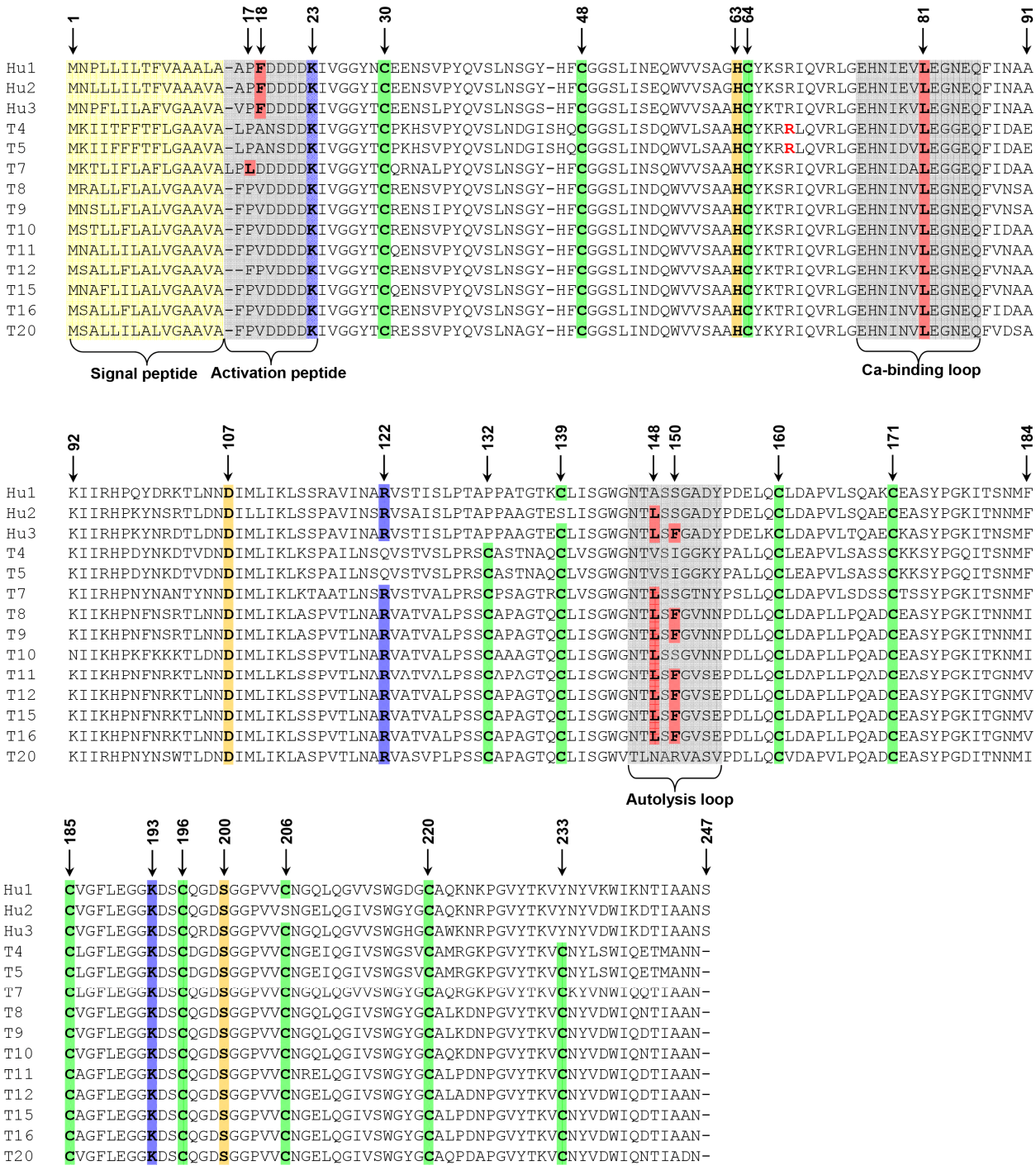

Supplementary Figure 1. Amino acid sequence alignment of human cationic (Hu1), anionic (Hu2), mesotrypsinogen (Hu3) and 11 potentially expressed mouse trypsinogen isoforms (T4, T5, T7, T8, T9, T10, T11, T12, T15, T16 and T20). Numbering starts with the initiator methionine. Note that due to insertions in T4, T5 and T7, the numbering is shifted by one after the insertion sites, relative to the indicated numbers. Similarly, a deletion in T12 shifts numbering. Trypsin cleavage sites are highlighted in blue and chymotrypsin C (Ctrc) cleavage sites in red. Cys residues are indicated in green and the catalytic triad in orange. The original annotation predicted deletion of Arg69 (in red letter) in T4 and T5 but more recent annotations include this residue.

T7

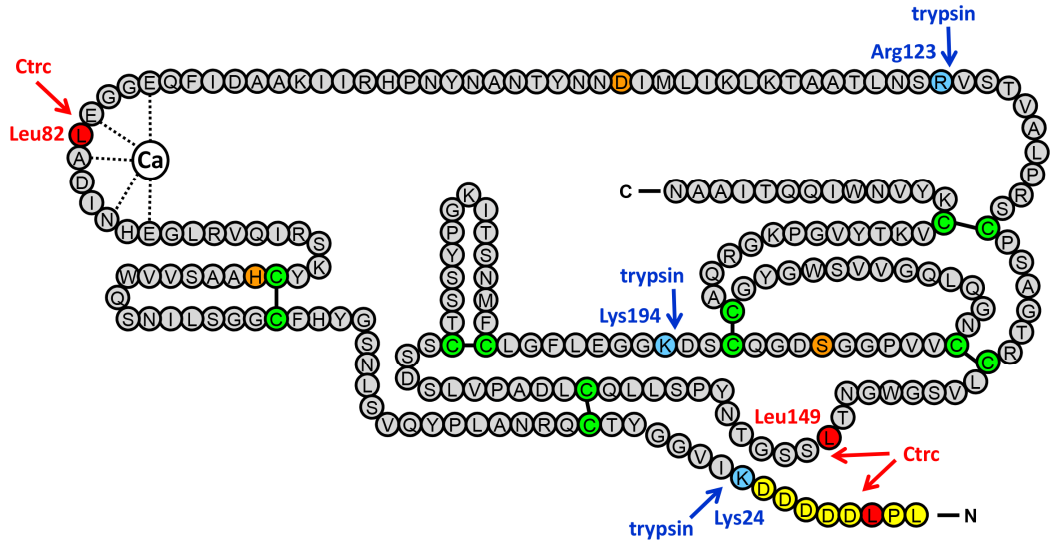

Supplementary Figure 2A. Primary structure of T7 moue trypsinogen. The activation peptide containing Lys24 is designated by yellow circles. Red circles indicate cleavage sites of chymotrypsin C (L18, L82 and L149), while blue background shows tryptic cleavage sites (K24, R123 and K194). Cys residues which form disulfide bonds are designated by green circles (C31-C161, C49-C65, C133-C234, C140-C207, C172-C186 and C197-C221). Members of the catalytic triad are shown by orange circles (H47, D108 and S201). "**Ca**" indicates a calcium ion (Ca^{2+}).

T8 (T9)

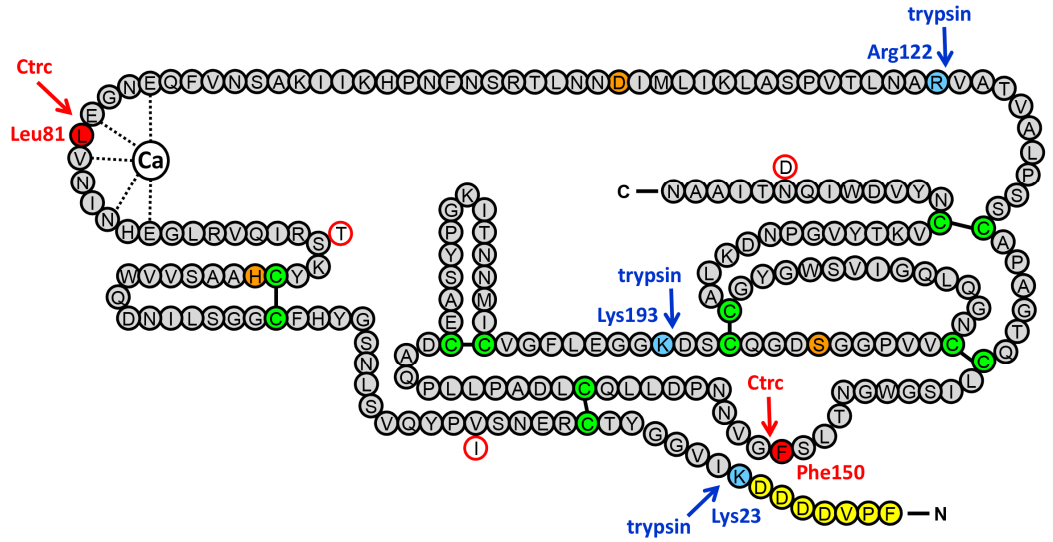

Supplementary Figure 2B. Primary structure of T8 and T9 mouse trypsinogens. The activation peptide containing Lys23 is designated by yellow circles. Solid red circles indicate cleavage sites of chymotrypsin C (L81 and F150), while blue background shows tryptic cleavage sites (K23, R122 and K193). Cys residues which form disulfide bonds are designated by green circles (C30-C160, C48-C64, C132-C233, C139-C206, C171-C185 and C196-C220). Members of the catalytic triad are shown by orange circles (H46, D107 and S200). Amino acid differences in T9 trypsinogen are indicated in empty red circles. "**Ca**" indicates a calcium ion (Ca^{2+}).

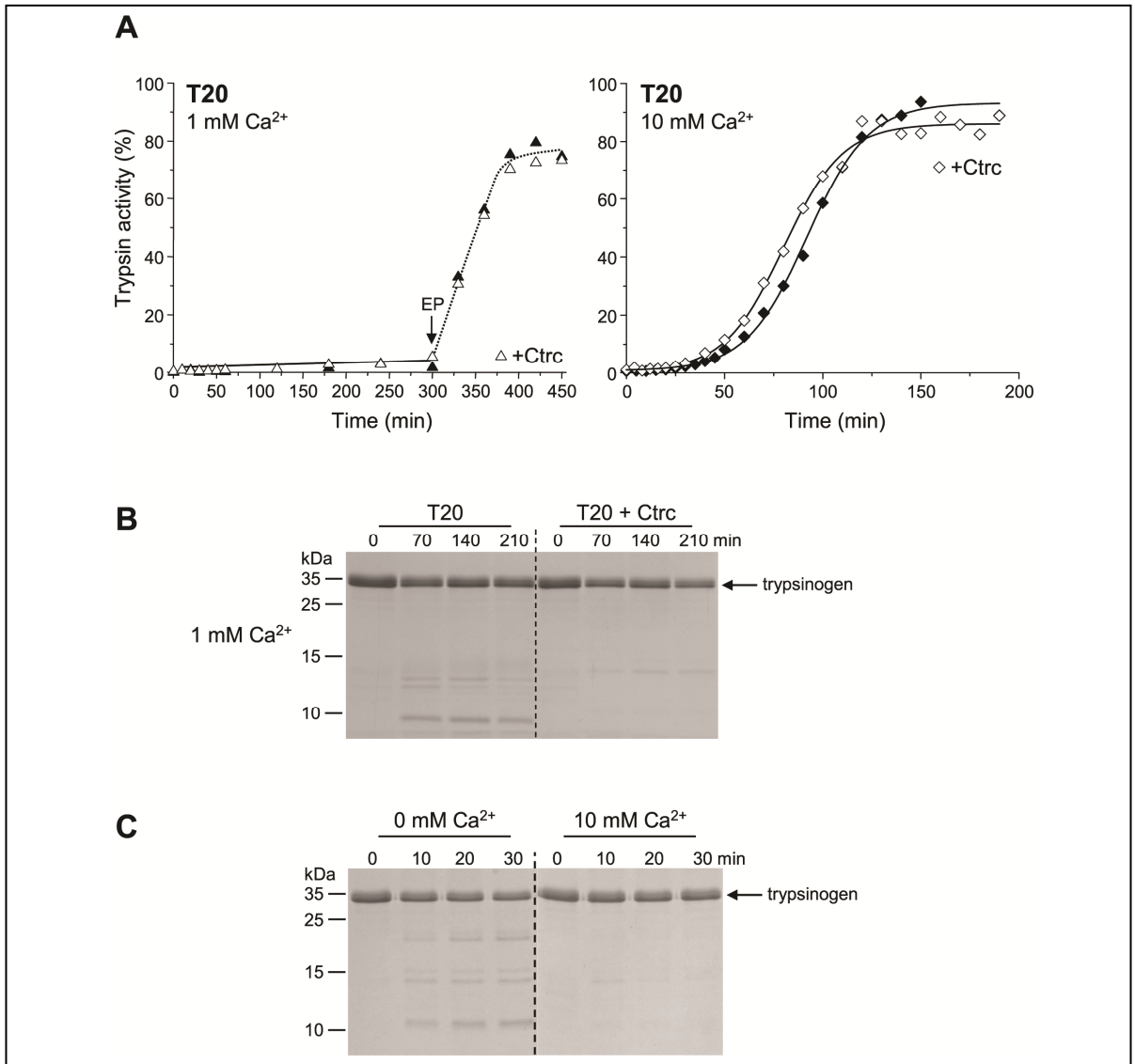

Supplementary Figure 3. Effect of mouse chymotrypsin C (Ctrc) on mouse trypsinogen T20. (**A**) Autoactivation was measured in 1 mM and 10 mM $CaCl_2$, in the absence (solid symbols) or presence (open symbols) of 25 nM mouse Ctrc, as described in *Patients and Methods*. Where indicated, 2 µL of 1.4 µg/mL human enteropeptidase (EP) was added. (**B**) SDS-PAGE analysis of the autoactivation reaction in 1 mM $CaCl_2$. Samples were withdrawn at the indicated time points, precipitated with trichloroacetic acid, electrophoresed and stained as described in *Patients and Methods*. (**C**) Cleavage of T20 trypsinogen by 25 nM mouse Ctrc. Incubations were performed and samples were analyzed as in Figure 13C. The faint Ctrc cleavage products seen in the absence of calcium were not identified. Representative experiments from three replicates are shown.

8. ACKNOWLEDGEMENTS

I would like to express my most sincere gratitude to my mentors, Professor Yvette Mándi M.D. Ph.D. D.Sc. and to Professor Miklós Sahin-Tóth M.D. Ph.D. for introducing me to miraculous worlds of immunobiology and biochemistry. I admire their broad knowledge of science, their way of analyzing scientific problems, and their ability to come up with exciting new ideas. I am most grateful for their patient guidance and inspiration during my Ph.D. studies.

I would like to express my special thank to Ferenc Somogyvári Ph.D. who showed me the fabulous applications of polymerase chain reaction.

I thank all the coworkers of the Department of Medical Microbiology and Immunobiology at the Faculty of General Medicine, University of Szeged, especially I am thankful for the help and advice I am received from Katalin Burián M.D. Ph.D., Klára Megyeri M.D. Ph.D., Zoltán László Tiszlavicz M.D. Ph.D., Ádám Horváth, Márta Szekeres M.D. and for the excellent technical assistance from Györgyi Müller and Mariann Ábrahám, and from Zsuzsanna Rosztóczy and Renáta Bognár for skilful administration.

I also express my greatest gratitude to all the coworkers of Department of Molecular and Cell Biology at the Henry M. Goldman School of Dental Medicine, Boston University for their support, especially to András Szabó Ph.D, Andrea Schnúr Ph.D, Andrea Geisz Ph.D., Anita Balázs M.D., Maren Ludwig, Sebastian Beer M.D., Jiayi Zhou M.D. Ph.D., Melinda Bence Ph.D. and Vera Sahin-Tóth.

It also gives me great pleasure to acknowledge the support and help of our research collaborators Walter Halangk and Thomas Wartmann at the Division of Experimental Surgery, Department of Surgery, Otto-von-Guericke-Universität Magdeburg and also our clinical partners Tamás Várkonyi M.D. Ph.D., Csaba Lengyel M.D. Ph.D., Katalin Fehértemplomi M.D, Szabolcs Nyiraty M.D., Rita Laurentzi M.D. at the First Department of Medicine, University of Szeged, and Péter Kempler M.D. Ph.D. at the First Department of Internal Medicine, Semmelweiss University, Budapest. Furthermore, my thankful words also reach Zoltán Szolnoki M.D. Ph.D. at the Department of Cerebrovascular Diseases, Pándy Kálmán County Hospital, Gyula, Professor László Sztriha M.D. Ph.D. D.Sc. and Professor László Vécsei M.D. Ph.D. D.Sc. at the Department of Neurology and Neuroscience Research Group of Hungarian Academy of Sciences, University of Szeged.

I acknowledge the contributions of János Borbás, as webmaster for the http://www.pancreasgenetics.org/ website. Furthermore I am very thankful for the help of

Amanda Watkins Ph.D. and Martin Minns for their suggestions of using professional level of English language in this thesis.

This work was supported by TÁMOP-4.2.2.A-11-1-KONV-2012-0035 and TÁMOP 4.2.2.B-10/1-KONV-2010-0012 research grants at the University of Szeged. In Boston this work was also supported by National Institutes of Health grants R01DK058088, R01DK082412, R01DK082412-S2, and R01DK095753 (to M. S.-T.) and by grant DFG HA2080/7-1 from the Deutsche Forschungsgemeinschaft.

I dedicate this thesis to my beloved parents, Mária Varga and Miklós Németh for their lifelong support and encouragement during my studies.

I.

Nemeth, Balazs

From: esps@wjgnet.com
Sent: Tuesday, April 08, 2014 9:08 PM
To: yvette@comser.szote.u-szeged.hu
Cc: Nemeth, Balazs
Subject: Manuscript acceptance-Express Submission and Peer-review System-Ms NO: 7997

Dear Dr. Mandi,

Thank you very much for submitting your high-quality paper to World Journal of Gastroenterology. We are pleased to inform you that your paper has been accepted for publication after a very rigorous review process. Congratulations!

We are happy to tell you that this paper will be given priority for publishing, with all publishing fees waived. The basic information about this manuscript is as follows:

Author: Y Mandi

ESPS Manuscript NO: 7997

Title: The relevance of alpha and beta defensins in diabetes

Received Date: 2013-12-10 04:43:11

Accepted Date: 2014-04-09 09:07

Baishideng Publishing Group (BPG) has a professional editorial team composed of science editors, language editors and electronic editors and currently edits and publishes 42 clinical medical journals. BPG has independently developed not only the world's leading Express Submission and Peer-review System and full-text online release system but also the world's leading Highly Cited Articles database. This database covers the most important international biomedical literature and contains 2,148,687 articles that were cited more than once over the past 100 years (For details please visit http://www.wjgnet.com/ESPS/HighlyCitedArticles.aspx). The bibliographic information for included articles includes rankings, total cites, author's name, journal name, and title. The title includes a link to Google, greatly facilitating the availability of knowledge to readers. In addition, BPG has independently developed the world's leading Express Submission and Peer-review System (ESPS) publishing system. Cutting-edge research papers from journals included in PubMed or Web of Knowledge will be selected to write a summary of less than 100 to outline the most innovative and important arguments and core contents in the papers. The summary, along with the bibliographical information of the papers, is submitted to the ESPS publishing system to guide readers to read the most important articles in the shortest possible time to improve their diagnostic and treatment skills.

A GENTLE REMINDER: You are recommended strongly to withdraw your paper in case of the following conditions: (1) Plagiarism; (2) Data fabricating and falsification; (3) Redundant publication; (4) Stealing from others; and (5) Divergence about the right of authorship. Once the paper is published on the Website of World Journal of Gastroenterology, the author who wishes to withdraw the paper must pay 10,000 USD for damages. The paper will then be withdrawn within four weeks.

Thank you for your cooperation. On behalf of the Editors of the World Journal of Gastroenterology, we look forward to your continued contributions to the journal.

If you have any questions, please feel free to contact us via e-mail: submission@wjgnet.com

Best regards,

Lian-Sheng Ma, President and Company Editor-in-Chief

Baishideng Publishing Group Co., Limited

Flat C, 23/F., Lucky Plaza,

315-321 Lockhart Road,

Wan Chai, Hong Kong, China

Telephone: +86-10-8538-1892

Fax: +86-10-8538-1893

E-mail: l.s.ma@wjgnet.com

http://www.wjgnet.com

Name of journal: World Journal of Gastroenterology

ESPS Manuscript NO: 7997

Columns: Retrospective study

Relevance of α-defensins (HNP1-3) and defensin β-1 in diabetes

Running title: Defensins in diabetes

Balázs Csaba Németh *

Department of Medical Microbiology and Immunology, University of Szeged,

Szeged, Hungary, H6720 tel: +36 62 545 115, fax: +36 62 545 113

Tamás Várkonyi

First Department of Internal Medicine , University of Szeged

Szeged, Hungary H6720 tel: +36 62 342 210, fax: +36 62 545 185

Ferenc Somogyvári

Department of Medical Microbiology and Immunology, University of Szeged,

Szeged, Hungary, H6720 tel: +36 62 545 115, fax: +36 62 545 113

Csaba Lengyel , Katalin Fehértemplomi , Szabolcs Nyiraty

First Department of Internal Medicine , University of Szeged

Szeged, Hungary H6720 tel: +36 62 342 210, fax: +36 62 545 185

Péter Kempler

First Department. of Internal Medicine, Semmelweis University, Budapest,Hungary H 1052

Tel: +36 1 210 02 78, fax: +36 1 313 02 50

Yvette Mándi

Department of Medical Microbiology and Immunology, University of Szeged,

Szeged, Hungary, H6720 tel: +36 62 545 115, fax: +36 62 545 113

*Present work place: Department of Molecular and Cell Biology, Boston University Henry M. Goldman School of Dental Medicine, Boston, Massachusetts 02118, USA.

Corresponding author**:** Yvette Mándi, MD, PhD, DSc, Department of Medical Microbiology and Immunobiology, University of Szeged, Dóm tér 10, H-6720 Szeged, Hungary. Tel: +36-62-545-115, Fax: +36-62-545-113. E-mail: mandi.yvette@med.u-szeged.hu

Authors contributions:

Németh B. Cs. performed all laboratory experiments, Várkonyi T. designed clinical research and analyzed the clinical data, F. Somogyvári designed the genetical experiments, K. Fehértemplomi, Cs. Lengyel and Sz.Nyiraty collected all the human material and analyzed the clinical data, P. Kempler provided the scientific clinical background, Y. Mándi designed and coordinated the study, provided the immunological background, ensured financial support for the research and wrote the manuscript.

ABSTRACT

AIM: To investigate the genetic background of human defensin expression in type 1 and 2 diabetes.

METHODS: Associations between *DEFA1/DEFA3* gene copy number polymorphism and diabetes as well as between the promoter polymorphisms of *DEFB1* and diabetes were studied. The copy number variation of the *DEFA1/DEFA3* genes was determined in 257 diabetic patients (117 patients with type 1 and 140 with type 2 diabetes). The control group consisted of 221 age- and gender-matched healthy blood donors. The cumulative copy numbers of the *DEFA1/DEFA3* genes were detected by using quantitative PCR analysis. To evaluate the HNP 1-3 (human neutrophil peptide 1-3 or α-defensin) levels in the circulation, plasma HNP 1-3 concentrations were measured by ELISA. The expression of *DEFA1/A3* in peripheral leukocytes ofthe diabetic patients was measured by quantitative RT PCR analysis. Three SNPs of the human *DEFB1* (human defensin β-1) gene: *DEFB1* G-20A (rs11362), *DEFB1* C-44G (rs1800972) and *DEFB1* G-52A (rs1799946) were genotyped by Custom TaqMan® Real Time PCR assay.

RESULTS: Significant differences were observed in HNP1-3 levels between the healthy subjects and both groups of diabetic patients. The mean ±SE was 28.78 ± 4.2 ng/ml in type 1 diabetes, and 29.82 ± 5.36 ng/ml in type 2 diabetes, vs. 11.94 ± 2.96 ng/mL in controls; $p<0.01$ respectively. There was no significant difference between patients with type 1 and type 2 diabetes in the high plasma concentrations of HNP1-3. The highest concentrations of α-defensin were found in diabetic patients with nephropathy (49.4 ± 4.8 ng/mL), neuropathy (38.7 ± 4.8 ng/mL) or cardiovascular complications (45.6 ± 1.45 ng/L).

There was no significant difference in the cumulative copy numbers of *DEFA1/DEFA3* genes between controls and patients, or between patients with the two types of diabetes. Comparisons of HNP 1-3 plasma level and *DEFA1/A3* copy number of the same patient did not reveal significant relationship between defensin-α levels and the gene copy numbers (r^2 = 0.01). Similarly, no positive correlation was observed between the copy numbers and the mRNA expression levels of *DEFA1/A3*. Regarding the C-44G polymorphism of *DEFB1*, the GG "protective" genotype was much less frequent (1–2%) among both groups of patients than among controls (9%).

CONCLUSION: Elevated HNP1-3 levels in diabetes are independent of *DEFA1/DEFA3* copy numbers, but GG genotype of C-44G SNP in *DEFB1* gene may result in decreased defensin β-1 production.

Key words: α-defensins, HNP1-3, β-defensin 1, diabetes, copy number polymorphism, single nucleotide polymorphism

CORE TIP:

There is growing evidence of the role of innate immunity in diabetes To our knowledge our data provide the first report on a complex investigation of defensin-α and defensin β-1 in type 1 and type 2 diabetes. The main conclusion of our manuscript is, that the elevated HNP1-3 levels in diabetes are independent of the DEFA1/DEFA3 copy numbers, but the GG genotype of C-44G SNP in the DEFB1 gene may result in a decreased level of defensin β-1 production. Our data support the view that both alpha and beta-defensins may have an important role in the pathogenesis of diabetes and diabetic complications.

INTRODUCTION

Defensins are members of small antimicrobial peptides of the innate immune system[1,2]. However, today these peptides are also known as danger signals or ”alarmins” playing important roles in inflammation and immunity[3]. Mammalian defensins are divided into two major families, the α- and β-defensins. Human α-defensins include human neutrophil peptide 1-4 (HNP1-4) and intestinal human defensins (HD-5 and HD-6) produced by Paneth cells. Besides the antimicrobial effects, alpha defensins display chemotactic activity and induce proinflammatory cytokines[4,5,6]. HNPs increase the binding of LDL (low density lipoprotein cholesterol) to the endothelial surface suggesting that alpha defensins may modulate the development of atherosclerosis [7]. Neutrophil granulocytes are considered to be the primary cellular origin of α-defensins; HNP 1-3 comprise 30–50% of the granule proteins. HNPs can be released into the extracellular milieu following granulocyte activation as a consequence of degranulation, leakage, cell death, and lysis during inflammation[8]. α-defensins are also involved in the formation of neutrophil extracellular traps[9].

Human β-defensins make up another family of antimicrobial peptides[1, 10]. In addition to their antibacterial and antiviral effects, the chemoattractive function of these defensins has been shown to play a role in immunological reactions that protect the host from various pathogens[11]. While the expression of human defensin beta-1 (HBD1) is generally constitutive, the levels of human defensin beta-2 (HBD2) are inducible by proinflammatory cytokines and bacteria[10, 12, 13]. Human beta defensins are expressed by epithelial cells of the skin, gut, respiratory and urogenital tissues, the pancreas and the kidneys. HBD1 is also constitutively expressed by leukocytes[14, 15, 16].

The level of defensin expression varies among individuals, and it has been suggested that this variation is due to genetic differences in the genes encoding defensins. Defensin genes have been mapped to 8p22-p23[17]. Two types of genetic polymorphisms have been identified in genes encoding defensins: copy number polymorphisms and single nucleotide poymorphisms (SNPs). Human defensin beta-1 (HBD-1) is encoded by the gene *DEFB1* (OMIM: 602056), in which several SNPs (single nucleotide polymorphisms) have been characterized. Three frequent SNPs at positions G-20A (rs11362), C-44G (rs 1800972) and G-52A (rs1799946) in the 5'-untranslated region (UTR) of *DEFB1* were described[18]. The untranslated variants influence HBD-1 expression or function[19].

The cluster of human alpha-defensin genes on chromosome 8 includes the genes *DEFA1 (OMIM:* 125220) and *DEFA3 (OMIM:* 604522), which are copy-variables. The genes *DEFA1* and *DEFA3* differ only in a single base substitution in the coding sequence, corresponding to a single amino acid difference between the peptides encoded[20]. HNP 1-3 differs only in a single N-terminal acid, and the HNP-2 peptide lacks this residue and might be a proteolytic product of the other two peptides because no separate gene has been identified to encode HNP-2[21]. Several copy number polymorphisms form the major source of genetic polymorphism of α-defensin genes *DEFA1* and *DEFA3*, encoding human neutrophil peptides HNP-1, -2 and 3[20, 22].These genes are present in a cluster that is close to but independent from the β-defensin cluster on 8p23. The total *DEFA1/DEFA3* copy number has been found to range between 4 and 11 copies per diploid genome with 5 to 9 copies being the most common[22].

To date, little is known about the genetic basis and the functions of α- and β-defensins in diabetes. Infections are frequent in diabetic patients because the antimicrobial function of their immune response is impaired. It has been reported that mRNA levels of rat β-defensin-1 are significantly low in the kidneys, which may explain the high incidence of urinary tract infections in diabetes mellitus[23]. The effects of glucose and insulin on the β-defensin

expression have recently been demonstrated[24], but no connection has been found between genetic polymorphisms of the HBD1 gene and diabetes in a Brazilian study on diabetic children[25].

Increased levels of alpha-defensin -1, -2 and -3 have recently been reported in patients with type 1 diabetes with nephropathy and in cardiovascular complications[26, 27]. It is tempting to speculate whether copy number polymorphisms and the *DEFA1/DEFA3* mRNA in the granulocytes may influence the levels of HNP1-3 in patients with types 1 and 2 diabetes.

The aim of our study was to investigate the genetic background of human defensin-α and human defensin β-1 production in adult patients with type 1 and type 2 diabetes, especially with complications. Therefore, we carried out an association study between *DEFA1/DEFA3* copy number polymorphism and diabetes, and between the promoter polymorphisms of DEFB1 and diabetes. We also measured the plasma levels of HNP 1-3 in both types of diabetes, and the mRNA expression of *DEFA1/DEFA3* in leukocytes.

MATERIALS AND METHODS

.

Patients

257 diabetic patients (122 men and 135 women) were enrolled in our study, which included 117 patients with type 1 and 140 patients with type 2 diabetes. All patients participating in the study were diagnosed according to the ADA criteria: Diagnosis and classification of diabetes mellitus. Diabetes Care 36 (Suppl.1.) 2013. S64-S74.

The mean age of type 1 diabetic patients was 40.6 years±1.51 years, the mean duration of diabetes was 17.7±1.12 years, and their mean HbA1c was 8.86±0.17%. In type 2 diabetic subjects, the mean age was 58.4±1.27 years, the mean duration of diabetes was 14.5±0.8 years, and the mean HbA1c was 8.03±0.13%.

71 subjects in the cohort had diabetic nephropathy (32 with type 1 and 39 with type 2 diabetes) defined as an albumin-to-creatinine ratio in a random spot collection being higher than 3.4 mg/mmol, or the protein content being over 300 mg/day in collected urine. Abnormal kidney function was described when the glomerular filtration rate (GFR) was lower than 60 mL/min/1.73 m^2.

115 patients suffered from retinopathy (47 with type 1 and 68 with type 2 diabetes). This complication was evidenced as the presence of background or proliferative retinopathy, macular edema or diabetes-related blindness, or the administration of retinal photocoagulation

therapy. The retinopathy status was checked by color stereo-ophthalmography and fluorescence angiography. Neuropathy was diagnosed in 95 patients (35 with type 1 and 60 with type 2 diabetes). Neuropathy was proven when abnormal peripheral sensory functions or altered lower limb tendon reflexes as well as impaired cardiovascular reflex tests were detected. 54 diabetic patients (14 with type 1 diabetes and 40 with type 2 diabetes) had previously been diagnosed with macrovascular disease including major coronary events, stroke or a transient ischemic attack, peripheral artery disease or amputation. A high number of the patients (182) had controlled hypertension (50 with type 1 and 132 with type 2 diabetes).

The control group consisted of 221 age- and gender-matched healthy blood donors. These control subjects were selected from blood donors at the regional Center of Hungarian National Blood Transfusion Service, Szeged, Hungary. The exclusion criteria for blood donors were diabetes, nephropathy, hypertension, or ischemic heart disease. All cases and controls were of Hungarian ethnic origin and resident in Hungary. Informed consent was obtained from all patients and controls, and the local Ethics Committee gave prior approval to the study. All patients consented to the study and were treated according to the Patient Right Protection Act of our institutions and according to international guidelines.

Assay of HNP 1-3 concentration

Blood samples containing EDTA were obtained from patients and controls. Plasma was isolated after the blood was centrifuged at 3,000g for 3 min and stored at -80^{o}C for further analysis. The HNP1-3 concentrations in plasma were determined by ELISA (Hycult-Biotech HK324, Uden, The Netherlands) according to the instructions of the manufacturer.

DNA isolation

Genomic DNA purified from peripheral blood was used. Leukocyte DNA was isolated using the High Pure PCR Template Preparation Kit according to the instructions of the manufacturer (Roche Diagnostic GmbH, Mannheim, Germany). DNA concentrations were measured with a Qubit™ fluorometer (Invitrogen, Carlsbad, CA, USA) according to the instructions of the manufacturer. Genomic DNA was stored at -20º C until further use.

Determination of DEFA1/DEFA3 gene copy numbers by quantitative real-time PCR

Genomic DNA purified from peripheral blood was used. Gene copy number determination was carried out as previously described by Linzmeier [20] with slight modifications. BIO-RAD CFX 96 instrument (Bio-Rad, Hercules, CA, USA) was used for quantitation. The reaction volume was 15 μL, containing 3 μL of DNA, 1 μmol L^{-1} each of the primers, 7.5 μL of reaction buffer (Fermentas Probe/ROX qPCR MasterMix, Fermentas, Lithuania) and 0.6 μL EVAGreen (20x EVAGreen™ Biotium Inc., Hayward, CA, USA). Forward primer: DEFA1 1 F (5' TAC CCA CTG CTA ACT CCA TAC 3'), reverse primer: DEFA1 1 R (5' GAA TGC CCA GAG TCT TCC C 3'); MPO (myeloperoxidase) reference gene primer set MPO 1 F (5' CCA GCC CAG AAT ATC CTT GG 3'), MPO 1 R (5' GGT GAT GCC TGT GTT GTC G 3'). PCR conditions were as follows: initial denaturation at 95°C for 10 min followed by 40 cycles of denaturation (95°C for 15 sec) and extension (54°C for 1 min).

Quantification was performed by monitoring the emitted fluorescence after each cycle of PCR reaction of genomic DNA samples in order to identify the exact time point at which the log-linear phase could be distinguished from the background (crossing point). The precise amount of DNA added to each reaction mix was based on optical density. Each DNA sample was analyzed in triplicate, in 2 independent experiments.

DEFA1/DEFA3 mRNA quantification by RT PCR

We collected further 2 mL of venous blood in EDTA tubes from patients with diabetes and controls. Leukocytes from blood were separated by centrifugation at 1200 rpm/min for 15 min. By using the reverse transcription polymerase chain reaction (RT-PCR), we examined the expression of *DEFA1/DEFA3* mRNA in 24 patients with diabetes (12 cases of type 1 and 12 cases of type 2 diabetes). Total RNA was extracted with High Pure RNA isolation kit (Roche) according the manufacturer's instruction. RNA concentration was determined by the A_{260} value of the sample. Complementary DNA (cDNA) was generated from 1 μg total RNA using the High-Capacity cDNA Reverse Transcription Kit (Applied Biosystems) in a final volume of 20 μL. After reverse transcription, amplification was carried out by using Light Cycler Fast Start DNA Master^{PLUS} SYBR Green I mix (Roche). Samples were loaded into capillary tubes and placed in the fluorescence thermocycler (LightCycler). Initial denaturation at 95°C for 10 min was followed by 45 cycles of 95°C for 10 sec, annealing at 58°C for 8 sec, and elongation at 72°C for 12 sec. DEFA1/DEFA3 sense, 5'-TCC CAG AAG TGG TTG TTT CC-3'; and antisense, 5'-GCA GAA TGC CCA GAG TCT TC-3', and for the housekeeping gene

GAPDH (glyceraldehyde-3-phosphate dehydrogenase) sense, 5′-AAG GTC GGA GTC AAC GGA TTT-3′; antisense, 5′-TGG AAG ATG GTG ATG GGA TTT-3′ primers were used to amplify specific products from cDNA samples. At the end of each run, melting-curve profiles were achieved by cooling the sample to 40°C for 15 sec, and then heating the sample slowly at 0.20°C/sec up to 95°C with continuous measurement of the fluorescence to confirm the amplification of specific transcripts. Cycle-to-cycle fluorescence emission readings were monitored and analyzed by using LightCycler software (Roche Diagnostics GmbH). All quantifications were normalized to the housekeeping GAPDH gene. Relative gene expression was determined by using the ΔΔCt method.

Genotyping of SNPs of human defensin beta -1 (DEFB1)

Genotyping was performed by means of Custom TaqMan® SNP Genotyping Assays (Applied Biosystems, CA). Fluorogenic minor groove binder probes were used for each case using the dyes 6-carboxyfluorescein (FAM; excitation, 494 nm) and VIC (excitation, 538 nm): beta-defensin-1 polymorphisms *DEFB1* G-20A (rs11362) Applied Biosystems code c_11636793_20, *DEFB1* C-44G (rs1800972) c_11636794_10 and *DEFB1* G-52A (rs1799946) c_11636795_20. Thermal cycling was performed on ABI Prism 7000 sequence-detection PCR systems. The amplification mix contained the following ingredients: 7.5 μL of TaqMan® universal PCR master mix (Applied Biosystems, CA), 0.375 μL of primer-probe mix, 6.375 μL of RNase- and DNase-free water (Sigma), and 0.8 μL of sample DNA, in a total volume of 15 μL per single tube reaction. Assay conditions were 2 min at 50°C, 10 min at 95°C, and 40 cycles of 95°C for 15 sec and 60°C for 1 min. Each 96-well plate contained 90 samples of an unknown genotype and six reactions with reagents but no DNA. DNase-free water was used as nontemplate control. Initial and postassay analysis was performed by using the Sequence Detection System (SDS) version 2.1 software (Applied Biosystems, CA) as outlined in the TaqMan Allelic Discrimination Guide. Genotypes were determined visually based on the dye-component fluorescent emission data depicted in the X-Y scatter plot of the SDS software. Genotypes were also determined automatically by the signal processing algorithms in the software. Results of each scoring method were saved in two separate output files for later comparison.

Statistical analysis

Comparisons of plasma concentrations were carried out by the Mann–Whitney test and with two-tailed paired Student test. The level of significance of the genotype frequency of different *DEFB1* SNPs was analyzed by using the χ^2 test and the Fischer test. Levels $p<0.05$ indicated statistical significance. All statistical calculations were performed with the Graph Pad Prism 5.0 statistical program (GraphPad Software, San Diego CA. USA). The genotype frequencies for each polymorphism of DEFB1 were tested for deviation from the Hardy–Weinberg equilibrium by the χ^2 test with 1 degree of freedom.

RESULTS

Plasma levels of human neutrophil peptide (HNP1-3) in patients with type 1 and type 2 diabetes

In a pilot study, plasma levels of α-defensin, human neutrophil peptide (HNP1-3), in 50 patients with type 1 diabetes and in 60 patients with type 2 diabetes were determined and compared with those of 50 healthy blood donors. There was a high individual variation in the plasma levels of α-defensin, but significant differences were observed between the healthy subjects and both groups of diabetic patients. The mean value ±SE was 28.78±4.2 ng/mL in patients with type 1 diabetes and 29.82±5.36 ng/mL in patients with type 2 diabetes vs. 11.94±2.96 ng/mL in controls ($p<0.01$ respectively). The difference between the high plasma concentrations of HNP1-3 in patients with type 1 or type 2 diabetes was not significant (Fig.1.).

Plasma levels of human neutrophil peptide (HNP1-3) in diabetic patients with complications

After that, we checked whether the generally high level of HNP1-3 in the peripheral blood of both groups (type 1 and type 2) of diabetic patients was connected to diabetic complications. Nephropathy was diagnosed in 71 patients (32 with type 1 and 39 with type 2 diabetes) and neuropathy in 95 ones (35 with type 1 and 60 with type 2 diabetes). 115 patients suffered from retinopathy (47 with type 1 and 68 with type 2 diabetes), 54 patients had cardiovascular diseases (14 with type 1 diabetes and 40 with type 2 diabetes), and 182 had hypertension (50 with type 1 and 132 with type 2 diabetes). Their data concerning the HNP1-3 levels were compared with those of the 67 patients who did not suffer from these complications, and with the data of the 100 healthy subjects (Fig.2.). The highest HNP 1-3 concentrations were found in the diabetic patients with nephropathy (49.4±4.8 ng/mL) and with neuropathy (38.7±4.8 ng/mL) or with cardiovascular complications (45.6±1.4 ng/mL). These concentrations were significantly higher than those in the diabetic patients without complications (25.4±3.5 ng/mL). These data are in accordance with previous observations[26, 27] of high levels of HNP 1-3 in type 1 diabetic patients with cardiovascular diseases. In a relatively smaller group of patients (n =28) with diabetic foot ulcer (20 with type 1 diabetes and 8 with type 2 diabetes), the HNP1-3 plasma levels were 35.9±1.1 ng/mL. These high HNP1-3 levels might be the consequence of the degranulation of recruited neutrophils from the skin frequently following

infections. Our results suggest that in diabetic complications such as nephropathy, neuropathy and cardiovascular diseases, the HNP1-3 level in the circulation is elevated independently of the type of diabetes. All diabetic patients, with or without complications, exhibited significantly higher plasma levels of HNP1-3 than the control subjects (Fig.2).

Copy number polymorphism of DEFA1/DEFA3

The cumulative copy numbers of *DEFA1/DEFA3* were determined by using quantitative PCR analysis. In the control group, 133 DNA samples were used for copy number determination and 100 DNA samples of diabetic patients with type 1 or type 2 diabetes. There was no significant difference in copy number between the controls and the patients or between the patients with the two types of diabetes (Fig.3). In the control group, *DEFA1/DEFA3* copy numbers ranged from 4 to 15 per genome with a median number of 10 copies. The median copy number of *DEFA1/DEFA3* in the patients with type 1 diabetes was 10 copies per genome (range 5 to16 copies), and that in the patients with type 2 diabetes was also 10 (range 5 to 15). Comparing the HNP 1-3 plasma level and the *DEFA1/A3* copy number of the same patient, no significant correlation was observed between defensin levels and genomic copy numbers (r^2=0.01; Fig.4.).

DEFA1/DEFA3 gene expression

The expression of *DEFA1/A3* was measured in the peripheral leukocytes of diabetic patients. *DEFA1/DEFA3* mRNA was determined in blood samples from 12 patients with type 1 and another 12 with type 2 diabetes, and the relative expressions of *DEFA1/DEFA3* were compared with the *DEFA1/DEFA3* copy numbers of the same patients (Fig.5). The data indicated that peripheral leukocytes had the ability to transcribe *DEFA1/DEFA3* genes (mean ± SE of relative expression 1.5±0.28) and to biosynthetize HNP1-3 peptides. However, no positive correlation was observed between the copy numbers and the expression levels of the human neutrophil peptide 1-3 (Fig.5). The variation in expression levels between individuals did not exhibit a positive correlation with the copy number. Similarly, the expression of specific mRNA in the leukocytes for HNP 1-3 did not parallel the HNP 1-3 plasma levels (data not shown).

DEFB1 G-20A, DEFB1 G-52A and DEFB1 C-44G polymorphisms

The genotypic distributions of *DEFB1* G-20A, and *DEFB1* G-52A and *DEFB1* C-44G polymorphisms are presented in Table 1.

The distribution of the *DEFB1* G-20A genotypes was in accordance with the Hardy–Weinberg equilibrium both in the control population and in the patients (p = 0.912 and p = 0.795, respectively). There was no significant difference in genotype distribution between the patients overall and the healthy controls. Similarly, no significant differences in genotypes were observed when the patients were grouped according to type 1 and type 2 diabetes.

As concerns the *DEFB1* G-52A SNP , distribution of the genotypes was in accordance with the Hardy–Weinberg equilibrium both in the control population and in the patients (p = 0.252 and p = 0.181, respectively). We did not detect any significant difference in genotypes between the patients and the controls, either in type 1 or type 2 diabetes.

The genotypic distribution of DEFB1 C– 44G polymorphism is shown in Table 1.

The distribution of genotypes was in accordance with the Hardy–Weinberg equilibrium among the patients with diabetes (p = 0.151) and also in the control population (p = 0.722). But there was a significant difference in genotype distribution between the patients overall and the healthy controls (χ^2 test, p = 0.002). The frequency of the GG genotype was significantly lower in both types of diabetes (2.5% and 2%, respectively) than in the healthy controls (9%) (Fisher test vs. control, p = 0.001, OR=9.136, 95% CI: 3.512–23.82). Conversely, the prevalence of the *DEFB1* CC genotype was 61 % in the group of diabetic patients vs. 45% in the controls (Fisher test: p = 0.0009, OR=2.055, 95% CI: 1.248–2.746). When the patients were grouped according to the diabetic complications, there was a lower frequency of the GG genotype among the patients with nephropathy and among those with neuropathy (1.4% and 1%, respectively).

DISCUSSION

HNP1-3 levels in the circulation were measured, and the copy number variation of *DEFA1/A3* genes was determined in diabetic patients. The diabetic patients exhibited overall higher plasma levels of HNP 1-3 (α-defensin) with either type 1 or type 2 form of the disease than the healthy controls. The highest concentrations of HNPs were detected in patients with nephropathic or neuropathic and cardiovascular complications. An essential

question arises as to why an increased concentration of plasma α-defensin (HNP1-3) level is associated with type 1 and type 2 diabetes, especially in the event of diabetic complications such as nephropathy, neuropathy or cardiovascular problems. The explanation might be that the elevation in the plasma HNP1-3 level is the consequence of the decreased renal degradation of the peptides in patients with advanced nephropathy [26]. HNP 1-3 promote the accumulation of low density lipoprotein in the vasculature, inhibit fibrinolytic activity on the surface of vascular cells, and accumulate in the intima of atherosclerotic plaques. Therefore, HNP 1-3 may have clinical implications in diabetic patients with hypercholesteremia or vascular dysfunction[7, 27].

The association of high levels of HNP1-3 in patients with neuropathy in type 1 and type 2 diabetes is yet to be clarified. The next question is whether there is an increased gene expression responsible for the elevated plasma levels of α-defensins. Our study revealed that there was no correlation between HNP1-3 plasma levels and the copy numbers of *DEFA1/A3* genes. The effect of copy number variations in *DEFA1/DEFA3* on the disease or even on the plasma concentrations of the peptides remain unclear. Controversal data have been published about the correlation between *DEFA1/A3* copy number and the α-defensin peptide concentration. Linzmeier and Ganz [20] have shown that the intracellular HNP1-3 levels in human neutrophils are proportional to the copy numbers of the *DEFA1* and *DEFA3* genes Copy numbers of *DEFA1/A3* may be proportional to the intracellular levels of HNP1-3 in neutrophil granulocytes but possibly not to the circulating HNP1-3 levels. Additionally, a discrepancy between gene copy number and the HNP1-3 protein levels has recently been reported in septic patients[28]. There are several potential explanations of the discrepancy between the gene copy number and the plasma levels. HNP1-3 is stored primarily in the granules of neutrophils and is released into the circulation during the activation of the neutrophils. Moreover, it might also be due to different transcriptional mechanisms modulating these genes or to an increased distance between the regulators of the genes [28, 29].

The fact that in our study no significant correlation was observed between the genomic copy number variation of *DEFA1/DEFA3* and the mRNA expression levels (Fig. 5.) suggests that the degranulation rather than the increased gene expression may be responsible for the increased plasma HNP 1-3 levels in diabetes.

Similar observations have been published about the copy number polymorphism and expression level variation of *DEFA1* and *DEFA3* genes[22]. In that study, the combined

expression levels of *DEFA1/A3* and the genomic copy number have not been correlated, suggesting the superimposed influence of trans-acting factors.

It is noteworthy that there are several examples of the absence of a correlation between copy number polymorphisms and the relative transcription level[29].

There are no direct data showing that exaggerated degranulation is linked to diabetic complications, or it is higher in DM patients than in controls. However, it has recently been published that pro-inflammatory conditions during hyperglycemia favor NET – neutrophil extracellular traps – formation [30], and HNP 1-3 are also involved in the formation of neutrophil extracellular traps[9]. It is noteworthy that diabetes is associated with low grade, sub-clinical and chronic inflammation characterized by abnormal cytokine production. Therefore, the diabetic microenvironment can induce NET formation, which may result in a basic high HNP-1 concentration in the circulations

In order to detect whether increased mRNA expression is responsible for elevated defensin levels in diabetic patients, quantitative RT-PCR reactions were performed. Expression of specific mRNA in the leukocytes was observed for HNP 1-3 but not parallel with HNP1-3 plasma levels. The mRNA values between patients and controls were rather equal (mean ± SE of relative expression 1.5±0.28 vs. 1.49±0.35, respectively) suggesting that not an increased gene expression may be responsible for increased plasma levels of HNP 1-3. Our findings were in good correlation with the observations of Fang X. M. et al. [31], that is, α-defensin genes were constitutively transcribed at low level in mature neutrophils, but they were not inducible

Eosinophils with transcriptionally active α-defensin production have recently been detected in the capillary blood of diabetic patients[32]. Eosinophils but not neutrophils displayed the augmentation of transcriptional activation of α-defensin expression. In our study, the majority of the cells in peripheral venous blood were neutrophils; therefore, our purified DNA and RNA samples were derived mostly from neutrophils.

The present study demonstrated that the distributions of the C-44G genotypes were different between patients with diabetes and healthy controls, whereas the frequency of the GG genotype was significantly higher in the control population. It indicates that the presence of G allele probably leads to strengthened HBD1 antimicrobial activity, which is less frequent in patients with diabetes. The G allele of C-44G SNP generates a putative binding site for nuclear factor κ B (NF-κB), and it is very likely to induce an overexpression. The proposed effect of this SNP could partially explain why the GG

genotype was considered to be a protective genotype in atopic dermatitis[33] and also in the susceptibility to Candida colonization in diabetic patients[34]. Conversely, in these studies, subjects carrying the CC genotype at the -44 locus site of the gene were at a greater risk of acquiring infection. It has been recently suggested that the C allele of *DEFB1* C-44G SNP probably abrogates NF-κB-dependent *DEFB1* upregulation[35].

These data are consistent with our present observation that the GG phenotype could also be protective in diabetes, and *vice versa*, the higher frequency of CC genotype might be connected with lower expression of human defensin β-1. Among the 257 patients with diabetes, only 6 (2%) were GG homozygotes, and 61% of the patients were CC homozygotes, as compared with 45% of CC homozygotes in the control group. Furthermore, the number of GG homozygotes was even lower (1%) among patients with nephropathy and neuropathy. These observations draw the attention to the importance of *DEFB1* polymorphisms in diabetes, especially in the cases with nephropathy and neuropathy. Foot ulcerations in diabetic patients are often combined with infections. None of the 28 patients with foot ulcer displayed GG genotype of C- 44G SNP of DEFB1 gene . A high blood glucose level itself can result in low levels of β-defensin[23], and it might be further downregulated in humans as a consequence of C-44G polymorphism. It is noteworthy that insulin is an important factor mediating hBD-1 expression[24].

Taken together, our study demonstrated elevated levels of α-defensin (HNP1-3) in type 1 and type 2 diabetes, which were more pronounced when there were diabetic complications. However, there was no correlation between the circulating HNP1-3 levels and the *DEFA1/DEFA3* copy number. Similarly, no correlation was found between the mRNA expression and the copy number variation. Further studies are needed to explore whether the elevated α-defensin levels of the plasma in diabetes are causally linked to this disease and its complications, or they are simply the consequences of the degranulation of neutrophils under pathologic conditions. Whatever the mechanism, the elevated HNP1-3 level might not be genetically determined or at least independent of the copy number variation of the *DEFA1/DEFA3* genes. In contrast, the CC genotype of the C-44G SNP of *DEFB1* was more frequent in diabetic patients than in healthy controls, which draws the attention to the genetic background of a potentially impaired function of hBD1 (human defensin β-1) in diabetes. These data support the view that both alpha and beta-defensins may have important roles in the pathogenesis of diabetes and diabetic complications. Our results should be regarded as preliminary results, which should be confirmed on a larger series of patients in a future multicenter study.

ACKNOWLEDGMENTS

We thank Mrs.Györgyi Müller for expert technical assistance. This work was supported by TÁMOP-4.2.2.A-11-1-KONV-2012-0035 Research Grant

COMMENTS

Background

There is a growing evidence of the role of innate immunity in diabetes. Defensins are members of small antimicrobial peptides of the innate immune system. **I**n addition to their antibacterial and antiviral effects, immunologic functions of defensins has been shown to play a role in the homeostasis. To date, little is known about the genetic basis and the functions of α- and β-defensins in diabetes. The aim of our study was to investigate the genetic background of human defensin-α and human defensin β-1 production in adult patients with type1 and type 2 diabetes, especially with complications.

R*esearch Frontiers*

Neutrophil granulocytes are considered to be the primary cellular origin of α-defensins; HNP 1-3 . HNPs can be released into the extracellular milieu following granulocyte activation as a consequence of degranulation, leakage, cell death, and lysis during inflammation . Human beta defensins are expressed mainly by epithelial cells of the skin, gut, respiratory and urogenital tissues, the pancreas and the kidneys . The level of defensin expression varies among individuals, and it has been suggested that this variation is due to genetic differences in the genes encoding defensins

Innovations and breakthroughs

To our knowledge our data provide the first report about a complex investigation of defensin-alpha and defensin β-1 in type 1 and type 2 diabetes. Increased levels of alpha-defensin -1, -2 and -3 have recently been reported in patients with type 1 diabetes with nephropathy and in cardiovascular complications (Ref 26, 27)..In our study not only HNP1-3 levels in the circulation were measured, but also the copy number variation of *DEFA1/A3* genes was determined in diabetic patients , together with the expression of *DEFA1/A3* in peripheral leukocytes. Several SNPs (single nucleotide polymorphisms) have been characterized of human *DEFB1* (human defensin β-1) gene in previous studies (Ref 18, 19) In our complex study we demonstrated that elevated HNP1-3 levels in diabetes are independent of *DEFA1/DEFA3* copy numbers, but the GG genotype of C-44G SNP in *DEFB1* gene may result in decreased β1-defensin production.

Applications

Our data support the view, that both alpha and beta-defensins may have an important role in the pathogenesis of diabetes and diabetic complications The results may contribute to a better understanding of the roles of defensins in the pathomechanism of diabetes and may represent a future possibility toward broadening of the prognostic laboratory markers.

Terminology

HNP 1-3 are Human Neutrophil Peptides, members of the human α-defensin family. Human defensin β-1 (HBD1) is the member of another family of antimicrobial peptides. Two types of genetic polymorphisms have been identified in genes encoding defensins: copy number

polymorphisms and single nucleotide poymorphisms (SNPs). Several copy number polymorphisms form the major source of genetic polymorphism of α-defensin genes DEFA1 and *DEFA3*, encoding human neutrophil peptides Human defensin beta-1 (HBD-1) is encoded by the gene *DEFB1*. Three frequent SNPs at positions G-20A (rs11362), C-44G (rs 1800972) and G-52A (rs1799946) in the 5'-untranslated region (UTR) of *DEFB1* were described. The untranslated variants influence HBD-1 expression or function.

DEFB1 G-20A	GG	GA	AA	χ^2 test*
Patients with diabetes n = 257	82 (32%)	131 (51%)	44 (17%)	0.568
Type 1 diabetes n = 117	36 (31%)	60 (51%)	21 (18%)	0.775
Type 2 diabetes n = 140	46 (33%)	71 (51%)	23 (16%)	0.573
Controls n = 200	62 (31%)	96 (48%)	42 (21%)	
DEFB1 G-52A	**GG**	**GA**	**AA**	**χ^2 test***
Patients with diabetes n = 257	114 (44%)	104 (40%)	39 (15%)	0.572
Type 1 diabetes n = 117	52 (44%)	47 (40%)	18 (17%)	0.702
Type 2 diabetes n = 140	62 (44%)	57 (41%)	21 (15%)	0.658
Controls n = 200	80 (40%)	84 (42%)	36 (18%)	
DEFB1 C-44G	**CC**	**CG**	**GG**	**χ^2 test***
Patients with diabetes n = 257	156 (61%) +	95 (37%)	6 (2%)**	0.002
Type 1 diabetes n = 117	70 (60%)	44 (37 %)	3 (2.5%)	0.01
Type 2 diabetes n = 140	86 (61%)	51 (36%)	3 (2%)	0.003
Controls n = 200	90 (45%)	92 (46%)	18 (9%)	

Table 1. Genotypes of DEFB1 G-20A, DEFB1 G-52A , and DEFB1 C-44G polymorphisms in patients with diabetes

* chi square test vs. controls

** Fisher test vs. controls, p = 0.001, OR = 9.136, 95% CI: 3.512–23.82

\+ Fisher test vs. controls, p = 0.0009, OR = 2.005, 95% CI: 1.218–2.746

Legends

Fig.1. Plasma levels of human neutrophil peptides (HNP1-3) in patients with type 1 and type 2 diabetes (DM1 and DM2) and healthy controls. The line represents the mean plasma levels of HNP1-3. Significant differences as determined by Mann–Whitney test are indicated.

Fig.2. Plasma levels of human neutrophil peptides (HNP1-3) in diabetic patients with different complications relative to those without complications, and to healthy controls. Mean and SE are indicated; significant differences between groups were determined by unpaired *t test.*

Fig.3. Genomic copy number of *DEFA1/DEFA3* in patients with diabetes and in healthy blood donors. Quantitative box-plot analysis (median, minimum, maximum value, 25% and 75% percentiles) of *DEFA1/A3* copy numbers determined in DNA samples from 133 controls, 100 patients with type 1 diabetes (DM1), and 100 patients with type 2 diabetes (DM2).

Fig.4. Plasma levels of human neutrophil peptides (HNP1-3) in diabetic patients vs. copy numbers of *DEFA1/DEFA3*. The *DEFA1/A3* copy numbers were determined by quantitative PCR analysis and compared to the HNP1-3 plasma level of the same patient (50 with type 1 and 50 with type 2 diabetes).

Fig.5. Relative mRNA expression levels of *DEFA1/DEFA3* in diabetic patients vs. copy numbers of *DEFA1/DEFA3*. The *DEFA1/A3* copy numbers were determined by quantitative PCR analysis and compared to the *DEFA1/DEFA3* mRNA measured by RT-PCR of the same patient (12 with type 1 and 12 with type 2 diabetes).

REFERENCES

1 **Ganz T.** Defensins: antimicrobial peptides of innate immunity. *Nature Reviews. Immunology* 2003; **3**: 710-720. [PMID: 12949495, DOI: 10.1038/nri1180]

2 **Chen H**, Xu Z, Peng L, Fang X, Yin X, Xu N, Cen P. Recent advances in the research and development of human defensins. *Peptides* 2006; 27:931-940. [PMID: 16226346, DOI: 10.1016/j.peptides.2005.08.018]

3 **Oppenheim JJ,** Yang D. Alarmins: chemotactic activators of immune responses. *Curr Opin Immunol* 2005; 17:359-365. [PMID: 15955682, DOI: 10.1016/j.coi.2005.06.002]

4 **Bowdish DME**, Davidson DJ, Hancock REW. A re-evaluation of the role of host defence peptides in mammalian immunity. *Curr Protein Pept Sci* 2005; 6:35-51. [PMID: 15638767, DOI: 10.2174/1389203053027494]

5 **Chertov O,** Yang D, Howard OMZ, Oppenheim JJ. Leukocyte granulate proteins mobilize innate host defenses and adaptive immune responses. *Immunol Rev* 2000; 177:68-78. [PMID: 11138786, DOI: 10.1034/j.1600-065X.2000.17702.x]

6 **Yang D,** Biragyn A, Kwak LW, Oppenheim JJ. Mammalian defensins in immunity: more than just microbibidal. *Trends Imunol* 2002; 23:291-296. [PMID: 12072367, DOI: 10.1016/s1471-4906(02)02246-9]

7 **Quinn K,** Henriques M, Parker T, Slutsky AS, Zhang H. Human neutrophil peptides: a novel potential mediator of inflammatory cardiovascular diseases. *Am J Physiol Heart Circ Physiol* 2008; 295: H1817-H1824. [PMID: 18805897, DOI: 10.1152/ajpheart.00472.2008]

8 **Ganz T.** Extracellular release of antimicrobial defensins by human polymorphonuclear leukocytes *Infect. Immun*. 55; 568-571. 1987. [PMID: 3643886,

9 **Papayannopoulos V**, Zychlinsky A. NETs: a new strategy for using old weapons. *Trends Immunol*. 2009;30:513-21. [PMID: 19699684, DOI: 10.1016/j.it.2009.07.011]

10 **Pazgier M,** Hoover DM, Yang D., Lu W, Lubkowski J. Human beta-defensins. *Cell Mol Life Sci* 2006; 63:1294-1313. [PMID: 16710608, DOI: 10.1007/s00018-005-5540-2]

11 **Durr M,** Peschel A. Chemokines meet defensins: the merging concepts of chemoattractans and antimicrobial peptides in host defense. *Infect Immun* 2002; **70**: 6515-6517 [PMID: 12438319, DOI: 10.1128/iai.70.12.6515-6517.2002]

12 **Boman HG** Antibacterial peptides: basic facts and emerging concepts. *J Intern Med* 2003; 254:197-215 [PMID: 12930229, DOI: 10.1046/j.1365-2796.2003.01228.x]

13 **De Smet K** and Contreras R. Human antimicrobial peptides: defensins, cathelicidins and histatins. *Biotechnol Lett* 2005; 27: 1337-1347. [PMID: 16215847, DOI: 10.1007/s10529-005-0936-5]

14 **Zhao C**, Wang I, Lehrer RI: Widespread of beta-defensin hBD-1 in human secretory glands and epithelial cells. *FEBS Letters* 1996;396:319-322. [PMID: 8915011, DOI: 10.1016/0014-5793(96)01123-4]

15 **Schnapp D**, Reid CJ, Harris A: Localization of expression of human beta defensin-1 in the pancreas and kidney. *J Pathol* 1998;186:99-103. [PMID: 9875146, DOI: 10.1002/(sici)1096-9896(199809)186:1<99::aid-path133>3.0.co;2-#]

16 **Duits LA,** Ravensbergen B, Rademaker M, Hiemstra PS, Nibbering PH (2002) Expression of β-defensin 1 and 2 mRNA by human monocytes, macrophages and dendritic cells. Immunology 106:517-525 [PMID: 12153515, DOI: 10.1046/j.1365-2567.2002.01430.x]

17 **Hollox EJ**, Barber JCK, Brookes AJ, Armour JAL. Defensins and the dynamic genome: what we can learn from structural variation at human chromosome band 8p23.1. *Genome Res* 2009; 1686-1697. [PMID: 18974263, DOI: 10.1101/gr.080945.108]

18 **Dork T**, Stuhrmann M: Polymorphisms of the human beta-defensin-1 gene. *Mol Cell Probes* 1998;12:171-173. [PMID: 9664579, DOI: 10.1006/mcpr.1998.0165]

19 **Sun CQ**, Arnold R, Fernandez-Golarz C, Parrish AB, Almekinder T, He J, Ho SM, Svoboda P, Pohl J, Marshall FF, Petros JA. Human beta-defensin-1, a potential chromosome 8p tumor suppressor: control of transcription and induction of apoptosis in renal cell carcinoma. *Cancer Res*. 2006; 66:8542-8549. [PMID: 16951166, DOI: 10.1158/0008-5472.can-06-0294]

20 **Linzmeier RM,** Ganz T. Human defensin gene copy number polymorphisms: comprehensive analysis of independent variation in α- and β-defensin regions at 8p22-p23. *Genomics* 2005; 86: 423-430. [PMID: 16039093, DOI: 10.1016/j.ygeno.2005.06.003]

21 **Selsted M.E**,. Ouellette A J. Mammalian defensins in the antimicrobial immune response, *Nat. Immunol.* 2006; 6: 551–557. [PMID: 15908936, DOI: 10.1038/ni1206]

22 **Aldred PM**, Hollox EJ, Armour JA. Copy number polymorphism and expression level variation of the human alpha-defensin genes DEFA1 and DEFA3. *Hum Mol Genet*. 2005;14:2045–2052. [PMID: 15944200, DOI: 10.1093/hmg/ddi209]

23 **Froy O**., Hananel A., Chapnik N, Madar Z. Differential effect of insulin treatment on decreased levels of beta-defensins and Toll-like receptors in diabetic rats. *Molecular Immunology* 2007; 44: 796-802 [PMID: 16740310, DOI: 10.1016/j.molimm.2006.04.009]

24 **Barnea M**, Madar Z, Froy O. Glucose and insulin are needed for optimal defensin expression in human cell lines. Biochem Biophys Res Commun. 2008; 367:452-456. [PMID:18178160, DOI: 10.1016/j.bbrc.2007.12.158]

25 **Guimarães RL,** Segat L, Rocha CR, Brandão LA, Zanin V, Araujo J, Naslavsky MS, de Lima Filho JL, Crovella S. Functional polymorphisms of DEFB1 gene in type 1 diabetes Brazilian children *Autoimmunity.* 2009; 42:406-413 [PMID: 19811257]

26 **Saraheimo M**, Forsblom C, Pettersson-Fernholm K, Flyvbjerg A, Groop PH, Frystyk J; FinnDiane Study Group Increased levels of alpha-defensin (-1, -2 and -3) in type 1 diabetic patients with nephropathy. *Nephrol Dial Transplant* 2008; 23: 914-918. [PMID: 18003664, DOI: 10.1093/ndt/gfm711]

27 **Joseph J,** Tarnow L, Astrup AS, Hansen T K, Parving H H, Flyvbjerg A, Frystyk J. Plasma alpha-defensin is associated with cardiovascular morbidity and mortality in type 1 diabetic patients. *J Clin Endocrinol Metab* 2008, 93: 1470-1475 [PMID: 18211979, DOI: 10.1210/jc.2007-1910]

28 **Chen Q X.,** Hakimi M., Wu S, Jin Y, Cheng B, Wang H H, Xie G, Ganz T, Linzmeier R M, Fang X M. Increased Genomic Copy Number of DEFA1 / DEFA3 Is Associated with Susceptibility to Severe Sepsis in Chinese Han Population. *Anesthesiology* 2010; 112:1428-1834. [PMID: 20502117, DOI: 10.1097/ALN.0b013e3181d968eb]

29 **Henrichsen C. N**, Chaignat E, Reymond A. Copy number variants, diseases and gene expression. *Human Molecular Genetics,* 2009, Vol.18, R1-R8. [PMID: 19297395, DOI: 10.1093/hmg/ddp011]

30 **Joshi MB**, Lad A, Bharath Prasad AS, Balakrishnan A, Ramachandra L, Satyamoorthy K. High glucose modulates IL-6 mediated immune homeostasis through impeding neutrophil extracellular trap formation. *FEBS Lett.* 2013; 587: 2241-2246. [PMID: 23735697 DOI: 10.1016/j.febslet.2013.05.053.]

31 **Fang X M,** Shu Q, Chen Q X, Book M, Sahl HG, Hoeft A, Stuber F : Differential expression of α - and β-defensins in human peripheral blood. *Eur J Clin Invest,* 2003; 11: 82-87 [PMID: 12492457 DOI: 10.1046/j.1365-2362.2003.01076.]

32 **Neuwirth A**., Dobeš J., Oujezdská J., Ballek O., Benesova M, Sumink Z, Vcelakova J, Kolouskova S, Obermannova B, Kolátr M, Stechova K, FilippD.:Eosinophils from patients with type 1 diabetes mellitus express high level of myeloid alpha-defensins and myeloperoxidase. *Cellular Immunol* 2012; 273: 158-163 [PMID: 22248881, DOI: 10.1016/j.cellimm.2011.12.001]

33 **Prado-Montes de Oca E,** Garcia-Vargas A, Lozano-Inocencio R, Gallegos-Arreola MP, Sandoval-Ramirez L, Davalos-Rodriguez NO, Figuera LE: Association of beta-defensin 1 single nucleotide polymorphisms with atopic dermatitis. *Int Arch Allergy Immunol* 2007; 142:211-218. [PMID: 17108702, DOI: 10.1159/000097023]

34 **Jurevic RJ,** Bai M, Chadwick RB, White TC, Dale BA. Single-nucleotide polymorphisms (SNPs) in human β-defensin 1: High-throughput SNP assays and association with Candida carriage in type I diabetics and nondiabetic controls. *J Clin Microbiol* 2003, 41: 90-6. [PMID: 12517831, DOI: 10.1128/jcm.41.1.90-96.2003]

35 **Prado-Montes de Oca E**, Velarde- Félix J S, Rios-Tosdaldo J J, Picos-Cárdenas J P, Figuera L E. SNP 668 C(-44) alters of NKκB1 putative binding site in non-coding strand of human β-defensin 1 (DEFB1) and is associated with lempromatous leprosy. *Infection, Genetics, and Evolution* 2009; 9: 612-625. [PMID: 19460328, DOI: 10.1016/j.meegid.2009.03.006]

Figure 1.

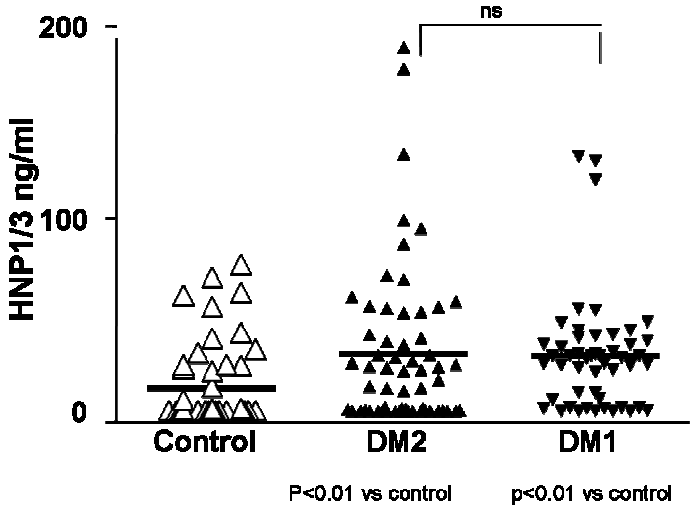

Figure 2.

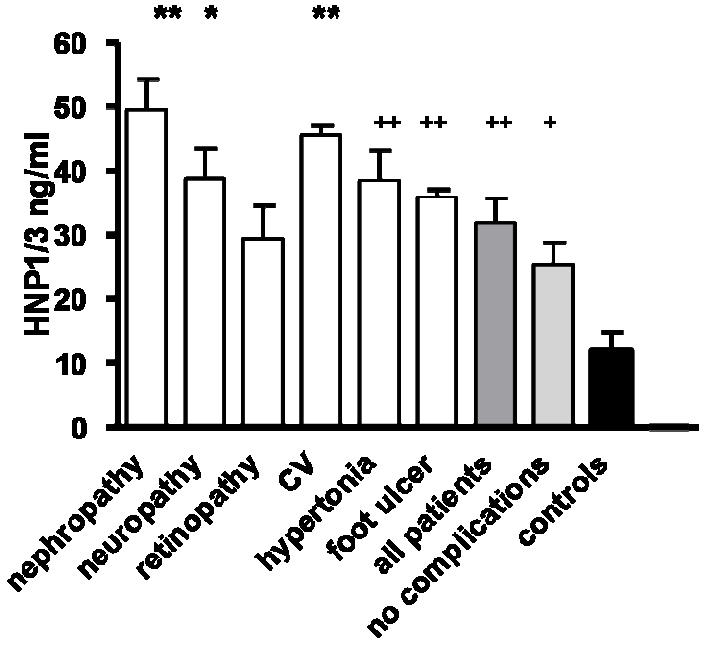

** p<0.001 , * p<0.05 vs without complications
++ p< 0.01 , + p<0.05 vs controls

Figure 3.

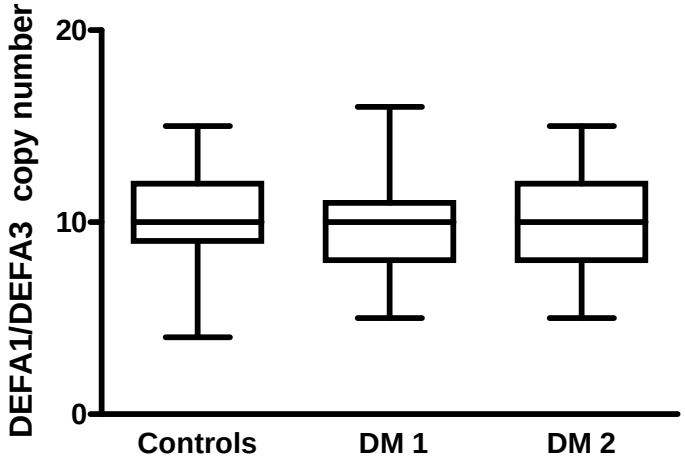

Figure 4.

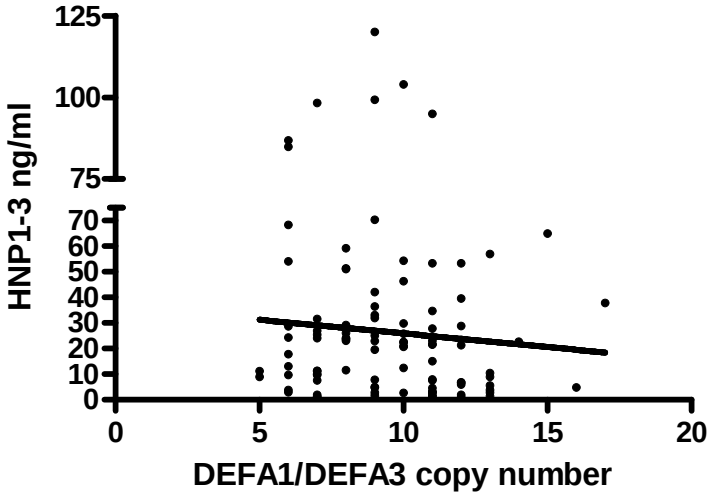

Figure 5.

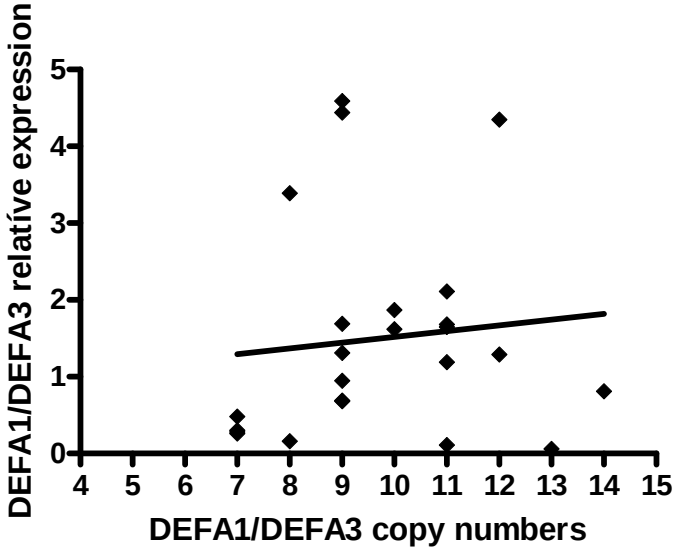

II.

Am J Physiol Gastrointest Liver Physiol 306: G466–G473, 2014.
First published January 23, 2014; doi:10.1152/ajpgi.00419.2013.

Human cationic trypsinogen (*PRSS1*) variants and chronic pancreatitis

Balázs Csaba Németh and Miklós Sahin-Tóth

Department of Molecular and Cell Biology, Henry M. Goldman School of Dental Medicine, Boston University, Boston, Massachusetts

Submitted 6 December 2013; accepted in final form 14 January 2014

Németh BC, Sahin-Tóth M. Human cationic trypsinogen (*PRSS1*) variants and chronic pancreatitis. *Am J Physiol Gastrointest Liver Physiol* 306: G466–G473, 2014. First published January 23, 2014; doi:10.1152/ajpgi.00419.2013.—Variations in the serine protease 1 (*PRSS1*) gene encoding human cationic trypsinogen have been conclusively associated with autosomal dominant hereditary pancreatitis and sporadic nonalcoholic chronic pancreatitis. Most high-penetrance *PRSS1* variants increase intrapancreatic trypsin activity by stimulating trypsinogen autoactivation and/or by inhibiting chymotrypsin C-dependent trypsinogen degradation. Alternatively, some *PRSS1* variants can cause trypsinogen misfolding, which results in intracellular retention and degradation with consequent endoplasmic reticulum stress. However, not all *PRSS1* variants are pathogenic, and clinical relevance of rare variants is often difficult to ascertain. Here we review the *PRSS1* variants published since 1996 and discuss their functional properties and role in chronic pancreatitis.

The PRSS1 Gene

The serine protease 1 (*PRSS1*, *PR*otea*S*e *S*erine *1*) gene in humans is located on chromosome 7q35, within the T cell receptor beta locus (43). The association of trypsinogen genes with this locus is important historically, because DNA sequencing of this region in 1996 and the fortuitous finding of eight trypsinogen genes intercalated here greatly facilitated the discovery of the susceptibility gene for hereditary pancreatitis. *PRSS1* codes for human cationic trypsinogen, the precursor for the most abundant digestive enzyme secreted by the human pancreas (45). Besides *PRSS1*, the locus also contains five trypsinogen pseudogenes, a relic gene, and *PRSS2*, that encodes anionic trypsinogen, the other major human trypsinogen isoform. The *PRSS3* gene coding for mesotrypsinogen, the relatively minor third human isoform, is found on chromosome 9p13.

Copy Number Mutations in PRSS1

Heterozygous triplication and duplication of a 605-kb segment containing the trypsinogen genes on chromosome 7 was found in French patients with hereditary and sporadic idiopathic chronic pancreatitis (5, 29, 33). Presumably similar heterozygous duplications of *PRSS1* were reported in two U.S. families with hereditary pancreatitis (26). Such copy number mutations should result in higher trypsinogen expression through a gene-dosage effect, although this has not been demonstrated directly. Higher trypsinogen concentrations, in turn, would increase the likelihood of autoactivation and development of intrapancreatic trypsin activity. A unique duplication event that resulted in an extra copy of a hybrid *PRSS2/PRSS1* trypsinogen gene was also described in a French family with hereditary pancreatitis (34).

Address for reprint requests and other correspondence: M. Sahin-Tóth, 72 E. Concord St., Evans-433, Boston, MA 02118 (e-mail: miklos@bu.edu).

Gene Conversions Within Trypsinogen Genes

Human trypsinogen genes exhibit a high level of sequence identity, which may facilitate gene conversion events. In fact, gene conversion was suggested as a mechanism for the evolutionary origin of the most common hereditary pancreatitis-associated mutations (6). A gene conversion event was identified in a 6-yr-old German girl with sporadic chronic pancreatitis, which replaced exon 2 in *PRSS1* with that from *PRSS2* (60). A gene duplication event in a French family with hereditary pancreatitis resulted in a similar hybrid gene, containing exons 1–2 from *PRSS2* and exons 3–4–5 from *PRSS1* (34). Since exon 1 codes for part of the signal peptide which is removed in the endoplasmic reticulum, only changes in exon 2 affect the mature trypsinogen protein. The amino acids encoded by exon 2 are nearly identical between the two isoforms, with the exception of Ile29 and Ser54 found in anionic trypsinogen (*PRSS2*). Consequently, the hybrid genes described in the German and French studies encode cationic trypsinogen with mutations p.N29I and p.N54S. Whereas the p.N54S variation is functionally innocuous (60), the p.N29I mutation causes hereditary pancreatitis.

Common Polymorphisms in PRSS1

Polymorphic variations with a population frequency >5% are relatively rare in *PRSS1*. Variant c.486C>T (p.D162= or p.D162D; dbSNP rs6666) in exon 4 and variant c.738C>T (p.N246= or p.N246N, dbSNP rs6667) in exon 5 are the only two variations within the coding region. The two variants are typically found in linkage disequilibrium and the C allele has a slightly higher frequency in Europeans (0.6), whereas it is less frequent (0.25) in subjects of Asian origin or subjects from India (0.1). No disease association has been demonstrated for either variant. Two additional common variants can be found in the 5′ region upstream of the ATG start codon: c.−204C>A (dbSNP rs4726576; C allele frequency is ~0.7 in Europeans

and ~0.4 in Asians) and c.−408C>T (dbSNP rs10273639; C allele frequency is ~0.6 in Europeans and ~0.3 in Asians). In a recent genomewide association study, variant c.–408C>T (i.e., the T allele) was demonstrated to have a small protective effect against chronic pancreatitis presumably by lowering trypsinogen expression (64). The C allele of the same variation (erroneously reported as −409C/T) was previously claimed to offer protection against pancreatic cancer in a Chinese population; however, independent confirmation is lacking (31).

PRSS1 Variants in the General Population

Published accounts indicate that sequencing the *PRSS1* gene of 200 French (7), 82 German (58), 420 Chinese (4, 68), 28 Korean (30), and 150 Brazilian (3) control subjects revealed only the p.E79K exon 3 variant in a French and a Brazilian individual. More recently, exon 3 of 1,000 healthy controls of German origin was sequenced and only the p.V123L variation was identified in a single subject (46). These observations indicate that *PRSS1* variants, other than the common polymorphisms, are exceedingly rare in the general population.

PRSS1 Mutations in Hereditary Pancreatitis

Autosomal dominant hereditary pancreatitis was first reported by Comfort and Steinberg in 1952 (10). Using genetic linkage analysis, three independent research groups localized the susceptibility gene to chromosome 7 in 1996 (27, 39, 62). In the same year, Whitcomb et al. (63) used candidate gene sequencing to identify the most common causative mutation p.R122H in *PRSS1*. Genetic heterogeneity underlying hereditary pancreatitis was soon recognized when the second most common *PRSS1* mutation, p.N29I, was described by two groups in 1997–1998 (16, 56). These two heterozygous mutations are found in ~90% of hereditary pancreatitis families worldwide, with p.R122H accounting for ~65% and p.N29I for ~25% of the cases. In the remaining 10% of the cases, *PRSS1* mutations p.A16V, p.D21A, p.D22G, p.K23R, p.K23_I24insIDK, p.N29T, p.V39A, p.R116C, and p.R122C were identified, always in the heterozygous state (2, 12, 22, 28, 40, 48, 55, 57, 65, 67). Mutations p.D21A, p.D22G, p.K23R, p.K23_I24insIDK, and p.V39A were found only in a single family each. Penetrance of *PRSS1* mutations in hereditary pancreatitis families is incomplete; it is estimated between 80 and 90% for carriers of p.R122H, although smaller pedigrees may exhibit lower apparent penetrance (21, 62, 41, 49). Note that mutations p.A16V and p.R116C exhibit variable penetrance and were also found in sporadic cases with no family history.

Hereditary pancreatitis-associated *PRSS1* mutations exert their effect via a so-called trypsin-dependent pathological pathway, which involves increased autoactivation of mutant trypsinogens resulting in elevated intrapancreatic trypsin activity. Rare mutations in the activation peptide of trypsinogen (p.D21A, p.D22G, p.K23R, and p.K23_I24insIDK) directly stimulate autoactivation (8, 15, 22, 37). In contrast, the more common hereditary pancreatitis-associated *PRSS1* mutations alter the regulation of activation and degradation of cationic trypsinogen by chymotrypsin C (CTRC), a digestive enzyme that controls trypsin levels generated through autoactivation of human trypsinogens (51) (Fig. 1). CTRC promotes degradation of trypsinogen by cleaving the Leu81-Glu82 peptide bond in the calcium binding loop and thereby attenuates trypsin levels during autoactivation (51, 52, 53). Importantly, trypsin-mediated autolytic cleavage of the Arg122-Val123 peptide bond is also required for CTRC-dependent degradation and inactivation of trypsinogen (51, 53). Paradoxically, CTRC also stimulates trypsinogen activation by processing the activation peptide at the Phe18-Asp19 peptide bond to a shorter form, which is cleaved by trypsin at a higher rate, resulting in increased autoactivation (38, 51).

PRSS1 mutations interfere with the CTRC-mediated cleavages described above and render trypsinogen resistant to degradation and/or increase processing of the activation peptide (Fig. 1). Typically, a combination of two or more effects results in the common phenotype of increased activation (51). Thus mutations p.R122H and p.R122C completely block cleavage at Arg122 by trypsin but also decrease cleavage at Leu81 by CTRC. Mutation p.N29I increases cleavage of the activation peptide and reduces cleavage both at Leu81 and Arg122. Mutations p.V39A and p.N29T decrease cleavage at Leu81 and Arg122, whereas mutation p.A16V increases processing of the activation peptide by CTRC (38, 51). Regardless of mechanistic details, the unifying biochemical phenotype of all hereditary pancreatitis-associated mutants is increased rates of autoactivation, with markedly elevated final trypsin activity levels, relative to wild-type cationic trypsinogen.

The only exception to the unifying pathological mechanism described above is mutation p.R116C, which does not change trypsinogen activation but causes misfolding, which results in intracellular aggregation and degradation and consequently reduced secretion (25). Mutation-induced misfolding can elicit endoplasmic reticulum stress, which is probably responsible for the increased disease risk in carriers of p.R116C, although the exact mechanism is unknown. Mutation p.R116C exhibits variable penetrance and is often found in sporadic cases, suggesting that the misfolding-dependent pathological pathway may confer relatively smaller risk.

PRSS1 Variants in Sporadic Nonalcoholic Chronic Pancreatitis

The first indication that *PRSS1* variants can cause chronic pancreatitis with lower penetrance came from the identification of the p.A16V variant by Witt et al. (65) in four children with chronic pancreatitis. Only one child had a positive family history consistent with hereditary pancreatitis, whereas in three children the disease was sporadic with no family history, even though inheritance from unaffected parents was demonstrated. Subsequent studies based on the EUROPAC database (18) confirmed the variable penetrance of this variant, demonstrating that p.A16V was found in six families with hereditary pancreatitis, in one family with familial (single-generation) chronic pancreatitis, and in three cases of chronic pancreatitis with no family history. The biochemical phenotype of the p.A16V explains its genetic properties: the mutation causes increased autoactivation in the presence of CTRC; however, the rate of autoactivation and the final trypsin levels attained are much lower than those observed with the highly penetrant *PRSS1* mutations such as p.R122H (51). Increased autoactivation is due to faster processing of the mutant trypsinogen activation peptide by CTRC (38, 51). As noted above, mutation

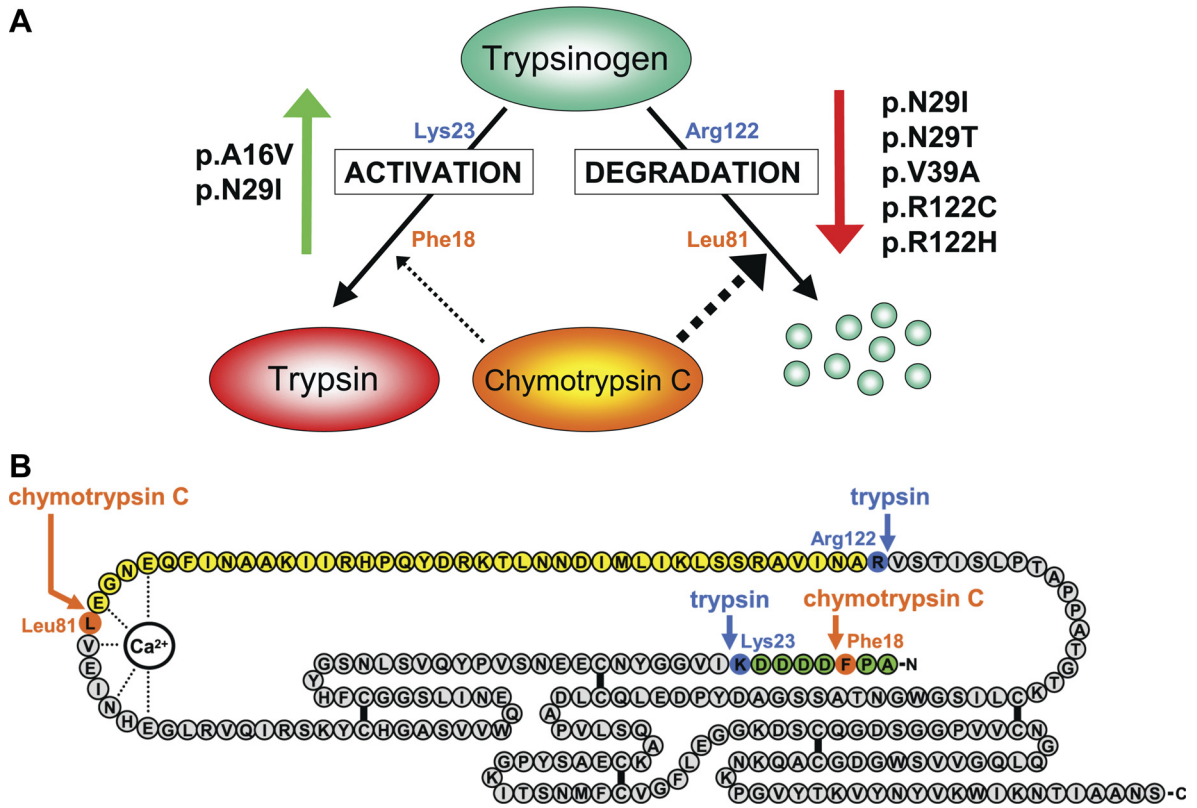

Fig. 1. Effect of pancreatitis-associated *PRSS1* mutations on the chymotrypsin C (CTRC)-dependent activation and degradation of human cationic trypsinogen. CTRC cleaves the Leu81-Glu82 peptide bond and trypsin cleaves the Arg122-Val123 peptide bond; these 2 cleavages result in the eventual degradation of trypsinogen. CTRC also stimulates autoactivation of cationic trypsinogen by cleaving the Phe18-Asp19 peptide bond in the activation peptide. The shortened activation peptide is more susceptible to trypsin-mediated activation at the Lys23-Ile24 peptide bond. The dominant effect of CTRC is degradation. *A*: *PRSS1* mutations can increase conversion of trypsinogen to trypsin by inhibition of CTRC-dependent trypsinogen degradation (red arrow) or by increasing CTRC-dependent stimulation of autoactivation (green arrow). See text for further details. *B*: proteolytic cleavage of human cationic trypsinogen by CTRC and trypsin. Primary structure of trypsinogen with disulfide bonds is shown. CTRC cleavage sites are highlighted in orange and trypsin cleavage sites are shown in blue. The activation peptide is in green. Note the yellow peptide segment not stabilized by disulfide bonds between the Leu81 and Arg122 cleavage sites. *B* is modified from Ref. 53, copyright by the National Academy of Sciences of the United States of America.

p.R116C is another example of a hereditary pancreatitis-associated mutation with variable penetrance. A recent study demonstrated that variant p.G208A was associated with ~4% of idiopathic and alcoholic chronic pancreatitis patients of Japanese origin, and increased disease risk by ~15- to 20-fold (32). This variant has no effect on trypsinogen activation but causes a moderate (~60%) reduction in trypsinogen secretion from transfected cells (46). Thus, as seen with variant p.R116C, mutation-induced misfolding and endoplasmic reticulum stress may be the pathologically relevant mechanism for variant p.G208A as well. It is also noteworthy that p.G208A is the first *PRSS1* variant for which an association with alcoholic pancreatitis has been demonstrated.

Screening of various patient populations with sporadic idiopathic chronic pancreatitis has led to the identification of a large number of rare missense variants (4, 7, 14, 23, 30, 35, 42, 55, 58). The clinical significance of such variants has been unclear because their low frequency did not allow statistical determination of genetic association with pancreatitis. Nevertheless, authors often described these as causative or pancreatitis-associated simply by analogy with well-characterized disease-relevant *PRSS1* mutations. Characterization of the functional phenotype of these variants revealed that only the activation peptide variant p.D19A increased autoactivation in a manner similar to the hereditary pancreatitis-associated activation-peptide mutations (8, 15, 37). A handful of mutants showed a marked (p.D100H, p.C139F, and p.C139S) or moderate (p.K92N and p.S124F) secretion defect, which suggested that these mutations exerted their pathogenic effect through a mechanism that involves mutation-induced misfolding and endoplasmic reticulum stress, as described above for mutations p.R116C and p.G208A (25, 46). Another subset of mutants showed no phenotypic alterations compared with wild-type trypsinogen (p.L81M, p.Q98K, p.A121T, p.T137M, and p.S181G) or suffered increased degradation by CTRC (p.P36R, p.G83E, p.I88N, and p.V123M) (46, 52, 54). These variants are likely harmless and their identification in patients with chronic pancreatitis may be accidental. One variant (p.K170E) caused slightly increased trypsinogen secretion, which, similarly to the copy number mutations, may translate to increased risk for pancreatitis (46).

Variant p.E79K should be highlighted because this is the only rare *PRSS1* variant that was found not only in patients but also in unrelated controls (3, 7, 20, 23, 41, 50, 59). Early biochemical studies demonstrated an increased propensity of this mutant to transactivate anionic trypsinogen; however, this small phenotypic change is unlikely to be of pathological consequence (59). More recent studies indicated that the rate of

Table 1. *Variants in the PRSS1 gene encoding human cationic trypsinogen*

Region	Nucleotide Change	Amino Acid Change	Number of CP Carriers Reported	Number of Non-CP Carriers Reported	Clinical Significance
	PRSS1 duplication		7		Pathogenic
	PRSS1 triplication		26	2	Pathogenic
5 prime	c.−408C>T		common polymorphism	common polymorphism	Protective
5 prime	c.−204C>A		common polymorphism	common polymorphism	Nonpathogenic
5 prime	c.−36G>A			1	Unknown
5 prime	c.−30_−28delTCC		1		Unknown
intron 1	c.40+1G>A			1	Protective
intron 1	c.40+40delC		1		Unknown
intron 1	c.41–49C>T		1		Unknown
exon 2	c.47C>T	p.A16V	39	24	Pathogenic
exon 2	c.56A>C	p.D19A	1		Pathogenic
exon 2	c.62A>C	p.D21A	3		Pathogenic
exon 2	c.65A>G	p.D22G	2	1	Pathogenic
exon 2	c.68A>G	p.K23R	2		Pathogenic
exon 2	c.63_71dup	p.K23_I24insIDK	3		Pathogenic
exon 2	c.86A>T	p.N29I	285	18	Pathogenic
exon 2	*PRSS1-PRSS2* hybrid	p.N29I + p.N54S	7	1	Pathogenic
exon 2	c.86A>C	p.N29T	5		Pathogenic
exon 2	c.107C>G	p.P36R	2		Nonpathogenic
exon 2	c.111C>A	p.Y37X		1	Protective
exon 2	c.116T>C	p.V39A	7		Pathogenic
intron 2	c.200+1G>A			1	Protective
exon 3	c.235G>A	p.E79K	13	6	Pathogenic?
exon 3	c.241C>A	p.L81M	4		Unknown
exon 3	c.248G>A	p.G83E	1		Nonpathogenic
exon 3	c.263T>A	p.I88N	1		Nonpathogenic
exon 3	c.273C>A	p.A91=	1		Unknown
exon 3	c.276G>T	p.K92N	1		Pathogenic
exon 3	c.292C>A	p.Q98K	1		Nonpathogenic
exon 3	c.298G>C	p.D100H	2	3	Pathogenic
exon 3	c.310C>G	p.L104V		4	Unknown
exon 3	c.311T>C	p.L104P	1	3	Pathogenic
exon 3	c.346C>T	p.R116C	16	4	Pathogenic
exon 3	c.361G>A	p.A121T	14	6	Nonpathogenic
exon 3	c.364C>T	p.R122C	35	23	Pathogenic
exon 3	c.365G>A	p.R122H	793	69	Pathogenic
exon 3	c.365_366GC>AT	p.R122H	3		Pathogenic
exon 3	c.367G>A	p.V123M	1		Nonpathogenic
exon 3	c.367G>T	p.V123L		1	Nonpathogenic
exon 3	c.371C>T	p.S124F	1		Pathogenic
exon 3	c.403A>G	p.T135A		1	Unknown
exon 3	c.410C>T	p.T137M	2	1	Nonpathogenic
exon 3	c.415T>A	p.C139S	11		Pathogenic
exon 3	c.416G>T	p.C139F	2	1	Pathogenic
exon 3	c.417C>T	p.C139=		1	Unknown
exon 3	c.443C>T	p.A148V		1	Unknown
intron 3	c.454+10A>C		5		Unknown
intron 3	c.454+36T>C			1	Unknown
intron 3	c.454+75A>G		24	4	Unknown
intron 3	c.454+127A>T		1		Unknown
intron 3	c.454+157C>A		1		Unknown
intron 3	c.454+157C>G		1	2	Unknown
intron 3	c.454+172C>T		4		Unknown
intron 3	c.455–192T>A		1		Unknown
exon 4	c.486C>T	p.D162=	common polymorphism	common polymorphism	Nonpathogenic
exon 4	c.508A>G	p.K170E	2		Pathogenic?
exon 4	c.541A>G	p.S181G	1	1	Nonpathogenic
intron 4	c.592–79G>A		1		Unknown
intron 4	c.592–78G>A		1		Unknown
intron 4	c.592–24C>T		1		Unknown
intron 4	c.592–11C>T		1		Unknown
intron 4	c.592–8C>T		1		Unknown

Continued

Table 1.—*Continued*

Region	Nucleotide Change	Amino Acid Change	Number of CP Carriers Reported	Number of Non-CP Carriers Reported	Clinical Significance
exon 5	c.623G>C	p.G208A	22	3	Pathogenic
exon 5	c.738C>T	p.N246=	common polymorphism	common polymorphism	Nonpathogenic

Adapted from www.pancreasgenetics.org, February 2, 2014. For a complete list of citations please visit the database website. The number of reported chronic pancreatitis (CP) carriers is an approximation for the most frequent variants, because authors often published the same patients in multiple publications without indicating the repetitive entries. Non-CP carriers include nonpenetrant family members, unrelated healthy control subjects or individuals with conditions other than pancreatitis. The clinical significance field indicates our interpretation of the available genetic and functional data with respect to the pathogenic potential of *PRSS1* variants. The following genetic evidence was considered as indicative of pathogenic nature: segregation with disease, multiple reports worldwide of affected carriers, and absence in unrelated controls. In case of rare variants, phenotypic similarity to well-characterized, hereditary pancreatitis-associated mutations served as the basis for classification. Thus variants were considered pathogenic if they caused *1*) increased autoactivation in the absence or presence of chymotrypsin C (CTRC), *2*) reduced secretion, indicative of potential misfolding, or *3*) increased trypsinogen expression or secretion. Conversely, variants that are expected to reduce trypsinogen expression were designated protective.

autoactivation of mutant p.E79K is suppressed in the presence of CTRC; however, the mutant reaches higher final trypsin levels than wild-type trypsinogen, because of its resistance to CTRC-mediated degradation (A. Szabó and M. Sahin-Tóth, unpublished observations). Thus the biochemical phenotype is inconclusive but, together with the genetic data, may be cautiously interpreted as p.E79K being a mild pathogenic variant with low penetrance.

PRSS1 Variants in Conditions Unrelated to Pancreatitis

Chen et al. (9) reported two loss-of-function *PRSS1* variants, a nonsense variant p.Y37X and a splice-site mutation c.200+1G>A in intron 2 found in chronic alcoholics without pancreatic disease. The authors suggested that the variants should be protective against chronic pancreatitis. Gullo et al. (19) investigated *PRSS1* variants in benign pancreatic hyperenzymemia and found variant p.A148V and the splice-site mutation c.40+1G>A in intron 1. Variant p.A148V has no functional consequences (A. Schnúr and M. Sahin-Tóth, unpublished observations), whereas variant c.40+1G>A should result in decreased trypsinogen expression, which might be protective against chronic pancreatitis. Two studies described *PRSS1* variants in Chinese patients with pancreatic cancer (p.T135A, p.T137M, c.454+36T>C, and c.454+157C>G in intron 3), which are in all likelihood incidental findings unrelated to pathology (13, 68). The same group proposed a strong protective effect for the C allele of the common polymorphic variant c.−408C>T (erroneously reported as −409C/T) against pancreatic cancer (31). Variant p.L104V was reported in two female members of a Chinese family with familial solid pseudopapillary tumor of the pancreas and in two healthy male relatives (17). Finally, patients with

Table 2. *Mechanism of action of pathogenic* PRSS1 *variants*

Region	Nucleotide change	Amino acid change	Pathogenic mechanism	Notes	Citations
	PRSS1 duplication		increased secretion	no direct evidence	
	PRSS1 triplication		increased secretion	no direct evidence	
exon 2	c.47C>T	p.A16V	increased activation	CTRC dependent	38, 51
exon 2	c.56A>C	p.D19A	increased activation		8, 15, 24, 37
exon 2	c.62A>C	p.D21A	increased activation		37
exon 2	c.65A>G	p.D22G	increased activation		8, 15, 22, 24, 57
exon 2	c.68A>G	p.K23R	increased activation		8, 15, 24, 57
exon 2	c.63_71dup	p.K23_I24insIDK	increased activation		15, 22
exon 2	c.86A>T	p.N29I	increased activation	CTRC dependent	51
exon 2	*PRSS1-PRSS2* hybrid	p.N29I + p.N54S	increased activation	CTRC dependent	51, 60
exon 2	c.86A>C	p.N29T	increased activation	CTRC dependent	51
exon 2	c.116T>C	p.V39A	increased activation	CTRC dependent	51
exon 3	c.235G>A	p.E79K	increased activation*	CTRC dependent	unpublished
exon 3	c.276G>T	p.K92N	misfolding		46
exon 3	c.298G>C	p.D100H	misfolding		46
exon 3	c.311T>C	p.L104P	misfolding		unpublished
exon 3	c.346C>T	p.R116C	misfolding		25
exon 3	c.364C>T	p.R122C	increased activation	CTRC dependent	51
exon 3	c.365G>A	p.R122H	increased activation	CTRC dependent	51
exon 3	c.365_366GC>AT	p.R122H	increased activation	CTRC dependent	51
exon 3	c.371C>T	p.S124F	misfolding		46
exon 3	c.415T>A	p.C139S	misfolding		25
exon 3	c.416G>T	p.C139F	misfolding		46
exon 4	c.508A>G	p.K170E	increased secretion		46
exon 5	c.623G>C	p.G208A	misfolding		46

See Table 1 for inclusion criteria. Mutations in *PRSS1* can increase activation of cationic trypsinogen via 4 independent but mutually nonexclusive mechanisms: *1*) inhibition of CTRC-dependent trypsinogen degradation, *2*) increasing CTRC-dependent stimulation of autoactivation; *3*) direct stimulation of autoactivation; and *4*) increased trypsinogen secretion. Alternatively, *PRSS1* mutations can cause misfolding and endoplasmic reticulum stress. See Fig. 1 for CTRC-dependent mechanisms of trypsinogen activation and degradation. *Note that the biochemical phenotype of p.E79K is ambiguous; see text for details. Citations refer to functional studies.

PRSS1-related hereditary pancreatitis have a 40–55% lifetime risk of developing pancreatic cancer (Ref. 66 and references therein).

The PRSS1 Database

The first database for *PRSS1* variants associated with chronic pancreatitis was created by Dr. Niels Teich at the University of Leipzig, Germany (61). Although the link is still active (http://www.uni-leipzig.de/pancreasmutation/db.html), the website has not been updated since 2006. To track the increasing number of *PRSS1* variants in the literature and to help with classification of their clinical relevance, in 2012 we created a new online database. Currently, the database lists 64 *PRSS1* variants: 2 copy number mutations, 34 missense variants, 4 synonymous variants, 1 nonsense variant, 1 microinsertion, 1 hybrid gene, and 21 variants in noncoding regions (Table 1). With respect to clinical significance, 25 variants are pathogenic (Table 2), 14 are nonpathogenic, 4 variants are protective, and 21 (mostly intronic) variants have unknown significance. The database can be accessed at www.pancreasgenetics.org.

Animal Models of PRSS1 Related Pancreatitis

Although considerable progress has been made in clarifying the mechanism of *PRSS1* mutations at the biochemical level, animal models that recapitulate salient features of human hereditary pancreatitis are still lacking. At the time of writing this review, only two publications documented attempts to generate such models. Selig et al. (47) created transgenic mice with the coding DNA of human *PRSS1* containing the p.R122H mutation. The animals did not develop spontaneous pancreatitis, and cerulein caused only slightly more severe pancreatitis in transgenic mice relative to controls. Archer et al. (1) described the spontaneous development of acute and chronic pancreatitis in a transgenic line with the p.R122H mutation introduced into the coding DNA of mouse trypsinogen isoform T8. Unfortunately, independent replications or additional studies on this promising model have not been published since 2006. It is also unclear whether the observed phenotype was related to the expression of the mutant trypsinogen. Nevertheless, this study focused attention to the question whether the biochemical effects human *PRSS1* mutations would be similar in the context of mouse and human trypsinogens and whether we can make use of mouse trypsinogens to model the human disease. Recently, we demonstrated that the mouse pancreas expresses four trypsinogen isoforms to high levels (T7, T8, T9, and T20), and mouse Ctrc strongly inhibits autoactivation of isoforms T8 and T9 through cleavage of the autolysis loop (36). In sharp contrast to the human situation (see Ref. 51 and Fig. 1), mutation p.R122H had no appreciable effect on the autoactivation of T8 trypsinogen in the presence of mouse Ctrc (36). These observations argue that human pancreatitis-associated mutations may not recapitulate the pathogenic biochemical phenotype in the context of mouse trypsinogens.

Genetic deletion of mouse T7 was recently shown to abolish intra-acinar trypsinogen activation in response to hyperstimulation with cerulein, whereas severity of acute pancreatitis was somewhat decreased but not diminished (11). Furthermore, development of cerulein-induced chronic pancreatitis was unaffected by the absence of T7 (44). These observations seem to call into question the direct role of trypsinogen in the development of pancreatitis and seem to be at odds with the preponderance of human genetic and biochemical data discussed in this review. However, a more likely explanation for the apparent contradiction is that the hyperstimulation model employed in these studies does not mimic the pathological pathway associated with human hereditary pancreatitis. Future studies will be needed to shed more light on this intriguing problem.

ACKNOWLEDGMENTS

The authors acknowledge the contributions of János Borbás, as webmaster for the www.pancreasgenetics.org website.

GRANTS

Studies in the senior author's laboratory were supported by NIH grants R01DK058088, R01DK082412, and R01DK095753.

DISCLOSURES

No conflicts of interest, financial or otherwise, are declared by the author(s).

AUTHOR CONTRIBUTIONS

B.C.N. and M.S.-T. conception and design of research; B.C.N. and M.S.-T. prepared figures; B.C.N. and M.S.-T. drafted manuscript; B.C.N. and M.S.-T. edited and revised manuscript; B.C.N. and M.S.-T. approved final version of manuscript.

REFERENCES

1. **Archer H, Jura N, Keller J, Jacobson M, Bar-Sagi D.** A mouse model of hereditary pancreatitis generated by transgenic expression of R122H trypsinogen. *Gastroenterology* 131: 1844–1855, 2006.
2. **Arduino C, Salacone P, Pasini B, Brusco A, Salmin P, Bacillo E, Robecchi A, Cestino L, Cirillo S, Regge D, Cappello N, Gaia E.** Association of a new cationic trypsinogen gene mutation (V39A) with chronic pancreatitis in an Italian family. *Gut* 54: 1663–1664, 2005.
3. **Bernardino AL, Guarita DR, Mott CB, Pedroso MR, Machado MC, Laudanna AA, Tani CM, Almeida FL, Zatz M.** CFTR, PRSS1 and SPINK1 mutations in the development of pancreatitis in Brazilian patients. *JOP* 4: 169–177, 2003.
4. **Chang YT, Wei SC, Tien YWLPC, Jan IS, Su YN, Wong JM, Chang MC.** Association and differential role of PRSS1 and SPINK1 mutation in early-onset and late-onset idiopathic chronic pancreatitis in Chinese subjects. *Gut* 58: 885, 2009.
5. **Chauvin A, Chen JM, Quemener S, Masson E, Kehrer-Sawatzki H, Ohmle B, Cooper DN, Le Maréchal C, Férec C.** Elucidation of the complex structure and origin of the human trypsinogen locus triplication. *Hum Mol Genet* 18: 3605–3614, 2009.
6. **Chen JM, Ferec C.** Gene conversion-like missense mutations in the human cationic trypsinogen gene and insights into the molecular evolution of the human trypsinogen family. *Mol Genet Metab* 71: 463–469, 2000.
7. **Chen JM, Piepoli Bis A, Le Bodic L, Ruszniewski P, Robaszkiewicz M, Deprez PH, Raguenes O, Quere I, Andriulli A, Ferec C.** Mutational screening of the cationic trypsinogen gene in a large cohort of subjects with idiopathic chronic pancreatitis. *Clin Genet* 59: 189–193, 2001.
8. **Chen JM, Kukor Z, Le Maréchal C, Tóth M, Tsakiris L, Raguénès O, Férec C, Sahin-Tóth M.** Evolution of trypsinogen activation peptides. *Mol Biol Evol* 20: 1767–1777, 2003.
9. **Chen JM, Le Maréchal C, Lucas D, Raguénès O, Férec C.** "Loss of function" mutations in the cationic trypsinogen gene (PRSS1) may act as a protective factor against pancreatitis. *Mol Genet Metab* 79: 67–70, 2003.
10. **Comfort MW, Steinberg AG.** Pedigree of a family with hereditary chronic relapsing pancreatitis. *Gastroenterology* 21: 54–63, 1952.
11. **Dawra R, Sah RP, Dudeja V, Rishi L, Talukdar R, Garg P, Saluja AK.** Intra-acinar trypsinogen activation mediates early stages of pancreatic injury but not inflammation in mice with acute pancreatitis. *Gastroenterology* 141: 2210–2217, 2011.
12. **Férec C, Raguénès O, Salomon R, Roche C, Bernard JP, Guillot M, Quéré I, Faure C, Mercier B, Audrézet MP, Guillausseau PJ, Dupont**

C, Munnich A, Bignon JD, Le Bodic L. Mutations in the cationic trypsinogen gene and evidence for genetic heterogeneity in hereditary pancreatitis. *J Med Genet* 36: 228–232, 1999.

13. **Gao F, Liu QC, Zhang S, Zhuang ZH, Lin CZ, Lin XH.** *PRSS1* intron mutations in patients with pancreatic cancer and chronic pancreatitis. *Mol Med Rep* 5: 449–451, 2012.
14. **Gao F, Li YM, Hong GL, Xu ZF, Liu QC, He QL, Lin LQ, Weng SH.** *PRSS1*_p Leu81Met mutation results in autoimmune pancreatitis. *World J Gastroenterol* 19: 3332–3338, 2013.
15. **Geisz A, Hegyi P, Sahin-Tóth M.** Robust autoactivation, chymotrypsin C independence and diminished secretion define a subset of hereditary pancreatitis-associated cationic trypsinogen mutants. *FEBS J* 280: 2888–2899, 2013.
16. **Gorry MC, Gabbaizedeh D, Furey W, Gates LK Jr, Preston RA, Aston CE, Zhang Y, Ulrich C, Ehrlich GD, Whitcomb DC.** Mutations in the cationic trypsinogen gene are associated with recurrent acute and chronic pancreatitis. *Gastroenterology* 113: 1063–1068, 1997.
17. **Gou S, Yu J, Wang C, Liu T, Cui P, Li X.** Three female familial cases of solid pseudopapillary tumors with a protease serine 1 gene mutation. *Pancreas* 42: 168–173, 2013.
18. **Grocock CJ, Rebours V, Delhaye MN, Andrén-Sandberg A, Weiss FU, Mountford R, Harcus MJ, Niemczyck E, Vitone LJ, Dodd S, Jørgensen MT, Ammann RW, Schaffalitzky de Muckadell O, Butler JV, Burgess P, Kerr B, Charnley R, Sutton R, Raraty MG, Devière J, Whitcomb DC, Neoptolemos JP, Lévy P, Lerch MM, Greenhalf W; European Registry of Hereditary Pancreatitis, and Pancreatic Cancer.** The variable phenotype of the p. A16V mutation of cationic trypsinogen (*PRSS1*) in pancreatitis families. *Gut* 59: 357–363, 2010.
19. **Gullo L, Laghi L, Migliori M, Lucrezio L, Bianchi P, Randolph AE, Mantovani V, Bastagli L, Pezzilli R, Malesci A.** *SPINK1* and *PRSS1* mutations in benign pancreatic hyperenzymemia. *Pancreas* 37: 31–35, 2008.
20. **Hamoir C, Pepermans X, Piessevaux H, Jouret-Mourin A, Weynand B, Habyalimana JB, Leal T, Geubel A, Gigot JF, Deprez PH.** Clinical and morphological characteristics of sporadic genetically determined pancreatitis as compared to idiopathic pancreatitis: higher risk of pancreatic cancer in CFTR variants. *Digestion* 87: 229–239, 2013.
21. **Howes N, Lerch MM, Greenhalf W, Stocken DD, Ellis I, Simon P, Truninger K, Ammann R, Cavallini G, Charnley RM, Uomo G, Delhaye M, Spicak J, Drumm B, Jansen J, Mountford R, Whitcomb DC, Neoptolemos JP; European Registry of Hereditary Pancreatitis, and Pancreatic Cancer (EUROPAC).** Clinical and genetic characteristics of hereditary pancreatitis in Europe. *Clin Gastroenterol Hepatol 2*: 252–261, 2004.
22. **Joergensen MT, Geisz A, Brusgaard K, Schaffalitzky de Muckadell OB, Hegyi P, Gerdes AM, Sahin-Tóth M.** Intragenic duplication: a novel mutational mechanism in hereditary pancreatitis. *Pancreas* 40: 540–546, 2011.
23. **Keiles S, Kammesheidt A.** Identification of *CFTR, PRSS1*, and *SPINK1* mutations in 381 patients with pancreatitis. *Pancreas* 33: 221–227, 2006.
24. **Kereszturi E, Sahin-Tóth M.** Intracellular autoactivation of human cationic trypsinogen mutants causes reduced trypsinogen secretion and acinar cell death. *J Biol Chem* 284: 33392–33399, 2009.
25. **Kereszturi E, Szmola R, Kukor Z, Simon P, Weiss FU, Lerch MM, Sahin-Tóth M.** Hereditary pancreatitis caused by mutation-induced misfolding of human cationic trypsinogen: a novel disease mechanism. *Hum Mutat* 30: 575–582, 2009.
26. **LaRusch J, Barmada MM, Solomon S, Whitcomb DC.** Whole exome sequencing identifies multiple, complex etiologies in an idiopathic hereditary pancreatitis kindred. *JOP* 13: 258–262, 2012.
27. **Le Bodic L, Bignon JD, Raguénès O, Mercier B, Georgelin T, Schnee M, Soulard F, Gagne K, Bonneville F, Muller JY, Bachner L, Férec C.** The hereditary pancreatitis gene maps to long arm of chromosome 7. *Hum Mol Genet* 5: 549–554, 1996.
28. **Le Maréchal C, Chen JM, Quéré I, Raguénès O, Férec C, Auroux J.** Discrimination of three mutational events that result in a disruption of the R122 primary autolysis site of the human cationic trypsinogen (PRSS1) by denaturing high performance liquid chromatography. *BMC Genet* 2: 19, 2001.
29. **Le Maréchal C, Masson E, Chen JM, Morel F, Ruszniewski P, Levy P, Férec C.** Hereditary pancreatitis caused by triplication of the trypsinogen locus. *Nat Genet* 38: 1372–1374, 2006.
30. **Lee YJ, Kim KM, Choi JH, Lee BH, Kim GH, Yoo HW.** High incidence of *PRSS1* and *SPINK1* mutations in Korean children with acute recurrent and chronic pancreatitis. *J Pediatr Gastroenterol Nutr* 52: 478–481, 2011.
31. **Liu Q, Lin X, Liu J, Liu A, Gao F.** The −409 C/T genotype of *PRSS1* protects against pancreatic cancer in the Han Chinese population. *Dig Dis Sci* 57: 573–579, 2012.
32. **Masamune A, Nakano E, Kume K, Takikawa T, Kakuta Y, Shimosegawa T.** *PRSS1* c.623G>C (p.G208A) variant is associated with pancreatitis in Japan. *Gut* 63, 366, 2014.
33. **Masson E, Le Maréchal C, Chandak GR, Lamoril J, Bezieau S, Mahurkar S, Bhaskar S, Reddy DN, Chen JM, Férec C.** Trypsinogen copy number mutations in patients with idiopathic chronic pancreatitis. *Clin Gastroenterol Hepatol* 6: 82–88, 2008.
34. **Masson E, Le Maréchal C, Delcenserie R, Chen JM, Férec C.** Hereditary pancreatitis caused by a double gain-of-function trypsinogen mutation. *Hum Genet* 123: 521–529, 2008.
35. **Masson E, Hammel P, Garceau C, Bénech C, Quéméner-Redon S, Chen JM, Férec C.** Characterization of two deletions of the *CTRC* locus. *Mol Genet Metab* 109: 296–300, 2013.
36. **Németh BC, Wartmann T, Halangk W, Sahin-Tóth M.** Autoactivation of mouse trypsinogens is regulated by chymotrypsin C via cleavage of the autolysis loop. *J Biol Chem* 288: 24049–24062, 2013.
37. **Nemoda Z, Sahin-Tóth M.** The tetra-aspartate motif in the activation peptide of human cationic trypsinogen is essential for autoactivation control but not for enteropeptidase recognition. *J Biol Chem* 280: 29645–29652, 2005.
38. **Nemoda Z, Sahin-Tóth M.** Chymotrypsin C (caldecrin) stimulates autoactivation of human cationic trypsinogen. *J Biol Chem* 281: 11879–11886, 2006.
39. **Pandya A, Blanton SH, Landa B, Javaheri R, Melvin E, Nance WE, Markello T.** Linkage studies in a large kindred with hereditary pancreatitis confirms mapping of the gene to a 16-cM region on 7q. *Genomics* 38: 227–230, 1996.
40. **Pfützer R, Myers E, Applebaum-Shapiro S, Finch R, Ellis I, Neoptolemos J, Kant JA, Whitcomb DC.** Novel cationic trypsinogen (PRSS1) N29T and R122C mutations cause autosomal dominant hereditary pancreatitis. *Gut* 50: 271–272, 2002.
41. **Rebours V, Boutron-Ruault MC, Schnee M, Férec C, Le Maréchal C, Hentic O, Maire F, Hammel P, Ruszniewski P, Lévy P.** The natural history of hereditary pancreatitis: a national series. *Gut* 58: 97–103, 2009.
42. **Rosendahl J, Landt O, Bernadova J, Kovacs P, Teich N, Bödeker H, Keim V, Ruffert C, Mössner J, Kage A, Stumvoll M, Groneberg D, Krüger R, Luck W, Treiber M, Becker M, Witt H.** *CFTR*, *SPINK1*, *CTRC* and *PRSS1* variants in chronic pancreatitis: is the role of mutated *CFTR* overestimated? *Gut* 62: 582–592, 2013.
43. **Rowen L, Koop BF, Hood L.** The complete 685-kilobase DNA sequence of the human beta T cell receptor locus. *Science* 272: 1755–1762, 1996.
44. **Sah RP, Dudeja V, Dawra RK, Saluja AK.** Caerulein-induced chronic pancreatitis does not require intra-acinar activation of trypsinogen in mice. *Gastroenterology* 144: 1076–1085, 2013.
45. **Scheele G, Bartelt D, Bieger W.** Characterization of human exocrine pancreatic proteins by two-dimensional isoelectric focusing/sodium dodecyl sulfate gel electrophoresis. *Gastroenterology* 80: 461–473, 1981.
46. **Schnúr A, Beer S, Witt H, Hegyi P, Sahin-Tóth M.** Functional effects of 13 rare *PRSS1* variants presumed to cause chronic pancreatitis. *Gut* 63: 337–343, 2014.
47. **Selig L, Sack U, Gaiser S, Klöppel G, Savkovic V, Mössner J, Keim V, Bödeker H.** Characterisation of a transgenic mouse expressing R122H human cationic trypsinogen. *BMC Gastroenterol* 6: 30, 2006.
48. **Simon P, Weiss FU, Sahin-Tóth M, Parry M, Nayler O, Lenfers B, Schnekenburger J, Mayerle J, Domschke W, Lerch MM.** Hereditary pancreatitis caused by a novel PRSS1 mutation (Arg-122→Cys) that alters autoactivation and autodegradation of cationic trypsinogen. *J Biol Chem* 277: 5404–5410, 2002.
49. **Solomon S, Gelrud A, Whitcomb DC.** Low penetrance pancreatitis phenotype in a Venezuelan kindred with a *PRSS1* R122H mutation. *JOP* 14: 187–189, 2013.
50. **Sultan M, Werlin S, Venkatasubramani N.** Genetic prevalence and characteristics in children with recurrent pancreatitis. *J Pediatr Gastroenterol Nutr* 54: 645–650, 2012.
51. **Szabó A, Sahin-Tóth M.** Increased activation of hereditary pancreatitis-associated human cationic trypsinogen mutants in presence of chymotrypsin C. *J Biol Chem* 287: 20701–20710, 2012.

52. **Szabó A, Sahin-Tóth M.** Determinants of chymotrypsin C cleavage specificity in the calcium-binding loop of human cationic trypsinogen. *FEBS* J 279, 4283–4292, 2012.
53. **Szmola R, Sahin-Tóth M.** Chymotrypsin C (caldecrin) promotes degradation of human cationic trypsin: identity with Rinderknecht's enzyme Y. *Proc Natl Acad Sci USA* 104: 11227–11232, 2007.
54. **Szmola R, Sahin-Tóth M.** Uncertainties in the classification of human cationic trypsinogen (*PRSS1*) variants as hereditary pancreatitis-associated mutations. *J Med Genet* 47: 348–350, 2010.
55. **Tautermann G, Ruebsamen H, Beck M, Dertinger S, Drexel H, Lohse P.** R116C mutation of cationic trypsinogen in a Turkish family with recurrent pancreatitis illustrates genetic microheterogeneity of hereditary pancreatitis. *Digestion* 64: 226–232, 2001.
56. **Teich N, Mössner J, Keim V.** Mutations of the cationic trypsinogen in hereditary pancreatitis. *Hum Mutat* 12: 39–43, 1998.
57. **Teich N, Ockenga J, Hoffmeister A, Manns M, Mössner J, Keim V.** Chronic pancreatitis associated with an activation peptide mutation that facilitates trypsin activation. *Gastroenterology* 119: 461–465, 2000.
58. **Teich N, Bauer N, Mössner J, Keim V.** Mutational screening of patients with nonalcoholic chronic pancreatitis: identification of further trypsinogen variants. *Am J Gastroenterol* 97: 341–346, 2002.
59. **Teich N, Le Maréchal C, Kukor Z, Caca K, Witzigmann H, Chen JM, Tóth M, Mössner J, Keim V, Férec C, Sahin-Tóth M.** Interaction between trypsinogen isoforms in genetically determined pancreatitis: mutation E79K in cationic trypsin (PRSS1) causes increased transactivation of anionic trypsinogen (PRSS2). *Hum Mutat* 23: 22–31, 2004.
60. **Teich N, Nemoda Z, Kohler H, Heinritz W, Mössner J, Keim V, Sahin-Tóth M.** Gene conversion between functional trypsinogen genes *PRSS1* and *PRSS2* associated with chronic pancreatitis in a six-year-old girl. *Hum Mutat* 25: 343–347, 2005.
61. **Teich N, Rosendahl J, Tóth M, Mössner J, Sahin-Tóth M.** Mutations of human cationic trypsinogen (*PRSS1*) and chronic pancreatitis. *Hum Mutat* 27: 721–730, 2006.
62. **Whitcomb DC, Preston RA, Aston CE, Sossenheimer MJ, Barua PS, Zhang Y, Wong-Chong A, White GJ, Wood PG, Gates LK Jr, Ulrich C, Martin SP, Post JC, Ehrlich GD.** A gene for hereditary pancreatitis maps to chromosome 7q35. *Gastroenterology* 110: 1975–1980, 1996.
63. **Whitcomb DC, Gorry MC, Preston RA, Furey W, Sossenheimer MJ, Ulrich CD, Martin SP, Gates LK Jr, Amann ST, Toskes PP, Liddle R, McGrath K, Uomo G, Post JC, Ehrlich GD.** Hereditary pancreatitis is caused by a mutation in the cationic trypsinogen gene. *Nat Genet* 14: 141–145, 1996.
64. **Whitcomb DC, Larusch J, Krasinskas AM, Klei L, Smith JP, Brand RE, Neoptolemos JP, Lerch MM, Tector M, Sandhu BS, Guda NM, Orlichenko L; Alzheimer's Disease Genetics Consortium, Alkaade S, Amann ST, Anderson MA, Baillie J, Banks PA, Conwell D, Coté GA, Cotton PB, Disario J, Farrer LA, Forsmark CE, Johnstone M, Gardner TB, Gelrud A, Greenhalf W, Haines JL, Hartman DJ, Hawes RA, Lawrence C, Lewis M, Mayerle J, Mayeux R, Melhem NM, Money ME, Muniraj T, Papachristou GI, Pericak-Vance MA, Romagnuolo J, Schellenberg GD, Sherman S, Simon P, Singh VP, Slivka A, Stolz D, Sutton R, Weiss FU, Wilcox CM, Zarnescu NO, Wisniewski SR, O'Connell MR, Kienholz ML, Roeder K, Barmada MM, Yadav D, Devlin B.** Common genetic variants in the *CLDN2* and *PRSS1-PRSS2* loci alter risk for alcohol-related and sporadic pancreatitis. *Nat Genet* 44: 1349–1354, 2012.
65. **Witt H, Luck W, Becker M.** A signal peptide cleavage site mutation in the cationic trypsinogen gene is strongly associated with chronic pancreatitis. *Gastroenterology* 117: 7–10, 1999.
66. **Yadav D, Lowenfels AB.** The epidemiology of pancreatitis and pancreatic cancer. *Gastroenterology* 144: 1252–1261, 2013.
67. **Yilmaz B, Ekız F, Karakaş E, Aykut A, Sımşek Z, Çoban Ş, Onay H, Özkınay F.** A rare PRSS1 mutation in a Turkish family with hereditary chronic pancreatitis. *Turk J Gastroenterol* 23: 826–827, 2012.
68. **Zeng K, Liu QC, Lin JH, Lin XH, Zhuang ZH, Gao F, Ou QS.** Novel mutations of *PRSS1* gene in patients with pancreatic cancer among Han population. *Chin Med J (Engl)* 124: 2065–2067, 2011.

III.

Volume 57(1):,47-50 2013
Acta Biologica Szegediensis
http://www.sci.u-szeged.hu/ABS

ARTICLE

Quantitation of *DEFA1A3* gene copy number polymorphism by allele specific amplification and real-time PCR

Balázs Csaba Németh, Ádám Horváth, Márta Szekeres, Yvette Mándi, Ferenc Somogyvári*

Department of Medical Microbiology and Immunobiology, University of Szeged, Szeged, Hungary

ABSTRACT Some of the PCR based genotyping methods are faster and less expensive than sequencing in population-wide studies. One of the cost effective solutions is the allele specific amplification (ASA). We applied this method for quantitative analysis of defensin α1 (*DEFA1*) and defensin α3 (*DEFA3*) genes which are known to have copy number polymorphism in the human genome. The proteins encoded by these genes are human alpha defensins / human neutrophil peptides 1 and 3. Their antimicrobial mechanisms have an important role in the function of innate immune system. Our aim was to improve the reproducibility of ASA using 14 different mastermixes (MMX). Unfortunately, not all MMX-s are suitable for ASA investigations due to their different characteristics of polymerase activity. Here we investigated 14 commercial MMX-s whether they are capable for ASA test. **Acta Biol Szeged 57(1):47-50 (2013)**

KEY WORDS

real-time PCR
SNP
ASA
defensin
mastermix

In allele specific amplification (ASA) the 3' end of the extension primer is perfectly complement to the mutation site of the target sequence (Fig. 1). The advantage of this technique is the low cost and fast detection (Nørby, 1993). One sign of the popularity is that all of the authors and scientific papers give a new name of all ASA variants, as "allele specific PCR" (AS-PCR), "PCR allele-specific amplification" (PASA), "simple allele-discriminating PCR" (SAP), "amplification refractory mutation system" (ARMS) etc. (Gaudet et al. 2009). All methods mentioned above are used agarose gel in order to detect amplification products. The technique can be combined also with real-time PCR, for instance with hybridization probes (Glaab and Skopek 1999) as a TaqMan mismatch amplification mutation assay (TaqMAMA). In a recent study (Baris et al. 2013) a single-tube strategy combined the tetra-primer ARMS PCR with SYBR Green I-based real-time PCR, and melting-point analysis (T-Plex real-time PCR). Since it is a real-time PCR method, this system is suitable for quantitation.

Defensins are small peptides of 12-50 amino acids which are important components of innate immunity (Ganz and Lehrer 1995). These antimicrobial peptides are divided into three groups: alpha, beta and theta defensins depending on the pattern of disulfide-bridge of the protein (Selsted at al. 1985). The genes encoding human neutrophil peptides 1 and 3 are *DEFA1* (MIM125220) and *DEFA3* (MIM604522) which map to 8p23.1 in the human genome and vary in copy number as a 19-kb tandem repeat unit. The numbers of *DEFA1* gene copies vary between 4 and 11 and the average copy number is 6. The *DEFA3* gene copy number mean is 1.5 and 10 to 37% of the tested subjects have been found to be absent for the *DEFA3* gene in the populations were tested. Exon sequences of *DEFA1* and *DEFA3* differ only one nucleotide. This paralogous sequence variant is C3400A that allows discrimination and separate quantitation of the two genes (Linzmeier and Ganz 2005).

The aim of the study was to improve the reproducibility of ASA using different commercially available mastermixes (MMX) suitable for real time PCR method. The investigations were carried out through determining *DEFA1 / DEFA3* gene copy number polymorphism using primers for specific amplification either only *DEFA1* or only *DEFA3* gene. The use of MMX-s is not only a convenient way of investigation but it minimizes the necessary pipetting steps, improves the reproducibility and reduces the standard deviation In this study we tested 14 commercial MMX-s for ASA quantification of *DEFA1 / DEFA3* genes.

Materials and methods

Patients

205 healthy blood donors were investigated. These control subjects were selected from blood donors at the Regional Centre of the Hungarian National Blood Transfusion Service, Szeged Hungary. All cases and controls were of Hungarian ethnic origin and resident in Hungary.

DNA preparation

Genomic DNA purified from peripheral blood was used. The leukocyte DNA was isolated according to the manufac-

Accepted Nov 14, 2013
*Corresponding author. E-mail: somogyvari.ferenc@med.u-szeged.hu

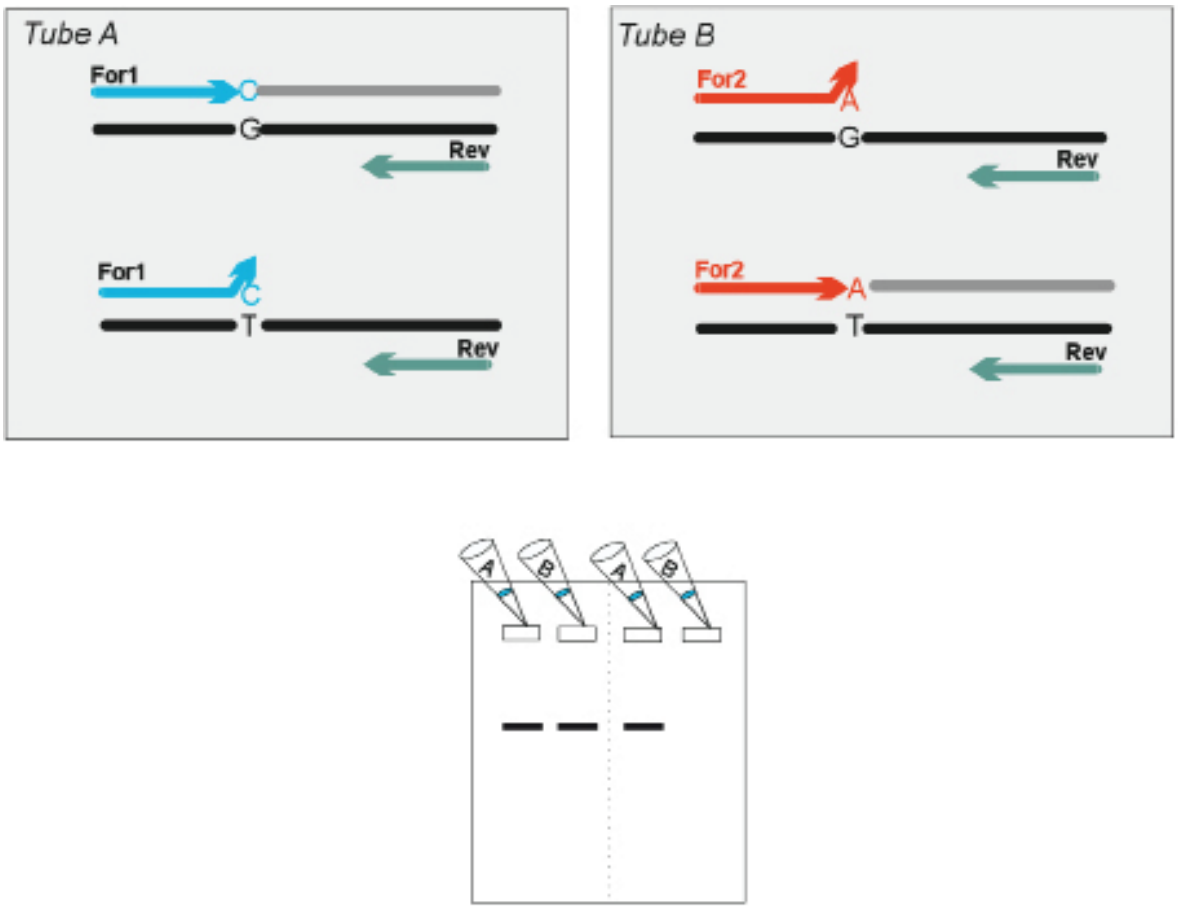

Figure 1. Principle of the allele specific amplification (ASA). The reaction takes place in two tubes. Each tube has one kind of forward extension primer which 3′ end perfectly complement to one of the target sequence. The reverse primer is common. The amplicon indicates the presence of the adequate allele. Investigating heterozygote's, there are amplicons in both tubes, in contrast in case of homozygosis just one of them has.

turer's instructions. (High Pure PCR Template Preparation Kit, Roche Diagnostic GmbH, Mannheim, Germany). DNA samples were stored at –20°C until further use.

Selection of the target DNA

Primarily we needed a suitable sample DNA for the examination of the different MMX-s. At least 10% of the populations investigated earlier (Ballana et al. 2007) had no *DEFA3* gene. For further ASA investigations we chose one of these genomic DNA samples which lacked *DEFA3* gene.

The *DEFA1A3* PCR was carried out as previously described (Linzmeier et al. 2005) with slight modifications. Briefly: BIO-RAD CFX 96 instrument (Bio-Rad, Hercules, CA, USA) was used. The reaction volume was 15 µL, containing 3 µL of DNA, 1 µM each of the primers and 7,5 µL of reaction buffer (Fermentas Probe/ROX qPCR MasterMix, Fermentas, Lithuania). We used the forward primer DEFA1 1 F (5' TAC CCA CTG CTA ACT CCA TAC 3'), reverse primer DEFA1 1 R (5' GAA TGC CCA GAG TCT TCC C 3'). The PCR conditions were as follows: initial denaturation at 95°C for 10 min followed by 40 cycles of denaturation (95°C for 15 s) and extension (54°C for 1 min).

DEFA1 and *DEFA3* genes differ only in a single nucleotide (C3400A) which is in the restriction site of *HaeIII* enzyme. The *DEFA1A3* PCR products were digested overnight at 37°C using 5 U of *HaeIII* izoschizomer *BsuRI* restriction enzyme (Fermentas, Vilnius, Lithuania). The restriction fragments were separated by electrophoresis on 2 % agarose gels containing GelRed Nucleic Acid Stain (Biotium Inc., Hayvard, CA, USA) and visualized by UV illumination. The resulted fragment lengths were 150 bp, 67 bp and 83 bp in case of presence of both alleles (*DEFA1* and *DEFA3*) in the investigated sample.

ASA PCR

All of the investigated MMX-s were used according to the manufacturer's recommendations. The precise amount of previously selected *DEFA1* homozygous DNA (contained

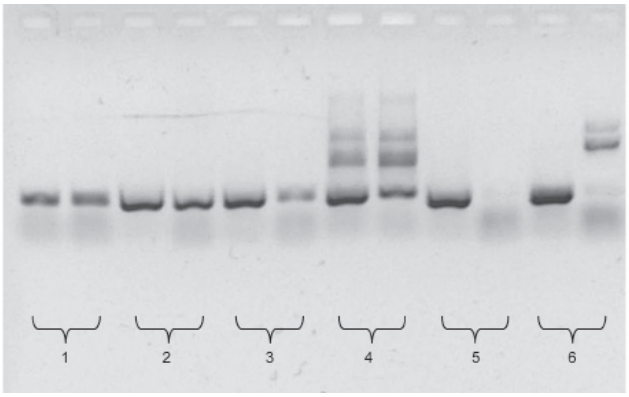

Figure 2. Test of the different mastermixes (MMX).MMX 1, 2 and 3 could not differentiate between the *DEFA1* and *DEFA3* genes because of the proof reading activity of the Taq polymerase. MMX 4 produced aspecific bands as a side effect due to the presence of dsDNA binding protein which stabilizes the polymerase-template complex and able to amplify the target DNA in the presence of inhibitors (BioRad SsoFast EvaGreen Supermix). MMX 5 is suitable for ASA (Fermentas Maxima SybrGreen qPCR Mastermix and BioRad iTaq SybrGreen Supermix). Followed by annealing temperature optimisation MMX 6 also could be used (Promega GoTaq qPCR Mastermix).

only *DEFA1* gene, but no *DEFA3* gene) was added to each reaction mix based on optical density. The reaction volume was 15 μL, containing 3 μL of DNA, 1 μM each of the primers and appropriate amount of MMX. Two separate reactions were carried out for each sample. The first reaction contained the common forward primer CommonF (5' CAG CCA GCA TCA CCT GTC AG 3') and *DEFA1* selective reverse primer 1ADR (5' GCT GGT ATT CTG CAA TAG CGG G 3'), while the second reaction was performed with common forward primer and *DEFA3* selective reverse primer 3ADR (5' GCT GGT ATT CTG CAA TAG CGG T 3'). The PCR conditions were the same as described previously except that the annealing/extension step was carried out at 68°C.

Real time PCR master mixes

We investigated 14 MMX-s from seven manufacturers. In alphabetic order:

Applied Biosystems (TaqMan Universal PCR Master Mix),

BioRad (SsoFast Probes Supermix; SsoFast EvaGreen Supermix; iQ SybrGreen Supermix; iTaq SybrGreen Supermix),

Eppendorf (RealMasterMix Probe)

Fermentas (Maxima SybrGreen qPCR Mastermix),

Promega (GoTaq HotStart Colorless Mastermix; GoTaq qPCR Mastermix),

Roche (LC HRM Mastermix; LC DNA Master SybrGreen; LC FastStart Colorless Mastermix) and

Sigma (JumpStart Taq ReadyMix; SybrGreen JumpStart Taq ReadyMix).

Real-time quantitation using ASA

For quantitation, the above described two tubes ASA PCR have supplemented the third, reference tube/reaction. Reference gene was MPO in quantitation using the primer set of MPO1F (5' CCA GCC CAG AAT ATC CTT GG 3') and MPO1R (5' GGT GAT GCC TGT GTT GTC G 3'). The emitted fluorescence was measured after each extension step. All conditions were the same as previously described with *DEFA1* / *DEFA3* gene amplification. Instead of electrophoresis, real-time quantification was performed by online monitoring for the identification of the exact time point at which the logarithmic linear phase could be distinguished from the background (crossing point). Determination of copy number polymorphism in diploid genome was calculated by ΔΔCt method as described previously (Linzmeier et al. 2005).

Results and Discussion

The *DEFA3* gene was absent in 9.27% (n=19) of the investigated study group (N=205) as determined by *HaeIII* (*BsuRI* izoschizomer) restriction enzyme digestion. This ratio was found to be less than it was in the previously investigated Caucasians (15%) and the same as in the Japanese/Chinese population (10%) (Ballana et al. 2007). The investigated study group was a control of an association study. Patients with diabetes, hypertension or ischemic heart disease were excluded from control group presumably causing the alteration compared to previous results. One of the *DEFA3* gene deficient samples were used for the MMX investigation with ASA PCR.

All of the investigated MMX-s successfully amplified the targeted sequence of the *DEFA1* gene. However, 10 MMX-s could not distinguish between *DEFA1* and *DEFA3* genes (Fig. 2, numbers 1-4). Two of them (*i.e.* Fig 2, number 4) produced aspecific bands (BioRad SsoFast Probes Supermix and SsoFast EvaGreen Supermix). These two MMX-s contain a dsDNA binding protein which stabilizes the polymerase-template complex and thus are able to amplify the target DNA in case of degenerate primers or highly concentrated inhibitors (Horvath et al. 2013). However, in general conditions they amplified aspecific bands.

Two MMX-s produced aspecific products (Promega GoTaq HotStart Colorless Mastermix and Promega GoTaq qPCR Mastermix) and a very week band in the *DEFA3* tube (Fig. 2, number 6). Some of the MMX components diminished the specificity of the reaction. This phenomenon could be fixed by optimization of the reaction which includes the selection of the optimal annealing temperature. Generally the empirical annealing optimum is 2-3°C higher than that calculated with thermodynamic methods. Moreover, the elevated annealing temperature improves the selectivity of the ASA PCR.

Two of the MMX-s (Fermentas Maxima SybrGreen qPCR Mastermix and BioRad iTaq SybrGreen Supermix) was com-

pletely suitable for ASA PCR, they successfully amplified the *DEFA1* alleles and did not amplify the *DEFA3* allele (Fig. 2, number 5). The BioRad iTaq SybrGreen Supermix was used for further investigations with quantitative ASA PCR.

After screening the 205 samples with the real-time ASA PCR the *DEFA1* gene copies varied between one and 13 and the average number were 5.7. The *DEFA3* gene copy mean was 1.7 and the gene copies varied between 0 and 5. These findings are in agreement with the previous data published (Linzmeier et al. 2005).

Acknowledgement

We want to thank Müllerné Deák Györgyi for skilled works. This work was supported by the project named „TÁMOP-4.2.2. A-11/1/ KONV-2012-0035 – Creating the Center of Excellence at the University of Szeged" and TÁMOP 4.2.4. A/2-11-1-2012-0001 'National Excellence Program' by the European Union and the State of Hungary, co-financed by the European Regional and European Social Fund.

References

Ballana E, González JR, Bosch N, Estivill X (2007) Inter-population variability of *DEFA3* gene absence: correlation with haplotype structure and population variability. BMC Genomics 8:14.

Baris I, Etlik O, Koksal V, Ocak Z, Baris ST (2013) SYBR green dye-based probe-free SNP genotyping: Introduction of T-Plex real-time PCR assay. Anal Biochem 441(2):225-231.

Ganz T, Lehrer RI (1995) Defensins. Pharmacol Ther 66:191-205.

Gaudet M, Fara AG, Beritognolo I, Sabatti M (2009) Allele-Specific PCR in SNP Genotyping. in: Komar AA (ed.), Single Nucleotide Polymorphisms, Methods in Molecular Biology, Humana Press, 2009

Glaab WE, Skopek TR (1999) A novel assay for allelic discrimination that combines the fluorogenic 5' nuclease polymerase chain reaction (TaqMan) and mismatch amplification mutation assay. Mutat Res 430(1):1-12.

Horvath A, Santha P, Horváth V, Torok N, Nagy I, Jancsó G, Vágvölgyi C, Somogyvári F (2013) Rapid genotyping of genetically modified laboratory animals from from whole blood samples without DNA preparation. Acta Biol Hung 64(2):262-265.

Linzmeier RM, Ganz T (2005) Human defensin gene copy number polymorphisms: comprehensive analysis of independent variation in alpha- and beta-defensin regions at 8p22-p23. Genomics 86:423-430.

Nørby S (1993) Mutation-specific PCR: a rapid and inexpensive diagnostic method, as exemplified by mitochondrial DNA analysis in Leber's hereditary optic neuropathy. DNA Cell Biol 12(6):549-552.

Selsted ME, Harwig SS, Ganz T, Schilling JW, Lehrer RI (1985) Primary structures of three human neutrophil defensins. J Clin Invest 76:1436-1439.

IV.

THE JOURNAL OF BIOLOGICAL CHEMISTRY VOL. 288, NO. 33, pp. 24049–24062, August 16, 2013

Autoactivation of Mouse Trypsinogens Is Regulated by Chymotrypsin C via Cleavage of the Autolysis Loop*

Received for publication, April 18, 2013, and in revised form, June 3, 2013 Published, JBC Papers in Press, June 28, 2013, DOI 10.1074/jbc.M113.478800

Balázs Csaba Németh[‡], Thomas Wartmann[§], Walter Halangk[§], and Miklós Sahin-Tóth[‡1]

From the [‡]Department of Molecular and Cell Biology, Boston University Henry M. Goldman School of Dental Medicine, Boston, Massachusetts 02118 and the [§]Division of Experimental Surgery, Department of Surgery, Otto-von-Guericke-Universität Magdeburg, D-39120 Magdeburg, Germany

Background: Hereditary pancreatitis-associated mutations alter regulation of trypsinogen activation by chymotrypsin C.
Results: Activation of mouse trypsinogens T8 and T9 is inhibited by chymotrypsin C-mediated cleavage of the autolysis loop.
Conclusion: Chymotrypsin C regulates activation of human and mouse trypsinogens by different mechanisms.
Significance: Introduction of human pancreatitis-associated mutations into mouse trypsinogens will not recapitulate the pathogenic biochemical effects.

Chymotrypsin C (CTRC) is a proteolytic regulator of trypsinogen autoactivation in humans. CTRC cleavage of the trypsinogen activation peptide stimulates autoactivation, whereas cleavage of the calcium binding loop promotes trypsinogen degradation. Trypsinogen mutations that alter these regulatory cleavages lead to increased intrapancreatic trypsinogen activation and cause hereditary pancreatitis. The aim of this study was to characterize the regulation of autoactivation of mouse trypsinogens by mouse Ctrc. We found that the mouse pancreas expresses four trypsinogen isoforms to high levels, T7, T8, T9, and T20. Only the T7 activation peptide was cleaved by mouse Ctrc, causing negligible stimulation of autoactivation. Surprisingly, mouse Ctrc poorly cleaved the calcium binding loop in all mouse trypsinogens. In contrast, mouse Ctrc readily cleaved the Phe-150–Gly-151 peptide bond in the autolysis loop of T8 and T9 and inhibited autoactivation. Mouse chymotrypsin B also cleaved the same peptide bond but was 7-fold slower. T7 was less sensitive to chymotryptic regulation, which involved slow cleavage of the Leu-149–Ser-150 peptide bond in the autolysis loop. Modeling indicated steric proximity of the autolysis loop and the activation peptide in trypsinogen, suggesting the cleaved autolysis loop may directly interfere with activation. We conclude that autoactivation of mouse trypsinogens is under the control of mouse Ctrc with some notable differences from the human situation. Thus, cleavage of the trypsinogen activation peptide or the calcium binding loop by Ctrc is unimportant. Instead, inhibition of autoactivation via cleavage of the autolysis loop is the dominant mechanism that can mitigate intrapancreatic trypsinogen activation.

Hereditary chronic pancreatitis is a human genetic disorder caused by heterozygous mutations in the serine protease 1 (*PRSS1*) gene, which codes for the digestive proenzyme cationic trypsinogen (1). High penetrance trypsinogen mutations such as p.N29I and p.R122H are associated with an autosomal dominant inheritance pattern, whereas mutations with lower penetrance, exemplified by p.A16V, may be found not only in hereditary but also in sporadic cases with no family history (2). The disease mechanism involves increased autoactivation of mutant trypsinogens within the pancreas due to altered regulation by chymotrypsin C (CTRC)[2] (3). Autoactivation of human trypsinogens is proteolytically regulated by CTRC that cleaves cationic trypsinogen at two distinct regulatory sites. Cleavage of the Phe-18–Asp-19 peptide bond in the activation peptide results in a shorter activation peptide and increased autoactivation (4). This cleavage is stimulated by pancreatitis-associated mutations p.N29I and p.A16V (3, 4). Cleavage of the Leu-81–Glu-82 peptide bond in the calcium binding loop, together with the trypsin-mediated autolytic cleavage of the Arg-122–Val-123 peptide bond, results in rapid degradation and inactivation of cationic trypsinogen (5). Mutations p.N29I and p.R122H hamper CTRC-mediated degradation and thereby increase trypsinogen autoactivation (3).

Despite the significant progress in understanding the mechanism of trypsinogen mutations at the biochemical level, animal models that recapitulate the human disease both phenotypically and mechanistically remain unavailable. Transgenic mice carrying the coding DNA for human cationic trypsinogen with the p.R122H mutation did not develop spontaneous pancreatitis, although small differences in the pathological responses were noted when pancreatitis was artificially induced (6). In contrast, when mice were made transgenic with the p.R122H mutation introduced into mouse trypsinogen isoform T8 (see Table 1), the resulting animals developed acute and eventually chronic pancreatitis (7). Unfortunately, this remarkable model has never been made available to the pancreas research community for independent replication nor have there been any follow-up studies published by the original authors since 2006. It thus remains unclear whether the

* This work was supported, in whole or in part, by National Institutes of Health Grants R01DK058088, R01DK082412, R01DK082412-S2, and R01DK095753 (to M. S.-T.). This work was also supported by Grant DFG HA2080/7-1 from the Deutsche Forschungsgemeinschaft.
[1] To whom correspondence should be addressed: 72 East Concord St., Evans-433, Boston, MA 02118. Tel.: 617-414-1070; Fax: 617-414-1041; E-mail: miklos@bu.edu.

[2] The abbreviations used are: CTRC, chymotrypsin C; IPG, immobilized pH gradient.

TABLE 1

Trypsinogen genes in the mouse genome

Table is based on the 1997 GenBank™ submissions AE000663.1, AE000664.1, and AE000665.1, which first reported the genomic sequence of the mouse T cell receptor β locus. The original annotation described genes T2 and T14 as relic genes based on the absence of exon 1. The more recent annotation to the mouse genome identified the first exons for both genes, and we re-classified these as pseudogenes.

Gene	Function	Notes
T1	Pseudogene	Exons give in-frame translation; product may serve unknown function Also known as protease, serine 58 (Prss58), GenBank™ NM_175020.3
T2	Pseudogene	Exons give in-frame translation; product may serve unknown function
T3	Pseudogene	A single nucleotide deletion in exon 2 leads to a frameshift
T4	Functional	
T5	Functional	
T6	Relic	This gene has only exons 2 and 3
T7	Functional	
T8	Functional	Also known as trypsin4 (Try 4), GenBank™ NM_011646.5
T9	Functional	Also known as trypsin5 (Try 5) GenBank™ NM_001003405.4 Also known as TESP4, GenBank™ AB017031.1
T10	Functional	
T11	Functional	Also known as protease, serine,3 (Prss3), GenBank™ NM_011645.2
T12	Functional	
T13	Relic	This gene has only exons 3 and 5
T14	Pseudogene	This gene has a defective splice site after exon 2
T15	Functional	
T16	Functional	Also known as protease, serine,1 (Prss1), GenBank™ NM_053243.2
T17	Relic	This gene is missing exons 1 and 2
T18	Relic	This gene is missing exons 1 and 2
T19	Relic	This gene has only exon 3
T20	Functional	Also known as protease, serine,2 (Prss2), GenBank™ NM_009430.2

observed phenotype was related to the expression of the mutant trypsinogen. Nonetheless, this study raises the question whether the biochemical effects of the p.R122H mutation are similar in the context of mouse and human trypsinogens and whether we can utilize mouse trypsinogens to model the human condition.

Considering the widespread use of mice in experimental studies of the pancreas, it is surprising how little is known about mouse trypsinogens. Watanabe and Ogasawara (8) reported the purification of three trypsinogen isoforms from the mouse pancreas. Stevenson *et al.* (9) cloned a trypsinogen cDNA, corresponding to isoform T20, from the pancreas and demonstrated that the mouse genome contained multiple different trypsinogen genes. This was later confirmed by Hood and coworkers in 1997 (10) who sequenced the mouse T cell receptor β locus on chromosome 6 and identified 20 trypsinogen genes organized in two groups, one containing genes T1–T7 and the other containing genes T8–T20 (Table 1). Eleven of the 20 genes are potentially functional (Table 1 and Fig. 1), whereas the other nine genes are pseudogenes or relic genes. Ohmura *et al.* (11) cloned the cDNA for isoform T9 from sperm acrosome. It remains unknown, however, which isoforms of the 11 potentially functional trypsinogen genes are expressed at the protein level in the mouse pancreas. More recently, genetic deletion of T7 indicated that this isoform may contribute as much as 60% of pancreatic trypsinogens (12, 13). The authors also found that despite the presence of other trypsinogen isoforms, mice deficient in T7 did not respond to secretagogue hyperstimulation with the characteristic intra-acinar cell trypsinogen activation, an early event in acute pancreatitis. These new findings suggest that the different mouse trypsinogen isoforms vary in their activation kinetics and highlight the need for their comparative biochemical characterization. Therefore, in this study, we identified the major trypsinogen isoforms in the mouse pancreas, expressed these recombinantly, and studied their autoactivation and regulation by mouse Ctrc.

EXPERIMENTAL PROCEDURES

Nomenclature—Amino acid residues are numbered starting with the initiator methionine of the primary translation product, according to the recommendations of the Human Genome Variation Society. Note that because of an extra Asp residue (Asp-23) in the activation peptide of T7, amino acid numbering in this isoform is shifted by one relative to human and other mouse trypsinogens. Autolysis loop refers to the flexible region between residues 146 and 154 in trypsinogen (Fig. 1).

Plasmid Construction and Mutagenesis—Construction of the pTrapT7-intein-Hu1 and pcDNA3.1(−)-CTRB2 expression plasmids harboring the coding sequence for human cationic trypsinogen (Hu1) and human chymotrypsinogen B2 (CTRB2) was reported previously (5, 14). Mutation p.S150F was introduced into human cationic trypsinogen using overlap-extension PCR mutagenesis. Expression plasmids for mouse trypsinogens were created in the pTrapT7 plasmid previously designed for bacterial expression of human trypsinogens (15, 16). The coding DNA was PCR-amplified from commercial IMAGE clones and cloned into pTrapT7 using NcoI and SalI restriction sites. In all constructs, the N-terminal secretory signal peptide was replaced with a Met-Ala sequence. In T20, the stop codon was changed from amber (TAG) to ochre (TAA). T7 was amplified from IMAGE clone 30306963 (GenBank™ accession BC061093.1) using T7 NcoI sense (5′-AAA TTT CCA TGG CTC TCC CCC TGG ATG ATG ATG ATG-3′, where the NcoI site is underlined) and T7 SalI antisense (5′-AAA TTT GTC GAC TTA GTT GGC AGC GAT GGT CTG CTG-3′, where the SalI site is underlined) primers. T8 was amplified from IMAGE clone 30306436 (GenBank™ accession BC061135.1) using T8 NcoI sense (5′-AAA TTT CCA TGG CTT TCC CTG TGG ATG ATG ATG ACA-3′, where the NcoI site is underlined) and T8 SalI antisense (5′-AAA TTT GTC GAC TTA GTT TGC AGC AAT GGT GTT TTG-3′, where the

SalI site is underlined) primers. T9 was amplified from IMAGE clone 6433372 (GenBank™ accession CF581321.1) using T8 NcoI sense and T9 SalI antisense (5′-AAA TTT GTC GAC TTA GTT TGC GGC AAT GGT GTC CTG-3′, where the SalI site is underlined) primers. T20 was amplified from IMAGE clone 6433384 (GenBank™ accession CF581305.1) using T20 NcoI sense (5′-AAA TTT CCA TGG CTT TCC CTG TGG ATG ATG ATG ACA-3′, where the NcoI site is underlined) and T20 SalI antisense (5′-AAA TTT GTC GAC TTA GTT GTC AGC AAT TGT GTT CTG-3′, where the SalI site is underlined) primers. Mutations p.L82A, p.R123H, and p.L149A in T7 and p.R122H in T8 were created by overlap extension PCR and cloned into the pTrapT7 plasmid.

Expression plasmids for mouse chymotrypsinogens carrying a His_{10} affinity tag were created in the pcDNA3.1(−) plasmid. The coding DNA for mouse chymotrypsinogen C (Ctrc) was PCR-amplified from a cDNA preparation from CD-1 mouse pancreas, using mouse CTRC XhoI sense (5′-AAA TTT CTC GAG ACC TGA ACC ATG TTG GGA ATT ACA GTC-3′, where the XhoI site is underlined) and mouse CTRC EcoRI antisense (5′-AAA TTT GAA TTC GGC GTC GAG ACT TCT GGA ACC GTC TCT-3′, where the EcoRI site is underlined) primers and cloned into pcDNA3.1(−) using XhoI and EcoRI. A His_{10} affinity tag was added to the C terminus using gene synthesis (GenScript, Piscataway, NJ) and the XcmI and EcoRI sites. In this synthetic construct Leu-268 was deleted to prevent autolytic cleavage of the His tag. The coding DNA for mouse chymotrypsinogen B (Ctrb, GenBank™ accession NM_025583.2) with a C-terminal His_{10} tag was custom-synthesized (GenScript) and cloned into pcDNA3.1(−) using XhoI and BamHI.

Purification and Identification of Trypsinogens from CD-1 Mouse Pancreas—Pancreata (2 to 3) were homogenized in 10 ml of 20 mM Na-HEPES (pH 7.4) buffer, briefly sonicated, and centrifuged at 13,500 rpm for 10 min, and ~4 ml of supernatant was loaded onto a 2-ml ecotin column. Ecotin is a pan-serine protease inhibitor from *Escherichia coli,* which can bind the inactive zymogen forms of pancreatic serine proteases (17, 18). The ecotin column was washed with 20 mM Tris-HCl (pH 8.0), 0.2 M NaCl, and trypsinogens were eluted with 50 mM HCl. The flow-through contained no trypsinogen, as judged by the lack of trypsin activity after incubation with enteropeptidase. The ecotin-eluate contained all trypsinogen isoforms and low levels of chymotrypsinogen and proelastase. Four ml of eluate was loaded onto a 2-ml Mono S column equilibrated with 20 mM sodium acetate (pH 5.0), and trypsinogens were eluted with a 0–0.5 M NaCl gradient at 1 ml/min flow rate (Fig. 2*A*). The eluted proteins were separated by SDS-PAGE and transferred to a PVDF membrane, and individual bands were subjected to N-terminal protein sequencing by Edman degradation (Midwest Analytical, St. Louis, MO). Peaks corresponding to T8, T9, and T20 were also subjected to in-gel digestion followed by LC-MS/MS mass spectrometry (ProtTech, Phoenixville, PA). Relative abundance of trypsinogen isoforms was calculated from the peak areas corrected for the ultraviolet extinction coefficient differences. The T9-T8 peaks were also corrected for Ctrb contamination, which was determined from the relative trypsin and chymotrypsin activities after activation with enteropeptidase. Because of the poor separation of T8 and T9, these two isoforms were calculated as one.

Identification of Trypsinogens from NMRI Mouse Pancreas by Two-dimensional PAGE and Mass Spectrometry—Pancreata were homogenized in a Potter homogenizer at 2,500 rpm in ice-cold homogenization buffer (HS buffer, 250 mM sucrose, 10 mM citric acid (pH 6.0), 0.5 mM EGTA, 0.1 mM $MgSO_4$) with Complete mini protease inhibitor mixture (Roche Applied Science). The homogenate was centrifuged for 5 min at 500 × *g*, and the post-nuclear supernatant was centrifuged at 1,300 × *g* for 15 min at 4 °C. This zymogen granule-enriched pellet was washed with HS buffer and dissolved in sample buffer (5 M urea, 2 M thiourea, 2 M CHAPS, 2% ASB-14, 0.05% SB3–10) with Complete mini protease inhibitor mixture and stored in aliquots at −80 °C.

Immobilized pH gradient (IPG) strips (pH 3–10, 13 cm) were rehydrated overnight in sample buffer containing 65 mM (10 mg/ml) dithiothreitol (DTT), 2% IPG buffer, and 0.01% Serva blue. The zymogen granule-enriched pancreatic extract dissolved in sample buffer (50–100 μg) was supplemented with 65 mM (10 mg/ml) DTT, 2% IPG buffer, 0.01% Serva blue and cup-loaded at the anode end of the strips. Isoelectric focusing was performed under mineral oil at 3,500 V with a current limit of 50 μA per strip up to 8,000 total volt hours using an IPGphor unit (Amersham Biosciences). Strips were subsequently incubated in equilibration buffer (0.5 M Tris-HCl (pH 8.8), 6 M urea, 2% SDS, 30% glycerol) containing 50 mM DTT followed by incubation in 0.3 M acrylamide, for 15 min each. For electrophoresis in the second dimension, the IPG strips were applied onto a 10.5% SDS-polyacrylamide gel, and proteins were separated according to Schaegger and van Jagow (19). Gels were stained with silver nitrate by a modified method of Blum *et al.* (20). For estimation of relative protein content of trypsinogen spots, gels were further stained with Serva blue, according to Neuhoff *et al.* (21). Gel images were analyzed, and spot intensities were quantitated with the ImageMaster 2D Elute version 3.10 software (Amersham Biosciences). Protein spots of interest were excised, de-stained, and digested in-gel with sequencing grade bovine trypsin (Roche Applied Science, 12.5 ng/μl) overnight at 37 °C. Peptides were extracted from gel slices, and mass spectra were analyzed using MALDI-TOF Reflex III mass spectrometer machine (Bruker Daltonics, Germany) in linear mode with external calibration. Peptide fingerprint data analysis was performed using the web-based ProFound database with a mass tolerance of 250 ppm.

Expression and Purification of Trypsinogens—Human cationic trypsinogen was expressed in the aminopeptidase P-deficient LG-3 *E. coli* strain as fusions with a self-splicing mini-intein, as described previously (14, 22). Mouse trypsinogens were expressed in *E. coli* BL21(DE3), as described for human trypsinogens previously (15, 16). Isolation of cytoplasmic inclusion bodies, *in vitro* refolding, and purification with ecotin affinity chromatography were performed according to published protocols (14–16, 18, 22). The preparations were more than 90% pure, as judged by SDS-PAGE and Coomassie Blue staining. Concentrations of trypsinogen solutions were calculated from their UV absorbance at 280 nm

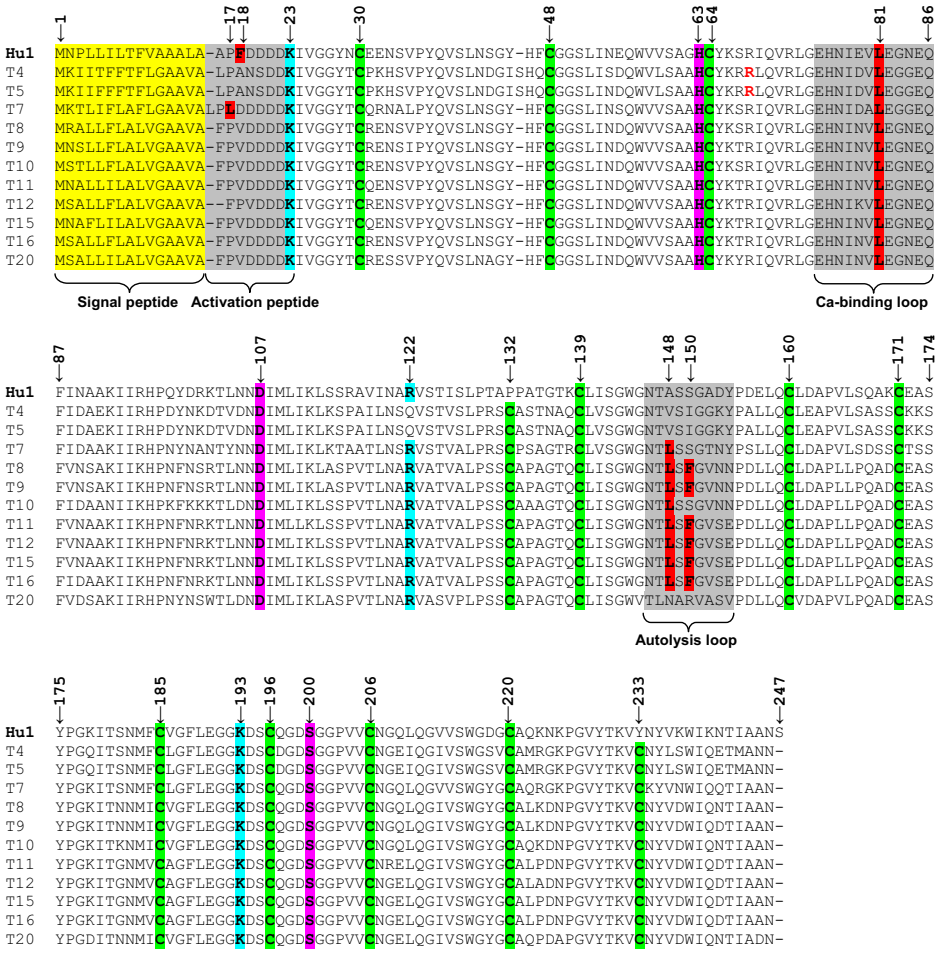

FIGURE 1. **Primary sequence alignment of human cationic trypsinogen (Hu1) and 11 potentially functional mouse trypsinogens.** Numbering starts with the initiator methionine. Note that due to insertions in T4, T5, and T7, the numbering is shifted by one after the insertion sites, relative to the indicated numbers. Similarly, a deletion in T12 shifts numbering. Trypsin cleavage sites are highlighted in *blue* and chymotrypsin C cleavage sites in *red*. Cys residues are indicated in *green* and the catalytic triad in *magenta*. The original annotation predicted deletion of Arg-69 (*red letter*) in T4 and T5, but more recent annotations include this residue. See text for details.

using the following extinction coefficients: 37,525 $M^{-1}cm^{-1}$ (human cationic trypsinogen), 39,140 $M^{-1}cm^{-1}$ (mouse T7), 34,670 $M^{-1}cm^{-1}$ (mouse T8 and T9), and 43,150 $M^{-1}cm^{-1}$ (mouse T20).

Expression and Purification of Chymotrypsinogens—Human CTRB2 and mouse Ctrb and Ctrc carrying His_{10} affinity tags were expressed in transiently transfected HEK 293T cells and purified from 450 ml of conditioned medium using nickel affinity chromatography as reported previously (3, 23). Aliquots (75 μl) of the eluted 5-ml fractions were analyzed by 15% SDS-PAGE and Coomassie Blue staining, and peak fractions with >90% purity were pooled and dialyzed for 72 h against three changes of 1 liter of 0.1 M Tris-HCl (pH 8.0) buffer containing 150 mM NaCl. The dialyzed chymotrypsinogen solutions were concentrated using a Vivaspin 20 concentrator (10-kDa molecular mass cutoff). Chymotrypsinogens were activated with trypsin, and active chymotrypsin concentrations were determined by active site titration with ecotin, as described previously (24).

Trypsinogen Autoactivation—Trypsinogen at 2 μM concentration was incubated in the absence or presence of 25 nM chymotrypsin, as indicated, and 10 nM initial trypsin in 0.1 M Tris-HCl (pH 8.0), 1 or 10 mM $CaCl_2$, and 0.05% Tween 20 (final concentrations) at 37 °C. At given times, 1.5-μl aliquots were withdrawn and mixed with 48.5 μl of assay buffer containing 0.1 M Tris-HCl (pH 8.0), 1 mM $CaCl_2$, and 0.05% Tween 20. Trypsin activity was measured by adding 150 μl of 200 μM *N*-CBZ-Gly-Pro-Arg-*p*-nitroanilide substrate dissolved in assay buffer and following the release of the yellow *p*-nitroaniline at 405 nm in a SpectraMax plus384 microplate reader (Molecular Devices, Sunnyvale, CA) for 1 min. Reaction rates were calculated from fits to the initial linear portions of the curves.

Trypsinogen Activation with Enteropeptidase—To determine the maximal trypsin activity attainable after full activation, 2 μM trypsinogen was incubated in 0.1 M Tris-HCl (pH 8.0), 10 mM $CaCl_2$, and 0.05% Tween 20 (final concentrations) at 37 °C with 140 ng/ml final concentration of human enteropeptidase (R&D Systems, Minneapolis, MN) for 1 h, and trypsin activity was measured as described above. This activity was designated as 100%, and trypsin activity measured in autoactivation experiments was expressed relative to this value. The 100% values corresponded to 500 (T7), 400 (T8), 400 (T9), and 300 (T20) milli-OD/min readings.

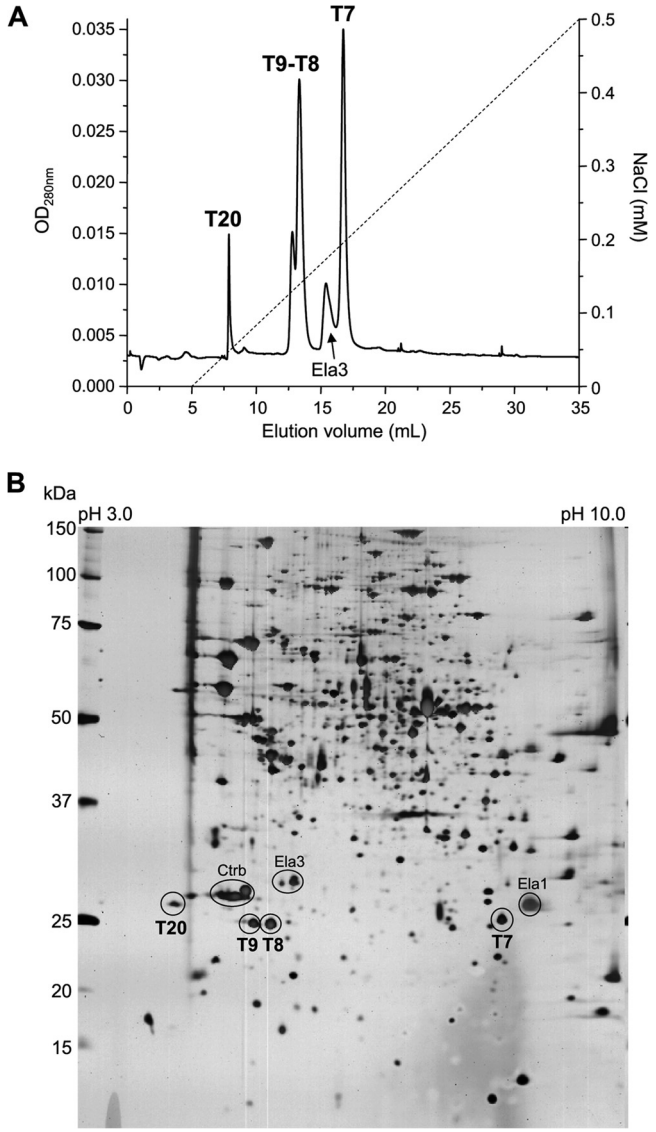

FIGURE 2. **Identification of major trypsinogen isoforms expressed in the mouse pancreas.** *A,* chromatographic separation of trypsinogen isoforms. Trypsinogens were purified from pancreas tissue extracts of CD-1 mice using ecotin affinity chromatography, and the ecotin eluate was loaded onto a Mono S column equilibrated with 20 mM sodium acetate (pH 5.0). The column was developed with a linear gradient of 0 – 0.5 M NaCl. Peaks were analyzed by SDS-PAGE, N-terminal sequencing, and mass spectrometry, as described under "Experimental Procedures" and "Results." *B,* two-dimensional PAGE of a zymogen granule-enriched fraction of pancreas tissue from NMRI mice. Silver-stained spots were digested with trypsin and analyzed by peptide mass fingerprinting, as described under "Experimental Procedures." Spots for trypsinogen isoforms T7, T8, T9, and T20, proelastase 3 (Ela3); chymotrypsinogen B (Ctrb), and proelastase 1 (Ela1) are indicated.

TABLE 2

Relative expression levels of major trypsinogen isoforms in the mouse pancreas determined by ion exchange chromatography (CD-1) or two-dimensional gel electrophoresis (NMRI)

The averages from four experiments ± S.D. are indicated. See text for details.

	Relative expression levels (% of total)			
Mouse strain	T7	T8	T9	T20
CD-1	41 ± 1	47 ± 3		12 ± 2
NMRI	25 ± 1	33 ± 1	27 ± 1	15 ± 2

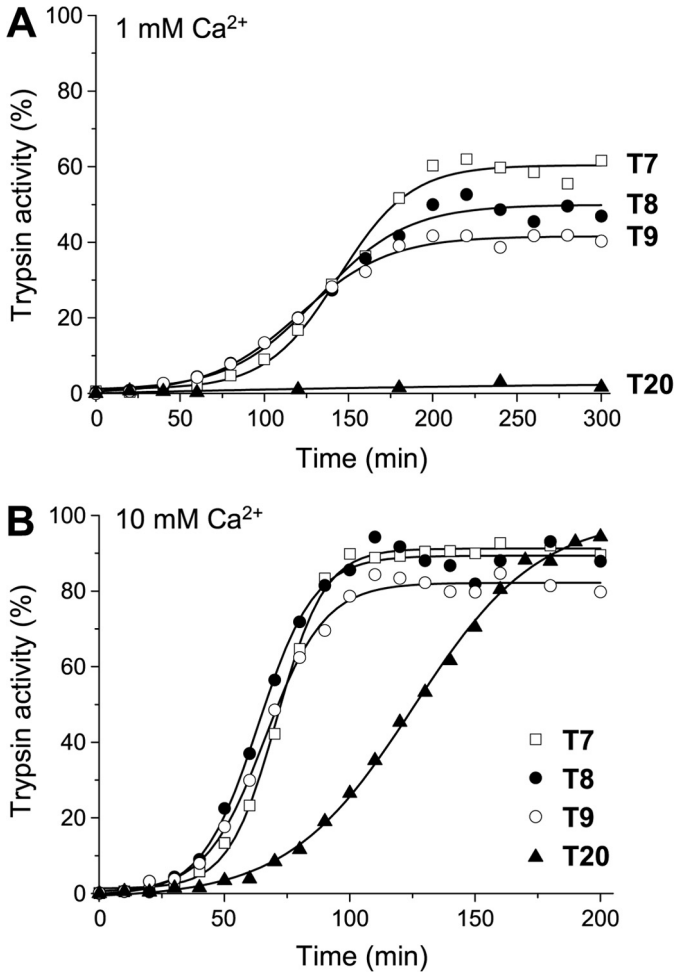

FIGURE 3. **Autoactivation of mouse trypsinogens.** Trypsinogens were incubated at 2 μM concentration with 10 nM initial trypsin in 0.1 M Tris-HCl (pH 8.0), 1 mM $CaCl_2$ (*A*) or 10 mM $CaCl_2$ (*B*) and 0.05% Tween 20 at 37 °C. Aliquots (1.5 μl) were withdrawn at the indicated times, and trypsin activity was determined as described under "Experimental Procedures." Trypsin activity was expressed as percentage of the maximal activity determined by full activation with enteropeptidase. Representative experiments from four replicates are shown.

Gel Electrophoresis—Trypsinogen samples (75 μl, ~3.8 μg of protein) were precipitated with trichloroacetic acid (10% final concentration), and the precipitate was recovered by centrifugation, dissolved in 15 μl of Laemmli sample buffer containing 100 mM DTT (final concentration), and heat-denatured at 95 °C for 5 min. Electrophoretic separation was performed on 15% SDS-PAGE mini gels in standard Tris-glycine buffer. Gels were stained with Brilliant Blue R-250 and destained as described earlier (25). Quantitation of bands was carried out with the GelDoc XR+ gel documentation system and Image Lab 3.0 software (Bio-Rad).

RESULTS

Identification of Major Trypsinogen Isoforms in the Mouse Pancreas—To identify trypsinogen isoforms expressed at high levels in the mouse pancreas, we used ecotin-affinity chromatography to purify trypsinogens *en bloc* from pancreas tissue extracts of the outbred CD-1 mouse strain. Trypsinogens were eluted under acidic conditions from the ecotin column and immediately loaded onto a Mono S cation exchange column equilibrated with 20 mM sodium acetate (pH 5.0). The Mono S column was developed with a NaCl gradient, resulting in five

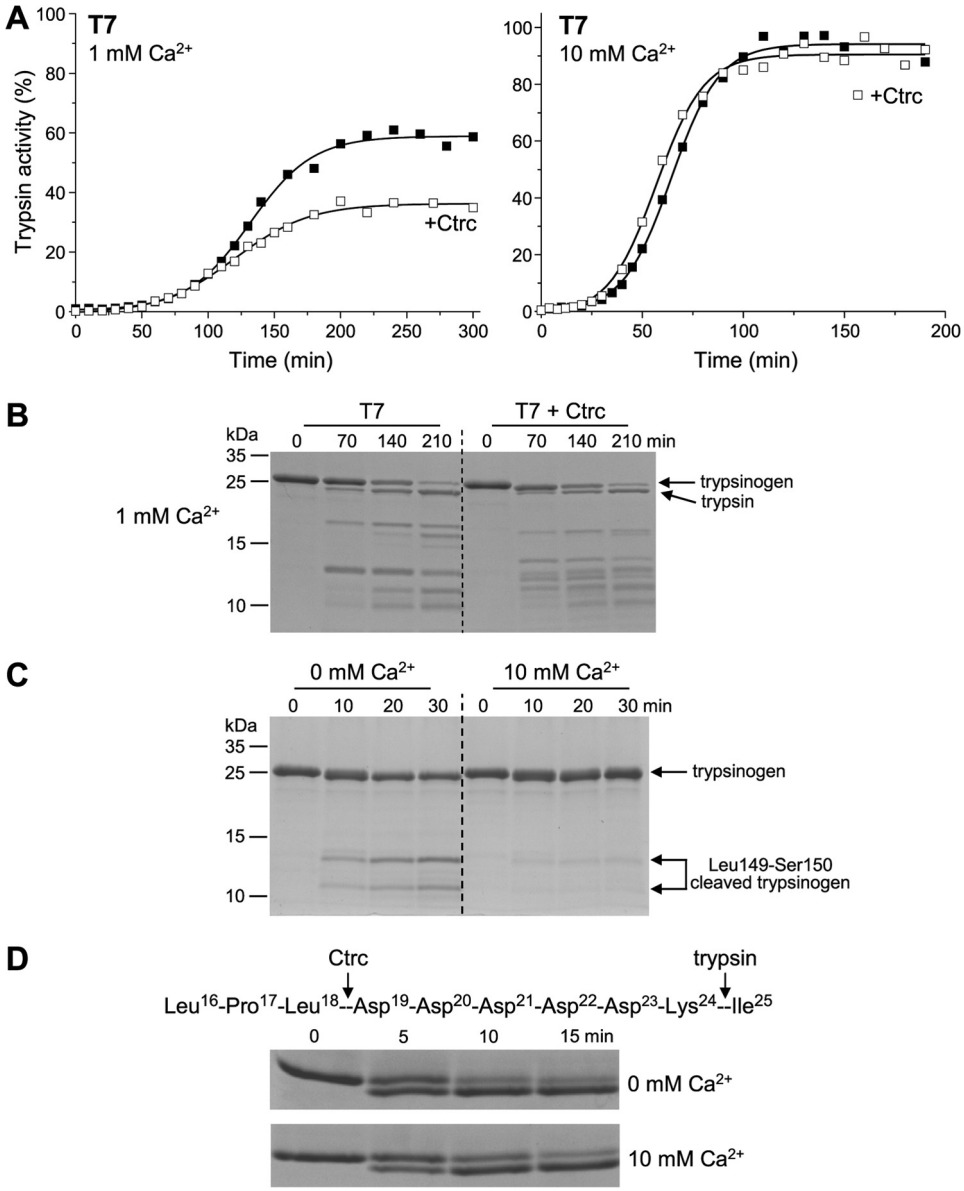

FIGURE 4. **Effect of mouse Ctrc on mouse trypsinogen T7.** *A,* autoactivation was measured in 1 and 10 mM $CaCl_2$ in the absence (*solid symbols*) or presence (*open symbols*) of 25 nM mouse Ctrc, as described under "Experimental Procedures." *B,* SDS-PAGE analysis of the autoactivation reaction in 1 mM $CaCl_2$. Samples were withdrawn at the indicated time points, precipitated with trichloroacetic acid, electrophoresed, and stained as described under "Experimental Procedures." *C,* cleavage of T7 trypsinogen by 25 nM mouse Ctrc. Incubations were performed with 2 μM trypsinogen in 0.1 M Tris-HCl (pH 8.0) in the absence or presence of 10 mM $CaCl_2$. Samples were precipitated with trichloroacetic acid and analyzed by SDS-PAGE and Coomassie Blue staining. Representative experiments from three replicates are shown. *D,* cleavage of the activation peptide of trypsinogen T7 by mouse Ctrc. Primary structure of the native T7 activation peptide with proteolytic cleavage sites for Ctrc and trypsin is also indicated. Note that the N-terminal amino acid of mature trypsinogen is Leu-16, as the 15-amino acid-long secretory signal peptide is removed in the endoplasmic reticulum. Trypsinogen was incubated at 2 μM concentration with 25 nM Ctrc in 0.1 M Tris-HCl (pH 8.0) and 0 or 10 mM $CaCl_2$ (final concentrations) at 37 °C. To prevent autoactivation, 25 nM human SPINK1 trypsin inhibitor was included. At the indicated times, reactions were terminated by precipitation with trichloroacetic acid, and samples were analyzed by nonreducing SDS-PAGE and Coomassie Blue staining. Relevant segments of representative gels (from two replicates) demonstrate the small mobility shift of the trypsinogen band caused by Ctrc-mediated cleavage of the Leu-18 –Asp-19 peptide bond. Note that the rapid rate of cleavage is partly due to the added Met-Ala sequence at the N terminus of recombinant T7.

peaks (Fig. 2*A*). Edman degradation unambiguously identified the small fourth peak as proelastase 3 (N terminus is CGQPS) and the large fifth peak as the cationic T7 trypsinogen isoform, which has a unique N-terminal sequence, LPLDD (Fig. 1). The other three peaks proved to be trypsinogens but had the same N termini, FPVDD; therefore, these were subjected to in-gel tryptic digestion followed by mass spectrometric nanosequencing, which revealed the identity of the first peak as isoform T20 and the second and third peaks as isoforms T9 and T8 (Fig. 2*A*). The latter two isoforms are nearly identical in their amino acid sequence (99% identity, Fig. 1) and MS/MS peptide coverage did not include any regions that were distinctive. On the basis of a slight difference in their ionic character, T9 was assigned to the second peak and T8 to the third peak. N-terminal sequencing of the combined second/third peaks after activation of trypsinogen to trypsin indicated a mixture of Val/Ile amino acids at position 35 (IVGGYTCRENS(**V**/**I**)P), with a preponderance of Val, confirming that the smaller second peak is T9 (containing

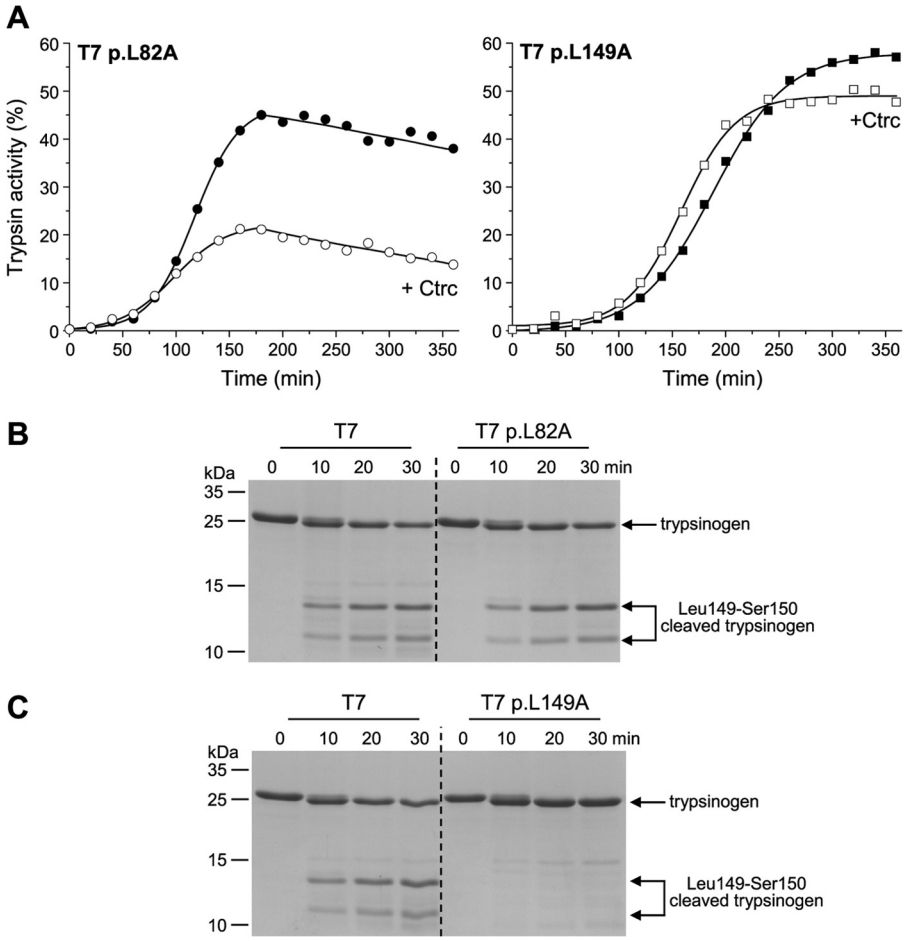

FIGURE 5. **Effect of mutations p.L82A and p.L149A on mouse trypsinogen T7.** *A,* autoactivation was measured in 1 mM $CaCl_2$ as described under "Experimental Procedures." Trypsin activity was expressed as percentage of the maximal activity determined by full activation with enteropeptidase. *B,* cleavage of wild-type and p.L82A T7 trypsinogen by 25 nM mouse Ctrc. *C,* cleavage of wild-type and p.L149A T7 trypsinogen by 25 nM mouse Ctrc. Incubations were performed with 2 μM trypsinogen in 0.1 M Tris-HCl (pH 8.0) in the absence of calcium. Trypsinogen samples were precipitated with trichloroacetic acid and analyzed by SDS-PAGE and Coomassie Blue staining. Representative experiments from two replicates are shown.

Ile-35) and the larger third peak is T8 (containing Val-35) (see Fig. 1). Both N-terminal sequencing (CGVPA) and MS/MS indicated that the T9/T8 peaks were contaminated with some Ctrb. Quantitative evaluation of trypsinogen peaks was performed as described under "Experimental Procedures," and the following relative expression levels were obtained (mean ± S.D., $n = 4$): 41 ± 1% for T7; 47 ± 3% for T8 and T9 combined, and 12 ± 2% for T20 (Table 2).

To confirm our findings with an independent method and in a different mouse strain, we used a proteomic approach based on two-dimensional PAGE, followed by in gel-digestion of silver-stained protein spots and peptide mass fingerprinting after MALDI-TOF mass spectrometry. Fig. 2*B* demonstrates two-dimensional PAGE protein patterns of a granule-enriched pancreas homogenate from the outbred NMRI mouse strain. In the 20–37-kDa molecular mass range, the same four trypsinogen isoforms were identified as with the chromatographic approach. The relative proportions of spot intensities (mean ± S.D., $n = 4$) were 25 ± 1% for T7, 33 ± 1% for T8, 27 ± 1% for T9, and 15 ± 2% for T20 (Table 2). These values compare fairly well, within experimental error, with those obtained for CD-1 mice.

Autoactivation of Mouse Trypsinogens—Large scale purification of different trypsinogen isoforms from the mouse pancreas is impractical, and preparations may be contaminated with low levels of other pancreatic proteases. In contrast, recombinant expression should provide highly purified homogeneous enzyme preparations. We previously established methodology for the expression and purification of human trypsinogens (15, 16), and here we used the same approach to obtain functionally competent mouse trypsinogen preparations. Trypsinogens were expressed in *E. coli* as inclusion bodies, renatured *in vitro* and purified by ecotin-affinity chromatography. When mouse trypsinogens were incubated in 1 mM $CaCl_2$ at pH 8.0, isoforms T7, T8, and T9 autoactivated and reached about 40–60% of potentially attainable trypsin levels, indicating that some autocatalytic (trypsin-mediated) degradation occurred (Fig. 3*A*) during autoactivation. In contrast, T20 did not autoactivate under these conditions. As expected, high concentrations of calcium (10 mM) increased the rate of autoactivation and stabilized trypsinogens against degradation, yielding 80–100% of attainable trypsin levels. The stimulatory effect of calcium on the autoactivation of T20 was particularly striking (Fig. 3*B*).

Effect of Mouse Ctrc on T7 Trypsinogen—Addition of 25 nM mouse Ctrc to the autoactivation assays of isoform T7 moderately (by ~35%) reduced trypsin levels in 1 mM calcium and slightly stimulated the rate of autoactivation in 10 mM calcium (Fig. 4*A*). SDS-PAGE analysis of the autoactivation reaction in 1 mM calcium, in the absence of Ctrc, confirmed conversion of the T7 trypsinogen band to trypsin and also indicated degradation fragments generated by cleavages of trypsin-sensitive peptide bonds Arg-123–Val-124 and Lys-194–Asp-195 (Fig. 4*B*, *left panel*, see also Fig. 1). These were identified by N-terminal sequencing, similarity to the published degradation fragments of rat anionic trypsinogen-2 (26), and comparison of the banding pattern with that of the T7 p.R123H mutant (see below). Note that because of an extra amino acid in the activation peptide of T7, amino acid numbering is shifted by one relative to human and other mouse trypsinogens (see Fig. 1). Cleavage after Arg-123 should result in a fully active two-chain trypsin (27, 28), whereas cleavage after Lys-194 causes inactivation (26, 29). Ctrc caused a small shift of the T7 trypsinogen band, suggesting cleavage of the activation peptide (Fig. 4*B*, *right panel*). In addition, the banding pattern of degradation fragments became more complex, which is consistent with the lower trypsin activity attained during autoactivation in 1 mM calcium in the presence of Ctrc.

To identify Ctrc-mediated cleavages of trypsinogen, we performed digestion experiments with short incubation times when no trypsinogen activation took place and no trypsin activity was present. Under these conditions, slow cleavage of the Leu-149–Ser-150 peptide bond in the autolysis loop was observed in the absence of calcium (Fig. 4*C*, *left panel*), and this was completely inhibited by 10 mM calcium (Fig. 4*C*, *right panel*, see also Fig. 1). The Leu-82–Glu-83 peptide bond (corresponding to Leu-81–Glu-82 in human trypsinogens and other studied mouse isoforms) in the calcium binding loop was not cleaved to a detectable extent. This finding suggested that in T7 the moderate degradation observed during autoactivation in 1 mM calcium in the presence of Ctrc is mediated by cleavage of the Leu-149–Ser-150 peptide bond. To confirm this assumption, we compared autoactivation of the T7 p.L82A and p.L149A mutants in 1 mM calcium and found that only mutation of p.L149A protected against degradation in the presence of Ctrc (Fig. 5). Interestingly, mutant p.L82A suffered Ctrc-dependent degradation during autoactivation to an even larger extent than wild-type T7.

N-terminal Processing of T7 Trypsinogen by Mouse Ctrc—Among the activation peptide sequences of mouse trypsinogens, only T7 contains a potentially Ctrc-sensitive peptide bond, Leu-18–Asp-19 (Fig. 1). Inspection of Fig. 4*B* revealed that the T7 trypsinogen band became slightly shifted as a result of treatment with Ctrc, suggesting that the activation peptide might be cleaved at Leu-18–Asp-19. When samples were run under nonreducing conditions, the mobility shift caused by N-terminal processing of the T7 activation peptide became more apparent (Fig. 4*D*), and N-terminal sequencing confirmed the predicted cleavage site. However, in contrast to human cationic trypsinogen, the rate of autoactivation of N-terminally processed T7 was only negligibly stimulated (see Fig. 4*A*, *right panel*), indicating that Ctrc does not regulate activation of mouse trypsinogens through cleavage of the activation peptide.

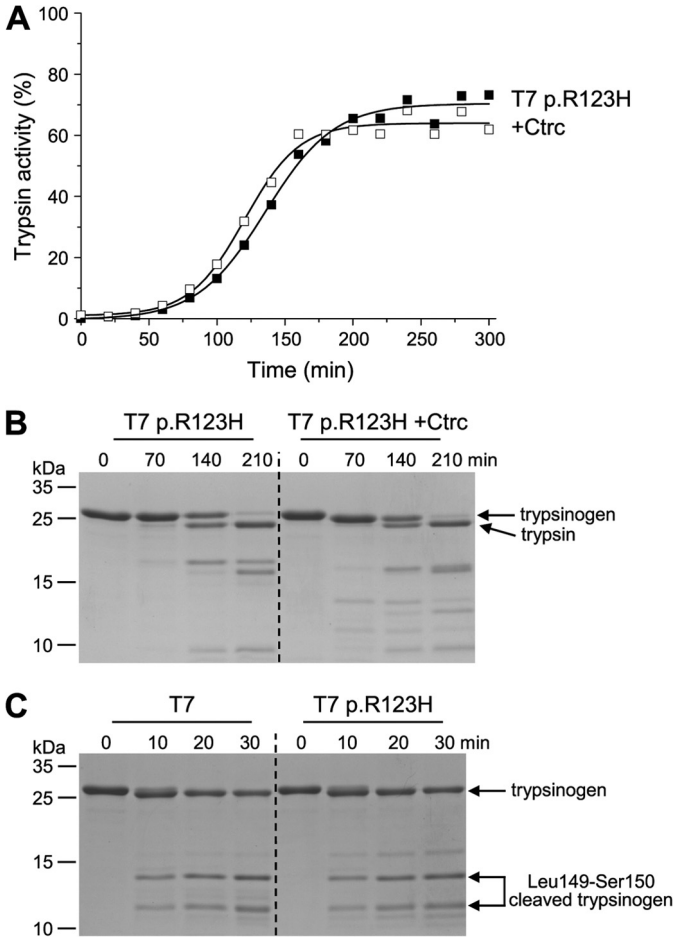

FIGURE 6. **Effect of mutation p.R123H on mouse trypsinogen T7.** *A*, autoactivation was measured in 1 mM $CaCl_2$ as described under "Experimental Procedures." Trypsin activity was expressed as percentage of the maximal activity determined by full activation with enteropeptidase. *B*, SDS-PAGE analysis of the autoactivation reaction. Samples were withdrawn at indicated times, precipitated with trichloroacetic acid, electrophoresed, and stained as described under "Experimental Procedures." *C*, cleavage of wild-type and p.R123H T7 trypsinogen by 25 nM mouse Ctrc. Incubations were performed with 2 μM trypsinogen in 0.1 M Tris-HCl (pH 8.0) in the absence of calcium. Samples were precipitated with trichloroacetic acid and analyzed by SDS-PAGE and Coomassie Blue staining. Cleavage products were identified with N-terminal sequencing. Representative experiments from two replicates are shown.

Effect of the p.R123H Mutation on T7 Trypsinogen—Mutation p.R123H protected T7 trypsinogen against degradation during autoactivation in 1 mM calcium in the presence of Ctrc (Fig. 6); however, it had no effect on the cleavage of the Leu-149–Ser-150 peptide bond *per se*. This observation indicates that moderate degradation of T7 during autoactivation is due to the combined effects of Ctrc-mediated and tryptic cleavages after Leu-149 and Arg-123, respectively (see Fig. 1).

Effect of Mouse Ctrc on T8 and T9 Trypsinogen—Mouse Ctrc almost completely inhibited autoactivation of T8 and T9 trypsinogen in 1 mM calcium and markedly reduced it in 10 mM calcium (Figs. 7 and 8). This inhibitory effect was not due to degradation, as addition of enteropeptidase to the Ctrc-treated samples resulted in the appearance of highly significant trypsin activity. SDS-PAGE analysis of autoactivation in 1 mM calcium,

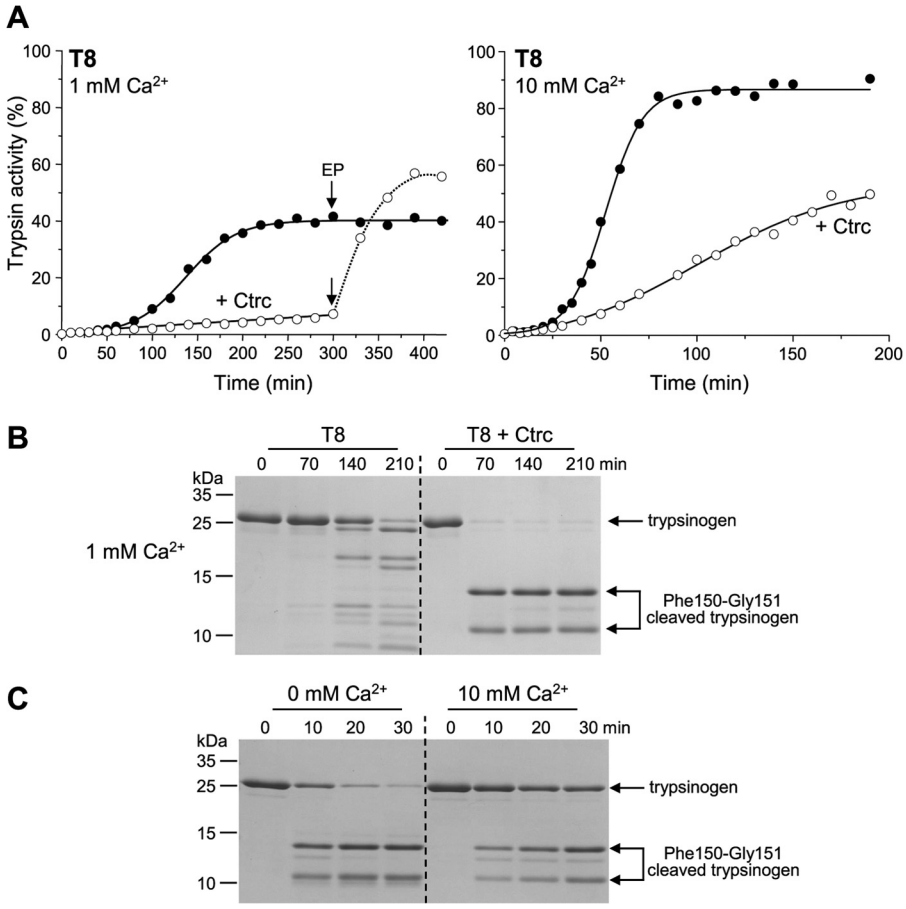

FIGURE 7. **Effect of mouse Ctrc on mouse trypsinogen T8.** *A,* autoactivation was measured in 1 and 10 mM $CaCl_2$, in the absence (*solid symbols*) or presence (*open symbols*) of 25 nM mouse Ctrc, as described under "Experimental Procedures." Where indicated, 2 μl of 1.4 μg/ml human enteropeptidase (*EP*) was added. *B,* SDS-PAGE analysis of the autoactivation reaction in 1 mM $CaCl_2$. Samples were withdrawn at indicated times, precipitated with trichloroacetic acid, electrophoresed, and stained as described under "Experimental Procedures." *C,* cleavage of trypsinogen by 25 nM mouse Ctrc. Incubations were performed with 2 μM trypsinogen in 0.1 M Tris-HCl (pH 8.0) in the absence or presence of 10 mM $CaCl_2$. Samples were precipitated with trichloroacetic acid and analyzed by SDS-PAGE and Coomassie Blue staining. Cleavage products were identified with N-terminal sequencing. In the absence of calcium (*left panel*), the faint bands above and below the major cleavage products correspond to fragments of trypsinogen cleaved at the Leu-81–Glu-82 peptide bond. The faint band visible in the presence of 10 mM calcium (*right panel*) could not be identified. Representative experiments from three replicates are shown.

in the absence of Ctrc, demonstrated conversion of trypsinogen to trypsin with the characteristic degradation fragments generated by tryptic cleavage of the Arg-122–Val-123 and Lys-193–Asp-194 peptide bonds (Figs. 7*B* and 8*B, left panel*, see also Fig. 1). In dramatic contrast, when autoactivation was followed in the presence of Ctrc, no trypsin band nor any of the tryptic degradation bands were observed. Instead, Ctrc rapidly and completely cleaved T8 and T9 trypsinogen at a single site, which N-terminal sequencing revealed as the Phe-150–Gly-151 peptide bond (Figs. 7*B* and 8*B, right panel*). This peptide bond lies within the so-called autolysis loop, a flexible segment between residues 146 and 154 (Fig. 1). When cleavage of T8 and T9 trypsinogen by Ctrc was studied with short incubation times (*i.e.* before autoactivation occurred), both isoforms were primarily cleaved at the Phe-150–Gly-151 peptide bond, with minimal cleavage observed at the Leu-81–Glu-82 peptide bond in the absence of calcium (Figs. 7*C* and 8*C*). Cleavage of the Phe-150–Gly-151 peptide bond was slower but still readily detectable in 10 mM calcium.

Cleavage of the Phe-150–Gly-151 Peptide Bond by Mouse Chymotrypsin B (Ctrb)—Regulation of autoactivation of human cationic trypsinogen by human CTRC is highly specific, and other chymotrypsins and elastases do not cleave the CTRC cleavage sites. To test whether the same Ctrc specificity exists in the mouse, we compared the effect of mouse Ctrb and Ctrc on T8 trypsinogen. As shown in Fig. 9*A*, autoactivation of T8 was much less effectively inhibited by 25 nM Ctrb than by an equimolar concentration of Ctrc. In degradation experiments, Ctrb cleaved the Phe-150–Gly-151 peptide bond at a more than 7-fold slower rate than Ctrc (Fig. 9, *B* and *C*).

Effect of the p.R122H Mutation on T8 Trypsinogen—Mutation p.R122H slightly stimulated autoactivation of T8 trypsinogen in 1 mM calcium, in the absence of Ctrc (Fig. 10*A*). In the presence of Ctrc, however, autoactivation was strongly inhibited by Ctrc, approximately to the same extent as seen with wild-type T8 (Fig. 10*B*, *cf.* Fig. 7*A*). Consistent with the robust inhibitory effect, the Phe-150–Gly-151 peptide bond was cleaved by Ctrc almost as well in T8 p.R122H trypsinogen as in wild-type T8 (Fig. 10*C*).

Cleavage of the Autolysis Loop in the p.S150F Human Cationic Trypsinogen Mutant Inhibits Autoactivation—The majority of mammalian trypsinogens do not contain Phe-150 in their autolysis loop. To test whether introduction of Phe-150 would reconstitute the chymotrypsin-dependent autoactivation inhi-

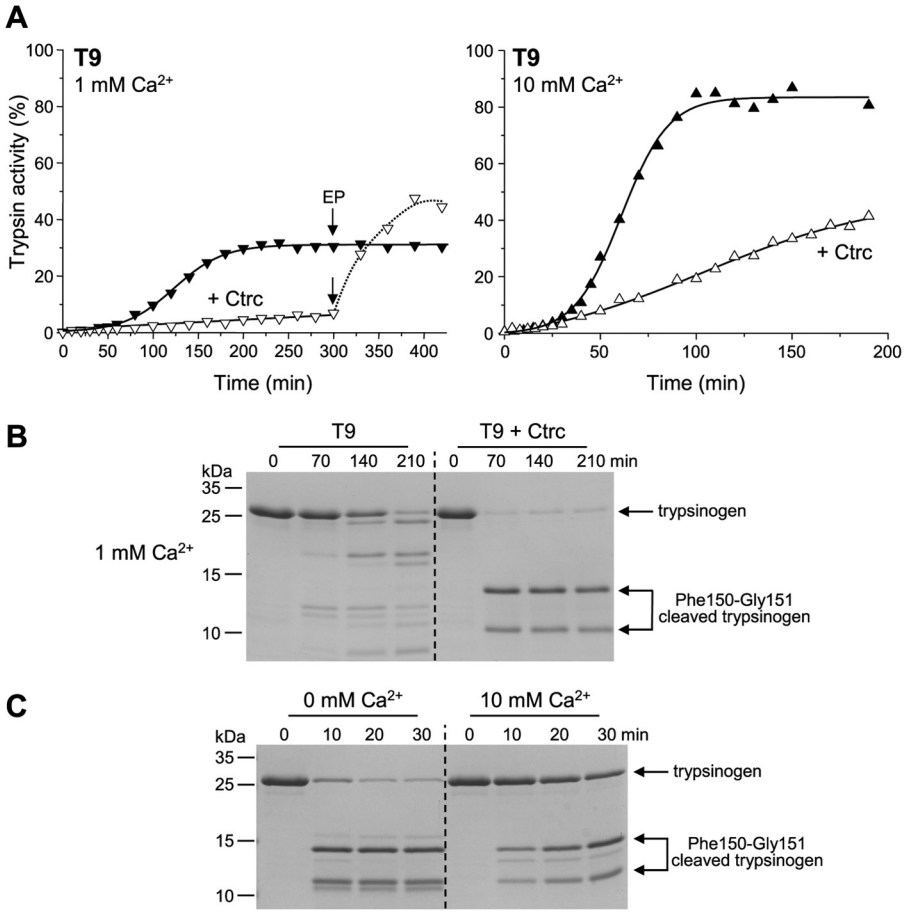

FIGURE 8. **Effect of mouse Ctrc on mouse trypsinogen T9.** See Fig. 7 for experimental details. *EP,* human enteropeptidase.

bition in another mammalian trypsinogen, we mutated Ser-150 in human cationic trypsinogen to Phe. Because human CTRC cleaves the Leu-81–Glu-82 peptide bond and causes trypsinogen degradation, we used human CTRB2 to selectively cleave the newly created Phe-150–Gly-151 peptide bond. CTRB2 at 25 nM concentration had no effect on the autoactivation of wild-type cationic trypsinogen (Fig. 11*A*), but it inhibited activation of the p.S150F mutant (Fig. 11*B*), via cleavage at the Phe-150–Gly-151 peptide bond (Fig. 11*C*).

Effect of Mouse Ctrc on T20 Trypsinogen—Finally, mouse Ctrc had essentially no effect on trypsinogen T20, except for a slight stimulation of the activation rate in 10 mM calcium (Fig. 12*A*). On SDS-PAGE, no trypsinogen to trypsin conversion was evident in 1 mM calcium, in the absence or presence of Ctrc (Fig. 12*B*). Note that T20 trypsinogen ran as a doublet on gels, which seems to represent differently denatured conformers, as N-terminal sequencing and mass spectrometry indicated molecular homogeneity (data not shown). Finally, cleavage of T20 with Ctrc resulted in very faint degradation bands even in the absence of calcium, indicating that this isoform is resistant to Ctrc (Fig. 12*C*).

DISCUSSION

The aim of this study was to identify the major trypsinogen isoforms expressed by the mouse pancreas and characterize their regulation of autoactivation by mouse Ctrc. These studies were undertaken to clarify whether introduction of trypsinogen mutations associated with human hereditary pancreatitis into mouse trypsinogens would offer a viable approach to model hereditary pancreatitis in mice. Previous attempts to generate transgenic mice expressing the coding DNA for human cationic trypsinogen with the p.R122H mutation failed to recapitulate hereditary pancreatitis, partly because of the low transgene expression levels (6). Introduction of mutation p.R122H into an endogenous mouse trypsinogen may circumvent the expression problem. However, the effect of p.R122H in human cationic trypsinogen is dependent on CTRC (3), and it has been unknown whether autoactivation of mouse trypsinogens is regulated by mouse Ctrc in a manner that mimics the human situation.

Using two independent biochemical approaches with two commonly used outbred mouse strains, we found that only four trypsinogen isoforms, T7, T8, T9 and T20, are expressed to high levels (Table 2) in the mouse pancreas, even though the mouse genome contains 20 trypsinogen genes, of which 11 are potentially functional (Table 1 and Fig. 1). The cationic isoform T7 was recently deleted in the C57BL/6 strain, and judging from the residual trypsinogen content the authors suggested that T7 contributes 60% of total mouse trypsinogens (12, 13). Here, we obtained smaller values (41% in CD-1 and 25% in NMRI mice); however, these differences seem to fall within experimental error and may even represent strain-specific differences. It is important to note that Prss1 (T16) and Prss3 (T11) (see Table

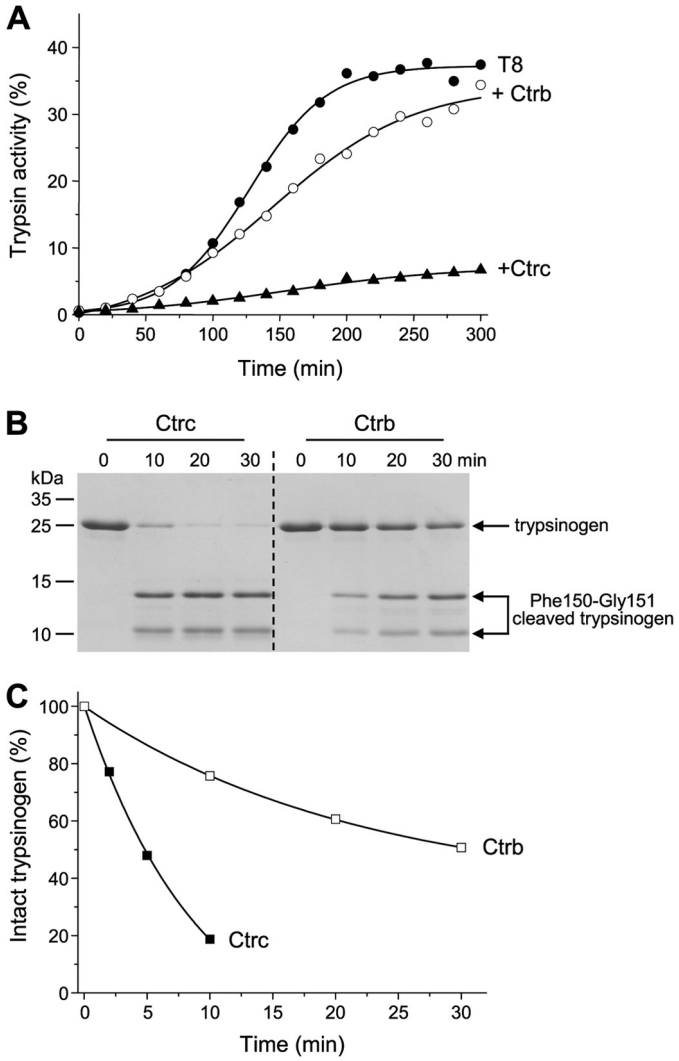

FIGURE 9. **Effect of mouse Ctrb on mouse trypsinogen T8.** *A,* autoactivation was measured in 1 mM $CaCl_2$ as described under "Experimental Procedures" in the absence or presence of 25 nM mouse Ctrb or Ctrc, as indicated. *B,* cleavage of trypsinogen by 25 nM Ctrb and Ctrc was compared in the absence of calcium, as described in Fig. 7*C*. Representative experiments from two replicates are shown. *C,* disappearance of the intact trypsinogen band was quantitated by densitometry, and data from two experiments were plotted. For clarity, *error bars* were omitted; the error was within 10% of the mean.

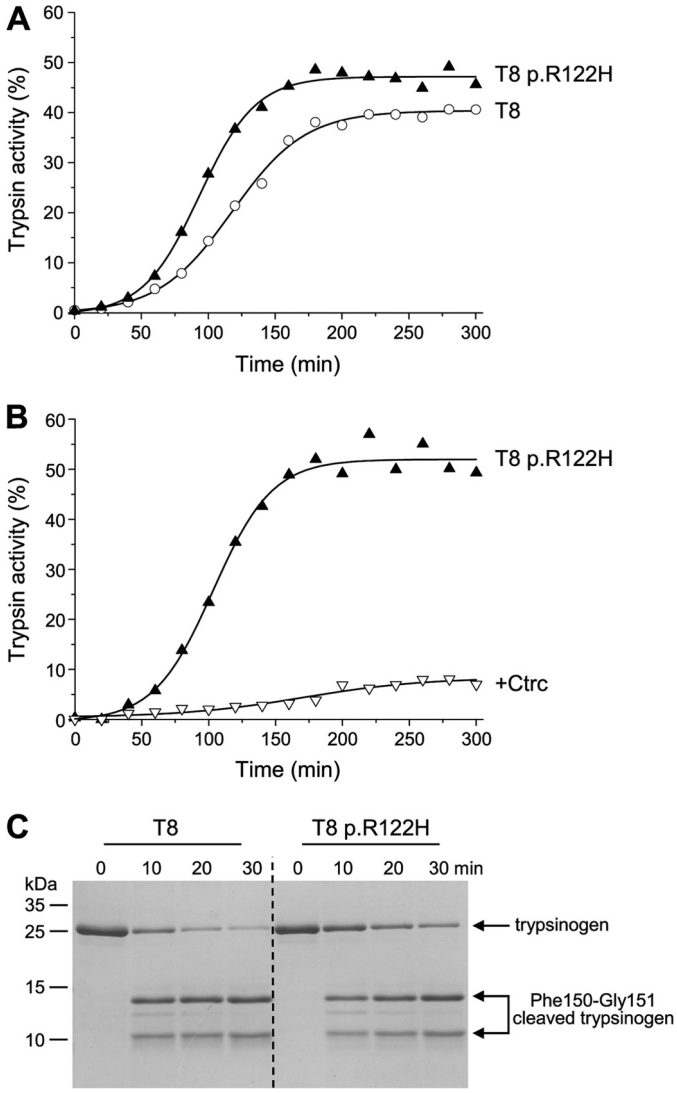

FIGURE 10. **Effect of mutation p.R122H on mouse trypsinogen T8.** *A,* autoactivation of wild-type and p.R122H mutant T8 trypsinogen was measured in 1 mM $CaCl_2$ as described under "Experimental Procedures." *B,* effect of 25 nM mouse Ctrc on the autoactivation of the p.R122H mutant T8. Conditions were the same as in *A*. *C,* cleavage of wild-type and p.R122H mutant T8 trypsinogen by 25 nM mouse Ctrc in the absence of calcium. Samples were incubated and analyzed as described in Fig. 7*C*. Representative experiments from two replicates are shown.

1), the presumed orthologs of human cationic trypsinogen (PRSS1) and mesotrypsinogen (PRSS3), are not expressed at detectable levels, indicating that assignment of orthology by database curators may be unreliable and even misleading to investigators, as evidenced by a recent study where expression of mouse Prss1 was studied (30). Finally, we emphasize that our data pertain to the resting, unstimulated mouse pancreas, and it is possible, even likely, that upon hormonal stimulation the trypsinogen expression pattern may change, as shown previously for rat p23, the ortholog of mouse T4 and T5, which becomes drastically up-regulated upon cerulein stimulation (31). Marked up-regulation of T5 was observed in a knock-out mouse strain deficient in interferon regulatory factor 2 (32).

Autoactivation of mouse trypsinogens T7, T8, and T9 was comparable, whereas T20 autoactivated more slowly, particularly in 1 mM calcium (see Fig. 3). Surprisingly, regulation of autoactivation by mouse Ctrc was isoform-specific and mechanistically different from the actions of human CTRC on human cationic trypsinogen. Whereas the human enzyme targets regulatory cleavage sites in the activation peptide and the calcium binding loop of cationic trypsinogen, these proved to be irrelevant in mouse trypsinogens. Thus, Ctrc-mediated cleavage of the activation peptide was observed only with the T7 isoform, however, this N-terminal processing had no significant effect on autoactivation. Cleavage of the Leu-81–Glu-82 peptide bond in the calcium binding loop (Leu-82–Glu-83 in T7) was not detectable in T7 or T20, and minimal cleavage was seen in T8 and T9. In contrast, isoforms T8 and T9 were rapidly cleaved at the Phe-150–Gly-151 peptide bond in the autolysis loop, and this cleavage resulted in marked inhibition of autoactivation. The Phe-150–Gly-151 peptide bond was also cleaved by Ctrb at a 7-fold slower rate. However, considering that Ctrb is the most abundant chymotrypsin in the pancreas, physiolog-

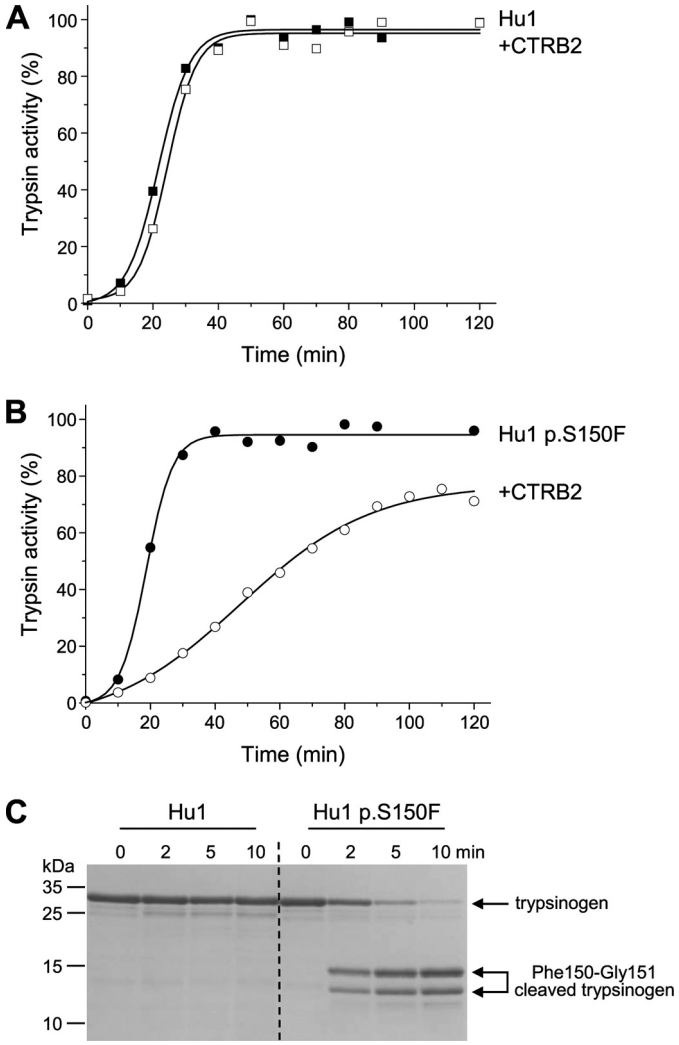

FIGURE 11. **Effect of human CTRB2 on the autoactivation of wild-type and p.S150F mutant human cationic trypsinogen (Hu1).** *A* and *B,* autoactivation was measured in 1 mM $CaCl_2$, in the absence or presence of 25 nM CTRB2, as described under "Experimental Procedures." *C,* cleavage of wild-type and p.S150F mutant human cationic trypsinogen by 25 nM CTRB2 in the absence of calcium. Incubations were performed, and samples were analyzed as given in Fig. 7*C*. To prevent autoactivation, 25 nM human SPINK1 trypsin inhibitor was included. Representative experiments from two replicates are shown.

ical regulation of activation of T8 and T9 may be also dependent on Ctrb. Isoform T7 was also cleaved in the autolysis loop, albeit slowly and at a different peptide bond (Leu-149–Ser-150), which resulted in moderate degradation during autoactivation. Nevertheless, isoform T7 was clearly less sensitive to chymotryptic regulation than human cationic trypsinogen or mouse trypsinogens T8 and T9.

The lack of cleavage at the Leu-81–Glu-82 (Leu-82–Glu-83 in T7) peptide bond by Ctrc may be partly explained by differences in the amino acid sequence of the calcium binding loop (see Fig. 1). Furthermore, as we learned from the recent crystal structure of human CTRC, recognition of the calcium binding loop is governed by long range electrostatic interactions between the negatively charged substrate and positively charged surface regions on CTRC (33). These macroscopic electrostatic interactions are less favorable in the mouse, due to missing positively charged residues in Ctrc (Arg-80 and Arg-240) and negatively charged residues in mouse trypsinogens T7 (Glu-32, Asp-156, and Glu-157) and T8, T9, and T20 (Glu-79 and Glu-157) (see Fig. 1).

The majority of mammalian trypsinogens do not contain Phe-150, indicating that this novel mechanism of autoactivation regulation may be unique to rodents. Human mesotrypsinogen contains Phe-150, and cleavage at this site by human CTRC was demonstrated previously (5), suggesting that activation of mesotrypsinogen may be under similar regulation. Human anionic and cationic trypsinogens contain Ser at position 150, but mutation S150F confers sensitivity to CTRB2-mediated cleavage of the autolysis loop, which inhibits autoactivation in a manner that is similar to the Ctrc-dependent inhibition of T8 and T9 in the mouse. Crystal structures of mouse trypsinogens are not available, and the autolysis loop in structures of rat anionic trypsinogen is disordered and not visible. Therefore, we used a bovine trypsinogen structure to model the potential effects of cleavage of the autolysis loop after Phe-150. As shown in Fig. 13, the autolysis loop may be in close proximity to the trypsinogen activation peptide, at least judged by the position of Val-25, the first visible residue of the otherwise disordered N-terminal segment. Cleavage of the Phe-150–Gly-151 peptide bond should increase the mobility of the autolysis loop, which may directly interact with the activation peptide thereby decreasing its accessibility. One possible interaction may occur between the positive charge of the newly created N terminus in the autolysis loop and the negatively charged tetra-Asp motif in the activation peptide.

The Ctrc-dependent inhibition of autoactivation of T8 and T9 trypsinogens may have evolved as a protective mechanism to curtail unwanted trypsinogen activation in the pancreas. This is conceptually analogous to the regulation of human trypsinogens by human CTRC even though mechanistic details are dissimilar. Interestingly, we found that cleavage of the Phe-150–Gly-151 peptide bond in T8 and T9 trypsinogens also inhibits activation by enteropeptidase, the physiological trypsinogen activator in the duodenum (data not shown). Although inhibition of digestive enzyme activation in the gut may seem counterintuitive, this chymotrypsin-dependent feedback mechanism likely ensures that intestinal trypsinogen activation proceeds with a slower, more prolonged kinetics, which may be favorable for food digestion.

Intra-acinar cell activation of trypsinogen in cytoplasmic vesicles of autophagic origin is an early event in experimental models of acute pancreatitis (34). Genetic deletion of T7 was recently shown to abolish intra-acinar trypsinogen activation in response to hyperstimulation with cerulein: a somewhat perplexing observation as other trypsinogen isoforms could have potentially be activated (12, 13). The results presented here offer a plausible explanation for this puzzle. When trypsinogen activation occurs, isoforms T8 and T9 may be inhibited in a Ctrc or Ctrb-dependent manner, whereas T7 is less sensitive to chymotryptic regulation. Because of its lower concentration and poor activation, isoform T20 is unlikely to contribute to intra-acinar trypsinogen activation to a detectable extent.

Finally, our data argue that in the context of mouse trypsinogens, human pancreatitis-associated mutations may not recapitulate the pathogenic biochemical phenotype observed with

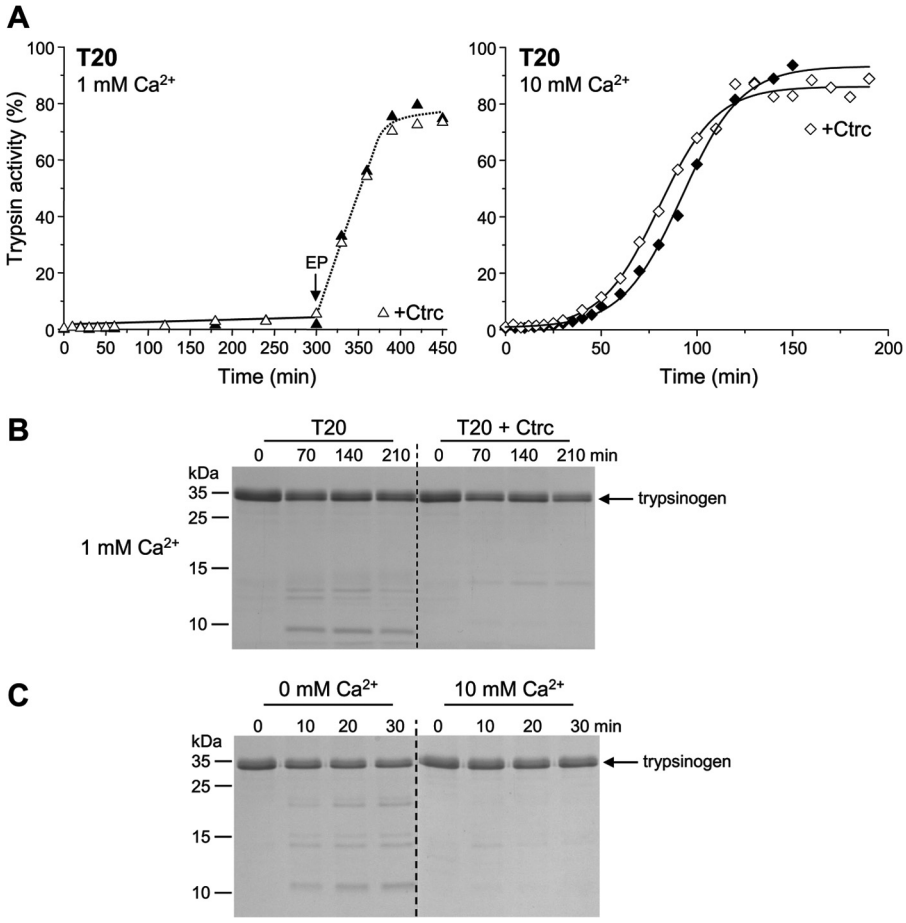

FIGURE 12. **Effect of mouse Ctrc on mouse trypsinogen T20.** *A,* autoactivation was measured in 1 and 10 mM $CaCl_2$, in the absence (*solid symbols*) or presence (*open symbols*) of 25 nM mouse Ctrc, as described under "Experimental Procedures." Where indicated, 2 μl of 1.4 μg/ml human enteropeptidase (*EP*) was added. *B,* SDS-PAGE analysis of the autoactivation reaction in 1 mM $CaCl_2$. Samples were withdrawn at the indicated time points, precipitated with trichloroacetic acid, electrophoresed, and stained as described under "Experimental Procedures." *C,* cleavage of T20 trypsinogen by 25 nM mouse Ctrc. Incubations were performed, and samples were analyzed as in Fig. 7*C*. The faint Ctrc cleavage products seen in the absence of calcium were not identified. Representative experiments from three replicates are shown.

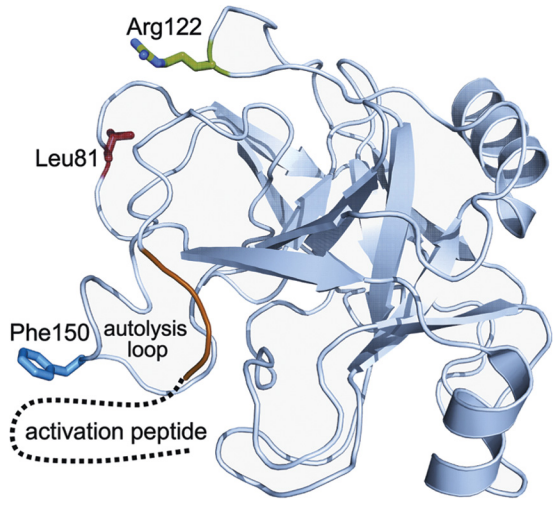

FIGURE 13. **Proximity of the autolysis loop and the activation peptide in trypsinogen.** Mouse trypsinogen T8 was modeled using a ribbon diagram of bovine trypsinogen (Protein Data Bank code 1TGN). The side chains for amino acids Leu-81, Arg-122, and Phe-150 are indicated. The putative activation peptide backbone is indicated by *dotted lines*. In the crystal structure the activation peptide (residues 16–23) is disordered, and the first visible N-terminal amino acid is valine 25. The image was rendered using PyMOL 1.3 (Schrödinger, LLC).

human cationic trypsinogen. We found that mutation p.R122H did not affect inhibition of autoactivation by Ctrc in T8 trypsinogen, which stands in contrast to the robust negative effect of this mutation on CTRC-dependent degradation of human cationic trypsinogen (3). Thus, introduction of human mutations into mouse trypsinogens may not be a practical approach for the generation of mouse models of human hereditary pancreatitis.

Acknowledgments—András Szabó is gratefully acknowledged for help with structural modeling and experimental advice. We thank Sebastian Beer for help with mutagenesis.

REFERENCES

1. Whitcomb, D. C., Gorry, M. C., Preston, R. A., Furey, W., Sossenheimer, M. J., Ulrich, C. D., Martin, S. P., Gates, L. K., Jr., Amann, S. T., Toskes, P. P., Liddle, R., McGrath, K., Uomo, G., Post, J. C., and Ehrlich, G. D. (1996) Hereditary pancreatitis is caused by a mutation in the cationic trypsinogen gene. *Nat. Genet.* **14,** 141–145
2. Teich, N., Rosendahl, J., Tóth, M., Mössner, J., and Sahin-Tóth, M. (2006) Mutations of human cationic trypsinogen (PRSS1) and chronic pancreatitis. *Hum. Mutat.* **27,** 721–730
3. Szabó, A., and Sahin-Tóth, M. (2012) Increased activation of hereditary pancreatitis-associated human cationic trypsinogen mutants in presence

of chymotrypsin C. *J. Biol. Chem.* **287,** 20701–20710
4. Nemoda, Z., and Sahin-Tóth, M. (2006) Chymotrypsin C (caldecrin) stimulates autoactivation of human cationic trypsinogen. *J. Biol. Chem.* **281,** 11879–11886
5. Szmola, R., and Sahin-Tóth, M. (2007) Chymotrypsin C (caldecrin) promotes degradation of human cationic trypsin: identity with Rinderknecht's enzyme Y. *Proc. Natl. Acad. Sci. U.S.A.* **104,** 11227–11232
6. Selig, L., Sack, U., Gaiser, S., Klöppel, G., Savkovic, V., Mössner, J., Keim, V., and Bödeker, H. (2006) Characterisation of a transgenic mouse expressing R122H human cationic trypsinogen. *BMC Gastroenterol.* **6,** 30
7. Archer, H., Jura, N., Keller, J., Jacobson, M., and Bar-Sagi, D. (2006) A mouse model of hereditary pancreatitis generated by transgenic expression of R122H trypsinogen. *Gastroenterology* **131,** 1844–1855
8. Watanabe, T., and Ogasawara, N. (1982) Purification and properties of multiple forms of mouse trypsinogen. *Biochim. Biophys. Acta* **717,** 439–444
9. Stevenson, B. J., Hagenbüchle, O., and Wellauer, P. K. (1986) Sequence organisation and transcriptional regulation of the mouse elastase II and trypsin genes. *Nucleic Acids Res.* **14,** 8307–8330
10. Glusman, G., Rowen, L., Lee, I., Boysen, C., Roach, J. C., Smit, A. F., Wang, K., Koop, B. F., and Hood, L. (2001) Comparative genomics of the human and mouse T cell receptor loci. *Immunity* **15,** 337–349
11. Ohmura, K., Kohno, N., Kobayashi, Y., Yamagata, K., Sato, S., Kashiwabara, S., and Baba, T. (1999) A homologue of pancreatic trypsin is localized in the acrosome of mammalian sperm and is released during acrosome reaction. *J. Biol. Chem.* **274,** 29426–29432
12. Dawra, R., Sah, R. P., Dudeja, V., Rishi, L., Talukdar, R., Garg, P., and Saluja, A. K. (2011) Intra-acinar trypsinogen activation mediates early stages of pancreatic injury but not inflammation in mice with acute pancreatitis. *Gastroenterology* **141,** 2210–2217
13. Sah, R. P., Dudeja, V., Dawra, R. K., and Saluja, A. K. (2013) Caerulein-induced chronic pancreatitis does not require intra-acinar activation of trypsinogen in mice. *Gastroenterology* **144,** 1076–1085
14. Király, O., Guan, L., Szepessy, E., Tóth, M., Kukor, Z., and Sahin-Tóth, M. (2006) Expression of human cationic trypsinogen with an authentic N terminus using intein-mediated splicing in aminopeptidase P-deficient *Escherichia coli*. *Protein Expr. Purif.* **48,** 104–111
15. Sahin-Tóth, M. (2000) Human cationic trypsinogen. Role of Asn-21 in zymogen activation and implications in hereditary pancreatitis. *J. Biol. Chem.* **275,** 22750–22755
16. Sahin-Tóth, M., and Tóth, M. (2000) Gain-of-function mutations associated with hereditary pancreatitis enhance autoactivation of human cationic trypsinogen. *Biochem. Biophys. Res. Commun.* **278,** 286–289
17. Pál, G., Sprengel, G., Patthy, A., and Gráf, L. (1994) Alteration of the specificity of ecotin, an *E. coli* serine proteinase inhibitor, by site-directed mutagenesis. *FEBS Lett.* **342,** 57–60
18. Lengyel, Z., Pál, G., and Sahin-Tóth, M. (1998) Affinity purification of recombinant trypsinogen using immobilized ecotin. *Protein Expr. Purif.* **12,** 291–294
19. Schägger, H., and von Jagow, G. (1987) Tricine-sodium dodecyl sulfate-polyacrylamide gel electrophoresis for the separation of proteins in the range from 1 to 100 kDa. *Anal. Biochem.* **166,** 368–379
20. Blum, H., Beier, H., and Gross, H. J. (1987) Improved silver staining of plant proteins, RNA and DNA in polyacrylamide gels. *Electrophoresis* **8,** 93–99
21. Neuhoff, V., Arold, N., Taube, D., and Ehrhardt, W. (1988) Improved staining of proteins in polyacrylamide gels including isoelectric focusing gels with clear background at nanogram sensitivity using Coomassie Brilliant Blue G-250 and R-250. *Electrophoresis* **9,** 255–262
22. Király, O., Guan, L., and Sahin-Tóth, M. (2011) Expression of recombinant proteins with uniform N termini. *Methods Mol. Biol.* **705,** 175–194
23. Szabó, A., and Sahin-Tóth, M. (2012) Determinants of chymotrypsin C cleavage specificity in the calcium-binding loop of human cationic trypsinogen. *FEBS J.* **279,** 4283–4292
24. Szabó, A., Héja, D., Szakács, D., Zboray, K., Kékesi, K. A., Radisky, E. S., Sahin-Tóth, M., and Pál, G. (2011) High affinity small protein inhibitors of human chymotrypsin C (CTRC) selected by phage display reveal unusual preference for P4′ acidic residues. *J. Biol. Chem.* **286,** 22535–22545
25. Kukor, Z., Tóth, M., and Sahin-Tóth, M. (2003) Human anionic trypsinogen: properties of autocatalytic activation and degradation and implications in pancreatic diseases. *Eur. J. Biochem.* **270,** 2047–2058
26. Sahin-Tóth, M. (1999) Hereditary pancreatitis-associated mutation $Asn^{21} \rightarrow$ Ile stabilizes rat trypsinogen *in vitro*. *J. Biol. Chem.* **274,** 29699–29704
27. Maroux, S., and Desnuelle, P. (1969) On some autolyzed derivatives of bovine trypsin. *Biochim. Biophys. Acta* **181,** 59–72
28. Kukor, Z., Tóth, M., Pál, G., and Sahin-Tóth, M. (2002) Human cationic trypsinogen. Arg-117 is the reactive site of an inhibitory surface loop that controls spontaneous zymogen activation. *J. Biol. Chem.* **277,** 6111–6117
29. Smith, R. L., and Shaw, E. (1969) Pseudotrypsin. A modified bovine trypsin produced by limited autodigestion. *J. Biol. Chem.* **244,** 4704–4712
30. Wang, J., Ohmuraya, M., Suyama, K., Hirota, M., Ozaki, N., Baba, H., Nakagata, N., Araki, K., and Yamamura, K. (2010) Relationship of strain-dependent susceptibility to experimentally induced acute pancreatitis with regulation of Prss1 and Spink3 expression. *Lab. Invest.* **90,** 654–664
31. Lütcke, H., Rausch, U., Vasiloudes, P., Scheele, G. A., and Kern, H. F. (1989) A fourth trypsinogen (P23) in the rat pancreas induced by CCK. *Nucleic Acids Res.* **17,** 6736
32. Hayashi, H., Kohno, T., Yasui, K., Murota, H., Kimura, T., Duncan, G. S., Nakashima, T., Yamamoto, K., Katayama, I., Ma, Y., Chua, K. J., Suematsu, T., Shimokawa, I., Akira, S., Kubo, Y., Mak, T. W., and Matsuyama, T. (2011) Characterization of dsRNA-induced pancreatitis model reveals the regulatory role of IFN regulatory factor 2 (Irf2) in trypsinogen5 gene transcription. *Proc. Natl. Acad. Sci. U.S.A.* **108,** 18766–18771
33. Batra, J., Szabó, A., Caulfield, T. R., Soares, A. S., Sahin-Tóth, M., and Radisky, E. S. (2013) Long-range electrostatic complementarity governs substrate recognition by human chymotrypsin C, a key regulator of digestive enzyme activation. *J. Biol. Chem.* **288,** 9848–9859
34. Sah, R. P., Garg, P., and Saluja, A. K. (2012) Pathogenic mechanisms of acute pancreatitis. *Curr. Opin. Gastroenterol.* **28,** 507–515

V.

Naunyn-Schmied Arch Pharmacol (2011) 383:447–455
DOI 10.1007/s00210-011-0605-2

ORIGINAL ARTICLE

Different inhibitory effects of kynurenic acid and a novel kynurenic acid analogue on tumour necrosis factor-α (TNF-α) production by mononuclear cells, HMGB1 production by monocytes and HNP1-3 secretion by neutrophils

Zoltán Tiszlavicz · Balázs Németh · Ferenc Fülöp · László Vécsei · Katalin Tápai · Imre Ocsovszky · Yvette Mándi

Received: 23 September 2010 / Accepted: 24 January 2011 / Published online: 19 February 2011

Abstract Kynurenic acid (KynA), a broad spectrum antagonist of excitatory amino acid receptors, may serve as a protective agent in neurological disorders. The potential anti-inflammatory effect of KynA in human leukocytes has not been characterized. The aim of this study was to compare the effects of KynA with those of a new analogue, 2-(2-*N*,*N*-dimethylaminoethylamine-1-carbonyl)-1*H*-quinolin-4-one hydrochloride on tumour necrosis factor-α (TNF-α) production and high mobility group box protein 1 (HMGB1) secretion. The effects of KynA on granulocyte activation were investigated via the secretion of human neutrophil peptide 1–3 (HNP1–3). Peripheral blood mononuclear cells and granulocytes or CD14 positive monocytes were applied as effector cells, or whole blood cultures were used. TNF-α, HMGB1 and HNP1–3 concentrations were determined by ELISA, TNF-α and HNP1–3 mRNA expressions were quantified by reverse transcription PCR. KynA attenuated the TNF-α production of human mononuclear cells activated by heat-inactivated *Staphylococcus aureus*, inhibiting TNF-α production at the transcription level. Furthermore, KynA diminished HMGB1 secretion by U 937 monocytic cells and by peripheral blood monocytes. KynA inhibited the HNP1–3 secretion in whole blood and in granulocyte cultures. The suppressive effect of the KynA analogue was more potent than that of an equimolar concentration KynA in TNF-α, HMGB1 and HNP1–3 inhibition. These results suggest that the new KynA analogue has a more potent immunoregulatory effect than KynA on human mononuclear cells, monocytes and granulocytes and indicate the potential benefits of further exploration of its uses in human inflammatory disease.

Keywords Kynurenic acid · TNF-α · HMGB1 · Defensin-α · Monocytes · Granulocytes

Z. Tiszlavicz · B. Németh · Y. Mándi (✉)
Department of Medical Microbiology and Immunobiology,
University of Szeged,
Dóm tér 10,
6720, Szeged, Hungary
e-mail: yvette@comser.szote.u-szeged.hu

F. Fülöp
Department of Pharmaceutical Chemistry, University of Szeged,
Szeged, Hungary

L. Vécsei
Department of Neurology, University of Szeged,
Szeged, Hungary

K. Tápai
Regional Centre of the Hungarian National Blood Transfusion Service,
Szeged, Hungary

I. Ocsovszky
Department of Biochemistry, University of Szeged,
Szeged, Hungary

Introduction

Kynurenic acid (KynA), an endogenous product of the tryptophan metabolism and a broad spectrum antagonist of excitatory amino acid receptors, may serve as a protective agent in neurological disorders (Stone 2000; Klivenyi et al. 2004; Nemeth et al. 2005; Sas et al. 2007; Gigler et al. 2007; Vamos et al. 2009). KynA is an *N*-methyl-D-aspartate (NMDA) antagonist (Stone 1993; Vecsei et al. 1992; Schwarcz et al. 1999; Robotka et al. 2008) and exerts a

wide range of biologically important action in the central nervous system, including the reduction of excitotoxic damage (Swartz et al. 1990; Kiss and Vecsei 2005; Robotka et al. 2008; Zádori et al. 2006). Exogenous KynA has been demonstrated to be able to inhibit leukocyte activation in a canine model of intestinal inflammation (Kaszaki et al. 2008). Furthermore, KynA decreases the inflammatory activation and colonic motility in the early phase of acute experimental colitis in the rat (Varga et al. 2010)

While most biological effects associated with KynA, such as neuroprotective activities, have been attributed to its antagonism on NMDA receptor, a novel mechanism by which KynA may regulate peripheral cellular responses through activation of GPR35 has been reported (Wang et al. 2006). It has been demonstrated that KynA acts as a ligand for GPR35, which is one of the members of the G-protein-coupled receptors (Lagerström and Schiöth 2008). Expression analysis has revealed prominent expression of GPR35 in immune and gastrointestinal tissues. In humans, GPR35 has mainly been detected in peripheral leukocytes, among them in monocytes, T cells, dendritic cells and neutrophils (Wang et al. 2006). Moreover, KynA was able to attenuate LPS-induced tumour necrosis factor-α (TNF-α) secretion of mononuclear cells. In view of its potential anti-inflammatory action, we considered it of interest to investigate the effects of KynA on TNF-α production and on the high mobility group box protein 1 (HMGB1) and defensin-α production of human white blood cells.

TNF is an inflammatory cytokine, an early mediator of proinflammatory reactions, orchestrating the production of the cytokine cascade (Fiers 1991). TNF-α has been shown to promote inflammation via the activation and induction of the cytokines interleukin 1 (IL-1), IL-6 and IL-8 and by the upregulation of adhesion molecules on endothelial cells, leading to increased leukocyte extravasation (Bradley 2008). Theoretically, the blockade of TNF should be of broad potential in the treatment of numerous inflammatory diseases (Mazza et al. 2010). HMGB1 functions as a proinflammatory late cytokine, actively secreted from monocytes and macrophages in response to proinflammatory stimuli, i.e. cytokines such as TNF-α, IL-1 or even lipopolysacharide (LPS; Harris and Andersson 2004; Lotze and Tracey 2005). Extracellular HMGB1 induces further release of proinflammatory mediators, thereby prolonging inflammatory processes (Andersson et al. 2002). In the present study, therefore the effects of KynA and a KynA analogue on the HMGB1 secretion of human monocyte cell line U 937 were investigated. Additionally, the effects of KynA on granulocyte activation were studied via the secretion of human neutrophil peptide 1–3 (HNP1–3), also known as defensin-α, which can be secreted and released into the extracellular milieu following the activation of polymorphonuclear neutrophils during inflammation (Ganz 1987; Quinn et al. 2008). Conventionally, α defensins are involved in microbial killing, but they also have an important immunomodulative role in inflammation (Yang et al. 2002). We further compared the effects of KynA with those of a novel, synthetic KynA analogue 2-(2-*N*,*N*-dimethylaminoethylamine-1-carbonyl)-1*H*-quinolin-4-one hydrochloride, which is able to cross the blood–brain barrier (Marosi et al. 2010).

Materials and methods

Reagents

The test compound KynA was purchased from SIGMA, while the new analogue (Fig. 1) was synthetized by Prof. Fülöp at the Department of Pharmaceutical Chemistry, University of Szeged. KynA and the analogue were dissolved in phosphate-buffered saline (PBS) and added in increasing concentration in the μ range to the cell cultures or whole blood samples.

Isolation and stimulation of human mononuclear cells

Peripheral blood mononuclear cells were prepared from EDTA-anticoagulated venous blood samples obtained from healthy volunteers by Ficoll-Hypaque (Sigma Chemicals) density gradient centrifugation. After washing, isolated cells (monocytes and lymphocytes) were resuspended in RPMI 1640 medium (GIBCO) supplemented with 10% foetal calf serum (FCS) to achieve a final concentration of 5×10^6 cells/ml.

Experimental cultures were incubated for 18 h with heat-inactivated *Staphylococcus aureus* 10^8/ml as a TNF inducer (Wang et al. 2000). In parallel experiments, mononuclear cells were pretreated for 30 min with KynA or with KynA analogue 2-(2-*N*,*N*-dimethylaminoethylamine-1-carbonyl)-1*H*-quinolin-4-one hydrochloride at concentrations of 500, 250, 125, 50 and 25 μM, respectively. Cell supernatants were tested for TNF-α content by ELISA (R&D).

Isolation and stimulation of human monocytes

Peripheral blood mononuclear cells were prepared from EDTA-anticoagulated venous blood samples from healthy

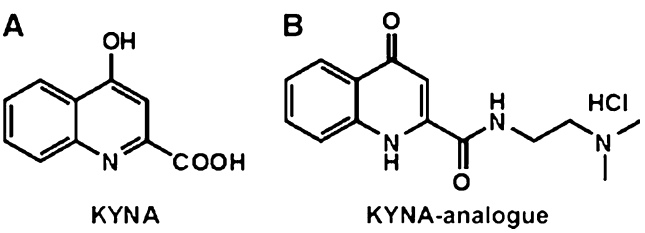

Fig. 1 The structures of kynurenic acid (*KynA*) and of the new KYNA analogue 2-(2-*N*,*N*-dimethylaminoethylamine-1-carbonyl)-1*H*-quinolin-4-one hydrochloride (Marosi et al. 2010)

volunteers by Ficoll-Hypaque (Sigma Chemicals) density gradient centrifugation. Cells were washed with PBS and resuspended in 80 μl of buffer consisting of PBS with 0.5% of bovine serum albumin and 2 mM EDTA per 10^7 total cells and 20 μl of magnetic MACS anti-CD14 MicroBeads (Miltenyi Biotec, Germany) per total 10^7 total cells and incubated for 15 min at 6–8°C. After washing, the cells were resuspended in 500 μl of buffer and run through a column (LS) placed in a magnetic field according to the instructions of the manufacturer. The magnetic anti-CD14 cell separation (positive selection) yielded a cell population consisting of 98% monocytes, as checked by flow cytometric analysis (FACstar, Becton Dickinson). Cells were cultured in RPMI 1640 medium (GIBCO) supplemented with 10% FCS to achieve final concentration of 2×10^6 cells/ml. The cells were stimulated for 24 h with 5 ng/ml phorbol-12-myristate-13-acetate (PMA; SIGMA), with or without heat-inactivated *S. aureus* at 10^8/ml. In parallel experiments, cultures were pretreated for 30 min with KynA or with KynA analogue at concentrations of 500, 250, 125 and 50 μM. Supernatants were tested for HMGB1 content by ELISA.

Isolation and stimulation of human polymorphonuclear neutrophilic granulocytes

Polymorphonuclear neutrophilic granulocytes were isolated from EDTA-anticoagulated blood by Ficoll-Hypaque density gradient centrifugation followed by brief hypotonic lysis of red blood cells. Thereafter, cells were resuspended in RPMI 1640 medium supplemented with 10% FCS. This technique yielded 90–95% neutrophils as assessed by Giemsa staining and by CD16 positivity. Cells were cultured in RPMI 1640 medium (GIBCO) supplemented with 10% FCS to achieve a final concentration of 2×10^6 cells/ml and were incubated in the presence of heat-inactivated *S. aureus* (10^8/ml) for 6 h. In parallel experiments, granulocyte cultures were pretreated for 30 min with KynA or with the KynA analogue at concentrations of 500, 250, 125 and 50 μM. Following the incubation period, the samples were centrifuged at 300 g and the supernatants were tested for HNP1–3 content by ELISA.

Cell line

Human monocytic cells U 937 were propagated in RPMI 1640 medium supplemented with 10% heat-inactivated FCS (GIBCO) at 37°C in a humidified CO_2 incubator. To analyse HMGB1 secretion from U 937 cells, the cell number was adjusted to 10^6/ml. The cells were stimulated for 24 h with 5 ng/ml PMA (SIGMA). In parallel experiments, cultures were pretreated for 30 min with KynA or with the KynA analogue at concentrations of 500, 250, 125 and 50 μM. Supernatants were tested for HMGB1 content by ELISA.

Whole blood incubation method

EDTA-anticoagulated freshly drawn peripheral blood samples (1 ml) from healthy blood donors (whose granulocyte count varied from 3.8×10^6/ml to 4.7×10^6/ml) were incubated in the presence of heat-inactivated *S. aureus* for 6 h. In parallel experiments, blood samples were pretreated for 30 min with KynA or with the KynA analogue at concentrations of 500, 250, 125 and 25 μM, respectively. Following the incubation period, the whole blood samples were centrifuged at 300×*g*, and the supernatants were tested for TNF-α and for HNP1–3 content by ELISA.

TNF-α ELISA

The TNF-α concentrations in the supernatants of whole blood cultures or in human mononuclear cells were quantified by using TNF-α ELISA kit (R&D) according to the instructions of the manufacturer.

HMGB1 ELISA

The HMGB1 concentrations of the supernatants of U 937 cells and of human monocytes were determined with an ELISA kit (IBL Hamburg) according to the instructions of the manufacturer.

HNP1–3 ELISA

The HNP1–3 ELISA kit was obtained from HyCult Biotechnology, The Netherlands. Plasma samples of whole blood cultures and the supernatants of purified granulocytes were analysed with standard measurements, according to the manufacturer's instructions.

TNF-α mRNA quantification by RT-PCR

Total RNA was isolated with High Pure RNA Isolation Kit (Roche) according to the manufacturer's instructions. RNA concentration was determined by the A_{260} value of the sample. Complementary DNA (cDNA) was generated from 1 μg total RNA using the High-Capacity cDNA Reverse Transcription Kit (Applied Biosystems) in a final volume of 20 μl. Reverse transcription PCR (RT-PCR) was performed in a thermal cycler (MJ Mini Gradient Thermal Cycler, Bio-Rad) according to the manufacturer's instructions. After reverse transcription, real-time quantitative PCR was carried out using a LightCycler (Roche). The mixture contained FastStart TaqMan® Probe Master (Roche), sample cDNA and the following primers and probes: TNF-α left primer: 5′-CAG

CCT CTT CTC CTT CCT GAT-3′, TNF-α right primer: 5′-GCC AGA GGG CTG ATT AGA GA-3′ and probe: UPL#29 (Roche). The thermal cycler conditions were initial denaturation at 95°C for 10 min and 45 cycles of 95°C for 15 s and 60°C for 1 min. 18S rRNA was used as a reference (18S rRNA left primer 5′-CTC AAC ACG GGA AAC CTC AC-3′, 18S rRNA right primer: 5′-CGC TCC ACC AAC TAA GAA CG-3′, probe: UPL#77). Results were obtained as threshold cycles (C_t) values, and the relative expression was calculated by using the delta–delta C_t method and given as a ratio between target and reference gene.

HNP1–3 mRNA quantification by RT-PCR

Total RNA was extracted from granulocytes with High Pure RNA Isolation Kit (Roche) according to the manufacturer's instructions. RNA concentration was determined by the A_{260} value of the sample. cDNA was generated from 1 μg total RNA using the High-Capacity cDNA Reverse Transcription Kit (Applied Biosystems) in a final volume of 20 μl. After reverse transcription, amplification was carried out using Light Cycler Fast Start DNA Master^{PLUS} SYBR Green I mix (Roche). Samples were loaded into capillary tubes and placed in the fluorescence thermocycler (LightCycler). Initial denaturation at 95°C for 10 min was followed by 45 cycles of 95°C for 10 s, annealing at 58°C for 8 s and elongation at 72°C for 12 s. For DEFA1 sense, 5′-TCC CAG AAG TGG TTG TTT CC-3′; antisense 5′-GCA GAA TGC CCA GAG TCT TC-3′ and for the housekeeping gene glyceraldehyde-3-phosphate dehydrogenase (GAPDH) sense, 5′-AAG GTC GGA GTC AAC GGA TTT-3′; antisense, 5′-TGG AAG ATG GTG ATG GGA TTT-3′ primers were used. At the end of each run, melting curve profiles were achieved by cooling the sample to 40°C for 15 s and then heating the sample slowly at 0.20°C/s up to 95°C with continuous measurement of the fluorescence to confirm the amplification of specific transcripts. Cycle-to-cycle fluorescence emission readings were monitored and analysed by using LightCycler software (Roche Diagnostics GmbH). All quantifications were normalized to the housekeeping GAPDH gene. Relative gene expression is given as a ratio between target gene and GAPDH gene expressions, calculated by using the delta–delta C_t method.

Statistical analysis

Data are expressed as means ± SD. Differences between group means were determined by ANOVA test followed by Bonferroni's multiple comparison test, or the unpaired Student t test. p values <0.05 were considered significant. All statistical calculations were performed with the GraphPad Prism 5 statistical program (GraphPad Software Inc., San Diego, CA, USA).

Results

KynA and the KynA analogue attenuates TNF-α production in whole blood

To study the effects of KynA and the KynA analogue on leukocyte TNF-α production, varying concentrations of the drugs were added to human whole blood activated with heat-inactivated *S. aureus*. Whole blood, which recapitulates the extracellular milieu of the physiological environment during infection or injury, is an ideal substrate on which to assess the activity of agents towards white blood cells directly.

During a 6-h incubation period, KynA significantly attenuated the TNF-α levels in whole blood in a dose-dependent manner (Fig. 2). The comparison of the inhibitory effect of KynA with that of the KynA analogue revealed that the KynA analogue was more effective ($p<0.01$) than an equimolar concentration of KynA in suppressing TNF-α production.

KynA and the KynA analogue attenuates TNF-α production in human mononuclear cells

As it was theoretically possible that KynA attenuates TNF-α in whole blood by acting indirectly on other cells than mononuclear cells, we ascertained the effect of KynA on isolated human mononuclear cells in vitro. Because of high individual differences in TNF producing capacity, the data in Fig. 3 are expressed as percentages of the TNF-α concentrations produced by untreated (only PBS-treated) cells in each experiment. Each concentration was tested in duplicate on mononuclear cell cultures obtained from five different blood donors. The maximum TNF-α concentrations in the supernatants in SA-induced cultures of mononuclear cells without KynA pretreatment were 12,500–50,000 pg/ml. At the highest

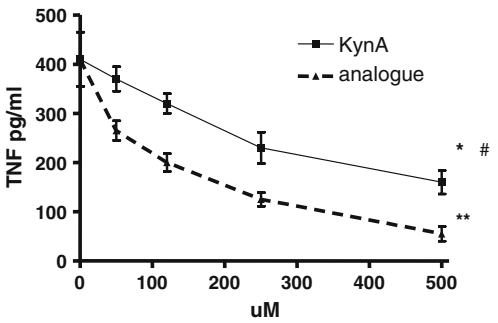

Fig. 2 KynA and the KynA analogue attenuate TNF-α levels in SA-stimulated human whole blood. Whole blood cultures were incubated with PBS (0 μM), KynA or the KynA analogue at concentrations of 50, 125, 250 and 500 μM for 30 min prior to the addition of heat-inactivated SA (10^8/ml), and the TNF-α levels in the plasma were determined 6 h later. Each concentration was tested in duplicate in whole blood obtained from three different donors. Data are shown as means±SD. *$p<0.01$; **$p<0.001$ vs the control (0 μM); #$p<0.01$ vs the KynA analogue, determined by the Student t test

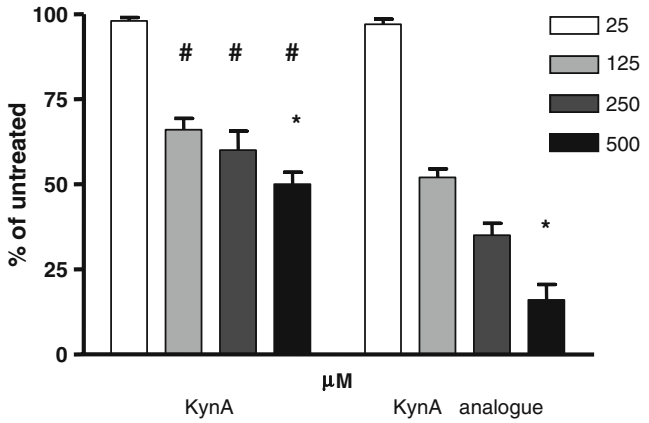

Fig. 3 KynA and the KynA analogue attenuate the TNF-α level in SA-stimulated human mononuclear cells. Mononuclear cells (5×10^6/ml) were incubated with PBS (untreated cells), or with KynA or the KynA analogue at the indicated concentrations 30 min prior to the addition of heat-inactivated SA (10^8/ml), and the TNF-α levels in the supernatants were determined after 18 h. Each concentration was tested in duplicate in mononuclear cell cultures obtained from five different blood donors. Data are expressed as percentages of the TNF values from untreated cell cultures, without KynA or the KynA analogue, and are shown as means±SD. *$p<0.001$ vs 25 μM KynA or vs 25 μM KynA analogue; #$p<0.001$ vs equimolar KynA analogue. The degree of significance between different experimental samples was determined by the ANOVA test followed by Bonferroni's multiple comparison test

concentration (500 μM), KynA suppressed the TNF-α level to 50±3.5%, while the KynA analogue did so to 16±4.5% ($p<0.001$). At 25 μM, the compounds proved ineffective. At each effective concentration (125, 250 and 500 μM), the KynA analogue exhibited a significantly higher inhibitory effect on TNF production than did KynA at equimolar concentration ($p<0.001$; Fig. 3). Together with the results obtained on whole blood, these findings indicate that the KynA analogue is significantly more potent than KynA in inhibiting TNF-α release from mononuclear leukocytes.

KynA and the KynA analogue inhibit TNF-α production in mononuclear cells at the transcription level

To gain further insight into the KynA mechanism of action, we next determined the effects of KynA on TNF-α mRNA expression. Both KynA and the KynA analogue significantly reduced the TNF-α relative expression (Fig. 4), indicating the attenuation of SA-induced TNF protein synthesis in human mononuclear lymphocytes via the inhibition of TNF-α gene transcription.

Effects of KynA and the KynA analogue on HMGB1 secretion of U 937 cells

PMA (5 ng/ml) induced HMGB1 secretion in U 937 cells after a 24-h incubation period. Pretreatment of the cells with KynA or the KynA analogue resulted in a decreased level of HMGB1 secretion. The KynA analogue exhibited a significantly higher inhibitory effect (Fig. 5).

Effects of KynA and the KynA analogue on HMGB1 secretion of human monocytes

To confirm that the inhibition of HMGB1 secretion by KynA is not characteristic only in the case of U 937, a monocytic cell line, we supplemented our experiments by applying freshly isolated human peripheral monocytes. Purified CD14-positive monocytes from peripheral blood of healthy donors were activated by PMA (5 ng/ml), or with PMA and heat-killed *S. aureus*, and HMGB1 was assessed by ELISA. KynA and KynA analogue exerted strong inhibitory effects on HMGB1 release in cultures of monocytes in doses ranging from 500 to 125 μM. The inhibition was significantly higher for the KynA analogue (Table 1).

Effects of KynA and the KynA analogue on secretion of HNP1–3

EDTA-anticoagulated freshly drawn peripheral blood samples were pretreated with increasing concentrations of KynA or the KynA analogue for 30 min and thereafter were incubated in the presence of heat-killed *S .aureus* for 6 h. Following a brief centrifugation at 300×*g*, the supernatants were assessed for HNP1–3 (defensin-α) concen-

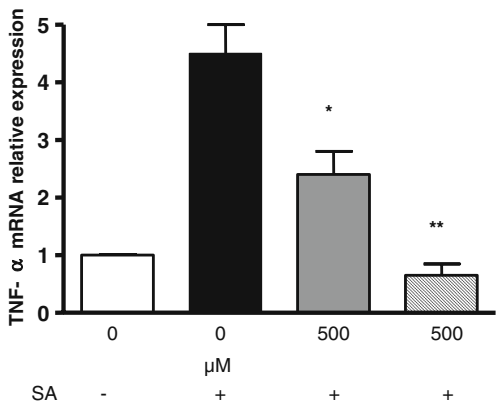

Fig. 4 Effect of 500 μM of KynA and KynA analogue on TNF-α mRNA levels in human mononuclear cells stimulated with SA. TNF-α levels were normalized to reference gene of 18S rRNA by using quantitative real-time PCR. Relative expression was calculated by using the delta–delta C_t method and is given as a ratio between the target and the reference gene. Data are shown as means±SD of the results of three independent experiments. *$p<0.01$ vs 0 μM; **$p<0.001$ vs 0 μM; determined by the Student *t* test. *Open bar* TNF-α mRNA expression without stimulation, *black bar* mRNA expression of SA-stimulated cells without KynA, *grey bar* SA-stimulated cells with 500 μM KynA, *hatched bar* SA-stimulated cells with 500 μM KynA analogue

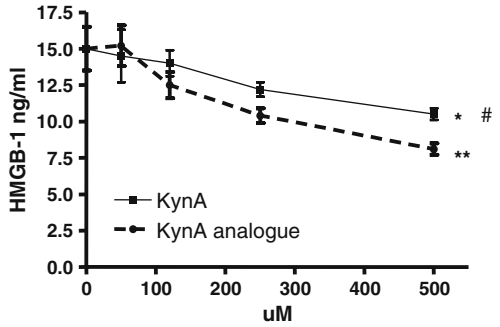

Fig. 5 Effects of KynA and the KynA analogue on HMGB1 secretion of U 937 cells. U-937 cells were pretreated for 30 min with KynA or the KynA analogue and thereafter incubated for 24 h with 5 ng/ml PMA. Supernatants were processed for HMGB1 ELISA. Data are means±SD of the results of three experiments.*$p<0.05$ vs control (0 μM); **$p<0.01$ vs control (0 μM); #$p<0.05$ vs the KynA analogue (determined by the Student *t* test)

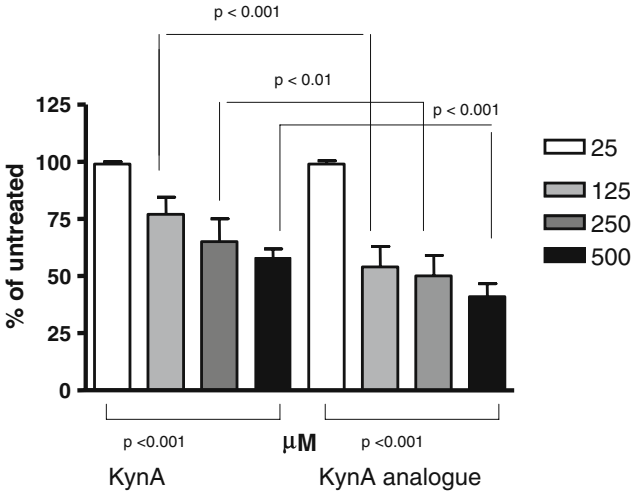

Fig. 6 Effects of KynA and the KynA analogue on secretion of HNP1–3. Whole blood cultures were incubated with KynA or the KynA analogue at the indicated concentrations for 30 min prior to the addition of heat-inactivated SA (10^8/ml), and the HNP1–3 levels in plasma was determined 6 h later. Each concentration was tested in duplicate in whole blood obtained from ten different blood donors. Data are expressed as percentages of the results obtained on untreated samples without KynA or the KynA analogue and are shown as means±SD. The degree of significance between different experimental samples was determined by the ANOVA test followed by Bonferroni's multiple comparison test

tration. The data in Fig. 6 are expressed as percentages of the control values (without KynA or the KynA analogue, respectively) in each experiment because of the high individual differences in HNP1–3 release. Each concentration was tested in duplicate on whole blood obtained from ten different blood donors. The HNP1–3 concentrations in the SA-activated blood samples without KynA treatment varied in the interval 350–650 ng/ml. Both KynA and the KynA analogue significantly reduced the secretion of HNP1–3 (Fig. 6), At 500 μM, KynA and the KynA analogue decreased the level of HNP1–3 to 58±12% and 41±5.6% of that for the untreated samples, respectively ($p<0.001$). The HNP1–3 present in the whole blood cultures can be regarded as mainly due to the activity of the granulocytes (Sthoeger et al. 2008). Our previous experiments demonstrated HNP1–3 secretion not only in the case of purified granulocytes but also when a whole blood incubation method was applied. In the peripheral blood, the neutrophil granulocytes are the main source of HNP1–3, and we therefore suggest that the elevation of the level of HNP1–3 following SA1 induction is mainly due to the activity of the granulocytes (Kocsis et al. 2009a). Accordingly, we conclude that the HNP1–3 (α-defensin) in the supernatants of whole blood cultures can be regarded as products of the granulocytes (this is all the more likely, if it is borne in mind, that the neutrophils account for the highest number of leukocytes in the peripheral blood). However, we ascertained the effect of KynA on isolated human neutrophils. There was a considerable HNP1–3 secretion by granulocytes following a 6-h induction with heat-killed SA (980±125 ng/ml). KynA and the KynA analogue resulted in significantly decreased HNP1–3 levels in the supernatants; at concentrations of 125–500 μM, the lowest levels of HNP1–3 were secreted in the presence of 500 μM KynA analogue (Table 2).

Table 1 Effects of KynA and the KynA analogue on HMGB1 secretion of human monocytes

		HMGB1 ng/ml	
		Induction with PMA	Induction with PMA + SA
Without KynA (control)		31±2.8	41.4±4.2
KynA	50 μM	29.0±2.8	33.2±4.1
Analogue	50 μM	27.1±3.1	28.2±3.5*
KynA	125 μM	26.2±2.7****	29.1±2.8*·****
Analogue	125 μM	21.5±2.2*	21.8±2.7**
KynA	250 μM	14.9±2.6**·****	18.2±2.4**·****
Analogue	250 μM	10.3±1.5***	12.5±1.8***
KynA	500 μM	13.7±2.1**·****	15.8±2.5***·****
Analogue	500 μM	9.5±1.5***	10.5±0.9***

Human peripheral blood monocytes (separated by the MACS (Miltenyi Biotec) magnetic bead method) were pretreated for 30 min with KynA or the KynA analogue and thereafter incubated for 24 h with 5 ng/ml PMA, or with 5 ng/ml PMA together with heat-inactivated SA (10^8/ml). Supernatants were processed for HMGB1 ELISA. Data are means ± SD of the results of three experiments

*$p<0.05$ vs control (without KynA); **$p<0.01$ vs control (without KynA); ***$p<0.001$ vs control (without KynA); ****$p<0.05$ vs the KynA analogue (determined by the Student *t* test)

Levels of HNP1–3 mRNA in granulocytes

We measured the α-defensin mRNA level in the granulocytes. While the induction of neutrophil granulocytes with SA

Table 2 Effects of KynA and the KynA analogue on the secretion of HNP1–3 of human granulocytes

		HNP1–3 (ng/ml)
Without KynA (control)		950±125
KynA	50 μM	915±130
Analogue	50 μM	850±125
KynA	125 μM	720±65*,****
Analogue	125 μM	410±51**
KynA	250 μM	660±62*,****
Analogue	250 μM	312±45**
KynA	500 μM	498±50**,****
Analogue	500 μM	230±32***

Human granulocytes (2×10^6/ml) were incubated with KynA or the KynA analogue at the indicated concentrations for 30 min prior to the addition of heat-inactivated SA (10^8/ml) and the HNP1–3 levels in the supernatants were determined 6 h later. Data are means±SD of the results of three experiments

*$p<0.05$ vs control (without KynA); **$p<0.01$ vs control (without KynA); ***$p<0.001$ vs control (without KynA); ****$p<0.01$ vs the KynA analogue (determined by Student t test)

resulted in an elevation of mRNA levels (relative mRNA expression 2.5±1.2; $n=3$), no significant influence of either KynA or the KynA analogue even at 500 μM was observed (data not shown).

Discussion

KynA was earlier shown to inhibit intestinal hypermotility and xanthine oxidase activity in experimental colon obstruction in dogs (Kaszaki et al. 2008), and it was presumed that KynA might influence intestinal inflammation. The aim of the present pilot study is to investigate the in vitro immunomodulatory effects of KynA and its analogue 2-(2-*N*,*N*-dimethylaminoethylamine-1-carbonyl)-1*H*-quinolin-4-one hydrochloride on human peripheral leukocytes and the human monocyte cell line.

In the whole blood model, which resembles closely the physiological milieu, both KynA and the KynA analogue attenuated TNF-α induction. KynA also dose-dependently inhibited the TNF-α production by purified human mononuclear cells, but in equimolar concentrations, the KynA analogue exhibited more pronounced inhibitory activity.

Not only the production of the "early inflammatory cytokine" TNF was inhibited by KynA but also the active secretion of a "late" cytokine, HMGB1. Active HMGB1 secretion induced in U 937 human monocytic cells following phorbol ester induction was inhibited more effectively by the KynA analogue. The inhibitory effects of KynA and the KynA analogue were also demonstrated when freshly isolated human peripheral blood monocytes were activated with phorbol ester, or with phorbol ester plus SA. HMGB1 plays important roles in various non-infectious and infectious inflammatory conditions including trauma, sepsis, rheumatoid arthritis and pancreatitis (Levy et al. 2007; Pisetsky et al. 2008; Sundén-Cullberg et al. 2006; Kocsis et al. 2009b). Inhibition of the production of TNF-α and the active secretion of HMGB1 draw attention to the anti-inflammatory effect of KynA and its analogue. Similarly, the secretion of human neutrophil peptides HNP1–3 (defensin-α) was inhibited by both compounds but significantly more strongly by the KynA analogue. The secretion of defensin-α by granulocytes was measured in our experiments in whole blood cultures. As granulocytes are the main source of HNP1–3 in the peripheral blood, the results obtained from the investigation of whole blood can be regarded as reflecting the granulocyte functions (Kocsis et al. 2009a; Sthoeger et al. 2008). To confirm this, we supplemented our study with experiments involving purified granulocytes from peripheral blood. The similar results proved the inhibitory effects of KynA and the KynA analogue on the HNP1–3 secretion of the granulocytes. KynA, however, did not result in a decreased HNP1–3 mRNA expression in the granulocytes, which could possibly explained by inhibition of the secretion or of the degranulation, rather than by impaired HNP1–3 transcription by KynA. HNP1–3 (defensin-α) has not only antibacterial properties but also important immune functions and inflammatory effects (Yang et al. 2002; Quinn et al. 2008). Inhibition of HNP1–3 secretion can therefore additionally result in anti-inflammatory effects.

Kynurenic acid is an NMDA antagonist (Stone 1993; Robotka et al. 2008; Klivenyi et al. 2004). It is likely that the inhibition of TNF transcription and production and the attenuation of defensin-α secretion are connected with NMDA antagonism (Mcnearney et al. 2010). Studies on the mechanism of action of KynA at micromolar concentrations are a competitive antagonist of the NMDA receptor (Rózsa et al. 2008). Another possibility is that the inhibitory effect on the TNF-α transcription is signalled through the α7-nicotinic acetylcholine receptor pathway. Activation of the α7-nicotinic acetylcholine receptor attenuates TNF-α and HMGB1 production through the inhibition of nuclear factor-κB activation (Rosas-Ballina and Tracey 2009; Wang et al. 2004). Nonselective nicotinic agonists, including acetylcholine and nicotine, attenuate proinflammatory cytokine production through an α7-dependent mechanism (Wang et al. 2003; Yoshikawa et al. 2006; Parrish et al. 2008). Interestingly, KynA is a nonselective antagonist of the α7-nicotinic acetylcholine receptor at nanomolar concentrations (Hilmas et al. 2001; Robotka et al. 2008), moreover exerts a biphasic, "Janus-face"-like effect (Rózsa et al. 2008). It is tempting to speculate whether KynA, an

antagonist of the α7-nicotinic acetylcholine receptor, could induce similar signalling effects towards TNF-α and HMGB1 transcription, as an agonist. It is noteworthy, however, that HMGB1 secretion by activated monocytes and macrophages requires a tightly controlled relocation program (Bonaldi et al. 2003; Ulloa and Messmer 2006). Lacking a leader signal sequence, HMGB1, cannot be released via the classical ER–Golgi secretory pathway. Instead, activated macrophages/monocytes acetylate HMGB1 at lysine-rich nuclear localization sequences, leading to translocation of nuclear HMGB1 into cytoplasmic vesicles and subsequent release into the extracellular milieu. Further studies are necessary to elucidate the exact mechanism, whereby the signalization is influenced by KynA, resulting in inhibition of HMGB1 secretion.

In our experiments, KynA and its analogue attenuated the secretion of TNF-α and HMGB1 of mononuclear cells and U-937 cells and monocytes, respectively. This is in good accordance with recent observations by Wang et al., who reported that KynA attenuated the LPS-induced TNF-α secretion of human mononuclear cells, expressing the GPR35 receptor (Wang et al. 2006). The predominant expression of GPR35 in immune cells and the elevation of KynA levels during inflammation (Lögters et al. 2009) suggest that the anti-inflammatory effect of KynA provides a feedback mechanism in modulating the immune response. The attenuation of HNP1–3 secretion of neutrophils by KynA may also be connected with the effect through GPR35, as this receptor is expressed on neutrophils. Further studies are necessary to elucidate the exact mechanisms that result in the attenuation of TNF-α and HMGB1 production, and it remains to be established whether the NMDA receptor or the GPR35 activation or even the α7-nicotinic acetylcholine receptor is involved in these effects.

Conclusion

Our preliminary results revealed that KynA attenuates TNF-α and HMGB1 production by human mononuclear white blood cells and by monocytic cells and the secretion of defensin-α by human granulocytes, indicating definitive anti-inflammatory action of the molecule, and the more potent effect of the KynA analogue. The suppressive effect of the KynA analogue is greater than that of an equimolar concentration of KynA both in whole blood and in separated mononuclear cells in vitro under comparable experimental conditions. This may be due to the cationic centre of the side chain, which is probably an additional binding site. Overall, these results suggest that KynA and the KynA analogue can regulate critical steps involved in a wide range of inflammation. The new analogue may therefore be considered a promising candidate for clinical studies.

Acknowledgements We thank Mrs. Györgyi Müller for expert technical assistance and Mrs. Zsuzsanna Rosztoczy for skillful administration. This work was supported by Hungarian Research Grant OTKA K67889/5K540.

References

Andersson U, Wang HC, Palmblad K, Aveberger AC, Bloom O, Erlandsson-Harris H, Janson A, Kokkola R, Zhang MH, Yang H, Tracey KJ (2002) High mobility group 1 protein (HMG-1) stimulates proinflammatory cytokine synthesis in human monocytes. J Exp Med 192:565–570

Bonaldi T, Talamo P, Scaffidi P, Ferrera D, Porto A, Bachi A, Rubartelli A, Agresti A, Bianchi ME (2003) Monocytic cells hyperacetylate chromatin protein HMGB1 to redirect it towards secretion. EMBO J 22:5551–5560

Bradley JR (2008) TNF-mediated inflammatory disease. J Pathol 214:149–160

Ganz T (1987) Extracellular release of antimicrobial defensins by human polymorphonuclear leukocytes. Infect Immun 55:568–571

Gigler G, Szenasi G, Simo A, Levay G, Harsing LG, Sas K, Vecsei L, Toldi J (2007) Neuroprotective effect of L-kynurenine sulfate administered before focal cerebral ischemia in mice and global cerebral ischemia in gerbils. Eur J Pharmacol 564:116–122

Fiers W (1991) Tumor necrosis factor. Characterization at the molecular, cellular and in vivo level. FEBS Lett 285:199–212

Harris HE, Andersson U (2004) The nuclear protein HMGB1 as a proinflammatory mediator. Eur J Immunol 34:1503–1512

Hilmas C, Pereira EF, Alkondon M, Rassoulpour A, Schwarcz R, Albuuqerque EX (2001) The brain metabolite kynurenic acid inhibits α7 nicotinic receptor activity and increases non-α7 nicotic expression: physiopathological implications. J Neurosci 21:7463–7473

Kaszaki J, Palasthy Z, Erczes D, Racz A, Torday C, Varga G, Vecsei L, Boros M (2008) Kynurenic acid inhibits intestinal hypermotility and xanthine oxidase activity during experimental colon obstruction in dogs. Neurogastroenterol Motil 20:53–62

Kiss C, Vecsei L (2005) Neuroprotection and kynurenine system. In: Vecsei L (ed) Kynurenines in the brain: from experiment to clinics. Nova Science, New York, pp 173–191

Klivenyi P, Toldi J, Vecsei L (2004) Kynurenines in neurodegenerative disorders: therapeutic consideration. In: Vecsei L (ed) Frontiers in clinical neuroscience: neurodegeneration and neuroprotection. Adv Exp Med Biol, vol 541. Kluwer, New York, pp 169–183

Kocsis AK, Ocsovszky I, Tiszlavicz L, Tiszlavicz Z, Mandi Y (2009a) Helicobacter pylori induces the release of alpha-defensin by human granulocytes. Inflamm Res 58:241–247

Kocsis AK, SzabolcsA HP, Hofner P, Takács T, Farkas G, BodaK G, Mandi Y (2009b) Plasma concentrations of high-mobility group box protein1, soluble receptor for advanced glycation end products and circulating DNA in patients with acute pancreatitis. Pancreatology 9:383–391

Lagerström MC, Schiöth HB (2008) Structural diversity of G protein-coupled receptors and significance for drug discovery. Nat Rev Drug Discov 7:339–357

Levy RM, Mollen KP, Prince JM, Kaczorowski DJ, Vallabhaneni R, Liu S, Tracey KJ, Lotze MT, Hackam DJ, Fink MP, Vodovotz Y, Billiar TR (2007) Systemic inflammation and remote organ injury following trauma require HMGB1. Am J Physiol Regul Integr Comp Physiol 293:R1538–R1544

Lotze MT, Tracey KJ (2005) High-mobility group box 1 protein (HMGB): nuclear weapon in the immune arsenal. Nat Rev Immunol 5:331–342

Lögters TT, Laryea MD, Altrichter J, Sokolowski J, Cinatl J, Reipen J, Linhart W, Windolf J, Scholz M, Wild M (2009) Increased plasma kynurenine values and kynurenine-tryptophan ratios after major trauma are early indicators for the developments of sepsis. Shock 32:29–34

Marosi M, Nagy D, Farkas T, Zs K, Rózsa É, Robotka H, Fülöp F, Vécsei L, Toldi J (2010) A novel kynurenic acid analogues: a comparison with kynurenic acid. An in vitro electrophysiological study. J Neural Transm 117:183–188

Mazza J, Rossi A, Weinberg JM (2010) Innovatives uses of tumor necrosis factor alpha inhibitors. Dermatol Clin 28:559–575

McNearney TA, Ma Y, Chen Y, Taglialatela G, Yin H, Zhang WR, Westlund KN (2010) A peripheral neuroimmune link: glutamate agonists upregulate NMDA NR1 receptor mRNA and protein, vimentin, TNF-alpha, and RANTES in cultured human synoviocytes. Am J Physiol Regul Integr Comp Physiol 298:R584–R598

Nemeth H, Toldi J, Vecsei L (2005) Role of kynurenines in the central and peripheral nervous systems. Curr Neurovasc Res 2:249–260

Parrish WR, Rosas-Ballina M, Gallowitsch-Puerta M, Ochani M, Ochani K, Yang LH, Hudson L, Lin X, Patel N, Johnson SM, Chavan S, Goldstein RS, Czura CJ, Miller EJ, Al-Abed Y, Traccy KJ, Pavlov VA (2008) Modulation of TNF release by choline requires alpha7 subunit nicotinic acethylcholine receptor-mediated signaling. Mol Med 14:567–574

Pisetsky DS, Erlandsson-Harris H, Andersson U (2008) High-mobility group box protein 1 (HMGB1): an alarmin mediating the pathogenesis of rheumatic disease. Arthritis Res Ther 10:209–223

Quinn K, Henriques M, Parker T, Slutsky AS, Zhang H (2008) Human neutrophil peptides: a novel potential mediator of inflammatory. Am J Physiol Heart Circ Physiol 295:1817–1824

Robotka H, Toldi J, Vécsei L (2008) L-Kynurenine: metabolism and mechanism of neuroprotection. Future Neurol 3:169–188

Rosas-Ballina M, Tracey KJ (2009) Cholinergic control of inflammation. J Intern Med 265:663–679

Rózsa É, Robotka H, Vécsei L, Toldi J (2008) The Janus-face kynurenic acid. J Neural Transm 115:1087–1091

Sas K, Robotka H, Toldi J, Vecsei L (2007) Mitochondria, metabolic disturbances, oxidative stress and the kynurenine system, with focus on neurodegenerative disorders. J Neurol Sci 257:221–239

Schwarcz R, Ceresoli-Borroni G, Wu HQ, Rassoulpour A, Poeggeler B, Hodgkins PS, Guidetti P (1999) Modulation and function of kynurenic acid in the immature rat brain. Adv Exp Med Biol 467:113–123

Sthoeger ZM, Bezalel S, Chapnik N, Asher I, Froy O (2008) High α-defensin levels in patients with systemic lupus erythematosus. Immunology 127:116–122

Stone TW (1993) Neuropharmacology of quinolinic and kynurenic acids. Pharmacol Rev 45:309–379

Stone TW (2000) Development and therapeutic potential of kynurenic acid and kynurenine derivatives for neuroprotection. Trends Pharmacol Sci 21:149–154

Sundén-Cullberg J, Norrby-Teglund A, Treutiger CJ (2006) The role of high mobility group box-1 protein in severe sepsis. Curr Opin Infect Dis 19:231–236

Swartz KJ, During MJ, Freese A, Beal MF (1990) Cerebral synthesis and release of kynurenic acid: an endogenous antagonist of excitatory amino acid receptors. J Neurosci 10:2965–2973

Ulloa L, Messmer D (2006) High-mobility group box 1 (HMGB1) protein: friend and foe. Cytokine Growth Factor Rev 17:189–201

Vamos E, Pardutz A, Klivenyi P, Toldi J, Vecsei L (2009) The role of kynurenines in disorders of the central nervous system: possibilities for neuroprotection. J Neurol Sci 283:21–27

Varga G, Erces D, Fazekas B, Fulop M, Kovacs T, Kaszaki J, Fulop F, Vecsei L, Boros M (2010) N-Methyl-d-aspartate receptor antagonism decreases motility and inflammatory activation in the early phase of acute experimental colitis in the rat. Neurogastroenterol Motil 22:217–221

Vecsei L, Miller J, MacGarvey U, Beal MF (1992) Kynurenine and probenecid inhibit pentylenetetrazol-induced and NMDLA-induced seizures and increase kynurenic acid concentrations in the brain. Brain Res Bull 28:233–238

Wang H, Yu M, Ochani M, Amella CA, Tanovic M, Susarla S, Li JH, Wang HC, Yang H, Ulloa L, Al-Abed Y, Czura CJ, Tracey KJ (2003) Nicotinic acetylcholine receptor alpha 7 subunit is an essential regulator of inflammation. Nature 421:384–388

Wang H, Liao H, Ochani M, Justiniani M, Lin XC, Yang LH, Al-Abed Y, Wang HC, Metz C, Miller EJ, Tracey KJ, Ulloa L (2004) Cholinergic agonists inhibit HMGB1 release and improve survival in experimental sepsis. Nat Med 10:1216–1221

Wang J, Simonavicius N, Wu X, Swaminath G, Reagan J, Tian H, Ling L (2006) Kynurenic acid as a ligand for orphan G protein-coupled receptor GPR35. J Biol Chem 281:22021–22028

Wang JE, Jorgensen PF, Almlof M, Thiemermann C, Foster SJ, Aasen AO, Solberg R (2000) Peptidoglycan and lipoteichoic acid from *Staphylococcus aureus* induce tumor necrosis factor alpha, interleukin 6 (IL-6) and IL-10 production in both T cells and monocytes in a human whole blood model. Infect Immun 68:3965–3970

Yang D, Biragyn A, Kwak LW, Oppenheim JJ (2002) Mammalian defensins in immunity: more than just microbicidal. Trends Immunol 23:291–296

Yoshikawa H, Kurokawa M, Ozaki N, Nara K, Atou K, Takada E, Kamochi H, Suzuki N (2006) Nicotine inhibits the production of proinflammatory mediators in human monocytes by suppression of I-kappa B phosphorylation and nuclear factor-kappa B transcriptional activity through nicotinic acetylcholine receptor alpha7. Clin Exp Immunol 146:116–123

Zádori D, Klivényi P, Vámos E, Fülöp F, Toldi J, Vécsei L (2006) Kynurenines in chronic neurodegenerative disorders: future therapeutic strategies. J Neural Transm 116:1403–1409